TECHNISCHE UNIVERSITÄT DRESDEN

Technische Universität Dresden
Fakultät Maschinenwesen
Institut für Productionstechnik

DIPLOMA THESIS

Title:

Influence of constructive materials, geometry and other variables on heat flow and output power of an air-cooled GTAW torch

Isabel Pilar Banegas Carrillo, born 12.10.1981

The Diploma Thesis contains:
72 Pages
46 Figures
4 Pictures
10 Tables
6 Appendixes

Dresden, 10.11.2006

Tutors: Prof. Dr.-Ing. Habil. Uwe Füssel
Dipl.-Ing. Julio Fuentes
Dipl.-Ing. Jörg Zschetzsche

NOMENCLATURE

LATIN SYMBOLS

Symbol	Units	Name
A	m^2	Area normal to the direction of heat flow
A	m^2	Area of the emitting surface
c_p	$\frac{J}{kg \cdot K}$	Specific heat
g	$\frac{m^2}{s}$	Gravitational acceleration
D	m	Cylinder/tube diameter
D_{eq}	m	Equivalent diameter
D_S	m	"Becoming element of turbulence" diameter
h	$\frac{W}{m^2 \cdot K}$	Convective heat transfer coefficient
$h_{3,i}$	$\frac{W}{m^2 \cdot K}$	Convective coefficient at inside head for model i = A, B, C, D.
$h_{4,i}$	$\frac{W}{m^2 \cdot K}$	Convective coefficient at normal collet surface for model i = A, B, C, D.
$h_{5,i}$	$\frac{W}{m^2 \cdot K}$	Convective coefficient at "becoming element of turbulence" surface for model i = A, B, C, D.
$h_{6,i}$	$\frac{W}{m^2 \cdot K}$	Convective coefficient at surface without "becoming element of turbulence" of the collet with this element for model i = A, B, C, D.
$h_{7,i}$	$\frac{W}{m^2 \cdot K}$	Convective coefficient due to free convection with shielding gas on collet body surface for model i = A, B, C, D.

Symbol	Units	Name
h_a	$\frac{W}{m^2 \cdot K}$	Convective coefficient due to free convection with air.
i	A	Electric current
k	$\frac{W}{m \cdot K}$	Thermal conductivity
L	m	Significant length
L	m	Cylinder height
L	m	Tube length
P	atm or Pa	Total pressure
q	W	Radiant energy emission rate
$\vec{q}$	$\frac{W}{m}$	Heat flux
q_x	W	Heat transfer rate in the x direction
$\dot{q}_v$	$\frac{W}{m^3}$	Volumetric rate of thermal energy generation
r	m	Radial coordinate
r_h	m	Hydraulic radius
$\Re$	$\Omega \cdot m$	Electrical resistivity
t	s	Time
T	K or $^\circ C$	Temperature
T_{bf}	K	Bulk fluid temperature
T_f	K	Temperature of fluid in motion
T_{mf}	K	Film temperature
T_{mp}	K	Melting point
T_s	K	Surface temperature
v	$\frac{m}{s}$	module of velocity

Symbol	Units	Name
y_3	m	y-coordinate of reference point T3
y_4	m	y-coordinate of reference point T4
z	m	Axial coordinate
z_1	m	z-coordinate of reference point T1
z_2	m	z-coordinate of reference point T2
z_{ew}	m	Distance between the tip of electrode and the workpiece
z_{ne}	m	Distance between the bottom of the nozzle and the tip of electrode

GREEK SYMBOLS

Symbol	Units	Name
α	$\frac{m^2}{s}$	Thermal diffusivity $\alpha = \frac{k}{\rho \cdot c_P}$
β	$\frac{1}{^\circ K}$	Coefficient of thermal expansion
ε	dimensionless	Emissivity
Φ	V	Electrical potential
μ	$\frac{kg}{m \cdot s}$	Viscosity
μ_S	$\frac{kg}{m \cdot s}$	Viscosity at the interior surface temperature of the tube
ϑ	$\frac{m^2}{s}$	Cinematic viscosity $\nu = \frac{\mu}{\rho}$
ρ	$\frac{kg}{m^3}$	Density
σ	$\Omega^{-1} \cdot m^{-1}$	Electrical conductivity
σ	$\frac{W}{m^2 \cdot K^4}$	Stefan-Boltzmann constant
ΔT	$^\circ K$ or $^\circ C$	Temperature difference

DIMENSIONLESS PARAMETERS

Symbol	Equation	Name
Eu	$\frac{P}{\rho \cdot \mathrm{v}^2}$	Euler Number
Gr	$\frac{\beta \cdot g \cdot \rho^2 \cdot L^3 \cdot \Delta T}{\mu^2}$	Grashof Number
Nu	$\frac{h \cdot L}{K}$	Nusselt Number
Pr	$\frac{\nu}{\alpha} = \frac{\mu \cdot c_P}{k}$	Prandtl Number
Pe	$\mathrm{Re} \cdot \mathrm{Pr}$	Peclet Number
Ra	$Gr \cdot \mathrm{Pr}$	Rayleigh Number
Re	$\frac{\rho \cdot \mathrm{v} \cdot \mathrm{L}}{\mu}$	Reynolds Number
St	$\frac{h}{\rho \cdot \mathrm{v} \cdot \mathrm{c_P}}$	Stanton Number

MATHEMATICAL OPERATORS

Symbol	Units	Name
$\frac{\partial}{\partial x}$	$\frac{1}{m}$	Gradient in x direction
$\frac{\partial T}{\partial t}$	$\frac{K}{s}$	Temperature variation with the time
$\nabla^2 T$	$\frac{K}{m^2}$	Laplace equation $\nabla^2 T = (\frac{\partial^2 T}{\partial x^2} + \frac{\partial^2 T}{\partial y^2} + \frac{\partial^2 T}{\partial z^2})$

CONTENTS

CHAPTER 1

INTRODUCTION

1 INTRODUCTION

The history of welding started several millennia ago, with the earliest examples of welding from the Bronze Age and Iron Age in Europe and the Middle East. However, it was during the 19th century when welding begun to be developed.

Since the early days of its invention, welding techniques play an important role in current state of living and technology. It is hard to imagine our world without any welding process. Nowadays, mostly all objects around us involve welding in some way; buildings, bridges, machinery, tunnels, highway, aircraft, bikes, cars, trains, space vehicles, sculptures, pipes, rails and even post mail boxes.

It is defined welding as the process of joining two pieces of material where the bonding is accompanied by an appreciable interatomic penetration that takes place at their original boundary surfaces. The boundaries more or less disappear at the weld, and integrating crystals develop across the interface. Welding is carried out by the use of heat and/or pressure, with or without added metal.

At present, there are many different welding processes. According to norm ISO 4063, these processes can be classified into two approaches: welding by fusion or welding by pressure. The fusion approach is the most common.

The study here is focused on Arc welding processes (AW), that use a welding power supply to create and maintain an electric arc between an electrode and the base material to melt materials at the welding point. They can use direct (DC) or alternating (AC) current, and consumable or non-consumable electrodes. The welding region is sometimes protected by some type of inert or semi-inert gas, known as a shielding gas, and filler material is sometimes used as well.

Particularly the case of interest here are non-consumable electrodes with inert gas with gas cooling. This approach to welding is known as gas-cooled GTAW (or air-cooled GTAW) and will be studied and developed in this work.

Getting good weld quality is important for welding production. This quality is related to current flow. Thus, higher currents provide penetration deeper weld penetration. However, the arc current is limited mainly by the inability to remove heat from the torch components.

In addition, increasing current might have unfavourable results in welding, when heat removal in the torch components is inadequate. The ability to remove the heat generated by these higher currents is the key factor for improving GTAW operation. GTAW* torch design until recently has not been sufficiently developed by the industry to achieve any improvement of their cooling capacity when using higher arc current without an associated increase in torch size.

Therefore, to increase an air-cooled GTAW torch's cooling capacity, it is fundamental to know how the torch behaves physically, i.e. how heat is transferred through the welding torch. Simulations with finite element method provide a powerful tool for better understanding this behaviour and trying to improve future designs.

So, this one will be major goal; studying the GTAW torch's heat transfer behaviour through simulations using Ansys Multiphysics. This aim will be reached by building four different welding geometries in Ansys. These models are validated by the experimentation in welding workshop and comparison of these results in awareness of all the errors with the simulations.

Firstly, a basic analysis of technical and economical situation of GTAW torch at present time will be introduced. The market state for this welding torch will be analyzed by presenting GTAW technical characteristics, advantages and disadvantages, and future field of this welding torch.

Some fundamental theory involved in the development of the project is also explained and the models construction is described systematically. This theory will be used with the experiments to validate the finite element models.

Later, some variables implicated in GTAW process will be studied through the models simulation in Ansys to know the behaviour of the welding torch and to identify improvements to its quality and power. Some of these variables include current intensity, electrode diameter, cycle duty, temperature, materials, geometry, shielding gas flow.

Finally, a general summary of results and a discussion about the possible future solutions to reduce the weakness of air-cooled GTAW torches and strengthen their advantages in industrial market are described in last chapter.

---

*GTAW is the acronym for Gas Tungsten Arc Welding.

CHAPTER 2

GOALS OF THE PROJECT

2 GOALS OF THE PROJECT

Most kinds of GTAW machines that are available in market are large, solid, expensive and with voluminous power sources. These great machines are water-cooled GTAW machines that require input power and water connections beside the electrical connections, making them heavier and less portable than other welding machines.

It could be easily stated that the water-cooled machines´ disadvantages are advantages for air-cooled GTAW. Several producers, like racecar, street or building constructors, would prefer the features of air-cooled welder machines because they are smaller, lighter, and easy to move, less complexity with fewer expensive internal components and less maintenance.

However, air-cooled GTAW has a disadvantage that water-cooled GTAW do not have, and it is that its amperage range is much shorter. That is, these machines cannot work with high current or over long times because the torch elements and internal electrical components tent to overheated. Mostly, all air-cooled GTAW that you can find in industrial market have a 200-250 amperes maximum output current. This is the project starting-point; how can we achieve a higher output current of air-cooled GTAW?

This project intends to answer to this question. It analyzes the physically behaviour of this torch and tries to improve air-cooled GTAW output power through increasing their cooling capacity. These are the processing steps:

1. Design new model

Four prototypes with different geometries were designed and built for making the experiments in the lab. At the same time, four finite element models (FEM) analogous to the real construction were constructed for simulation in Ansys by: (1) creating the geometry, defining material and properties; (2) Defining element type and meshing; (3) Applying the adequate boundary conditions and loads that make the simulations behave as close to physicality as possible.

2. Validation

Once all models were built, the prototypes were assembled in the lab and finite element models were ready to simulate, the next step was to validate. In the workshop some experiments were performed with the same experimental conditions for FEM models that were simulated in Ansys. The results of FEM are compared with experimental results to know if its behaviour is similar enough to the prototypes.

3. Variables in heat transfer

After comparing Ansys models with the prototype, some variables that might have an influence on heat transfer were simulated to know how the heat transfer in welding torch behaves physically.

4. Conclusion

In this last step, a short summary of the results and a discussion of the air-cooled GTAW's weakness and strengths are made. Also, some possible suggestions for the initial problem are described.

On the next page Figure 2.1 shows a schematic diagram of the project´s work line, that is, a summary of all steps made for getting some solutions to the problem of low amperage range of air-cooled GTAW.

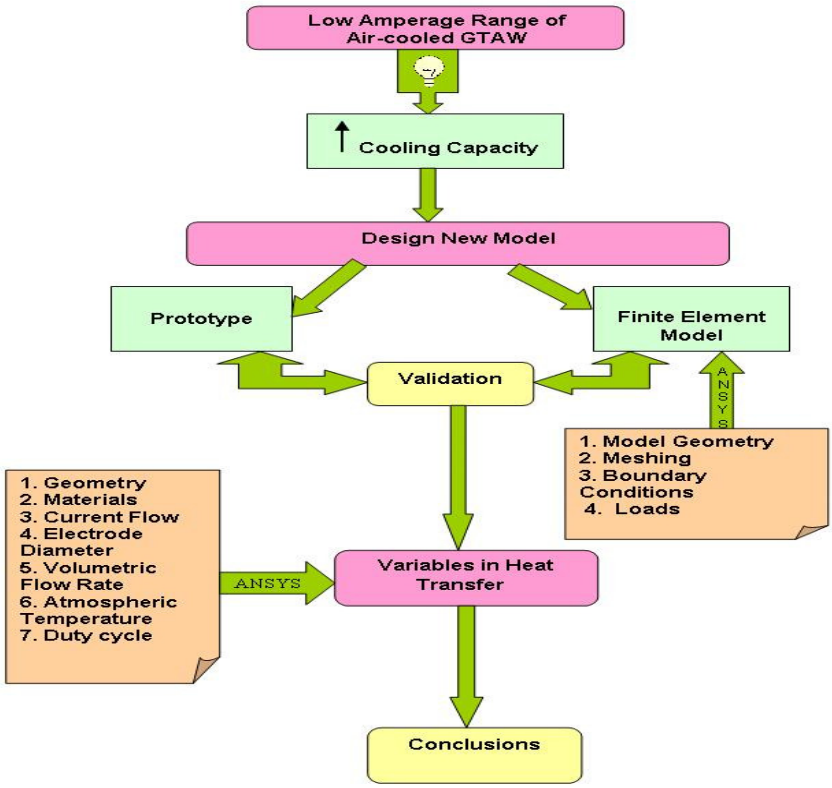

Figure 2.1 Schematic diagram of the project's work line.

CHAPTER 3

TECHNICAL BACKGROUND

3 TECHNICAL BACKGROUND

GTAW has become indispensable as a tool for many industries because of the high quality welds produced and low equipment costs. Today GTAW is used heavily in the military, nuclear, aerospace, chemical processing, racecar construction, motorsports, commercial aircraft, and decorative fabricating industries and stainless and aluminum products that are made for the medical, dental or food-handling services.

While GTAW can be used to weld a range of metal thicknesses, it is best suited for welding thin metals in applications with exacting requirements for quality and finish. Although typically filler metal is not added when GTAW is applied to thin materials, it may be added either manually or automatically.

The main classification of GTAW torches is made according how the heat that is generated in GTAW torch during welding is removed:

- Gas-cooled GTAW or air-cooled GTAW, use ambient air and shielding gas to dissipate excess heat.
- Water-cooled GTAW: these torches provide cooling by the continuous flow of water through small conduits in the torch. As illustrated in Figure 3.1, the cooling water enters the torch through the inlet hose, circulates through the torch, and exits through an outlet hose. The power cable from the power supply to the torch is typically enclosed within the cooling water outlet hose.

The equipment for both types of GTAW includes the following elements:

(a) electrode, which serves as one of the electrical terminals of the arc;
(b) collet, is the electrode holder typically made of a copper alloy;
(c) collet body, what hold the collet;
(d) torch body;
(e) shielding gas, which protect the electrode and the molten weld metal;
(f) nozzle, which direct shielding gas to weld zone;
(g) power supply.

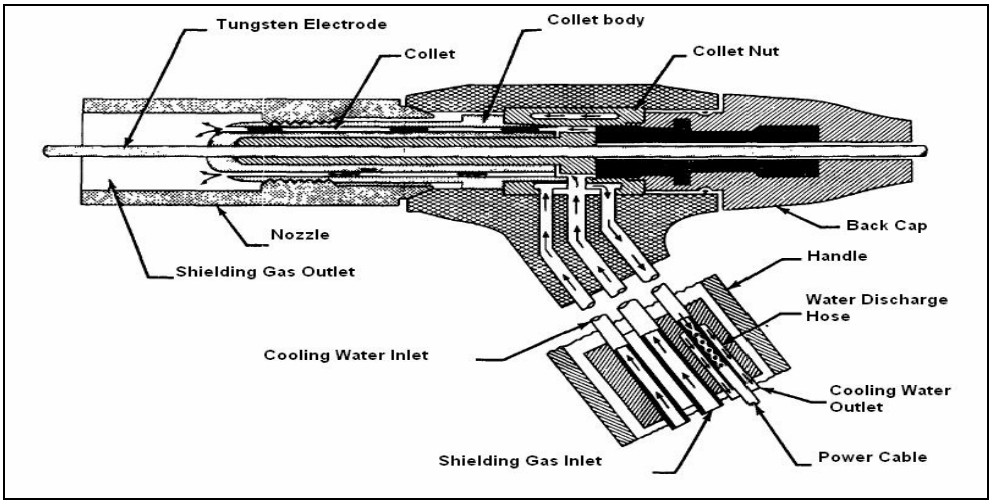

Figure 3.1 Cross-Sectional View of a Typical Water-cooled Torch for Manual Gas Tungsten Arc Welding. [1]

Brass and copper are the common materials used to build GTAW torches. The differences between the air and water cooled GTAW are that air-cooled GTAW torch does not have an inlet hose and an outlet hose for cooling water; it just has a conduit for the shielding gas. In addition, air-cooled GTAW torch do not need neither a heat exchanger nor a pump to circulate and remove the heat from the coolant. For the water-cooled torches, it is also necessary to use treated coolant solution to avoid algae growth or scale formation on the internal torch surfaces and cable assembly. These additional elements mean more money; water-cooled GTAW torches require a higher initial investment and these torches also have greater operating and maintenance costs than air-cooled GTAW torches.

The advantage of this cooling system in water-cooled torch is that the cooling time and welder fatigue is reduced. The flexible cable, lighter weight, and smaller size can provide more comfort to the welder when compared to the similar-amperage air-cooled torch, which contains more copper in its power cable to help protect the cable insulation. For example, the average 250 amperes water-cooled GTAW torch weighs approximately 85 grams and is about 165 mm long, while a 150-amp air-cooled GTAW torch weighs around 170 grams and is about 200 mm long.

However, water-cooled GTAW machines are heavier. The cooling system, extra hoses, water connection besides electrical connection and solid power source make them less portable than its brother the air-cooled GTAW machine. Air-cooled torches are more practical for outdoor work sites because they require fewer parts. This simplifies transport, setup procedures, and parts management. Water-cooled guns and torches generally are better suited for indoor use.

Water-cooled GTAW torches usually are rated between 200 and 500 amps. They are designed for use at higher welding currents on a continuous duty cycle than similar sizes of gas-cooled torches.

In general, technical features air-cooled GTAW, which are found in the industrial market, vary between 50 and 250 amp models. Mostly all manual air-cooled torches have a head angle (angle between the electrode and handle) between 60 and 90 degrees. The electrode diameter uses ranges from 0.5 to 4mm. Torches are also available with adjustable angle heads, 90º heads, or straight-line (pencil type) heads. Manual GTAW torches often have auxiliary switches and valves built into their handles for controlling current and gas flow.

It seems to be a general trend that the welding process is becoming more precise, applying the correct amount of heat in exactly the right place. In order to meet quality requirements and reduce costs, the welding industry has developed process control and automation. The article “Intelligent Robotic GTAW System for 3D Welding” [21] is a clear example how GTAW process is improving. This automation will reduce one of its main drawbacks of GTAW; its high labor cost.

Studies on control of the welding process that analysed the radiation from arc light in order to improve the control of GTAW have also been performed; “Analysis of an Arc Light Mechanism and its Application in Sensing of the GTAW Process” [20].

Welding industry is in a continuous movement toward the development of better technologies. Competing manufacturers of welding tools are in a battle to invent new systems and better products with substantial cost savings.

If air-cooled GTAW torch producers would want their product to remain a competitive product and increase its share of the market against water-cooled GTAW, they must find more efficient and better methods of production.

One way might be increasing cooling capacity of air-cooled torches without increasing torch size. Higher torch cooling capacity allows the use of higher arc current without overheating of components and power cables. About this subject, there isn’t so much literature. Normally, researches are made from effects view on workpiece, heat-affected zone and welding quality, therefore, there have not been many studies of this phenomenon.

However, this project was intended to study how heat transfer in a GTAW torch is influenced by the geometry, materials, air flow rated used and set some possible ideas for improving the air-cooled GTAW efficiency.

*Numbers in brackets indicate references at the bibliography.

CHAPTER 4

FUNDAMENTAL CONCEPTS AND DEFINITIONS

4 FUNDAMENTAL CONCEPTS AND DEFINITIONS

This chapter defines concepts and ideas that are necessary to obtain a general view of the case studies and the tools required to meet the aims what were mentioned in previous chapters. Firstly, a general description of the GTAW process is given. This will be followed by a short introduction to heat transfer. Finally, some concepts the finite element method used in this project will be introduced.

4.1 Gas Tungsten Arc Welding (GTAW)

4.1.1 Definition

Gas tungsten arc welding (GTAW) is an electric arc welding process that produces an arc between a nearly nonconsumable tungsten or tungsten-alloy electrode and the workpiece. Tungsten electrodes are nonconsumable if the process is properly used, because they do not melt or transfer to the weld.
The weld is shielded from the atmospheric by a shielding gas that forms an envelope around the weld area. This gas pushes the air away from the welding area and prevents oxidation of the electrode, weld puddle, and heat-affected zone.

This process has been called TIG (tungsten inert gas) welding and Heliarc®, named for the helium shielding gas originally used. However, the terminology for this process is, gas tungsten arc welding (GTAW), because shielding gas mixtures which are not inert can be used for certain applications. Although helium was originally used as the shielding gas, actually argon is the most common used shielding gas for GTAW welding [1].

Figure 4.1.1 shows the gas tungsten arc welding process and its correspondent nomenclature.

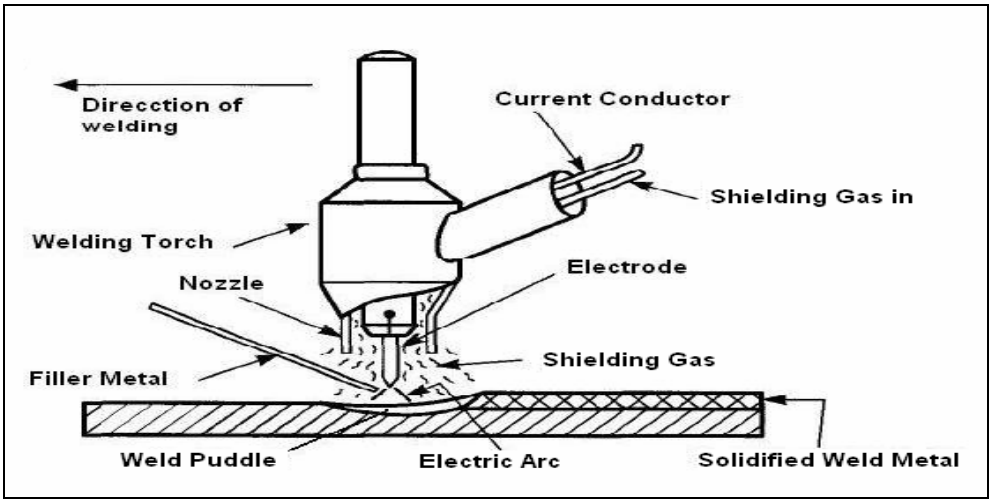

Figure 4.1.1 Schematic View of the Gas Tungsten Arc Welding Operation. [1]

4.1.2 GTAW Process Description

The typical equipment used for the gas tungsten arc welding process is illustrated in Figure 4.1.2. The process uses a nonconsumable tungsten (or tungsten alloy) electrode held in a torch. Shielding gas is fed through the torch to protect the electrode, molten weld pool, and solidifying weld metal from contamination by the atmosphere.

The electric arc is produced by the passage of current through the conductive, ionized shielding gas. The arc is established between the tip of the electrode and the workpiece. Heat generated by the arc melts the base metal. Once the arc and weld pool are established, the torch is moved along the joint and the arc progressively melts the surfaces. Filler wire, if used, is usually added to the leading edge of the weld pool to fill the joint.

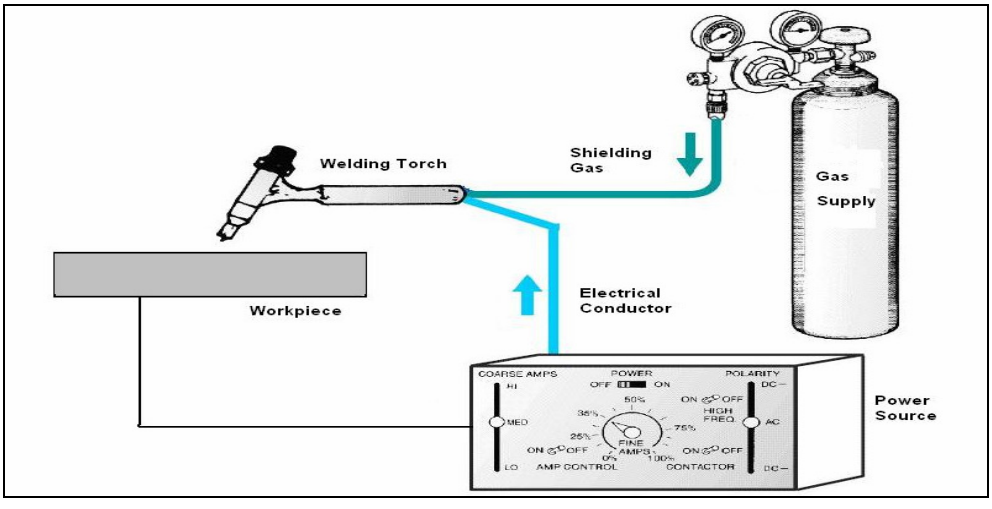

Figure 4.1.2 Typical Equipment Used for Gas Tungsten Arc Welding. [2]

4.1.3 Advantages and Disadvantages of GTAW process

Advantages

GTAW is versatile and can be used on ferrous and nonferrous metals and, depending on the base metal, in all welding positions. The process can be used to weld thin or thick materials with or without the addition of filler metal.

The following are some advantages of the Gas Tungsten Arc Welding:

a) It produces superior quality welds, generally free of defects.
b) It is free of the spatter which occurs with other arc welding processes.
c) It can be used with or without filler metal as required for the specific application.
d) It allows excellent control of root pass weld penetration.
e) It can produce inexpensive autogenous welds at high speeds.
f) It can use relatively inexpensive power supplies.
g) It allows precise control of the welding variables.
h) It can be used to weld almost all metals, including dissimilar metal joints, all with minimal distortion or corruption of the adjoining base metal.
i) It allows the heat source and filler metal additions to be controlled independently.
j) It is generated very little smoke, so welder has a good view of the process, allowing him to make very precise joints.

Disadvantages

The following are some limitations of the Gas Tungsten Arc process:

a) Deposition rates are lower than the rates possible with consumable electrode arc welding processes.
b) There is a need for slightly more dexterity and welder coordination than with gas metal arc welding or shielded metal arc welding for manual welding.
c) It is less economical than the consumable electrode arc welding processes for sections thicker than 10 mm.
d) There is difficulty in shielding the weld zone properly in drafty environments.
e) It is produces high heat input.

Potential problems with the process include:

a) Tungsten inclusions can occur if the electrode is allowed to contact the weld pool.
b) Contamination of the weld metal can occur if proper shielding of the filler metal by the gas stream is not maintained.
c) There is low tolerance for contaminants on filler or base metals.
d) Possible contamination or porosity can be caused by coolant leakage from water-cooled torches.
e) Arc blow or arc deflection, has similar problems that occur with other processes.

4.2 Heat Transfer in GTAW Process

This chapter gives an introductory description of the modes of transfer that exist. There are three types of energy transfer: conduction, convection, and radiation. All heat transfer processes involve one or more of these types.

All of these energy transfer modes are presented in air-cooled GTAW torch. The main heat-input is produced at the tip of the electrode (cathode). The workpiece works as anode. The function of electrode is to serve as one of the electrical terminals of the arc which supplies the heat required for welding. Approaching its high temperature, tungsten becomes thermionic; it is a ready source of electrons as shown in Figure 4.2.

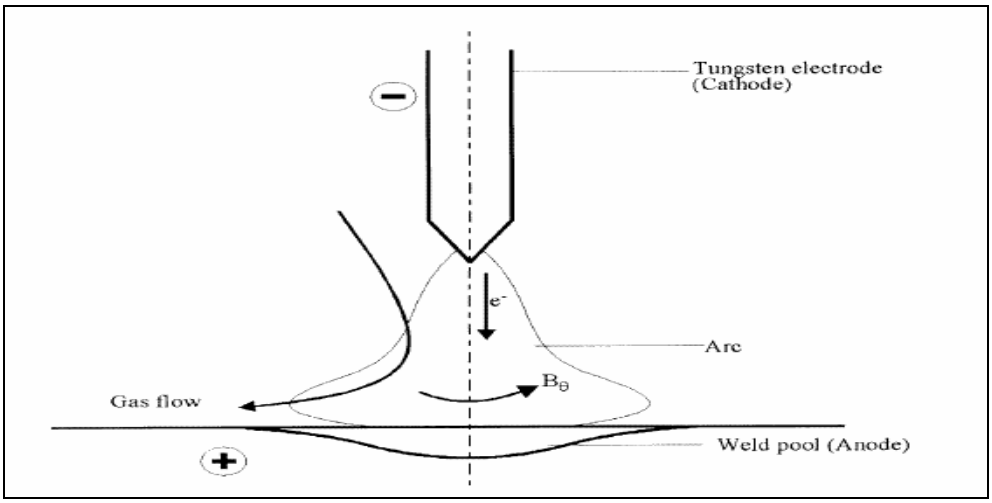

Figure 4.2 Schematic diagram of the welding arc (GTAW). [22]

Continuity of current can be written in terms of the electrical pontential as [22]:

$$\frac{\partial}{\partial z}\left(\sigma \cdot \frac{\partial \phi}{\partial z}\right)+\frac{1}{r}\cdot\frac{\partial}{\partial r}\left(\sigma \cdot r \cdot \frac{\partial \phi}{\partial r}\right)=0 \qquad (4\text{-}0)$$

where r is the radial coordinate, in m; z is the axial coordinate, in m; Φ is the electrical potential, in V; σ is the electrical conductivity, in $\Omega^{-1}\cdot m^{-1}$.

A rate of heat generated by the electric arc is transferred to the torch by conduction between components. The main radioactive heat is between the collet surface and collet body surface; there is also radiation between collet body and nozzle. The shielding gas produces cooling effect by convection with surface in touch besides its protector function.

4.2.1 Conduction

Conduction heat transfer is the energy exchange mechanism from one body to another body or from one part of this body to another. Conduction refers to that mode of heat transfer that occurs when exists a temperature gradient in a medium exists. Energy transfer is accomplished by two ways. The first mechanism is that of molecular interaction, molecules at a higher energy level impart energy to adjacent molecules at lower energy levels, in other words, energy is moved from regions of higher temperatures to regions of lower temperatures by the excitation of lower energy molecules. The second mechanism of conduction heat transfer is by free electrons.

The expression to describe basic conduction heat transfer was first stated by Fourier in the following equation:

$$q_x = -k \cdot A \cdot \frac{\partial T}{\partial x} \tag{4-1}$$

where q_x is the heat transfer rate in the x direction in Watts; A is the area normal to the direction of heat flow, in m^2; $\frac{\partial T}{\partial x}$ is the temperature gradient in the x direction, in K/m; and k is the thermal conductivity, in $W/m \cdot K$.

A more general equation for the heat flux is defined by Fourier's first law of heat conduction:

$$\vec{q} = -k \cdot A \cdot \nabla^2 T = -k \cdot A \cdot \left(\frac{\partial^2 T}{\partial x^2} + \frac{\partial^2 T}{\partial y^2} + \frac{\partial^2 T}{\partial z^2}\right) \tag{4-2}$$

This expresses the heat flux as proportional to the temperature gradient. The negative sign in equations indicates that heat flow is in the direction of a negative temperature gradient. The thermal conductivity, k, is a property of a conducting medium and is a function of temperature, varying significantly with pressure only in the case of gases subjected to high pressures.

Conduction heat at welding torch is a transient process, this means that the temperature at a given point varies with time. In general, the solution of an unsteady state (transient) conduction problem is more difficult than that for a steady-state problem because of the dependence of temperature on both time and position.

For the welding torch, it is also necessary to consider an internal energy source, that is, joule heating (also known as ohmic heating). The temperature in materials of welding increases as a result of resistance to electrical current running through them and an internal heat is generated.

As shown in Figure 4.2.1, consider the control volume in a solid having dimensions Δx, Δy and Δz the characteristic equation for conduction heat is obtained as:

$$\boxed{\rho \cdot c_p \cdot \frac{\partial T}{\partial t} = k \cdot \nabla^2 T + \dot{q}_v} \qquad (4\text{-}3)$$

where ρ is the density, in $^{kg}/_{m^3}$; c_p is specific heat, in $^{J}/_{kg \cdot K}$; $\frac{\partial T}{\partial t}$ is temperature variation with the time, in $^{K}/_{s}$; k is the thermal conductivity, in $^{W}/_{m \cdot K}$; $\dot{q}_v$ is volumetric rate of thermal energy generation, in $^{W}/_{m^3}$; and $\nabla^2 T$ is the Laplace equation: $\nabla^2 T = (\frac{\partial^2 T}{\partial x^2} + \frac{\partial^2 T}{\partial y^2} + \frac{\partial^2 T}{\partial z^2})$.

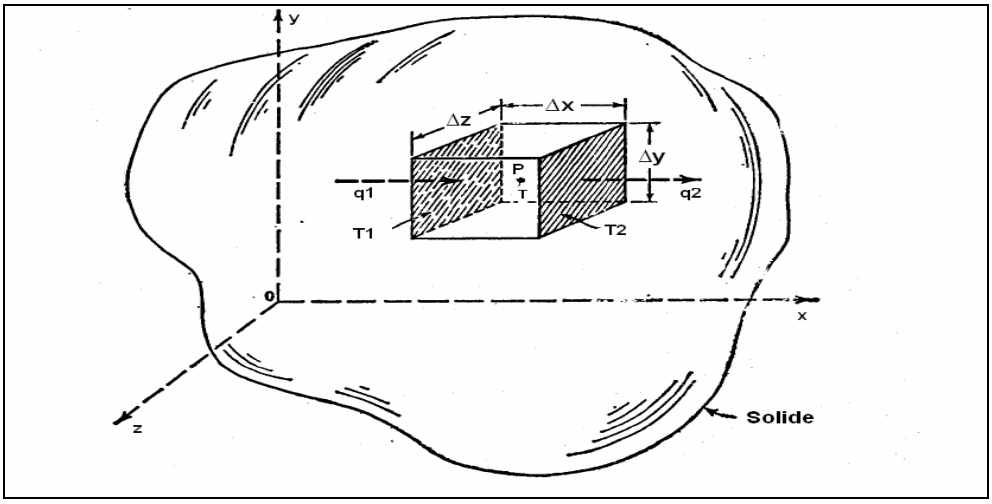

Figure 4.2.1 Diagram of energy balance for an element with dimensions Δx, Δy and Δz focused on point P of the solid. T is the temperature at the point P. [9]

For a system in which heat sources are present but there is no time variation, the equation is reduced to Poisson equation:

$$\nabla^2 T + \frac{\dot{q}_v}{k} = 0 \qquad (4\text{-}4)$$

4.2.2 Convection

Heat transfer due to convection involves the energy exchange between a surface and an adjacent fluid. There are two kind of convective heat transfer: (1) natural or free convection, type of process wherein fluid motion next to the solid boundary is the result from the heat transfer. (2) Force Convection when fluid circulation is produced by an external agent such as a fan or pump.

The equation for convective heat transfer is expressed by the following expression. This equation is known as Newton's Law of Cooling:

$$q = h \cdot A \cdot (T_S - T_f) \tag{4-5}$$

where q is convective heat, in W, h is convective coefficient, in $W/m^2 \cdot K$; A is the area normal to direction of heat flow, in m^2; T_s is the surface temperature, in K or ºC, and T_f is the temperature of the fluid in motion, in K or ºC.

There are four methods of evaluating convective coefficients; (a) dimensional analysis coupled with experimental results, (b) exact analysis of the boundary layer, (c) approximate integral analysis of the boundary layer, (d) analogy between energy and momentum transfer.

For obtaining the convective coefficients of our model, it was used method (a).

Calculating the different convective coefficients involved in the welding model is arduous and it will be need to make some approximations. The acquisition process of these coefficients is explained in Chapter 5 with the dimensionless numbers used are found in Section 5.3.5.

4.2.3 Radiation

Radiant heat transfer between surfaces differs from conduction and convection in that no medium is required for its propagation. In addition energy transfer by radiation is at a maximum when the two surfaces, which are exchanging energy, are separated by a perfect vacuum.

The amount of energy emitted by a surface is given by the equation Stefan-Boltzmann ´s Law of thermal radiation:

$$q = A \cdot \in \cdot \sigma \cdot T^4 \tag{4-6}$$

where q is the rate of radiant energy emission, in W; A is the area of the emitting surface, in m^2; ε is the emissivity of the surface $0 < \varepsilon < 1$, is dimensionless; T is the absolute temperature, in K, and σ is the Stefan-Boltzmann constant, which is equal to 5.676.10-8 $W/m^2 \cdot K^4$

Considering heat due to radiation makes the finite element models complex and extends running time. It is wanted to get a model simple of analyzing, so the radiation will not be considered in the models. Probably, it will be taken into account in future model improvements. Note that the radiation absence will involve some error in simulation results.

4.3 Finite Element Method (FEM) Introduction

The objective of this subsection is to give a short explanation of fundamental concepts behind finite element method.

In recent years, the use of finite element analysis as a design tool has grown rapidly. Numerical simulation plays an important role in production, manufacturing process. Virtual prototyping - based on the finite element modelling approach- has replaced the traditional build-and-break prototyping. One of the many reasons of importance of numerical simulation tools is the advantage to save time and money building the model and making the necessary experiments.

With numerical simulation software, the first step, building the design, requires some great money investment, but after this, it is really worth the effort. These simulation tools allow you change all conditions and get the results without any extra cost.

In general, engineering problems are mathematical models of physical situations. The mathematical models used are differential equations with a set of corresponding boundary and initial conditions. These mathematical models are differential equations that are derived by applying the fundamental laws and principles of nature to a system or a control volume. In heat transfer problems, these governing equations represent the balance of mass, momentum, and energy for a medium.

There are two common classes of numerical methods: (a) finite difference methods and (b) finite element methods. With finite difference methods, the differential equation is written for each node, and the derivatives are replaced by difference equations. This approach results in a set of simultaneous linear equations. Although finite difference methods are easy to understand and employ in simple problems: they become difficult to apply to problems with complex geometry or complex boundary conditions. This situation is also true for problems with no isotropic material properties.

In contrast, the finite element method uses integral formulations rather than difference equations to create a system of algebraic equations. Moreover, an approximate continuous function is assumed to represent the solution for each element. The complete solution is then generated by connecting or assembling the individual solutions, allowing for continuity at the interelemental boundaries.

The finite element method is a numerical procedure that can be applied to obtain solutions to a variety of problems in engineering. Steady, transient, linear, or nonlinear problems in stress analysis, heat transfer, fluid flow, and electromagnetism problems may be analyzed with finite element methods.

The origin of the modem finite element method may be traced back to the early 1900s, when some investigators approximated and modelled elastic continuo using discrete equivalent elastic bars.
However, Courant (1943) has been credited with being the first person to develop the finite element method. In a paper published in the early 1940s, Courant used piecewise polynomial interpolation over triangular subregions to investigate torsion problems.

The basic steps involved in any finite element analysis consist of the following:

1. Create and discretize the solution domain into finite elements; that is, subdivide the problem into nodes and elements.

2. Assume a shape function to represent the physical behaviour of an element; that is, an approximate continuous function is assumed to represent the solution of an element.

3. Develop equations for an element.

4. Assemble the elements to present the entire problem. Construct the global stiffness matrix.

5. Apply boundary conditions, initial conditions, and loading.

6. Solve a set of linear or nonlinear algebraic equations simultaneously to obtain nodal results. Such as temperature values at different nodes in a heat transfer problem.

However, we are not going to make any element finite formulation by hand. The numerical simulation software will do all steps described earlier in discretising the domain, we just need to create the model, mesh and resolve the algebraic equations.

Ansys Multiphysics is the finite element computer program chosen for reaching the project aims because of being a very powerful and impressive engineering tool that it is used to solve a large class of engineering problems.

The Next chapters are focused on designing the model; geometry, attributes, meshing and applying boundary conditions. That is, all what is necessary to build the welding model in Ansys. Later, that model will be verified through some experiments in welding lab.

Once, we know that it is possible to use the model; we are going to analyze the heat conducted by using the model in Ansys to modify some welding variables and then studying possible improvements for GTAW process.

CHAPTER 5

FINITE ELEMENT MODEL IN ANSYS MULTIPHYSICS

5 FINITE ELEMENT MODEL IN ANSYS MULTIPHYSICS

The main objective of this chapter is describing in detail the model building in Ansys; characteristics, components, materials, element type, meshing, boundary conditions, what were used for designing GTAW torch in Ansys Multiphysics.

5.1 Designing the Model

This section is important to give a general idea of geometry obtained. It is important that reader review again the information which will be explained here, for the analysis in the next chapters to obtain a better understanding.

5.1.1 Creating the Geometry

For studying influence of welding torch elements geometry in heat transfer, it was decided to apply four different models of GTAW torch. As illustrated in Figures 5.1.1 and 5.1.2 there are two main differences between them. First, if collet body and collet are long (l_{cb} = 50 mm and l_c = 55 mm respectively) or short (l_{cb} = 38 mm and l_c = 43 mm respectively). Second, if handle of the torch is hollow or solid.

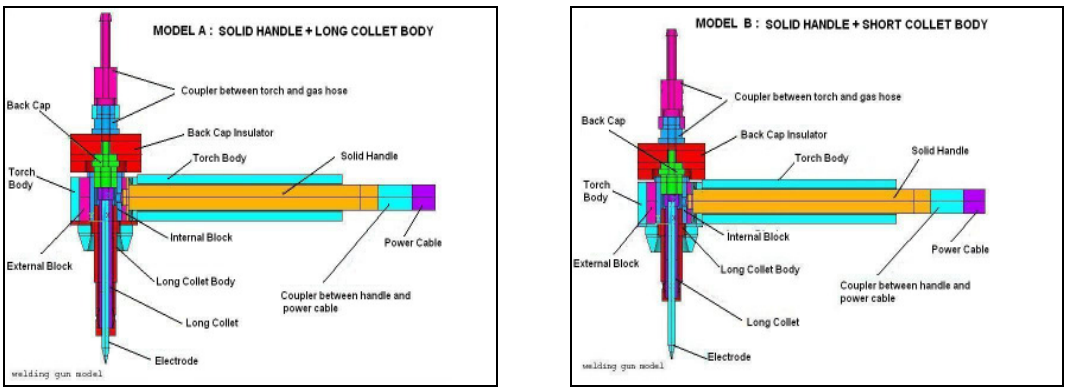

Figure 5.1.1 Cross-sectional view of welding torch model A and B.

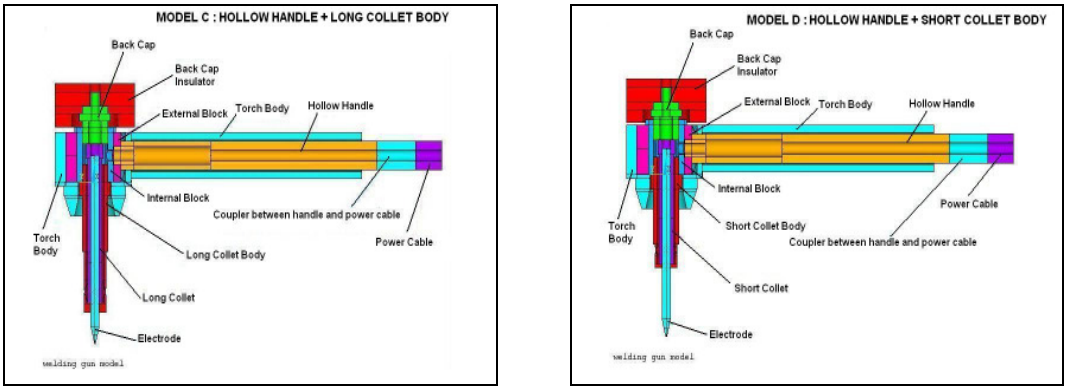

Figure 5.1.2 Cross-sectional view of welding torch model C and D.

In Appendix F; Section 1, you can see these pictures in more detail.

5.1.2 Defining materials and its properties

At the present GTAW torch are mostly constructed of copper due to its high electrical conductivity. It is used brass for the connections because of its hardness.

However, there are not studies about advantages or disadvantages of using different materials in the torch for making good use of the thermal resistance. Thus, in this section some materials properties are defined to study its influence on heat transfer in next chapters.

Between all materials that are available in industry for welding torch elements, the following five materials were chosen: aluminium, brass (70%Cu, 30%Zn), copper, stainless steel, Teflon and tungsten.

Tungsten electrodes are used in gas tungsten arc welding because of their satisfactory performance when operated with high-current arcs and because of its melting point, at 3410 ºC. It has the highest melting point and lowest vapour pressure of all metals.

To create the model, it is needed to determine those materials properties that are fundamental to define the model in the problem in Ansys. Material properties are required as an element input data.

In this case, it is essential to define the thermal conductivity, density, specific heat and electrical resistivity as each torch element has two degrees of freedom, temperature and voltage. Materials properties what were used in the Ansys model are specified in Appendix B.

The graphics above –Figures 5.1.1 and 5.1.2– show a cylindrical part that represents the power cable in welding torch. Its dimensions, diameter and length, were chosen arbitrarily, but it needs to obey some request:

a) It is assumed to be made from copper.

b) Its mass must be same as the cable:

$$m_k = m \quad \longrightarrow \quad \rho_K = \rho \cdot \left(\frac{d}{d_K}\right)^2 \cdot \left(\frac{L}{L_K}\right) \tag{5-1}$$

where m_k is the mass of the cylindrical piece that represents the cable while me is the cable mass, in kg; ρ is the cable density, in kg/m^3; ρ_K is the cylindrical piece density, in kg/m^3; d is the cable diameter, in m; d_K is the cylindrical piece diameter, in m; L is the length of the cable, in m; and L_K is the length of the cylindrical piece, in m.

c) Its specific heat is same as cable specific heat:

$$c_{pk} = c_p$$

where c_{pk} is the cylindrical piece specific heat and c_p is the cable specific heat, in $\frac{J}{kg \cdot K}$.

d) Its total thermal conductivity must be same as the cable:

$$K_K = K \cdot \left(\frac{L}{L_K}\right) \tag{5-2}$$

where K_k is the thermal conductivity of cylindrical piece and K is the thermal conductivity of cable, in $\frac{W}{m \cdot K}$.

e) Its electrical resistivity per length must be same as the cable:

$$\Re_K = \Re \cdot \left(\frac{L_K}{L}\right) \tag{5-3}$$

where $\Re_k$ is the electrical resistivity of cylindrical piece and $\Re$ is the electrical resistivity of cable, in $\Omega \cdot m$.

5.1.3 Defining Reference Points

Figure 5.1.3 shows the localization of thermoelectric thermometer in the welding torch during experimental test. These thermocouples measure the surface temperature of the torch on that position by means of thermoelectric current (this exploits the relationship between difference of temperature and potential difference in order to measure the temperature). A picture of the torch with the thermocouples positioned as shown in Appendix G, Picture G-1.

These points are also used as reference points in Ansys, to make the validation between the experimental results and simulation results by comparing the results at these points.

In Ansys, besides those points, sometimes three more points are used. These ones are; a) T5, is the point in collet surface in touch with collet body with maximum temperature, b) T6 is the point on the top of collet with maximum temperature, c) T7 is the point with maximum temperature localized on external surface of internal block at 5 mm from the symmetry axes of its hole.

Experimentally, two more parameters were used: z_{ne} is the distance between the bottom of the nozzle and the tip of the electrode and z_{ew} is the distance between the workpiece and the tip of the electrode. Both of them were fixed during the experiments, that means that all experiments were made with the same value for each parameter, z_{ne} = 5 mm and z_{ew} = 5 mm. For the simulation in Ansys, just z_{ne} were taken into account and it was used the same value of 5 mm for all simulations.

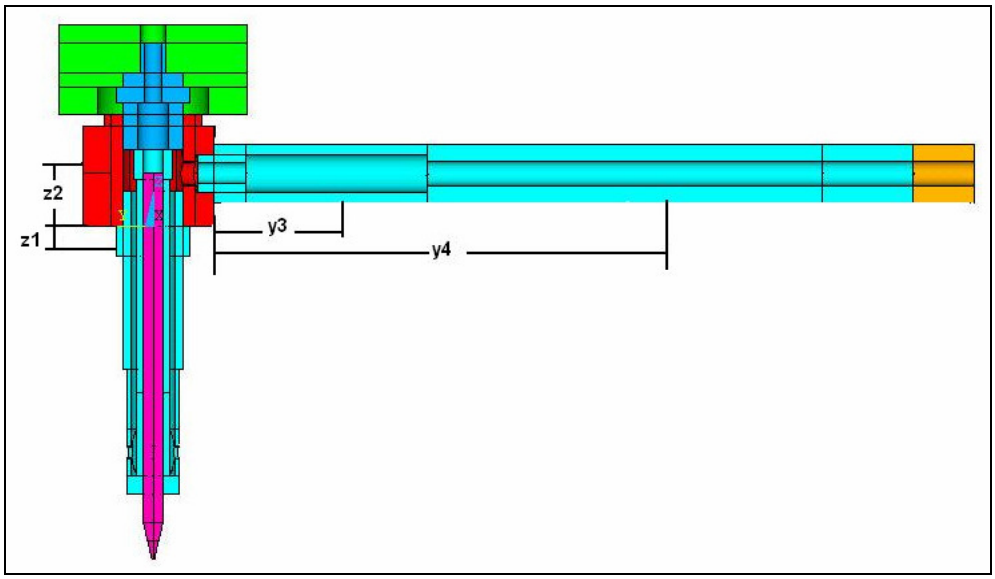

Figure 5.1.3 Reference points used for Ansys and for experimental tests: (a) T1 situated at collet body surface at z1 = 1.5 mm; (b) T2 situated at external block surface at z2 = 11 mm; (c) T3 situated at handle surface at y3 = 18 mm; (d) T4 situated at handle surface at y4 = 70 mm.

5.2 Meshing the Model

After defining the materials properties and reference points, the following step to build the model is generating the finite elements (nodes and elements) that correctly describe each of geometries that are analyzed in design process. Meshing the model is a very important part of any finite element analysis. Inappropriate element shape and size will affect the accuracy of the results.

The process for generating the mesh of nodes and elements of the models consisted of two steps: (1) set the element attributes, (2) generating the finite element models.

5.2.1 Set the Element Attributes

The element attributes include element type, real constants, and material properties.

In the previous chapter, a small explanation of the materials and their properties to be used was given, these material properties are also summarized in Appendix B.

Realize that the materials are one of the study variables, through simulations in Ansys it is wanted to know the influence of materials on temperature. In this section, the material for each piece is defined. However, later on in Chapter 7, Section 7.2, different combinations of materials are examined and their influence on heat transfer will be studied.

For the following simulations, except for the simulations for the study of the material influence in Section 7.2, a basic combination of materials will be employed, known as combination 0. Table 5.2.1 illustrates materials used for this combination.

Table 5.2.1 The basic material combination used in Ansys simulations, combination 0.

Piece	Material
Back Cap	Steel
Back Cap Insulator	Teflon
Collet	Copper
Collet Body	Copper
Coupler torch/gas pipe	Brass
Coupler handle/cable	Copper
Electrode	Tungsten
External Block	Copper
Handle	Copper
Internal Block	Copper
Power Cable	Copper
Torch Body	Teflon

After defining materials properties, the next step for meshing the models is determining the right element type to be used for the geometries.

The first questions to be asked in order to decide the type of elements used from a selection of 150 types available in the Ansys finite element libraries are: is it in 2 or 3 dimensions? how many degrees of freedom are there?

The choice of element type is significant for any Ansys analysis because the accuracy of the results is strongly dependent on the elements used. Each element type has a set degree of freedom, which establishes the primary nodal unknowns to be calculated. The degrees of freedom may be based on rotations, temperatures, pressures, voltages, etc. Derived results, such as stresses, heat flows, etc., are resolved from the degree of freedoms.

The element type chosen should be such that the degrees of freedom are enough to characterize the model's response. Including unnecessary degrees of freedom increases the solution memory requirements and running time. Similarly, selecting element types with unnecessary features, also unnecessarily increases the analysis run time.

In each case studied it was necessary to define a volume element, that has a tetrahedral or hexahedral shape, because it will be worked in 3D space. Two degrees of freedom were defined, these were: temperature and voltage. Now, with the answers to these questions it is possible go to Ansys help [7] in chapter “Element reference: 3.1 element classifications” and choose the element type.

According to the degrees of freedom, voltage and temperature, the field of study is Thermal-Electric, with four choices; PLANE67, LINK68, SOLID69, SHELL157.

Between them, SOLID69 is the best element type to create the finite element models. Figure 5.2.1, in next page, shows the geometry of Solid69 used for the simulations in Ansys.

SOLID69 has a 3-D thermal and electrical conduction capability. Joule heating generated by the current flow is also included in the heat balance. The element has eight nodes with two degrees of freedom, temperature and voltage, at each node. The thermal-electric solid element is applicable to a 3-D, steady state or transient thermal analysis, although no transient electrical capacitance or inductance effects are included in the element. Elements are connected to the nodes in the sequence and orientation shown on the following figure.

Note that using more nodes gives an improved accuracy, but this also increases the run time.
When using Solid 69 with 8 nodes, a good balance between getting accurate results and the computational costs can be applied.

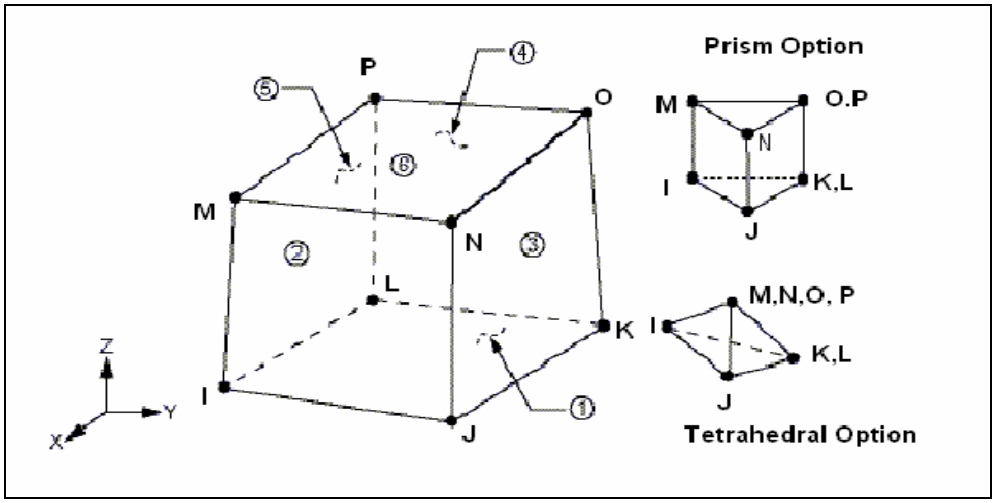

Figure 5.2.1 Solid69 geometry. [7]

5.2.2 Generating the Finite Element Model

Firstly, it is important to think about whether a free mesh or a mapped mesh is appropriate for the analysis. A mapped mesh is restricted in terms of the element shape it contains and the pattern of the mesh. A mapped area mesh contains either only quadrilateral or only triangular elements, while a mapped volume mesh contains only hexahedral elements. In addition, a mapped mesh typically has a regular pattern, with obvious rows of elements.
To get this mapped mesh, models geometry were built as a series of fairly regular volumes that could accept a mapped mesh, sometimes it was necessary divided the torch pieces into smaller volumes. In Figure 5.2.2, some examples of these divisions can be seen.

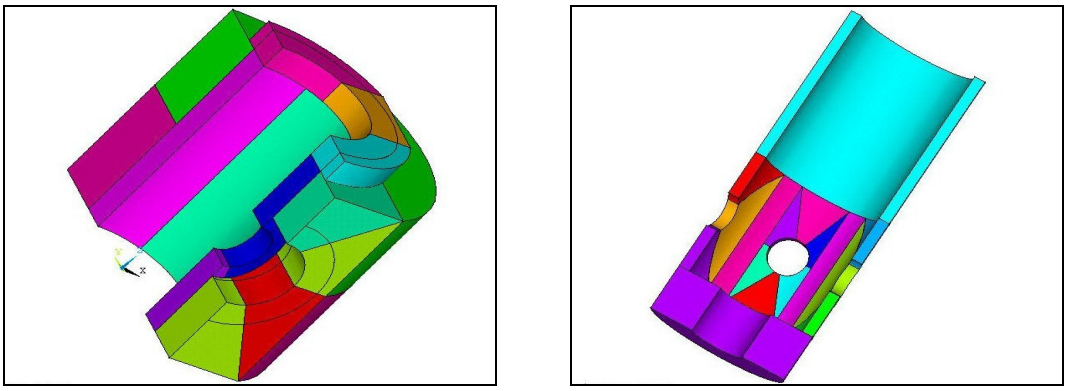

(a) (b)

Figure 5.2.2 Division of welding model in small volumes: (a) Detail of internal block and external block; (b) Detail of collet body.

After dividing the volumes and choosing the elements' attributes, the geometries can be meshed. At this point is especially important to specify the element size. The element size controls the resolution of the mesh; the smaller the element size, the finer the mesh is. Before meshing, it has to be carefully decided which parts of the welding torch, it is necessary to have a small size and the parts in where it is not important. Not all parts play same role in the model, some volumes will need tiny elements, because these volumes influence on the solution is large. That is, the bigger an element is, less accurate it is. Therefore, element size in electrode, in collet and collet body will be much smaller than element size in the rest of torch parts, to better account for the heat fluxes in these regions. Appendix F; Section 2 shows the meshing of some parts of the torch.

To avoid wasting simulation time and money, an element size optimization was performed. What is an element size optimisation? Is there any change if element number is modified? How small do I need to make the elements before I can trust the solution?
Element size is important for convergence time, if the size is too small, more than necessary to get enough accuracy, then running time will be longer. The main aim is to save simulation time. This is achieved by decreasing the number of elements.

In general, it is necessary to make convergence tests on the finite element model to confirm that a fine enough element discretization has been used. In a solid mechanics problem, this would be done by creating several models with different mesh sizes and comparing the results. Hexahedral elements were chosen to make the next simulations.

This consists of simulating with a number of elements. For next simulation this number is increased and the solution is compared with the previous one. If they are not similar, the number is raised again and the following simulation is compared. This process is done until difference between results of simulation i and simulation i+1 will be quite small.

This process of element number optimization was started by simulating with Ne = 24367 elements (Ne is the elements number), getting the results as shown in table 5.2.2. For next simulation, Ne is increased to 50013 and it was found that difference between both simulation solutions was big. Then the simulation was performed with Ne = 74389 and it was observed that the difference with previous simulation where Ne was 50013 was insignificant. As economizing is a goal in industry, it is better use Ne = 50013 instead Ne = 74389 because the solution is nearly the same. However, convergence time for Ne = 50013 is smaller than for Ne = 74389. Note that less convergence time means less calculating time and less memory required. In conclusion, the model with mesh size Ne = 50013 will be used for simulations made in next chapters.

The following table summarizes the process done to get the optimal elements number and Table 5.2.3 shows the convergence time for elements number used.

Table 5.2.2 Temperature in ºC at reference points for different elements number. *

	Elements Number		
Reference Points	Ne = 24367	Ne = 50013	Ne = 74389
T1	105.21	189.67	191.34
T2	94.87	182.38	185.83
T3	51.65	115.75	116.52
T4	44.23	74.76	78.13

*Data from simulation with model C, 300 amperes, “becoming element of turbulence” element with turbulent regime, uniform temperature 298 K, electrode diameter equal 3.2 mm and simulation time 3.5 min.

Table 5.2.3 Convergence time against elements number for Ansys simulations.*

Elements Number	Convergence Time
Ne = 74389	12 hours
Ne = 50013	3.5 hours
Ne = 24367	2 hours

*Data from simulation with model C, 300 amperes, “becoming element of turbulence” element with turbulent regime, uniform temperature 298 K, electrode diameter equal 3.2 mm and simulation time 3.5 min.

5.3 Boundary Conditions and Loads

This step is usually the most difficult aspect of modelling. It involves taking an actual problem and estimating the loading and the appropriate boundary conditions for a finite element model.

Now starts the purely physics part, it is essential that physical behaviour of the model must be similar to real model behaviour. In general, engineering problems are mathematical models of physical situations. Mathematical models are usually defined as differential equations with a set of corresponding boundary and initial conditions. The differential equations are derived by applying the fundamental laws and principles of nature.

It what follows, it will be explained systematically how the boundary conditions and loading have been applied to the models to get the analogy with real construction.

Two approaches were used to apply the loads: applying the loads on the solid model (at keypoints, lines and areas) or applying loads on the finite element model (at the nodes and elements).

Advantages of solid model loads are that they are independent of the finite element mesh. That is, you can change the element mesh without affecting the applied loads. This allows make mesh modifications and conduct mesh sensitivity studies without having to reapply loads each time.

Advantages of finite element loads are that reduced analyses present no problems, because you can apply loads directly at master nodes. The disadvantage is any modification of the finite element mesh invalidates the loads, requiring deleting the previous loads and re-applying them on the new mesh.

The following boundary conditions were applied: temperature and voltage at tip of electrode, current excitation at cable area, surface load on those surfaces there were convection with air or Argon on.
In a later chapter, the influence of some variables will be studied for example, current flow, or atmospheric temperature. So, all of these parameters were programmed into the Ansys model for an easy and fast modification.

5.3.1 Surface Temperature at the Tip of the Electrode

The models will be unsuccessful, if it does not included the effect of the electric arc. Key question: how can we configure the models for adapting that effect? The answer for this question is by applying a temperature of around 3000 K at the tip of the electrode. This action is based on the results obtained from earlier studies on the measurements of the surface temperature for tungsten-based cathodes [19]. This article showed that cathode surface temperature affects the distribution of the current density over the cathode surface and as a result has an important role in determining the arc mode of operation.

Figure 5.3.1 on next page, obtained from [19], represents the surface temperature profiles against distance from the tip of the electrode, in mm, for different current densities. It was observed that there was a decreased tendency with the distance. However, the average temperature at conical surface of tip of electrode along 3 mm was around 3000 K. Thus, this approximation of 3000 K was applied as a temperature boundary condition to the nodes of the model at surface of the tip of the electrode along 3 mm; as shown in Figure 5.3.2.

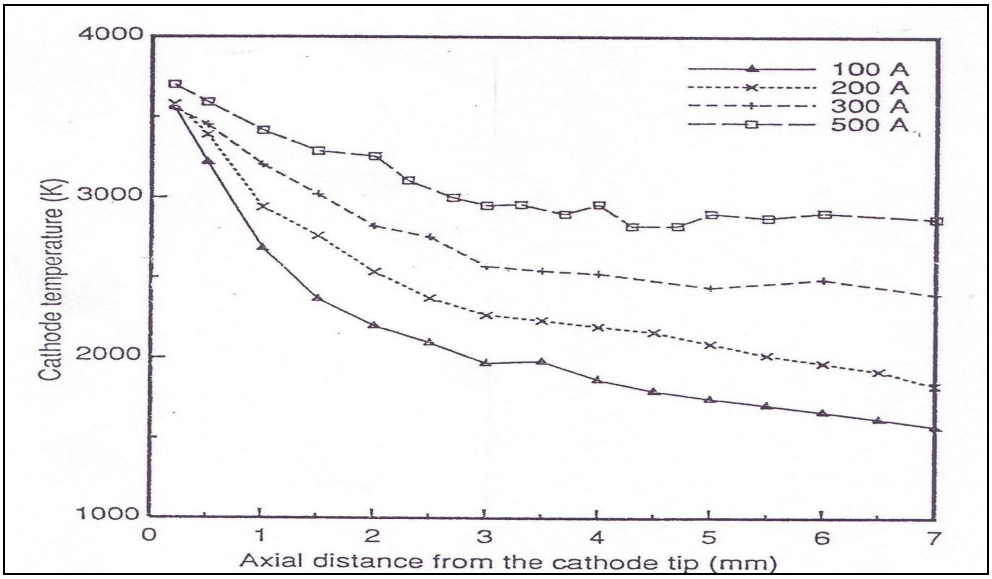

Figure 5.3.1 Temperature against axial distance from the tip of the electrode [19].

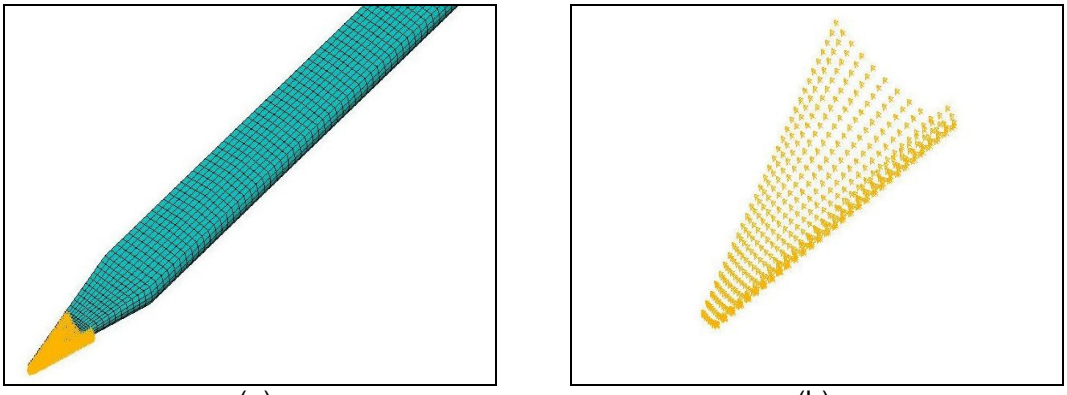

(a) (b)

Figure 5.3.2 (a) Temperature boundary condition on nodes at surface of the tip of electrode along 3 mm. (b) Detail of temperature boundary on nodes.

5.3.2 Excitation Current

The current flow through the welding torch generates heating increasing temperature values in the torch. An interesting study might be eliminate temperature boundary condition at tip of the electrode and simulate just with current flow. Then, estimates of the heat caused by application of the current can contribute to total heat transferred in the model.
Ansys allows apply an excitation current, so modifying current flow is possible as is modifying arc current and therefore it would be possible study has the greatest influence on temperatures observed. To create the same effect, a current excitation was applied at the area cable. For further details see Figure F-3.2 in Appendix F, Section 3.

5.3.3 Zero Voltage

After defining the excitation current value, next step is setting the zero voltage. Without the condition of zero voltage on the tip of electrode (detailed in Figure F-3.3 Appendix F), there will not be current density through the designed model.
The tungsten electrode becomes source electrons because of its high melting. The function of a tungsten electrode is to serve as cathode of the electrical arc produced between the workpiece and the tip of the electrode. Tungsten electrode becomes thermionic; thus, it is a ready source of electrons.

5.3.4 Uniform Temperature

Temperatures vary as the simulation is progressed through time. Therefore, the thermal analysis is transient. Thus, an initial uniform temperature must be set.
In transient thermal analysis, the uniform temperature is used during the first iteration of a solution: as the starting nodal temperature (except where temperatures are explicitly specified) and to evaluate temperature dependent on material properties.

Atmospheric temperature was used as uniform temperature and its value used for simulation conditions is 298 K (25 ºC) except for the section where the influence of atmospheric temperature will be studied. In that section, it is utilized two more temperatures besides the atmospheric condition (298 K) and compared their simulation results.

5.3.5 Convective Heat

Convective heat transfer occurs when a fluid in motion meets a surface whose temperature differs from the moving fluid. The value of the heat transfer coefficient for a particular situation is determined from experimental correlations.

Convective surface loads are applied to the surfaces of the Ansys models to take account of heat transferred to argon gas used to cool the welding torch.

The determination of convective coefficient is not a simple task, because it is related to the mechanism of fluid flow, the properties of the fluid, and the geometry of the specific system of interest.

The Grashof, Prandtl and Reynolds numbers are needed to evaluate convective coefficients. The Prandtl number is dependent on the properties of the fluid and therefore on the temperature. In Appendix C, the temperatures over working range of the welding are tabulated.

Before starting the calculations, it must be clear that free convection is different to forced convection*. Therefore, the equations for free convection are guide different from those for forced convection and there are many experimental correlations to use for many cases. In this section, it is explained which correlations have been chosen and how they were applied.

As said earlier in Section 4.2.2, it will be used dimensional analyses method to obtain the convective coefficients. From the consideration of the dimensional analyses, the following functions for correlating convection data:

Forced convection: $Nu = f_1 (Re, Pr)$
Free convection: $Nu = f_2 (Gr, Pr)$

In Table 5.3.1 it can be seen certain dimensionless parameters are useful for the correlations of convective coefficient:

Table 5.3.1 Dimensionless parameters used to calculate convective coefficient.

Dimensionless Parameters	Symbol	Equation
Euler Number	Eu	$\frac{P}{\rho \cdot \mathrm{v}^2}$
Grashof Number	Gr	$\frac{\beta \cdot g \cdot \rho^2 \cdot L^3 \cdot \Delta T}{\mu^2}$
Nusselt Number	Nu	$\frac{h \cdot L}{k}$
Prandtl Number	Pr	$\frac{\nu}{\alpha} = \frac{\mu \cdot c_P}{k}$
Peclet Number	Pe	$\mathrm{Re} \cdot \mathrm{Pr}$
Rayleigh Number	Ra	$Gr \cdot \mathrm{Pr}$
Reynolds Number	Re	$\frac{\rho \cdot \mathrm{v} \cdot \mathrm{L}}{\mu}$
Stanton Number	St	$\frac{h}{\rho \cdot \mathrm{v} \cdot \mathrm{c_P}}$

*Free and forced convection were defining in earlier sections, if the reader wants review his/her knowledge, please check Chapter 4, Section 4.2.2.

In the following section, a description of the equations used for the estimation of convective coefficients with forced convection and free convection are presented.

Forced convection

In the welding torch, there is forced convection in all channels, through which shielding gas circulates through, see Figure 5.3.3 in page 35.

There are two class of flow; laminar and turbulent. Until now, welding torches use a flow with laminar regimen because the turbulence causes oxygen to enter the envelope around the weld area that is protected by shielding gas. Thus, oxidation of the electrode and increased temperatures occur, furthermore the possible apparition of oxide film on the workpiece.

Therefore, which regime of flow is better, turbulent or laminar flow?
The type of flow is one of many variables that were defined to study its influence on welding temperature. However, we are not searching to know if turbulent regime is better than laminar. What we are interested in is how turbulence influences in temperature profiles and finding out if turbulent flow produces lower temperature profiles than for laminar flow. For the hypothetical case that improvements in the heat transferred is observed, it would provide route for future studies to try to improve the design of existing welding torches that are available in market by taking advantage of the cooling capacity of turbulent flow.

The result of a dimensional analysis of forced convection in tubes indicates that a possible relation is of the form: $Nu = f_1 (Re,Pr)$. The experimental work consists of calculating function f_1 for each particular case; geometry of the solid surface, velocity, type of fluid, etc…

Energy transfer associated with forced convection inside closed conduits will be considered separately for laminar and turbulent regime:

- **laminar flow Re < 2300**

Sieder and Tate correlated, equation (5-4), experimental data for heat transfer in pipes under laminar flow conditions [14]:

$$Nu = 1.86\left[\frac{D}{L}\cdot \mathrm{Re}\cdot \mathrm{Pr}\right]^{1/3}\cdot\left(\frac{\mu}{\mu_S}\right)^{0.14} \qquad (5\text{-}4)$$

where D is tube diameter, in m; L is tube length, in m; μ is the fluid viscosity at the bulk fluid temperature, in $\frac{kg}{m\cdot s}$; and μ_S is the fluid viscosity at the interior surface temperature of the tube, in $\frac{kg}{m\cdot s}$.

For equation (5-4), the fluid must be in the range: 0.48 < Pr < 16700 and $\left(\frac{D}{L}\right)\cdot \mathrm{Re}\cdot \mathrm{Pr} > 10$.

The fluid temperature varies accordingly as the fluid circulates through inside pipe and exchanges heat energy from the fluid to the pipe wall. Due to the loss of heat in the pipe, the arithmetic mean fluid temperature (bulk fluid temperature) should be chosen as the reference temperature. This temperature is defined by the following equation:

$$T_{bf} = \frac{(T_{f1} + T_{f2})}{2} \tag{5-5}$$

where T_{f1} is the temperature at entrance of the pipe, in K and T_{f2} is the temperature at the outlet of the pipe, in K.

All properties are evaluated at the bulb fluid temperature except μ_S that is evaluated at surface temperature.

The expression $\left(\frac{\mu}{\mu_S}\right)^{0.14}$ does not have a strong influence; it is just corrective expression to take into account the variation of fluid viscosity with temperature.

- **turbulent regime Re > 2300**

When considering the energy exchanged between a conduit surface and a fluid experiencing a turbulent flow, it must be resorted to correlations of experimental data as suggested by dimensional analysis.

An empirical isothermal-wall correlation was developed by Dittus and Boelter for turbulent regime in pipes [15]:

$$Nu = 0.023 \cdot \mathrm{Re}^{0.8} \cdot \mathrm{Pr}^{n} \tag{5-6}$$

where n = 0.4 because the fluid in the welding torch is heated (n = 0.3 for the reversed case when the fluid is cooled).

Using this equation, all fluid properties were evaluated at bulk temperature as defined earlier.

In the region at the collet in the welding torch, the shielding gas must circulate between the external surface of the collet and internal surface of the collet body. This geometry is not exactly cylindrical as equations, (5-4) and (5-6) were defined for the application to cylindrical geometries.

Therefore, to be able to use equations (5-4) and (5-6) will be able to use, the tube diameter (D) in the equations must be substituted for the "equivalent diameter" concept (D_{eq}), as calculated according to the following expression:

$$D_{eq} = 4 \cdot r_h \tag{5-7}$$

where r_h (hydraulic radius) is the ratio of the cross-sectional area of flow to the wetted perimeter. Note that both equations, (5-4) and (5-6), are an empirical isothermal-wall correlation.

To increase the effect of turbulence, i.e. to increase the cooling capacity of the torch, a "becoming element of turbulence"* was designed, built and used for the experiments. A "becoming element of turbulence" was put inside the hollow handles (model C and D). This element wasn't modelled in Ansys because it would cause a complicate model with long running time. It was decided to follow another method. This method took into account the effect of this element on heat transfer by the use of appropriate convection equations.

The next equation allows us to calculate the convective coefficient for a cylinder with "becoming element of turbulence" [11]:

$$h_C = \left(1 + 3.54 \cdot \frac{D_S}{D}\right) \cdot h \tag{5-8}$$

where D_S is the "becoming element of turbulence" diameter, in m; D is the cylinder diameter without this "becoming element of turbulence", in m; h is the convective coefficient, in $\frac{W}{m^2 \cdot K}$, that is obtained by firstly estimating the Nusselt number from equations (5-4) and (5-6) and then solving according to the Nusselt number definition in Table 5.3.1.

Free convection

There is free convection between the external surface of collet body (vertical cylinder surface) and shielding gas, see Figure 5.3.4 in page 35. It is considered the method of heat convection for the parts of electrode that are in touch with shielding gas. However, the convection with air is despised since it hasn't so much influence in the results during welding torch is working. Note that air has a greater importance when the torch is cooling down, in that case there will be free convection with air where before there was convection with the shielding gas.

---

* Due to patent processing, it isn't detailed the nature of this component called "becoming element of turbulence" (BET).

The mechanism of energy transfer by natural convection involves the motion of a fluid, which is the result of the density differences resulting from the energy exchange. Therefore, the convective coefficients and the equations to estimate the coefficients will vary with the geometry of the model.

The correlations of convection data for free convection are used to express dimensionless numbers, like the function before: Nu = f_2 (Gr, Pr). These correlations are obtained experimentally and it already exists many literature what summarize all of these.

The process to get the convective coefficients requires choosing the correlating convection data that has been obtained empirically and is appropriate for the model and its geometry. Then, we evaluate the physical properties at the film temperature and calculate the dimensionless parameters at this temperature. Once, the Nusselt number is obtained through its definition (Table 5.3.1), the convective coefficient can be determined.

Equations (5-4) and (5-6) were used for forced convection. However, these equations are not valid for free convection; therefore, it is needed a particular equation for free convection shielding gas at the external surface of the collet body and for some part of electrode. These correlations of experimental data are available for the most common geometries and flow conditions in many convection bibliographies.

An empirical isothermal-wall correlation that reports the wall-averaged Nusselt number for the entire Rayleigh number range –laminar, transition, turbulent- was constructed by Churchill and Chu [13]:

$$Nu = \left\{ 0.825 + \frac{0.387 Ra^{1/6}}{\left[1 + \left(\frac{0.492}{\mathrm{Pr}} \right)^{9/16} \right]^{8/27}} \right\}^2 \qquad (5\text{-}9)$$

where $Ra = Gr \cdot \mathrm{Pr}$.

Note that the significant length for equation (5-9) is the height of the cylinder. This correlation is applicable over the range $10^{-1} \leq Ra \leq 10^{12}$ and for all Prandtl numbers.

In the same way as for forced convection the Reynolds number marks the transition from laminar to turbulent flow (~ 2300 for conduit flow), in free convection the transition between the flow regimes is showed by Grashof number in all fluids. This transition occurs when Gr ~ 10^9 (for fluids in the range $10^{-3} \leq Pr \leq 10^3$).

Equation (5-9) can be applied for vertical plates and cylinder. Specifically, the surface with free convection is a vertical cylinder, so, equation (5-9) can be used for calculating Nusselt number when:

$$\frac{D}{L} \geq \frac{35}{Gr^{1/4}} \tag{5-10}$$

The physical properties used in the definition of the dimensionless numbers, Nu, Gr and Pr, are evaluated at the film temperature (T_{mf}):

$$T_{mf} = \frac{(T_S + T_f)}{2} \tag{5-11}$$

where T_s is the surface temperature, in K; T_f is the temperature of the fluid in motion, in K.

The three equations, (5-4), (5-6) and (5-9), are for isothermal-walls, which is obviously not the case for the torch as there is local variation of forced or free convection. This is due to a temperature distribution along the welding torch, and in addition, the temperature changes with the time. To simplify the model and decreasing running time, it was built without considering fluids existence.

For both conditions of free and forced convection, the physical properties are calculated at the film temperature. Therefore, it is necessary to know surface temperature (T_s) and fluid temperature (T_f) or bulk fluid temperature (T_{bf}). This involves a problem as T_S is an unknown variable that must be estimated through by simulation. Similar problems are also found for T_f and T_{bf}.

How were the temperatures resolved? By making an iterative approximation and checking the behaviour of the model. It is supposed that an average temperature for Ts and that the fluid would increase its temperature by about 30 ºC. For the Ansys model, the earlier equations and this supposition will be used, but it must be aware of error that this introduces.

According to which model is studied, the torch presents regions with unequal convective coefficients due to their different geometry. Therefore, it is required to apply the appropriate equations, as described before, to each region. A summary of all coefficients calculated for each model, region, uniform temperature and flow is tabulated in Appendix D.

The next figures show the different convective coefficients for each region and the convection mode; free or forced. Note that h_4 is not included. This coefficient would be used in case of that collet didn't have "becoming element of turbulence". In that instance, the region with h_5 and h_6 is replaced by h_4.

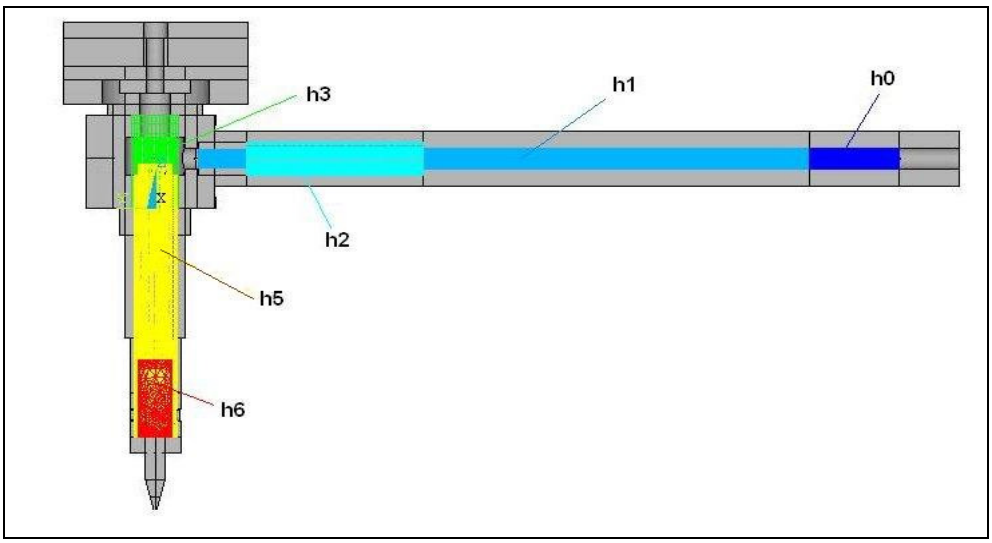

Figure 5.3.3 Convective coefficients for different regions in welding torch due to forced convection. Geometry: model C.

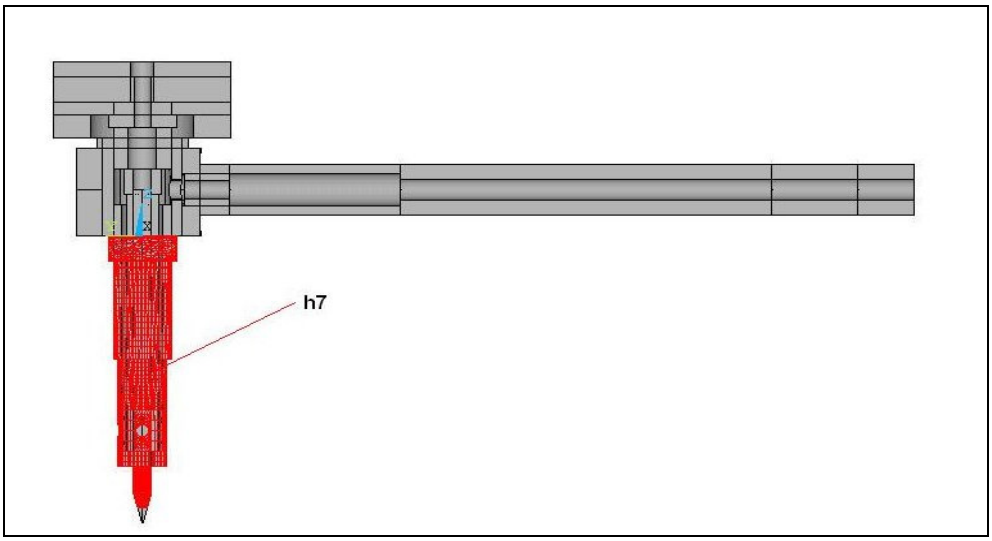

Figure 5.3.4 Convective coefficient (h_7) in welding torch due to free convection between the nozzle and the external surface of collet body and the electrode. Geometry: model C.

In Appendix F, Figure F-3.6 and Figure F-3.7, is shown another clarifier example of the applied convective loads.

CHAPTER 6

VALIDATION OF ANSYS MODEL

6 VALIDATION OF ANSYS MODEL

After designing the geometry, meshing and applying the appropriate boundary conditions and loads in Chapter 5, the Ansys models must be validated to whether verify that the simulated model has a behaviour that is similar to the real construction. Therefore, you must always find ways to validate your results. This was achieved by performing experiments in the welding workshop and comparing the results with the solutions resolved by Ansys.

In these sections, the steps for checking results, as well as the experimental process in the lab, will be shown.

6.1 Method of Operation

Working in a lab requires knowing all the details and proper experimental design to be made before starting making experiments in order to avoid possible surprises that consume time and money.

In this subsection, it an explanation will be given on the materials, machines, gas, type of electrode, modus operandi and everything pertinent to GTAW process that were studied in the workshop.

For making the experiments, it was used a GTAW power supply that had the following features:

- features: input power voltage; AC 400 (3 phases) -25% +20%
- frequency; 50/60 Hz
- output current range; 5-500 A
- arc starting with high frequency.

Argon was utilized as shielding gas. The characteristics of the electrode what was employed are the following ones: tungsten electrode with 1% LaO_2, 30º cone angle and diameter 2.4, 3.2 and 4 according to experiment realized.

The materials available for the experiments are shown in Table 6.1.1. The properties of these materials are summarized in Appendix B.

Table 6.1.1 Available material for each GTAW torch elements.

	Aluminium	Brass	Copper	Steel	Teflon	Tungsten
Back Cap		X		X		
Back Cap Insulator					X	
Collet			X			
Collet Body	X	X	X	X		
Coupler handle/cable			X			
Coupler torch/gas pipe		X				
Electrode						X
External Block	X	X	X	X		
Handle	X		X			
Internal Block	X	X	X	X		
Power Cable			X			
Torch Body					X	

A set distance (z_{ew}) between the tip of the electrode and the workpiece of 5 mm was specified. The separation (z_{ne}) between the bottom of the nozzle and the tip of the electrode was 5 mm.

Four main reference points (T1, T2, T3 and T4) to measure the temperature were chosen. Four thermocouples, type K (Cr-Ni-Cr), were positioned at these points. Figure 5.1.3 in Chapter 5 showed a schematic diagram with these parameters.

In the welding lab, the experiments were made with either laminar or turbulent flow. The flow rate required to obtain a turbulent regimen was calculated from the Reynolds number. In other words, the velocity was obtained by ensuring that the flow gave a Reynolds number above the limit of the critical Reynolds number for conduit flow. The critical Reynolds number is approximately 2300.

Using the critical Reynolds number, it was found that the flow is turbulent when the volumetric flow rate is greater than 13 l/min. Therefore, 10 l/min gave a laminar flow and 15 l/min gave a turbulent flow.

The modus operandi of the experiments involves: (1) preparing the electrode; getting the tip, taking pictures with microscope before experiments, (2) assembling the elements, (3) verifying that the flow is right, (4) checking z_{ew} and z_{ne}, (5) putting the thermocouples at the main reference points, (6) welding and (7) cooling the torch until the temperature is below 35 ºC.

Three measurements are made for each experiment, except when the electrode is so damaged after welding that further welding is impossible as is shown in Picture 6.1.1.

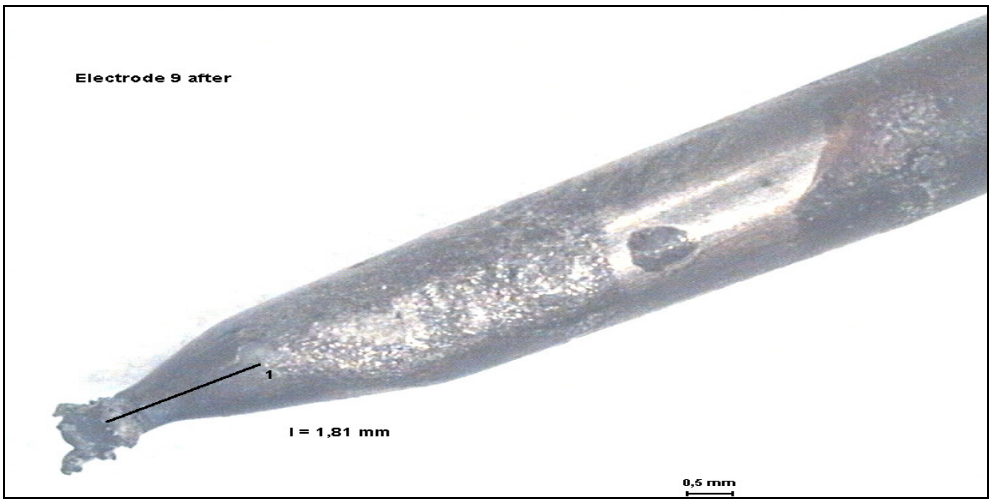

Picture 6.1.1 Example of an electrode used once for welding during 3.5 min. Details of this experiment shown in Appendix A, experiment number 9.

Further details on the technical conditions and specific details on the experiment realized such as flow, materials combination, intensity, geometry and etc can be found in Appendix A. Refer to Section 5.1.1 for an explanation of the torch geometry.

6.2 Experimental Results

Experimental testing is the best way to obtain the tendencies and behaviour of any tool, but this is also expensive and consumes a great deal of time. This disadvantage does not happen when using finite element methods. The initial phase of model construction is the most expensive phase after which it is possible to perform further simulation with minor modifications to get results with just a little investment.

Only a small selection of all the possible combinations of experiments will be made in the workshop, with the intention that the Ansys models will be used for simulating the remaining configurations and conditions. However, before work starts on these simulations, it must be verify that the finite element models work adequately. This is achieved through comparison of the simulation results with the corresponding experiments. Four experiments were made, one experiment for each geometry (model A, model B, model C and model D). All the experimental conditions were the same for four experiments.

See Appendix A for specifications of the experimental and numerical conditions applied. Figure 6.2.1 shows the experimental results for the validation of the Ansys models.

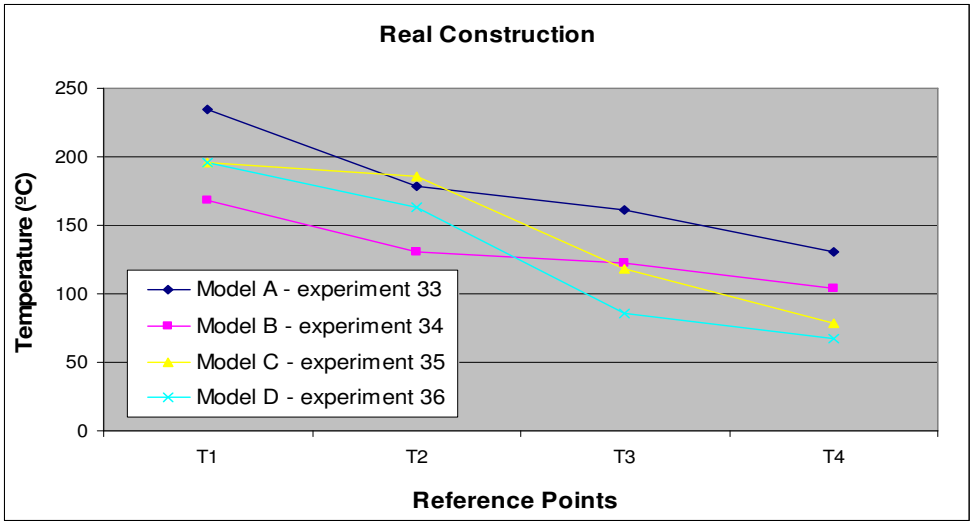

Figure 6.2.1 Experimental temperatures at main reference points used for the Ansys model validation. Experimental conditions; welding time 3.5 min, 3.2 mm electrode diameter, z_{ne} 5 mm , z_{ew} 5 mm, turbulent regime with "becoming element of turbulence", 250 A, 25 º C. Model A: long collet body with solid handle; Model B: short collet body with solid handle; Model C: long collet body with hollow handle; Model D: short collet body with hollow handle.

6.3 Comparison between Experimental and Simulation Results

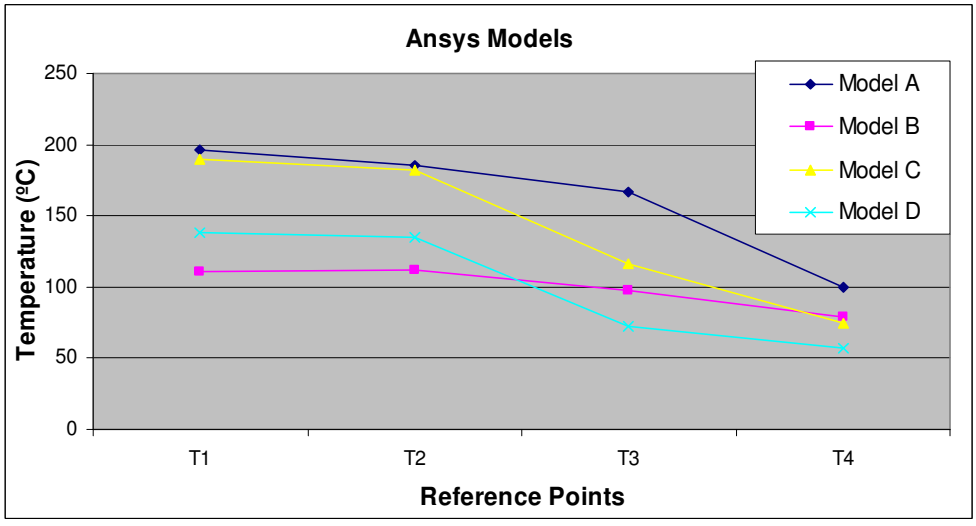

Figure 6.3.1 Temperatures profiles for each Ansys model at main reference points. Simulation conditions: 250 A, diameter 3.2 mm, uniform temperature 298 K (25ºC), collet with "becoming element of turbulence", material combination 0, turbulent regime (15 l/min) and simulation time 3' 30". Model A: long collet body with solid handle; Model B: short collet body with solid handle; Model C: long collet body with hollow handle; Model D: short collet body with hollow handle.

Figure 6.2.1 and Figure 6.3.1 display similarities in their general appearance. For example, it is observed in both figures that the temperature profiles for the configuration with the long collet body (model A and model C) are higher than for the configuration with short collet body (model B and D)*. Also, the configuration with solid handle (model A and model B) shows higher temperatures at handle zone (at reference points T3 and T4) than the configuration with hollow handle (model C and model D) **.

For both figures, the model with the lowest temperatures in handle zone is the model D. Lower temperatures in the handle are important in that the welder avoids suffering discomfort from holding the torch.

In the following subsection, each geometry will be analyzed. Experimental and simulation results will be compared to determine how error is.

6.3.1 Validation Model A

In Figure 6.3.2, it is observed that the behaviour of the model A in Ansys and the experimental results are similar. However, the error between the curves is not small, especially on the collet body at reference point T1.

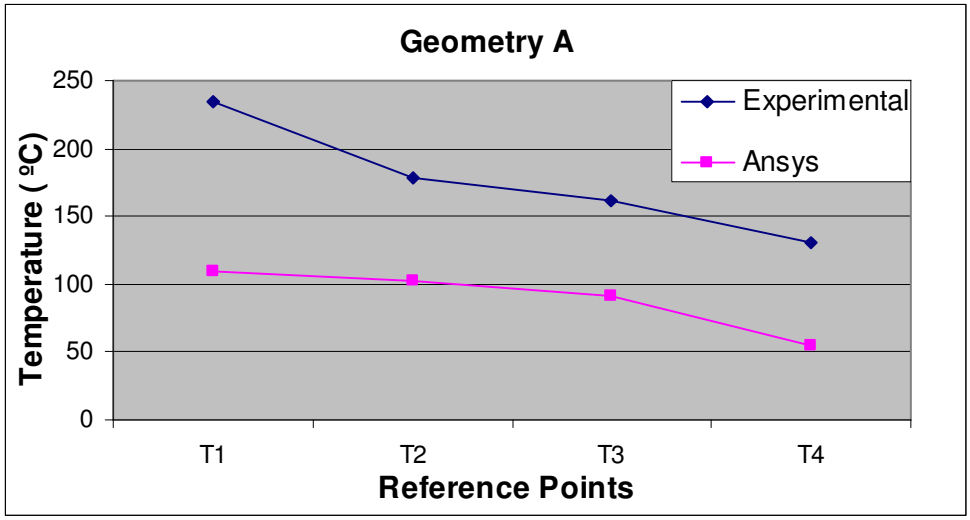

Figure 6.3.2 Temperature profiles of experimental results and Ansys results at reference points with Model A. Parameters: welding time 3.5 min, 3.2 mm electrode diameter, z_{ne} 5 mm , 250 A, 25 º C, turbulent regime with "becoming element of turbulence" (see Appendix A; experiment 33). Model A: long collet body with solid handle.

---

* Compare model A with model B and model C with model D.
** Compare model A with model C and model B with model D.

One of the possible reasons of the error at T1 might be the influence of the turbulent flow on temperature. The effect of the turbulence was more important with the geometry A than with the other geometries. The turbulent regimen caused unstable and inclined arc. Therefore, it was impossible to finish this experiment (number 33) and it was stopped at 2 min and six seconds.

Picture 6.3.1 shows the workpiece from experiment 33. It can be observed that there is some yellow dust on workpiece surface around weld pool. The dust could be oxides formed as a consequence of the oxygen entering the zone that is shielded by argon. The same dust was found at the bottom of the collet body as Picture 6.3.2 shown. The electrode used for this experiment was not able to be used again as it was completely destroyed.

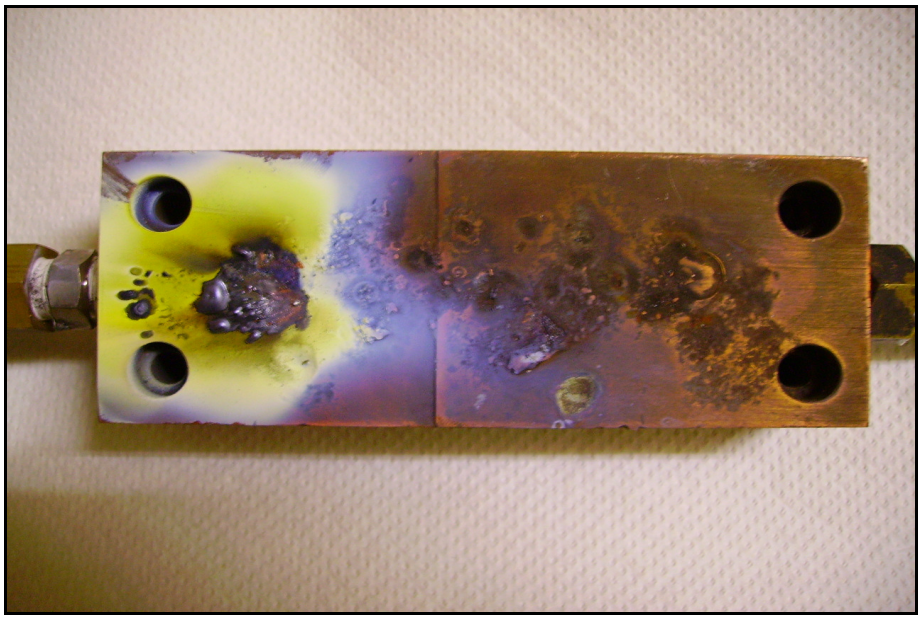

Picture 6.3.1 Status of workpiece cooled by water after making experiment 33 for validation of model A.

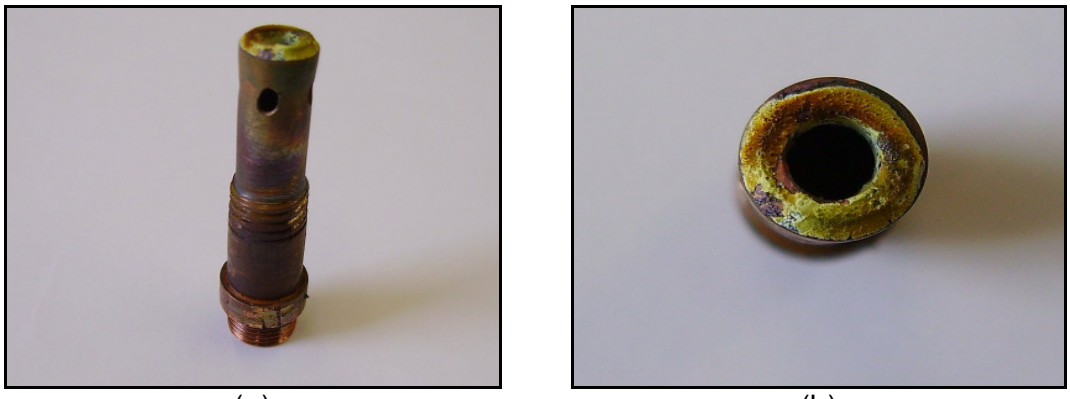

(a) (b)

Picture 6.3.2 Status of collet body after making experiment 33: (a) upright projection of collet body; (b) bird's-eye view of the collet body.

Picture 6.3.3 Status of electrode used for the validation experiment of model A. Parameters: 3.2 mm electrode diameter, welding time 3.5 min, 250 A, z_{ne} 5 mm, turbulent regime with "becoming element of turbulence" regimen, z_{ew} 5 mm, 25 º C. Model A: long collet body with solid handle.

The model used here is not able to simulate the effect that the turbulent flow of the shielding gas influences on the temperatures profile of model A. A further experiment was performed under laminar flow conditions to eliminate this effect and to obtain an error for model A when this effect is not present. Model A was simulated again, but this time with flow laminar conditions. The comparison between their results is showed in Figure 6.3.3:

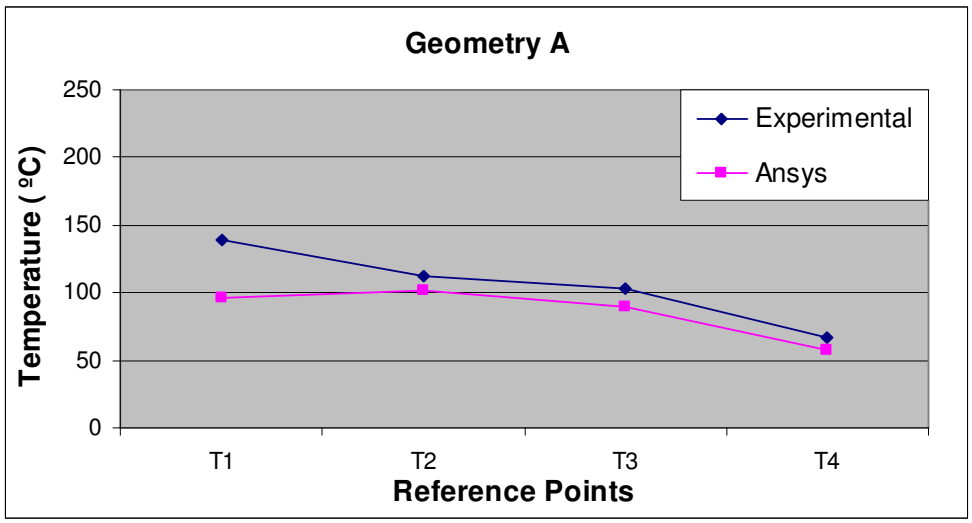

Figure 6.3.3 Temperature profiles of experimental results and Ansys results at reference points with Model A. Parameters: welding time 3.5 min, 3.2 mm electrode diameter, z_{ne} 5 mm , 250 A, 25 ºC, laminar flow with "becoming element of turbulence" (see Appendix A; experiment 3). Model A: long collet body with solid handle.

The difference between the curves in Figure 6.3.3 has been reduced. Nevertheless the error is still around 30% at reference point T1. The reason might be the absence of heat transfer by radiation, which was not taken into account. This may be of particular importance for the region between collet and collet body.

6.3.2 Validation B

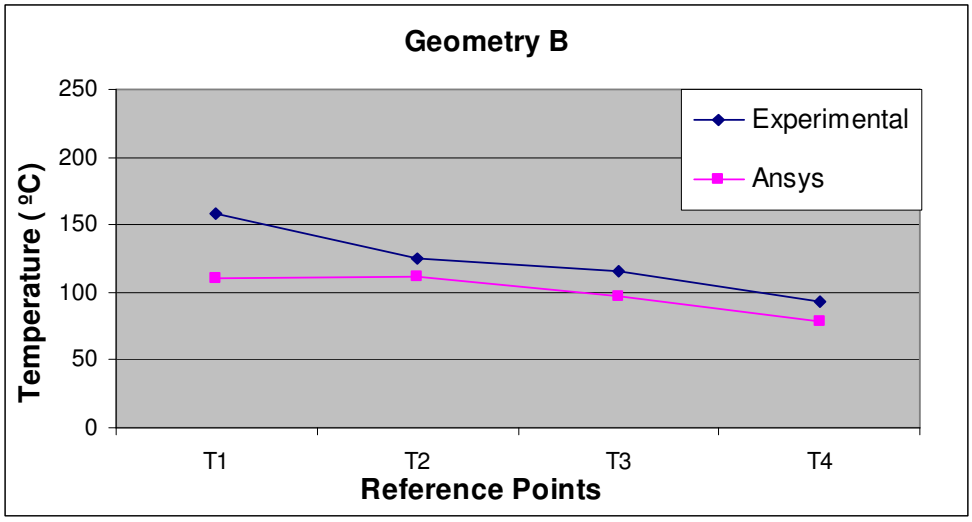

Figure 6.3.4 Temperature profiles of experimental results and Ansys results at reference points with Model B. Parameters: welding time 3.5 min, 3.2 mm electrode diameter, z_{ne} 5 mm , 250 A, 25 º C, turbulent regime with "becoming element of turbulence" (see Appendix A; experiment 34). Model B: short collet body with solid handle.

The shape of the temperature profiles given in Figure 6.3.4 for the simulated and experimental results at the reference points are quite similar. As for the validation model A, the difference between the two data sets is greatest at T1. Again the most probable reason is the absence of heat transfer by radiation.

6.3.3 Validation C

The analysis for this model is singular. As Figure 6.3.5 shown on the next page, the temperature profiles for experimental result and simulation result are quite close. The error between the two profiles is small, around 4%.

An irregular contact between thermocouples and torch surface at reference points might have made the temperatures smaller than really is the case. This inadequate contact might be one of the causes of obtaining such a small error. Also, it might be that the mathematical equations used for model C were more accurate.

The boundary conditions and loads applied play an important role on the torch behaviour. If the conditions and loads are more appropriately applied the more exact the model will be. It must be remembered that some approximations were made in order to obtain the boundary conditions. For example, temperature at the tip of the electrode was assumed to the value of 3000 K for all models.

Therefore, it could be that model C is better adapted to the boundary conditions and loads applied according to Chapter 5, Section 3.

It was said that radiation is one of the heat transfer modes existing in the GTAW torch. However, it was not taken into account for any of the models. The error of the radiation absence is proportional to its influence on the model. According to the proportion found with the error for model C, the influence of radiation may be lower than for other models.

The results of the simulation in Ansys and the experiment for the validation of model C are illustrated in Figure 6.3.5:

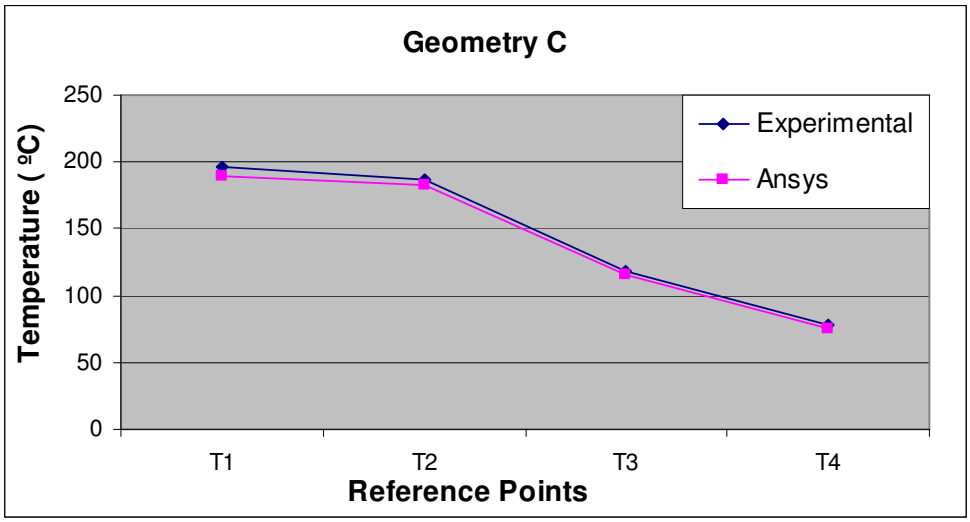

Figure 6.3.5 Temperature profiles of experimental results and Ansys results at reference points with Model C. Parameters: welding time 3.5 min, 3.2 mm electrode diameter, z_{ne} 5 mm , 250 A, 25 º C, turbulent regime with "becoming element of turbulence" (see Appendix A; experiment 35). Model C: long collet body with hollow handle.

6.3.4 Validation D

The behaviour of model D is similar to the behaviour of model A and model B. The error is within acceptable bounds at reference points T2, T3 and T4. However, at reference point T1 the error is much larger. Its value at T1 is around 28%. The error is getting smaller as the reference point is getting farther away from the torch tip.

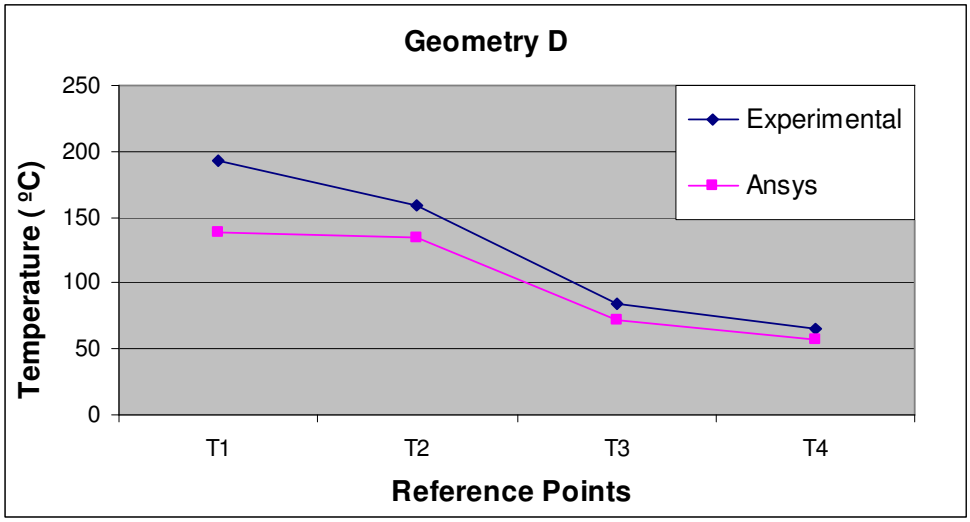

Figure 6.3.6 Temperature profiles of experimental results and Ansys results at reference points with Model D. Parameters: welding time 3.5 min, 3.2 mm electrode diameter, z_{ne} 5 mm , 250 A, 25 º C, turbulent regime with "becoming element of turbulence" (see Appendix A; experiment 36). Model D: short collet body with hollow handle.

6.4 Possible Reasons of Error

Figure 6.4.1 summarizes the error for each model in a block diagram. In the diagram, it can be seen that almost all the models have a similar error for all reference points except for T1 where the error is around 30%.

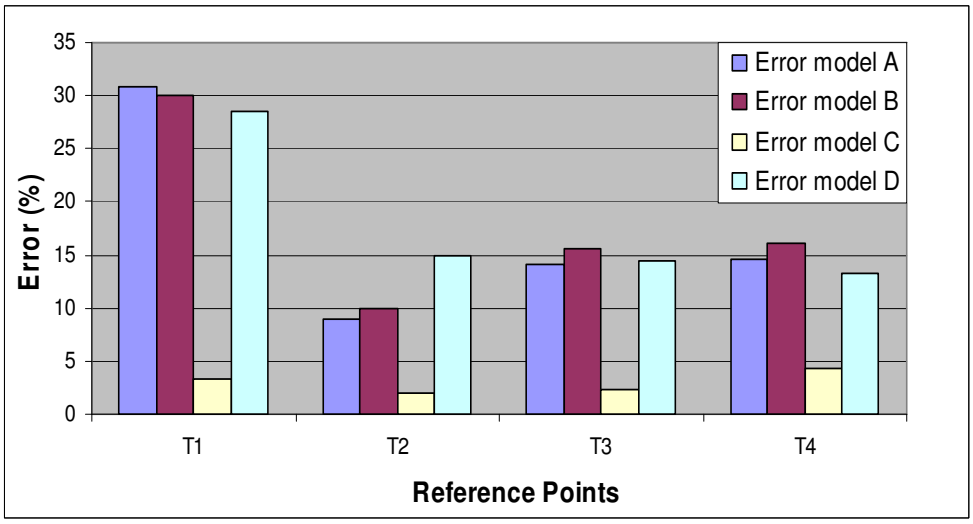

Figure 6.4.1 Block diagram of the error between experimental results and Ansys results at reference points for each model.

Radiation is present and it is relevant in zones where heat source has high energy (high temperature) and its distance from the receiving surface is small. In the real construction of GTAW torch, the heat radiation is emitted between the collet and collet body, between collet body and nozzle and also between the nozzle and the arc. However, this was not taken into account in the radiation in the Ansys models. The absence of heat radiation in the models could be one of the possible reasons of the error at reference point T1.

The mathematical error due to the finite element method also influences the results. In general, engineering problems are mathematical models of physical situations. Mathematical models are differential equations with a set of corresponding boundary and initial conditions. The solution of this system of differential equations allows the calculation of the heat transferred for each part of the continuous solid (GTAW torch). However, finite element method uses integral formulations to create a system of algebraic equations. Moreover, an approximate continuous function is assumed to represent the solution for each element. The complete solution is then generated by connecting or assembling the individual solutions, and by allowing for continuity at the interelemental boundaries. The finite element method is a numerical process what involves some mathematical error due to iterative procedure and assembling the algebraic equations between elements.

On the other hand, during the experiments there are always some parameters that produce disturbances in the system. These disturbances can not be modelled in Ansys for the cases examined here. Therefore, a small part of the error will be caused by absence of these disturbances.

Another reason to have obtained these error values could be the boundary conditions what were applied to the models. The solution might also be influenced to such a degree by the approximation of convective coefficients (see Chapter 5, Section 5.3.5) made during the model construction that large errors could be produced.

Once the reasons behind the errors in the models are known, further improvements can be included in the design of future models in order to reduce the limitations of the older models. For example, some improvements might be including the radiation in the analysis, using a fluid dynamics model or introducing a mathematical model for the electric arc in the finite element model [22].

Finally, to conclude this chapter, it must be said that model C was selected from all models because of low error. This model will be used as base model for next simulations. The aim of these simulations is to improve understanding of the behaviour of heat transfer in GTAW torch by studying the influence of different variables on the heat transferred.

CHAPTER 7

VARIABLES IN HEAT TRANSFER IN GTAW

7 VARIABLES IN HEAT TRANSFER IN GTAW

It is already well known that there are many factors that have an influence on the welding results such as the characteristics of the arc current, arc voltage, shape of the electrode tip, arc length, type of shielding gas and travel speed. In the same way, there will be also many variables that have an effect on the heat transferred in the torch.

The goal in this chapter is to study the influence of different variable, which affect the behaviour of the GTAW torch. These variables are: intensity, electrode diameter, cycle duty, temperature, materials, geometry and the flow rate of the shielding gas. For this chapter it is important to be constantly aware of the geometry of each model and the positions of the reference points (refer to Chapter 5; Section 5.1 for further information).

7.1 Geometry

Examining Figure 7.1.1 on next page, it can be observed that:

(1) Temperatures at reference points for model B (short collet body with a solid handle) are smaller than for model A (long collet body with a solid handle), and respectively the temperatures for model D (short collet body with a hollow handle) are shorter than for model C (long collet body with a hollow handle). In other words, heat flow with long collet body is bigger than with short collet body. This can be found in Appendix F, in Section 4.1; where more temperature plots are presented.
The reason is the temperature gradient at short collet body is smaller as is shown in Figure 7.1.2. The distance between the electrode tip and the bottom of the collet body is greater for short collet body than for long collet body (S > L). At the point where the electrode and the collet body are joined, a lower temperature is observed for the short collet body than for the long collet body. Consequently the energy transferred upward is lower. Also, increased free surface convection of heat between the argon and electrode helps to decrease the temperature at this point.

Nevertheless the surface convection with argon for the long collet body is greater than for the short collet. This cooling effect is not compensated by the larger temperature gradient for the long collet body. Therefore, it can be concluded that using a short collet body gives lower temperatures profiles than are observed when using a long collet body.

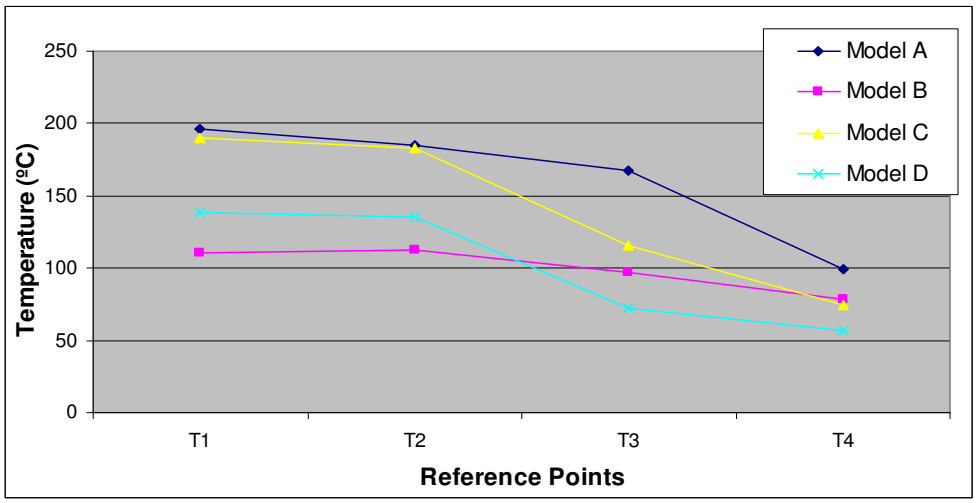

Figure 7.1.1 Temperatures profiles for each Ansys model at main reference points. Simulation conditions with 250 A, diameter 3.2 mm, uniform temperature 298 K, collet with "becoming element of turbulence", material combination 0, turbulent regime (15 l/min) and simulation time 3' 30". Model A: long collet body with solid handle; Model B: short collet body with solid handle; Model C: long collet body with hollow handle; Model D: short collet body with hollow handle.

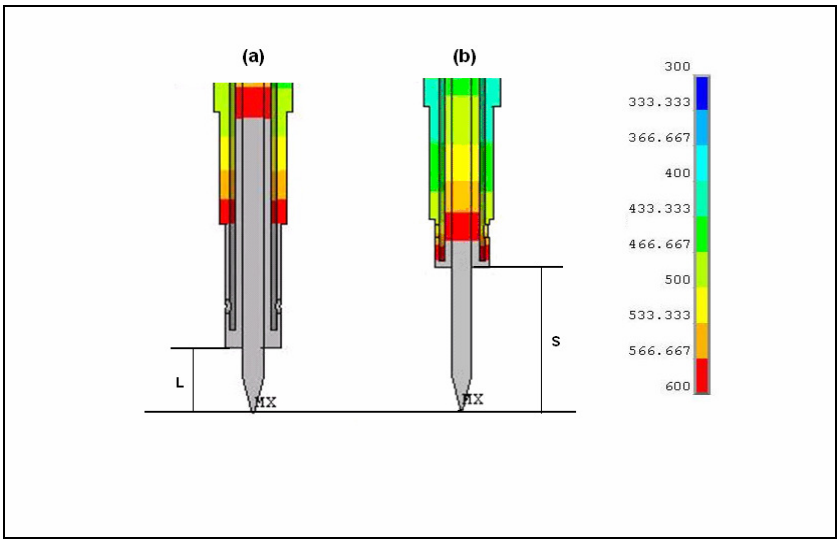

Figure 7.1.2 Ansys plot detail: (a) long collet body from model C; (b) short collet body from model D. Simulation conditions with 250 A, diameter 3.2 mm, uniform temperature 298 K, collet with "becoming element of turbulence", material combination 0, turbulent regime (15 l/min) and simulation time 3' 30". Model C: long collet body with hollow handle; Model D: short collet body with hollow handle.

As described earlier and confirmed in Table 7.1.1, the temperature differences observed for the long and short collet bodies can be distinguished. Therefore, as model A and C use the long collet body, the temperature differences observed between reference points T2 and T4 are greater than those observed for model B and D.

Table 7.1.1 Temperature difference between points T2 and T4 for each model.*

	T2- T4 (ºC)
Model A	85.77
Model B	33.73
Model C	107.62
Model D	77.88

*Note that the temperature at reference point T1 has not been taken into account, because the error at this point was substantial for all models, except for model C, where the error was small.

(2) The geometries with solid handles (model A and model B) give greater temperatures in the handle zone than is observed for geometries handles that are hollow. According to equation (4-2) the bigger transversal surface of the solid handle causes less thermal resistance, and therefore more heat is transferred toward the power cable. Cooling that occurs with argon in the region of the hollow handle reduces the observed temperatures at T3 and T4 as compared to the solid handle. On other hand, the hollow handles have smaller transversal surface areas. This obstructs the heat transferred, thus the temperatures observed in the external block at T2 are higher.

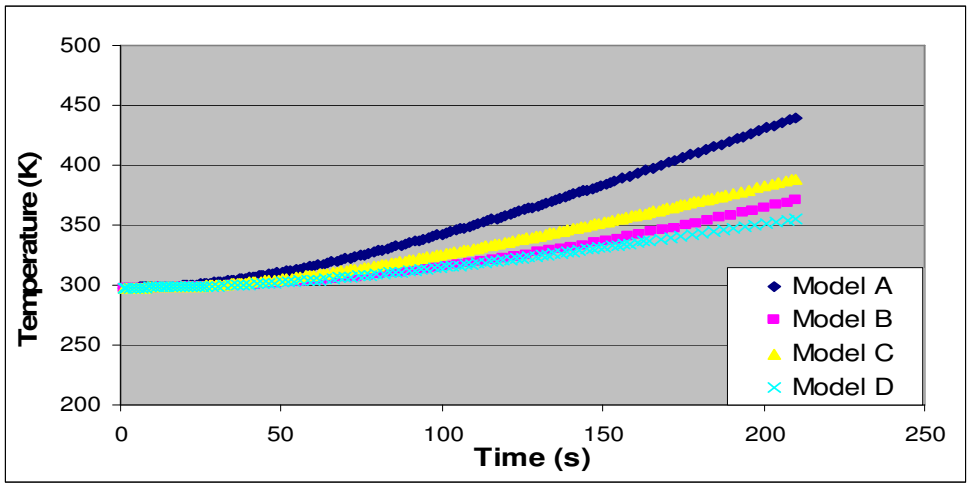

Figure 7.1.3 Heating curves for each Ansys model at reference point T3.

In Figure 7.1.1 it can be seen that model A is the model with highest temperatures at all reference points. Note that in Figure 7.1.3 the corresponding heating curve for model A has the highest tangent; thus the heat transfer rate of this model has the greatest rate.

7.2 Materials

Materials influence the heat conducted through in the welding torch. Therefore, in this chapter, different material combinations will be simulated to better understand the behaviour of the torch. Table 7.2.1 lists the combinations that have been simulated and the following figures illustrate the results.

Table 7.2.1 Material combinations simulated in Ansys: material for each element of the model.

	C.0	C.1	C.2	C.3	C.4	C.5	C.6	C.7
Back Cap	Steel	Steel	Steel	Steel	Steel	Steel	Steel	Steel
Back Cap Insulator	PTFE	PTFE	PTFE	PTFE	PTFE	PTFE	PTFE	PTFE
Collet	Copper	Copper	Copper	Copper	Copper	Copper	Copper	Copper
Collet Body	Copper	Steel	Copper	Copper	Aluminium	Copper	Copper	Copper
Coupler handle/ cable	Copper	Copper	Copper	Copper	Copper	Copper	Copper	Copper
Coupler torch/ gas pipe	Brass	Brass	Brass	Brass	Brass	Brass	Brass	Brass
Electrode	Tungsten	Tungsten	Tungsten	Tungsten	Tungsten	Tungsten	Tungsten	Tungsten
External Block	Copper	Copper	Copper	Steel	Copper	Aluminium	Aluminium	Brass
Handle	Copper	Copper	Copper	Copper	Copper	Copper	Aluminium	Copper
Internal Block	Copper	Copper	Steel	Copper	Copper	Aluminium	Aluminium	Brass
Power Cable	Copper	Copper	Copper	Copper	Copper	Copper	Copper	Copper
Torch Body	PTFE	PTFE	PTFE	PTFE	PTFE	PTFE	PTFE	PTFE

Generally, the collet, collet body, internal block, external block and the handle are built with copper. The element that connects to the handle with the power cable used to be brass, because its hardness allows better joints than when copper is used. This is the usual material combination for GTAW and therefore it will be used as the reference combination, “combination 0” (C.0). The combinations shown in Table 7.2.1 are compared with combination 0.

In next Figure 7.2.1, temperature profiles of three combinations are compared with “combination 0” to study the possible use of steel as the thermal block. Each combination in Figure 7.2.1 was obtained by replacing a copper piece of the torch to steel. For example, “combination 1 has the same composition as “combination 0” except that the collet body is made of steel instead of copper. For “combination 2”, the internal block, for “combination 3”, the external block; the materials of these elements were replaced from copper to steel.

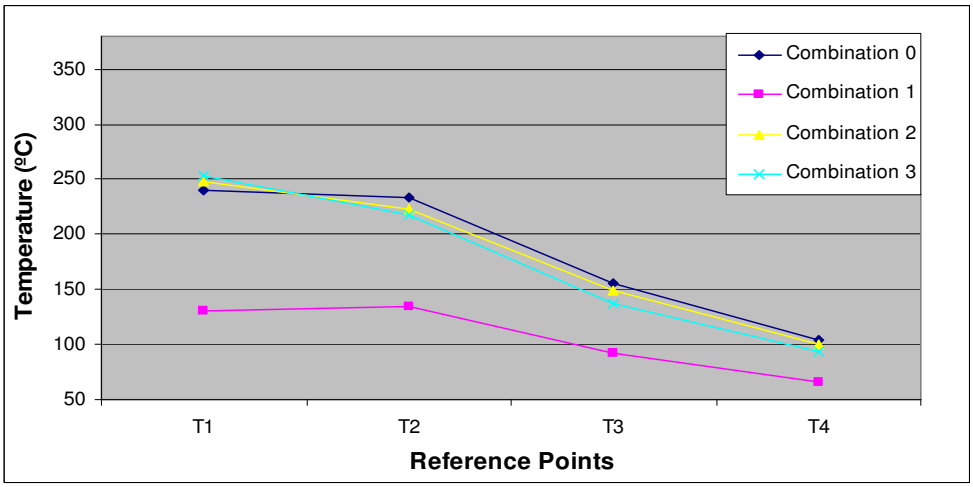

Figure 7.2.1 Temperature profile at main reference points for the material combinations: combination 0, combination 1, combination 2 and combination 3. Simulation conditions with 300 A, diameter 3.2 mm, uniform temperature 298 K, collet with “becoming element of turbulence”, model C, turbulent regime (15 l/min) and simulation time 3’ 30”. *Combination 1: steel collet body; Combination 2: steel internal block; Combination 3: steel external block.*

Note that the biggest temperature decrease is caused by changing collet body from copper to steel (“combination 1”). Steel has a lower thermal conductivity compared to copper, which causes the heat transfer rate away from the torch tip to be lower. This greater heat resistance caused by the lower thermal conductivity of steel results in a thermal block of the heat. The effect is that temperatures at reference points with steel collet body are lower.
The temperature at T2 for “combination 1” is also interesting; it is possible to observe that the temperature at T2 is slightly higher than temperature at T1. The reason behind this is the same as previously mentioned. The heat transferred in the collet body is much lower than the heat transferred in collet in contact with the back cap. The head receives more heat from the collet than from the collet body.

Using a steel internal block (“combination 2”) or a steel external block (“combination 3”) results in a decrease temperatures observed compared to those observed with the reference “combination 0”. However, their effect is much smaller than changing the material of the collet body (“combination 1”).

The temperature decrease is larger for “combination 3” than for “combination 2”, as the thickness of the internal block is smaller than thickness of the external block. The heat resistance of the internal block is smaller than of the external block and causes less of thermal obstruction. Therefore, the temperatures observed at reference points for “combination 2” will be higher than the temperatures of “combination 3”.

Figure 7.2.2 depicts that the heat conducted along the copper collet body is greater than along the steel collet body. This is shown by the higher temperatures along the length of the torch body and the smaller temperature gradient in the collet body.

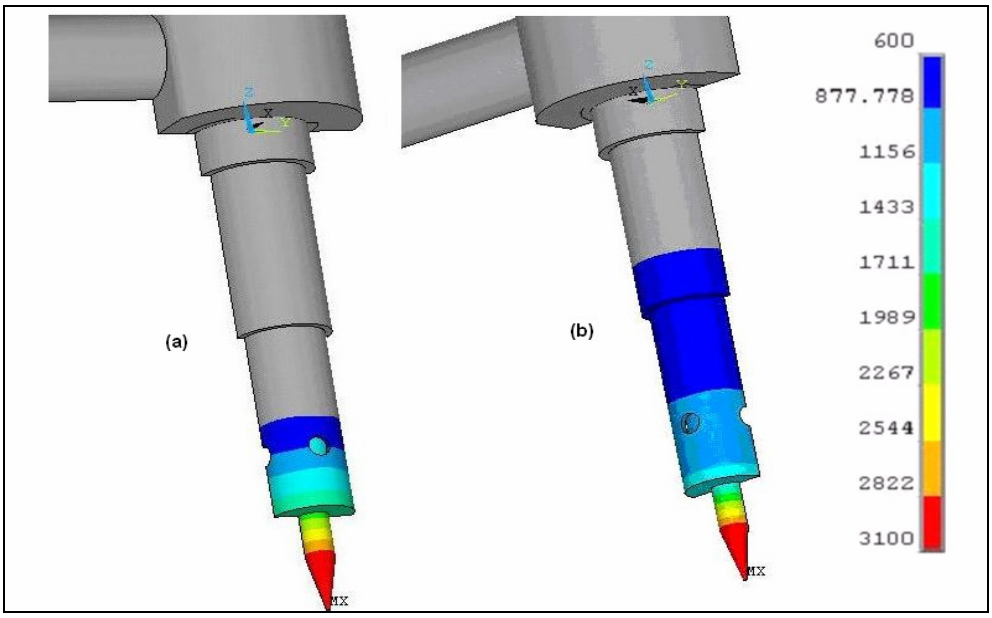

Figure 7.2.2 Temperature plots for two different material combinations: (a) Combination 1; (b) Combination 0. Simulation conditions with 300 A, diameter 3.2 mm, uniform temperature 298 K, collet with “becoming element of turbulence”, model C, turbulent regime (15 l/min) and simulation time 3’ 30”. Combination 0: copper collet body; *Combination 1: steel collet body.*

More plots of the differences in the rate of heat transferred between the copper and steel collet bodies can be found in Figures F-4.2.1 to F-4.2.6 in Appendix F.

Figure 7.2.3 shows how the heat transfer rate varies at reference point T2 is for these material combinations.

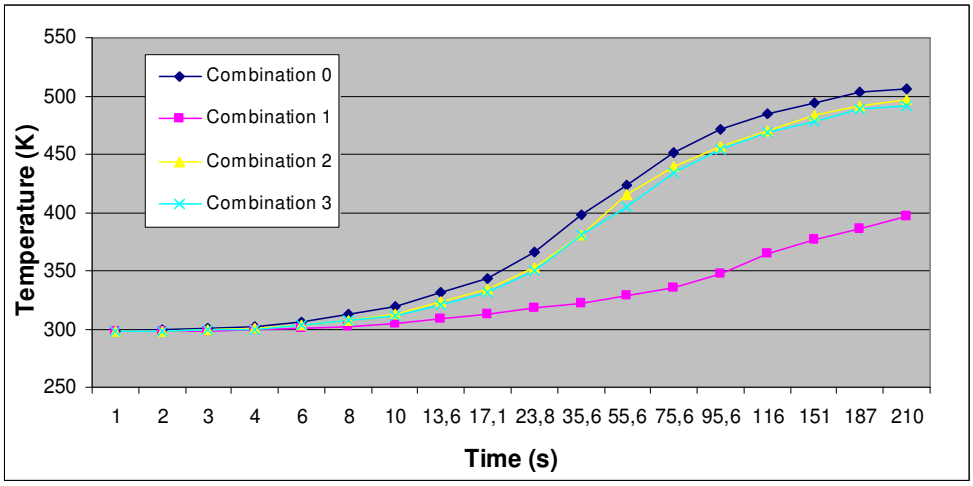

Figure 7.2.3 Heating curve at main reference point T2 for four material combinations: combination 0, combination 1, combination 2 and combination 3. Simulation conditions with 300 A, diameter 3.2 mm, uniform temperature 298 K, collet with "becoming element of turbulence", model C, turbulent regime (15 l/min) and simulation time 3' 30". *Combination 1: steel collet body; Combination 2: steel internal block; Combination 3: steel external block.*

Finding a possible substitute for copper with similar physical properties might be of interest due to the current high price of copper. The next plot (see Figure 7.2.4 on the next page) shows whether aluminium could be used as this substitute and how some components of the torch behave when they are made with aluminium.

As for the study of thermal block, "combination 0" is the reference combination. For each combination some components of the torch materials are changed from copper to aluminium. For "combination 4" the collet body is changed from copper to aluminium. Both the internal and external blocks of "combination 5" are changed from copper to aluminium. Finally for "combination 6" the internal and external blocks, plus the handle are changed from copper to aluminium.

As can be seen in Figure 7.2.4 the use of an aluminium collet body ("combination 4") produces the best results at all reference points as the temperature profile is lowest of all the combinations. However, this combination is not good because of the low melting point of aluminium, around 660 ºC (see Appendix B for a list of the physical properties of the solids). This is confirmed in Figure 7.2.5, which shows that the temperature at the bottom of collet body (T5) is around 940 ºC, which is above the melting point, In other words for "combination 4", the bottom of the collet body would have melted.

Comparing C.0 and C.5 in Figure 7.2.4, it can be observed that there is little difference between the two profiles. This is an interesting result, as the behaviour of the torch similar when aluminium is used for both the internal and external blocks. Therefore, aluminium could be a good cheap alternative for the internal and external block.

Both “combination 5” and “combination 6”, have aluminium internal and external blocks and the only the difference between them is that “combination 6” has aluminium handle. As Figure 7.2.4 shows the temperatures at the torch head (points T1 and T2) increase and temperatures at handle zone decrease lightly when an aluminium handle instead copper (“combination 6”) is used. As aluminium has a lower thermal conductivity, i.e. more heat resistance, the heat transfer transferred toward power cable is lower, which causes a thermal block at the torch head.

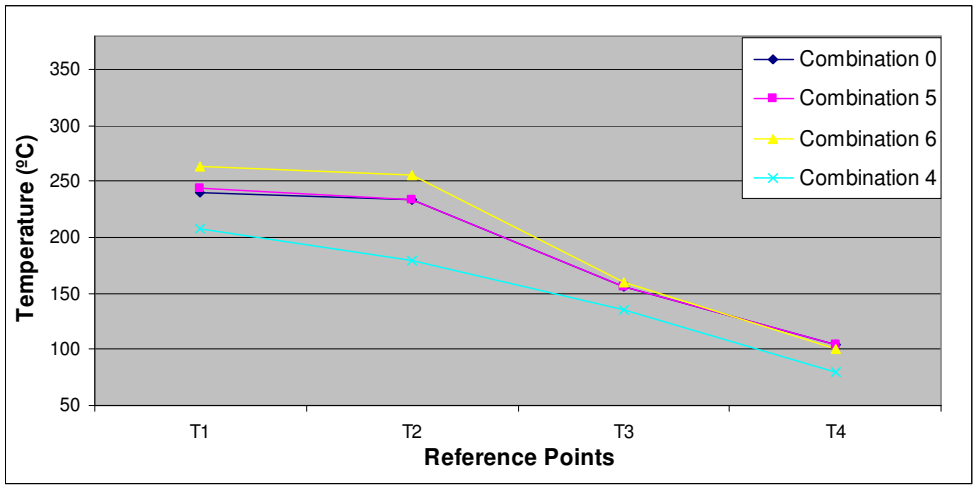

Figure 7.2.4 Temperature profile at main reference points for four material combinations: combination 0, combination 4, combination 5 and combination 6. Simulation conditions with 300 A, diameter 3.2 mm, uniform temperature 298 K, collet with “becoming element of turbulence”, model C, turbulent regime (15 l/min) and simulation time 3’ 30”. *Combination 4: aluminium collet body; Combination 5: aluminium internal block and external block; Combination 6: aluminium internal and external blocks with an aluminium handle.*

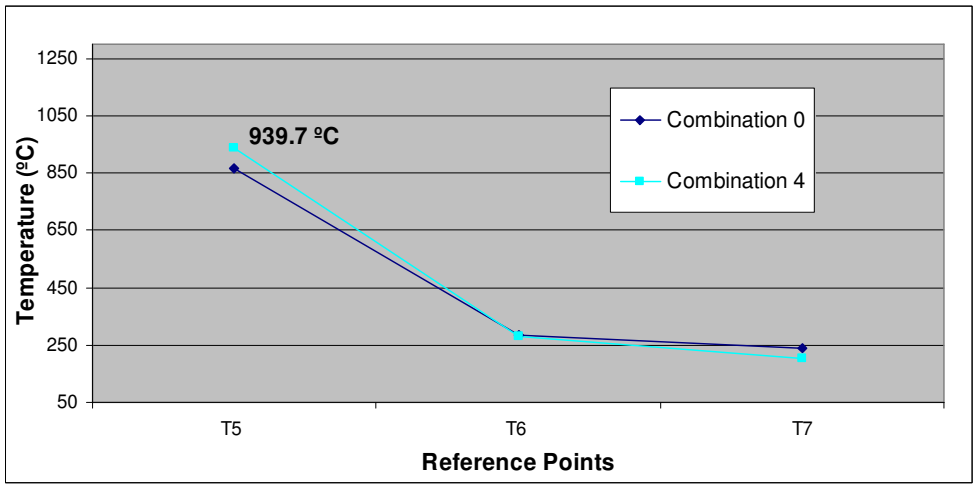

Figure 7.2.5 Temperature profile at other reference points for two different material combinations; combination 0 and combination 4. Simulation conditions with 300 A, diameter 3.2 mm, uniform temperature 298 K, collet with “becoming element of turbulence”, model C, turbulent regime (15 l/min) and simulation time 3’ 30”. *Combination 4: aluminium collet body.*

The main advantage of “combination 5” is that is achieved a similar temperature profile to “combination 0” and with the current copper prices this could lead to cost reduction. Another advantage is that the torch weight decreases as the density of aluminium density smaller than copper (review the physical properties in Appendix B). This weight reduction improves handling of the torch as the welder will feel less discomfort after long usage times.

Some GTAW torch manufacturers use brass as the material for the internal and external blocks. The use of brass is supported by results depicted in Figure 7.2.6. In this plot it can be seen that “combination 7” (brass internal block and external block) has similar temperature profiles to “combination 0”. However, the prices of brass and copper are quite different. Economically, substituting the head material from copper to brass is profitable as brass is a copper-zinc alloy, thus it is cheaper to buy.

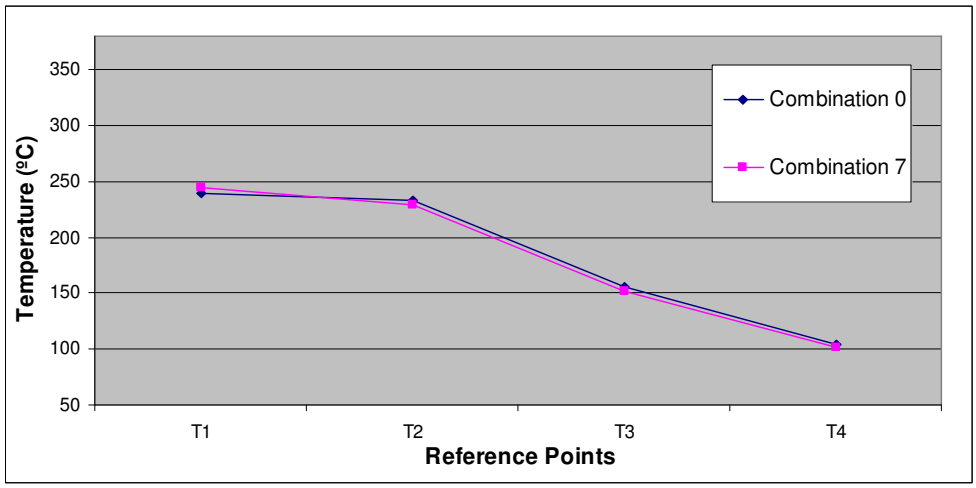

Figure 7.2.6 Temperature profile at main reference points for two different material combinations; combination 0 and combination 7. Simulation conditions with 300 A, diameter 3.2 mm, uniform temperature 298 K, collet with “becoming element of turbulence”, model C, turbulent regime (15 l/min) and simulation time 3’ 30”. *Combination 7: brass internal and external blocks.*

7.3 Current Flow

In this section, the parameter of simulation is the current flow. How temperatures change as current changes is the task in this section.

Electrical current causes two effect in the torch; first, joule heating is generated due to materials resistance to the electrical current running through them. Second, the electrical current influences on electric arc. The amount of energy produced by the arc is proportional to the electrical current. If it increases, the energy increases too.

Figure 7.3.1 shows the temperatures at the main reference points for different current values (200 A, 300 A and 400 A). It can be seen that there is not so much difference between them as the variation is about four Celsius degrees. These results indicate that the model is not sensitive to the second effect. The temperature increase is due to the first effect; joule heating.

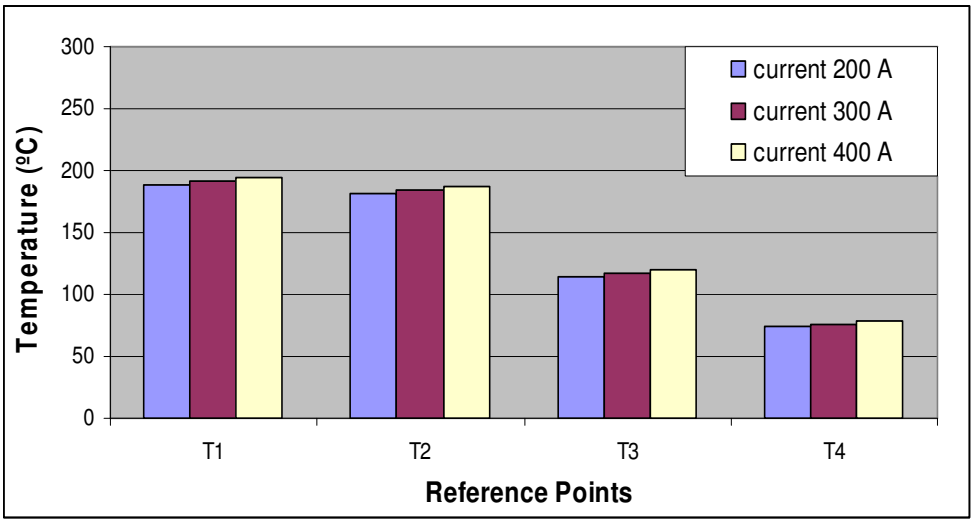

Figure 7.3.1 Block diagram of temperatures at main reference points for different values of current flow. Simulation conditions with diameter 3.2 mm, materials combination 0, uniform temperature 298 K, collet with "becoming element of turbulence", model C, turbulent regime (15 l/min) and simulation time 3' 30".

As Figure 7.3.2 shows the greatest change takes place when the electrode diameter is 2.4 mm due to joule heating is bigger as diameter goes up.

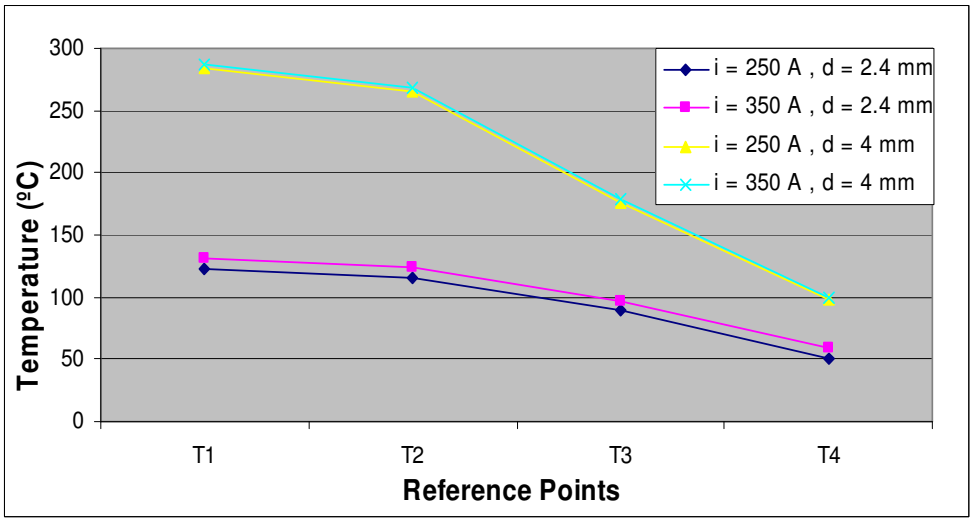

Figure 7.3.2 Temperature profile at main reference points for different values of current flow and diameters. Simulation conditions with materials combination 0, uniform temperature 298 K, collet with "becoming element of turbulence", model C, turbulent regime (15 l/min) and simulation time 3' 30".

7.4 Electrode Diameter

More likely is that there for the same current, the current per unit cross sectional area is signicantly increased. The electrode diameter has an important effect on temperature profiles of GTAW torch. As illustrated in Figure 7.4.1, the temperature rises as diameter increases. According to this diagram, welding with 2.4 mm diameter is better, because the temperatures that are achieved are lower than with the other diameters. However, there is one more factor to take into account; electrode deterioration. The electrode deterioration that occurs when a diameter of 2.4 mm is used has a more significant effect than the other electrodes as the current flow rises because of the joule heating. Using too much current is a major cause of excessive electrode consumption. This is solved by restricting the current flow to a level that is appropriate for the electrode size. There are some tables where current intervals for each diameter are recommended. Table 7.4.1 shows an example of these recommendations for the current intervals for different electrode diameters.

Table 7.4.1 Recommended tungsten electrode diameter for alternating current. [1]

Diameter (mm)	0.25	0.5	1	1.6	2.4	3.2	4	4.8	6.4
Current (A)	up to 15	5-15	10-60	50-100	100-160	150-210	200-275	250-350	325-450

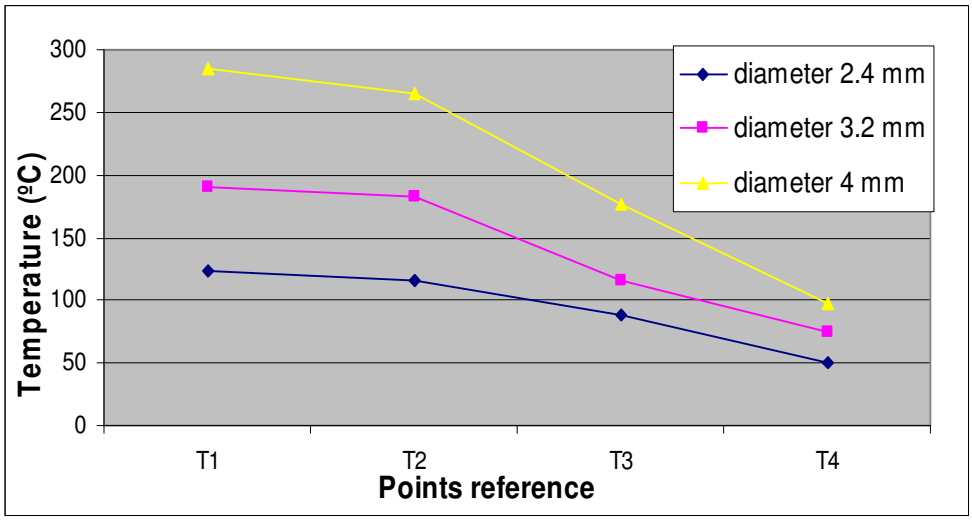

Figure 7.4.1 Temperature profiles at main reference points for different electrode diameters of GTAW torch. Simulation conditions; 250 A, materials combination number 0, uniform temperature 298 K, collet with “becoming element of turbulence”, model C, turbulent regime (15 l/min) and simulation time 3’ 30”.

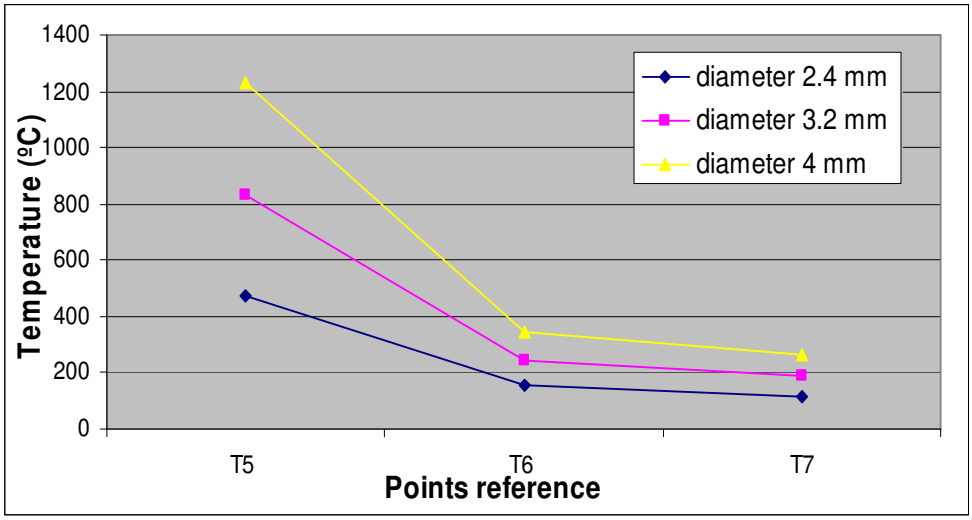

Figure 7.4.2 Temperature profiles at other reference points for different electrode diameters of GTAW torch. Simulation conditions; 250 A, materials combination number 0, uniform temperature 298 K, collet with "becoming element of turbulence", model C, turbulent regime (15 l/min) and simulation time 3' 30".

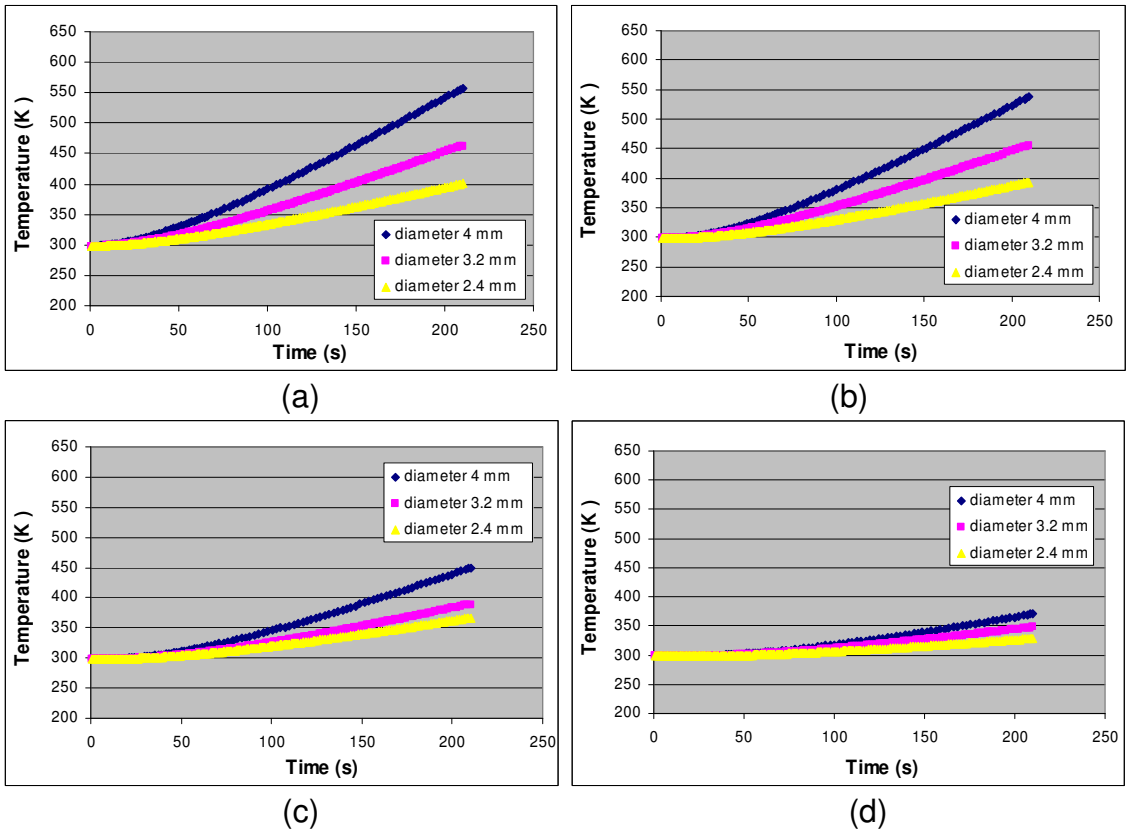

Figure 7.4.3 Temperature against time (heating curve) for different electrode diameter at reference points: (a) T1; (b) T2; (c) T3 and (d) T4. Simulation conditions; 250 A, materials combination number 0, uniform temperature 298 K, collet with "becoming element of turbulence", model C, turbulent regime (15 l/min) and simulation time 3' 30".

As shown in both Figures 7.4.1 and 7.4.2, the difference between the profiles decreases in proportion to the distance of the reference point locations from the tip of electrode. The same deduction is observed in Figure 7.4.3; note how curves are getting converging upon one another.
Figure 7.4.3 shows that the tangent of heating curves is greater for larger diameters. Thus, the heat transferred with diameter 4 mm is higher than with a diameter of 2.4 mm. See Appendix F for further comparisons particularly between Figures F-4.3.2 and F-4.3.4.

7.5 Volumetric Flow Rate

As was expected from the experimental results (see Appendix E, Figure E-5), the use of turbulent flow causes a decrease in the temperatures observed in the GTAW torch model. As Figure 7.5.1 and 7.5.2 show, there is a considerable temperature difference between profiles obtain with turbulent flow conditions and those for laminar flow conditions. Using turbulent flow increases cooling capability of GTAW torch; therefore, the temperatures are lower than with laminar flow. Note that the tangent of the line that joins T2, T3 and T4 is smaller when the flow is turbulent than compared to when it is laminar. Thus, there is more uniformity in the temperature distribution in the torch for turbulent flow.

In Ansys model, the “becoming element of turbulence” (BET) effect and gas volumetric flow rate are taken into account by modifying convection coefficients that were calculated by hand with the appropriate thermal equations described in Section 5.3.5.

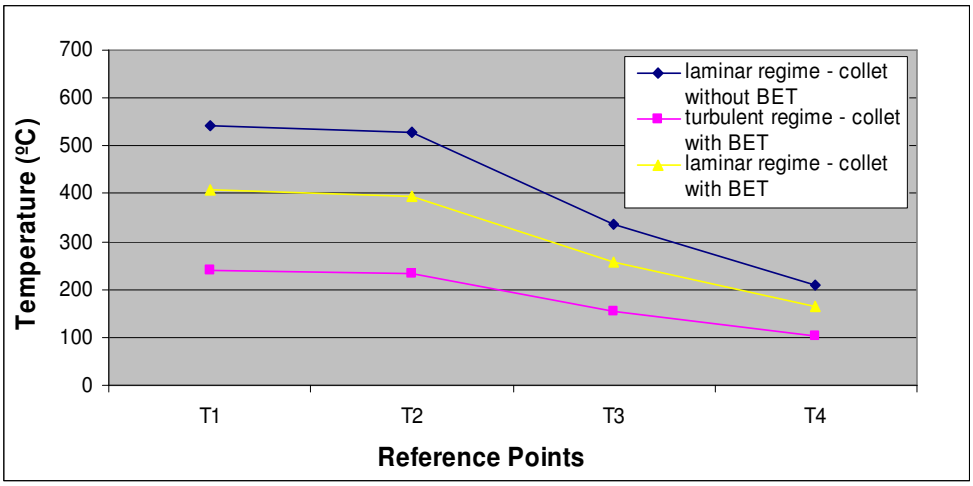

Figure 7.5.1 Temperature profiles at reference points for laminar and turbulent regime. Simulation conditions with 300 A, materials combination number 0, uniform temperature 298 K, diameter 3.2 mm, model C and simulation time 3’ 30”.

According to Figure 7.5.2, the collet body for the case with laminar flow and without “becoming element of turbulence” (line blue) will be melted at the bottom, since the temperature at T5 (1230 ºC) is higher than its melting point of 1083 ºC.

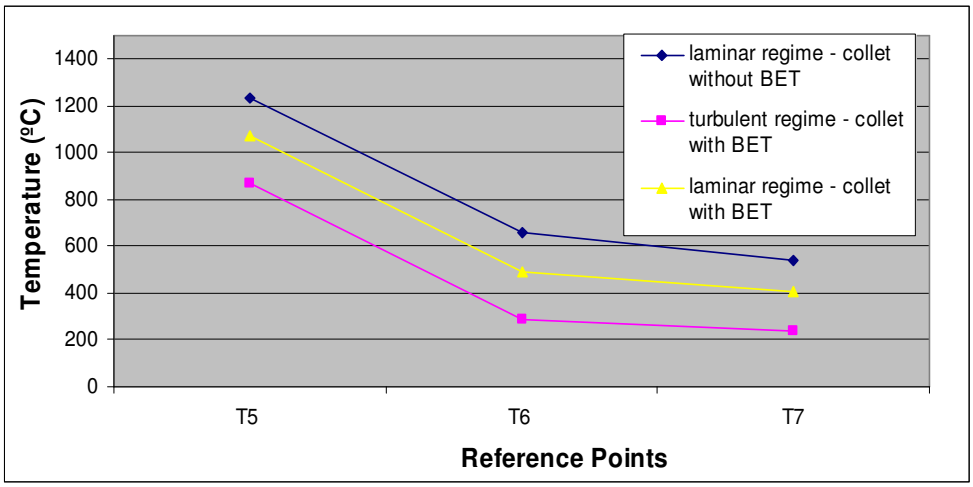

Figure 7.5.2 Temperature profiles at other reference points for laminar and turbulent regime. Simulation conditions with 300 A, materials combination number 0, uniform temperature 298 K, diameter 3.2 mm, model C and simulation time 3' 30".

The effect of the "becoming element of turbulence" at collet is also important; observe how using laminar flow with "becoming element of turbulence" also causes a reduction in the temperatures. Building future collets with "becoming element of turbulence" would be a good way to design the GTAW torch more effectively and to take advantage of cooling capability of the shielding gas, in this case argon.

It must be noted that the heat transfer along the welding torch is faster with laminar flow than with turbulent. This is illustrated in next figure (Figure 7.5.3). In Appendix F, Section 4.4, there are some simulation plots that further illustrate this effect.

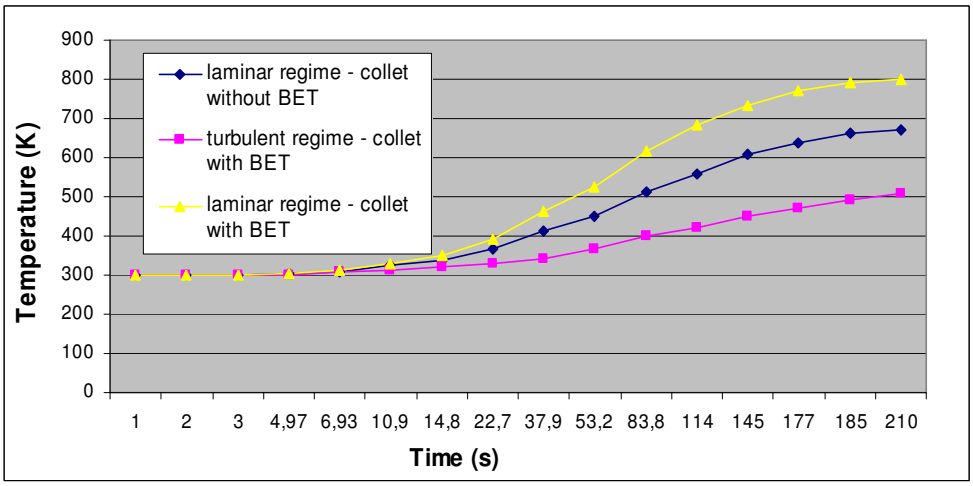

Figure 7.5.3 Heating curves for laminar and turbulent regime at T2. Simulation conditions with 300 A, materials combination number 0, uniform temperature 298 K, diameter 3.2 mm, model C and simulation time 3' 30".

7.6 Atmospheric Temperature

Figure 7.6.1 shows that atmospheric temperature has influence on temperature profiles along the torch length. If the atmospheric temperature increases, temperatures in the torch also increase. If the atmospheric temperature drops below the standard temperature (25 ºC), the temperatures observed are also lower. To design a welding torch correctly, this effect must be considered for all the possible the working environments that the torch would experience. The increase of the temperature associated with working in hot environments could affect the cooling capacity of the systems used on the torch. The opposite case, when the torch would be used in cold environments, involves a decrease of temperature profile in reference to temperature profile at the standard temperature.

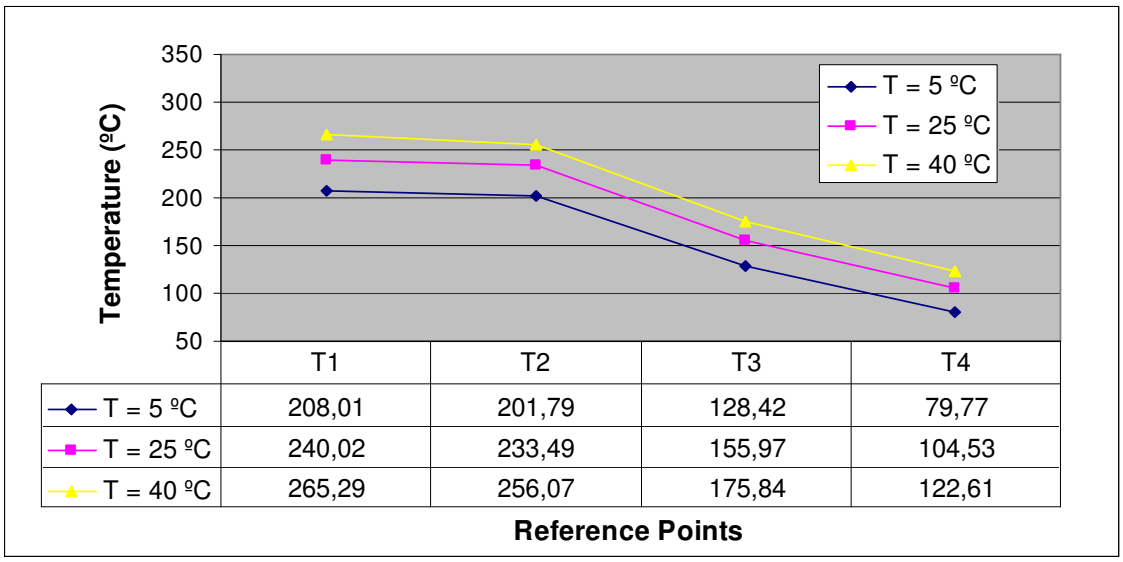

	T1	T2	T3	T4
T = 5 ºC	208,01	201,79	128,42	79,77
T = 25 ºC	240,02	233,49	155,97	104,53
T = 40 ºC	265,29	256,07	175,84	122,61

Figure 7.6.1 Temperature profiles at reference points for different atmospheric temperatures. Simulation conditions with 300 A, materials combination number 0, turbulent regime (15 l/min), collet with “becoming element of turbulence”, diameter 3.2 mm, model C and simulation time 3’ 30”.

The results, in Figure 7.6.1, indicate that if atmospheric temperature increases by approximately 15 ºC (from 25 to 40 ºC), the temperatures in the torch will rise by up to 25 ºC. It is also interesting to know how the temperature in the torch increases as the atmospheric temperature is increased when the torch is working at or near to its maximum power. For example, a GTAW torch with a maximum power of P_n and a maximum temperature at the torch head of T_{max} causes a reduction of its power output by 3 %. Therefore, its maximum power will be $0.97P_n$. Thus, in this case, the allowed maximum temperature will not be exceeded at the torch head. In general, the new maximum power after a change of atmospheric temperature is expressed by equation: $P_n \cdot \left(1 - \frac{\Delta T}{T_{\max}}\right)$ where ΔT is the temperature increase in the torch due to the increase in atmospheric temperature.

7.7 Duty Cycle

The duty cycle is defined as the number of minutes per 10-minute cycle that an arc welding system can operate at maximum level before needing to cool down. The component with the lowest duty cycle in the welding system determines the duty cycle capacity. It is expressed as a percentage. Therefore, a 35% duty cycle means that welding for 3.5 minutes requires 6.5 minutes of cooling before welding can restart.

The duty-cycle of a welding machine is usually given at the maximum current of the machine. As the amperage is reduced, the effective duty-cycle is increased. Thus, it is possible for a point on the welding machine's "curve" to exist where the duty-cycle is close to 100%.

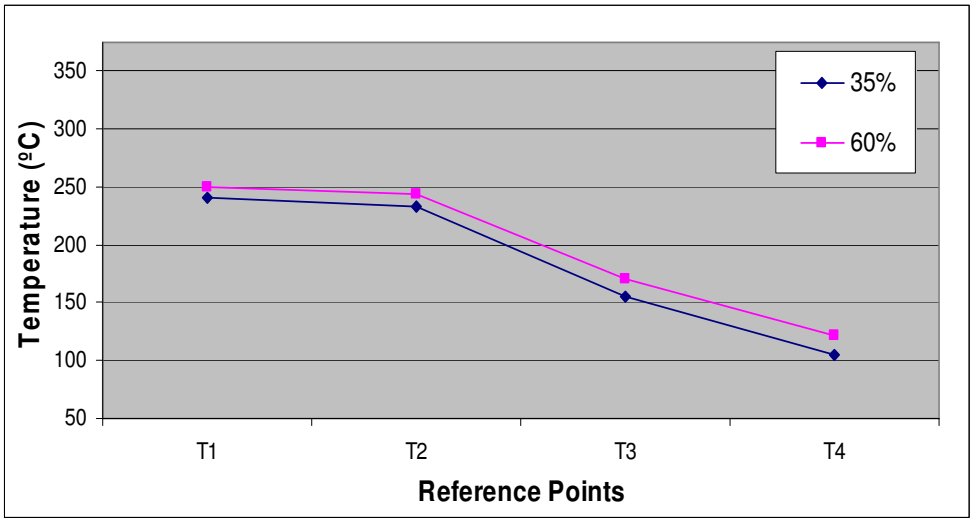

Figure 7.7.1 Temperature profiles at reference points for duty cycle of 35% and 60%. Simulation conditions; 300 A, materials combination number 0, turbulent regime (15 l/min), collet with “becoming element of turbulence”, uniform temperature 298 K, diameter 3.2 mm, model C.

As Figure 7.7.1 shows, the temperature is larger for higher duty cycles. The behaviour of GTAW torch model in Ansys is similar to real construction as is depicted in Figure E-6 in Appendix E.

The average increase in the temperature between the two duty cycles in Figure 7.7.1 was 13 ºC. This is confirmed with Table 7.7.1, where a comparison with the experimental measurements is made.
Note that the biggest increase takes place in the handle zone (between reference points T3 and T4)*.

---

* Please be aware that temperatures observed at T1 for the simulation were not reliable (as mentioned in Section 6.3).

Table 7.7.1 Temperature increase due to duty cycle increase from 35% to 60% for experimental and simulation results.

	ΔT_{simul} (ºC)	ΔT_{exp} (ºC)
T1	10.33	62
T2	10.73	10.1
T3	14.02	13.3
T4	16.98	17.02

The temperature profiles depicted in Figure 7.7.2 show the temperature after a single cycle, then for 2 and 3 repeated duty cycles that were simulated with a duty cycle of 35% and an atmospheric temperature of 25℃.

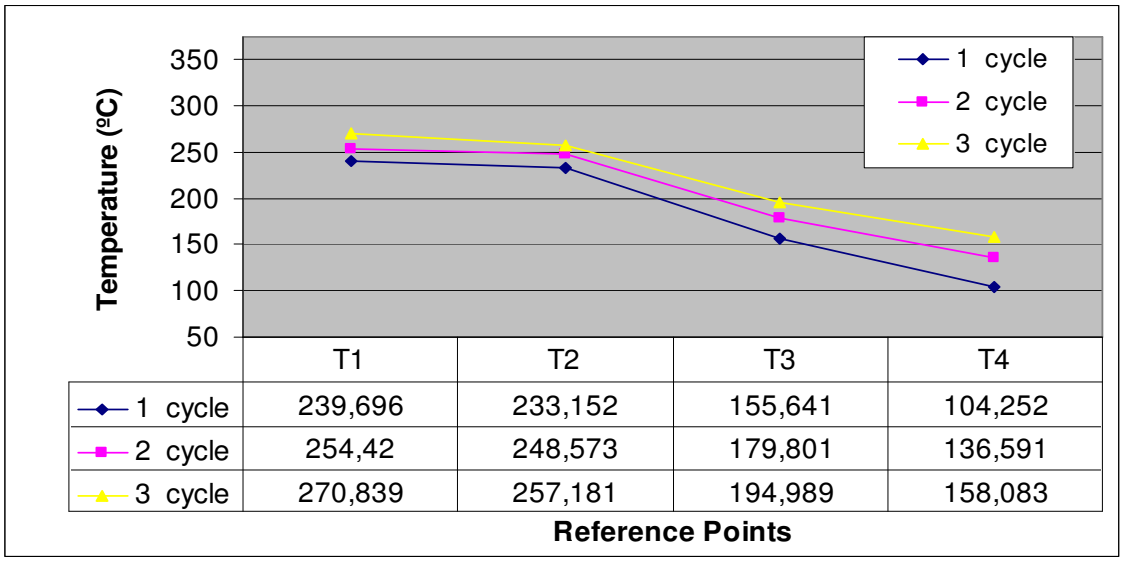

	T1	T2	T3	T4
1 cycle	239,696	233,152	155,641	104,252
2 cycle	254,42	248,573	179,801	136,591
3 cycle	270,839	257,181	194,989	158,083

Figure 7.7.2 Temperature profiles at reference points after welding in each cycle. Simulation conditions; 300 A, materials combination number 0, turbulent regime (15 l/min), collet with “becoming element of turbulence”, uniform temperature 298 K, diameter 3.2 mm, model C and welding time 3.5 min, cooling time is 6.5 min per cycle. Model C: long collet body with hollow handle.

Figure 7.7.2 illustrates that temperature increases at each point after each cycle. In addition, the temperature increase between the cycles is smaller as the cycle number rises. The increase between a cycle and next one must be equal to or less than 2 ºC before one hour of operation. After that time, the torch must reach a state of thermal equilibrium.

As can be found in Table 7.7.2, the Ansys model shows the tendency of the torch to reach the thermal equilibrium. The greatest temperature increase is between the first and second cycles and this is obtained at T4. This change in the temperature is reduced from 32.339 to 21.492 between the second and third cycle. It can be supposed that the temperature increase between the cycles is an arithmetic progression given by the following equation:

$$\Delta T_{n\to n+1} = \Delta T_{1\to 2} + (n-1)\cdot d \le 2 \qquad (7\text{-}1)$$

where $\Delta T_{n\to n+1}$ is the temperature increase between the nth and the n+1th cycle, in ºC; $\Delta T_{1\to 2}$ is the temperature increase between the first and the second cycle, in ºC; n is the cycle number, dimensionless; and d is the common difference of successive terms (d= $\Delta T_{2\to 3}$ - $\Delta T_{1\to 2}$), in ºC. *

The necessary cycle number to get the thermal equilibrium is obtained by next inequality:

$$\Delta T_{n\to n+1} = \Delta T_{1\to 2} + (n-1)\cdot d \le 2 \to 23.97 + (n-1)\cdot -8.87 \le 2 \to n \ge 3.48 \to n = 4$$

This means that the thermal equilibrium will be reached after the fourth cycle. As one cycle is 10 min, it will be reached after 40 min.

Table 7.7.2 Temperature increase between cycles: $\Delta T_{1\to 2}$ between the first and the second cycle; $\Delta T_{2\to 3}$ between the second and the third cycle.

	$\Delta T_{1\to 2}$	$\Delta T_{2\to 3}$
	(ºC)	(ºC)
T1	14.724	16.419
T2	15.421	8.608
T3	24.16	15.188
T4	32.339	21.492

*It is used the average of temperature increase between cycles at the reference points.

Figure 7.7.3, on the following page, shows the temperature profile at the reference point, T2 (torch head), for a simulation with 3 cycles that had a 35% duty cycle applied to one of the cycles.

Note that there are kind of three waves. Each wave is a cycle (i.e. 3.5 minutes of welding and 6.5 minutes of cooling). The ascent of the wave belongs to the temperature increases observed during the welding time and the descent of the wave to the temperature decreases observed during the cooling time.

Three points have been marked in the graph; they correspond to the temperatures in Kelvin at T2 at the end of each of the welding phases of the cycle. Note how the temperature keeps increasing even after the electric arc has been stopped. The temperatures continue to rise due to accumulation of energy in the tip of the cathode. This energy is transferred upward. The increase continues for around 20 seconds, after which the temperatures start to fall.

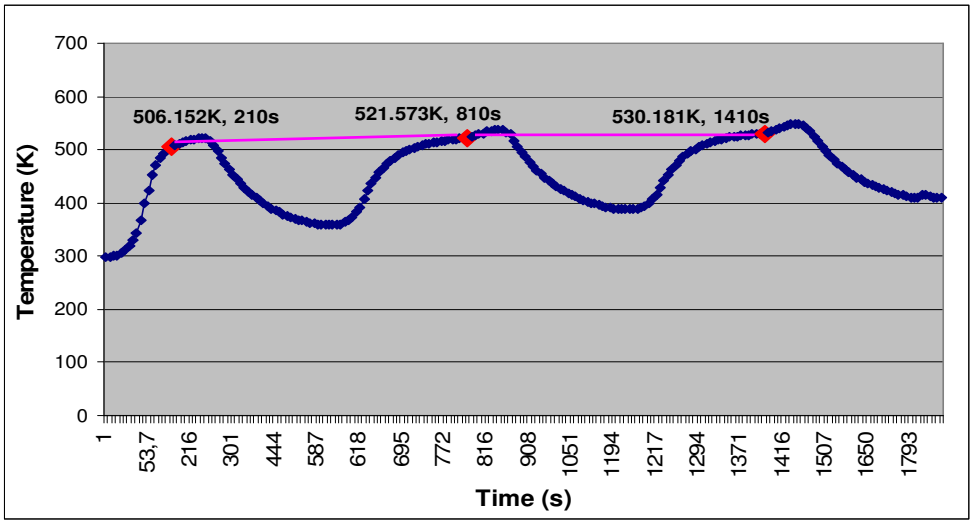

Figure 7.7.3 Temperature profile at reference point T2 after welding three times for 3.5 min. Simulation conditions; 300 A, materials combination number 0, turbulent regime (15 l/min), collet with “becoming element of turbulence”, uniform temperature 298 K, diameter 3.2 mm, model C, 3 cycles and welding time 3.5 min, cooling time is 6.5 min per cycle. Model C: long collet body with hollow handle.

The curve for the first cycle (first 10 min) is sharper than for the rest cycles due to specific heat of power cable is bigger at first cycle. That is, the power cable is able to absorb more energy.

If the atmospheric conditions change, the temperatures after the welding phase of each cycle also vary, as Figure 7.7.4 shows. It can be seen that temperature increase between both blocks per cycle is on average 23 ºC. The same result was also obtained in Section 7.6; the increase here was approximately 25 ºC.

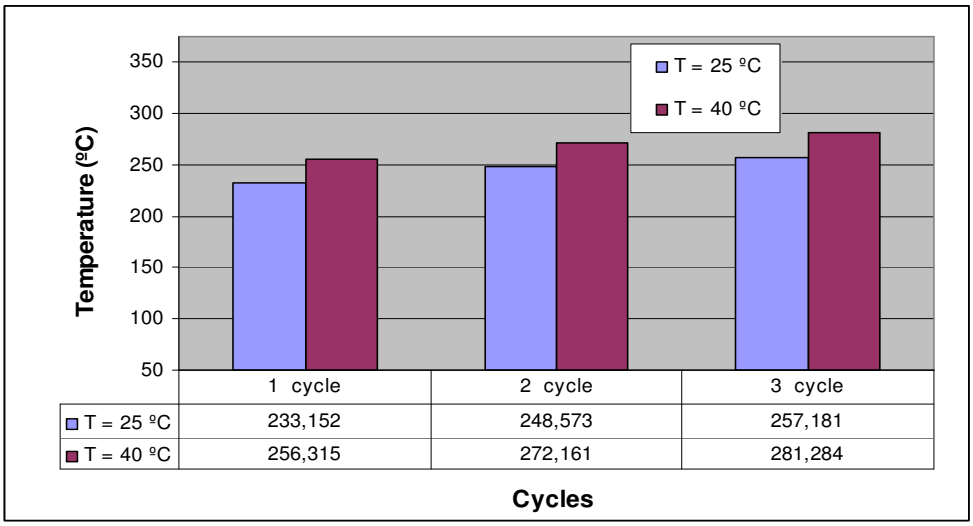

Figure 7.7.4 Block diagram at reference point T2 for different atmospheric temperature after welding three times for 3.5 min. Simulation conditions; 300 A, materials combination number 0, turbulent regime (15 l/min), collet with "becoming element of turbulence", diameter 3.2 mm, model C, 3 cycles and welding time 3.5 min, cooling time is 6.5 min per cycle. Model C: long collet body with hollow handle.

In Figure 7.7.5, the temperature profiles at the different reference points are shown.

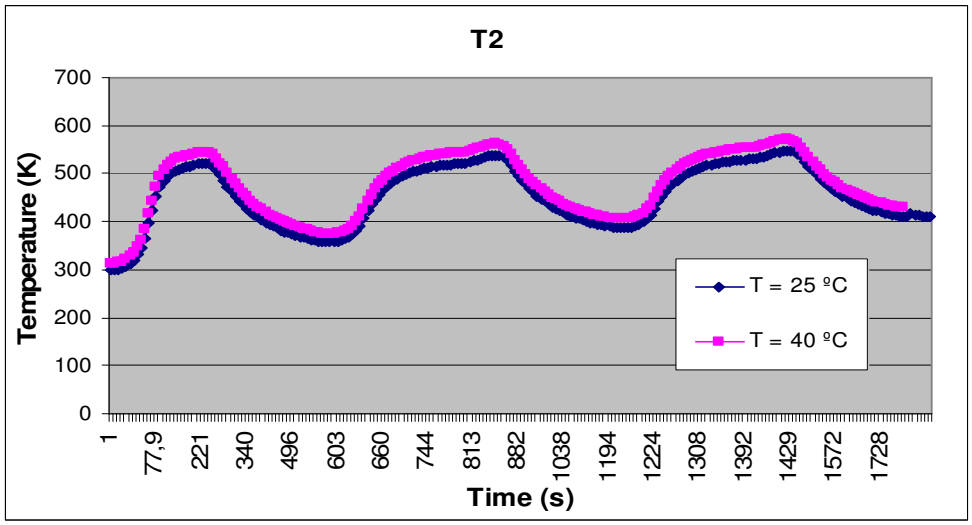

(a)

Figure 7.7.5 Temperature profile for different atmospheric temperature after welding three times for 3.5 min at reference points: (a) T2; (b) T3 (c) T4. Simulation conditions; 300 A, materials combination number 0, turbulent regime (15 l/min), collet with "becoming element of turbulence", uniform, diameter 3.2 mm, model C, 3 cycles and welding time 3.5 min, cooling time is 6.5 min per cycle. Model C: long collet body with hollow handle.

Note that the amplitude in the waves or temperature oscillations at T4 is not as strong as the other reference points. However, the temperature increase between cycles at T4 is greater than the other points. This means that the rate temperatures decrease is much slower for T4 over the cooling time than the rate of temperature change observed for the associated temperature increase during the welding time.

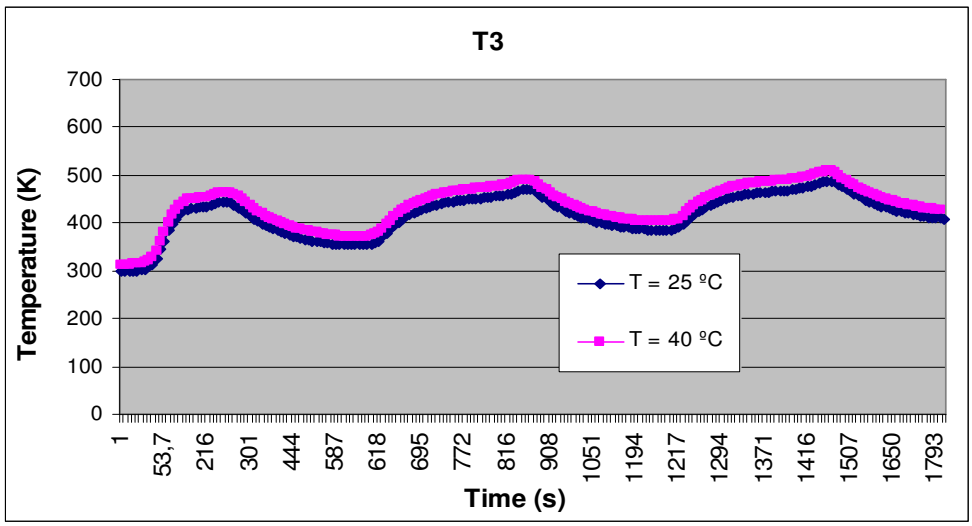

(b)

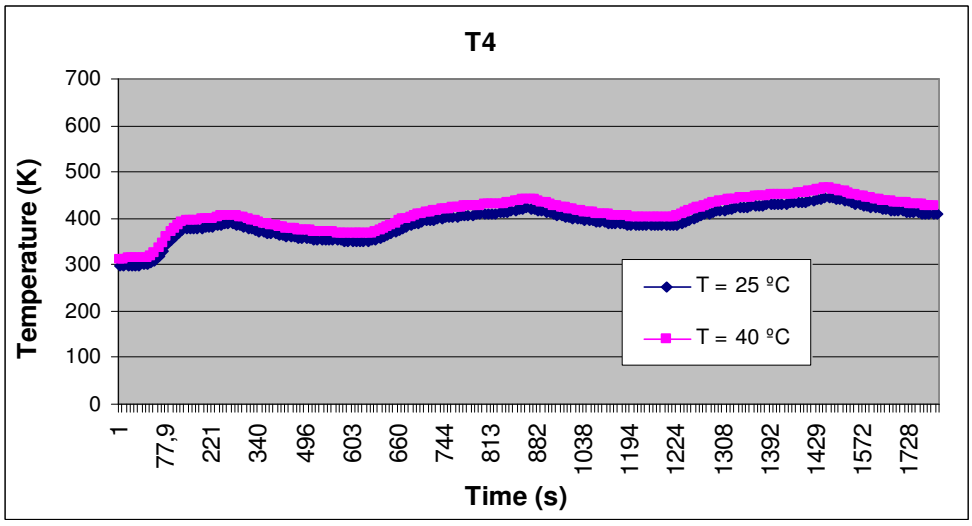

(c)

Figure 7.7.5 Continued. Temperature profile for different atmospheric temperature after welding three times for 3.5 min at reference points: (a) T2; (b) T3 (c) T4. Simulation conditions; 300 A, materials combination number 0, turbulent regime (15 l/min), collet with “becoming element of turbulence”, uniform, diameter 3.2 mm, model C, 3 cycles and welding time 3.5 min, cooling time is 6.5 min per cycle. Model C: long collet body with hollow handle.

CHAPTER 8

RESULTS DISCUSSION

8 RESULTS DISCUSSION

Four finite element models of a common GTAW torch were built:

(1) geometry A: long collet body and solid handle;
(2) geometry B: short collet body and solid handle;
(3) geometry C: long collet body and hollow handle;
(4) geometry D: short collet body and hollow handle.

Some of the influential variables of the welding process were simulated. Such variables include: geometry, materials used, current flow, volume flow rate, electrode diameter, atmospheric temperature and duty cycle. The results in Sections 6 and 7 are summarized in this chapter:

Geometry

At present, GTAW torch manufacturers produce a torch configuration with a hollow handle. The results of the experimental and numerical investigation supported this approach to designing the torch; the configuration with a solid handle (geometry A and B) showed around 27% higher temperatures in the handle zone than the configuration with the hollow handle (geometry C and D). The bigger transversal surface of the solid handle caused less thermal resistance, this involved that the heat flow toward the power cable was bigger. Another reason is that cooling at the handle by convection with argon caused the temperatures decrease as compared with solid handle.
It was also found that a GTAW torch whose geometry has long collet body (geometry A and C) gives 31% higher temperatures than geometry with short collet body (geometry B and D). Therefore, the heat transferred with the long collet body was greater than that with shorter collet body.
According to experimental and simulation results, the worst configuration was geometry A, because it had the highest temperatures at all the reference points. The geometry with the lowest temperature in the handle zone is model D. Such low temperatures in the handle are necessary to comply with safety regulations. DIN EN 60974-7 set that any point of torch handle must have a temperature in range $[T_a , T_a + 30]$ where T_a is the atmospheric temperature.

Materials

In general, substituting pieces of the torch made with copper to steel caused a decrease in the estimated temperatures. The biggest temperature reduction was produced by changing the collet body. The steel has less thermal conductivity than copper. This bigger heat resistance causes a thermal block of the heat at the collet body. The heat transfer toward up the torch is slower. The effect is that temperatures at reference points with steel collet body are smaller.

Replacing the internal block or external block material from copper to steel also caused a temperature decrease. Their effects were depreciable in comparison with temperature decrease produced by changing collet body material from copper to steel. In addition, using a steel external block causes the temperature reductions to be more significant than when using an internal steel block. The steel internal block had higher temperatures than the external steel block as its heat resistance was smaller than external block due to the internal block being the thinner of the two.

Aluminium is not a suitable material for substituting copper in the collet body. It was simulated as a material combination. Even though the temperature profile was lower than with copper, it was found that the aluminum collet body exceeded its melting point at the bottom of the collet body.

Another option would be to use aluminium for both the internal and external blocks. It was achieved the same temperatures as with copper. Yet the cost will be lower, because the price of aluminium is cheaper than copper. Another advantage is that the torch weight is also decreased; as aluminium density is lower than copper. The weight reduction can therefore improve the handling of the torch and the welder will feel less discomfort after welding for long time periods.

Nowadays, there are some GTAW torches with head (internal block and external block) made with brass. The simulation results supported the use of brass. The simulations with a brass head obtained temperatures that are similar to the simulation with a copper head. However, their prices are quite different. Economically, substituting the head material from copper to brass is profitable; since copper in metal market is becoming expensive and the brass, an alloy of copper and zinc, is cheaper.

Current

Electrical current causes two effect in the torch; first, joule heating is generated due to materials resistance to the electrical current running through them. Second, the electrical current influences on electric arc. The amount of energy produced by the arc is proportional to the electrical current. If it increases, the energy increases too. The simulations results indicated that the model is not sensitive to the second effect. The model was just able to measure an increase of 4 º C due to joule heating.

Diameter

The electrode diameter had an important effect on temperature profiles of GTAW torch. The temperatures rose as diameter increased. Heat flow that gets in the torch through the arc is bigger as diameter increases (bigger diameter, less heat resistance, bigger heat flow). The results seem indicate that smaller diameters are better than larger diameters because the observed temperatures are lower. However, using too much current is a major cause of excessive electrode consumption when the diameter size is wrong. The effect of current on the tip of the cathode was not modeled here. Therefore, the models are not sensitive to electrode deterioration.

.

Volumetric Flow Rate

It was obtained that using a "becoming element of turbulence" at collet reduces 24% the temperatures by increasing cooling capability of the shielding gas. The temperature reduction was 54% greater when it was used this element with turbulent regime.

Temperature

The results for the simulation of atmospheric conditions indicated that the temperature had influence on temperature profiles along the torch. The temperature in the torch was raised by around 25 ºC when the atmospheric temperature was increased by 15 ºC ($\Delta T_{torch} = 1.65 \cdot \Delta T_a$). To design a welding torch correctly, this effect must be considered, as it may be possible that such an increase of temperature could occur when the welding torch is operated in hot environments. For the opposite case, when in the torch is exposed to cold environments, a decrease from the temperature profile at the standard atmospheric temperature (25ºC) is observed.

Duty cycle

The models were simulated for different duty cycles of 35% and 60%. The results showed that the temperatures rose with longer duty cycles. The average increase in temperature over the increase from 35 to 60% was 13ºC.

It was observed that the models showed a tendency to achieve thermal equilibrium after 40 min of welding using the 35 % duty cycle and that the maximum temperature at reference points was not reached when the electric arc was stopped; the maximum temperature was reached around 20 seconds after the arc current was switched off. It was only after this lag time that temperatures started to fall. The temperature increase between cycles was smaller as the cycle number was raised.

The curve for the first cycle (first 10 min) is sharper than for the rest cycles due to specific heat of power cable is bigger at first cycle.

CHAPTER 9

CONCLUSION

9 CONCLUSION

The increasing need for accuracy and precision in welding is a great strength of GTAW welding. Water-cooled and air-cooled GTAW torch produce high-quality welding. Regardless of the price of air-cooled GTAW's at one-half to one-third the cost of water-cooled torch, air-cooled GTAW's still have weaknesses in welding industry due to its small power range and possible elements overheating.

The aim of the project was to study possible solutions in order to develop an air-cooled GTAW torch that is more competitive in the hard industrial market by improving its cooling capability.

A finite element model was used to examine such solutions. It was found from simulating the torches that there are many variables that can positively or negatively influence the welding process.

The materials used were one of the parameters. Studying the replacement of common copper elements with materials such as aluminium or steel indicated reduced temperature profiles. The simulations concluded some of the new material combinations for air-cooled GTAW torch that might be of interest. For example a steel collet body could be used instead of conventional copper elements. The substitution causes a general temperature reduction along the torch, allowing using more power to be used. In the same direction, using a steel torch head (external and internal block) decreases temperatures, but its effect is smaller than using steel collet body.

If a reduction in the weight of the torch is required, an aluminium torch head would be a good option. The temperature profiles obtained from the simulations of an aluminium torch head did not significantly differ from the simulation with a copper torch head. However, it is interesting due to two factors; the density and the price of aluminium. Aluminium's lower density decreases the torch weight, making the torch more manoeuvrable and reducing operator fatigue.

The second factor, price, is also important since copper the current high demand for copper has lead to high prices. This is not the case for aluminium and as a result the price is much lower. Thus, using this material for the head would be a good way to save money.

Another option to build torches with the same effectiveness and with lower costs would be to use brass in the torch head. The simulations showed that temperatures with a brass torch head were similar to a copper torch. Using brass instead copper for torch head reduces material costs, as again brass is currently cheaper than copper.

It was obtained by simulations that an aluminium collet body can not be used because the temperatures at the bottom of the collet body exceeded its melting point.

The model can be used to estimate temperature increases due to changes to atmospheric conditions or duty cycle of the torch.

The geometry is another factor that must be considered as it influences the temperature profiles. The simulations indicated that the optimal configuration was with using a hollow handle with short collet body.

A “becoming element of turbulence” was used for the hollow handle and short collet body configuration to examine the effect of the flow regime on cooling. . It was put into the collet and hollow handle. The results indicated that this element made temperatures decrease. The temperature reduction was further improved when a turbulent regime was applied. Thus, using turbulence increases the cooling capability of shielding gas.

Finally, the work developed in the report represents the first step to build future and better GTAW torch models. Such improvements may be to include mathematical models of radiation and fluids analysis. A mathematical model could be developed that characterizes the sensitivity of the electrode tip deterioration and electric effects by modelling mathematical equation of the arc. These new models will be fundamental to understand the parameters that affect arc-welding and to offer manufacturers insights into making welding machines that are more effective.

BIBLIOGRAPHY

BOOKS

[1] R. L. O'Brien, *Jefferson's Welding Encyclopedia*, American Welding Society, Miami, 1997.

[2] P. C. Rodríguez, *Manual de Soldadura*, Alsina, Buenos Aires, 2001.

[3] J. R. Welty, C. E. Wicks, R. E. Wilson, and G. Rorrer, *Fundamentals of Momentum, Heat, and Mass Transfer*, Wiley Book Company, New York, 2000.

[4] A. Bejan, *Convection Heat Transfer*, Wiley Book Company, New York, 2004.

[5] M. Mier, *Electrical Resistivity as a Function of Temperature*, Department of Chemical Engineering and Material Science, University of California, Davis, September 13 2004.

[6] CRC Handbook of Chemistry and Physics, CRC Press, Florida, 1984-1985, pages F114-120.

[7] Ansys Multyphysics Release 10 Documentation, Ansys Inc.

[8] S. Moaveni, *Finite Element Analysis: Theory and Application with Ansys*, Prentice Hall, New Jersey, 1999.

[9] A. J. Chapman, *Transmisión del calor*, Interciencia, Madrid, 1977.

[10] A. Herranz, "Lecciones de transmisión de calor", UPCT, 2003.

[11] J. Huhn, *Lehrveranstaltung Technische thermodynamic*, Institut für Thermodynamik und Technische Gebäudeausrüstung, TUD, 2003.

[12] A. B. Murphy and C. J. Arundell, *Transport coefficients of Argon, Nitrogen, Oxygen, Argon-Nitrogen and Argon-Oxygen Plasmas, Plasma Chemistry and Plasma Processing*, Vol. 14 No. 4 1994.

[13] S. W. Churchill and H. H. S. Chu, *Int. J. Heat & Mass Tr.*, 18, 1323, 1975.

[14] F. N. Sieder and G. E. Tate, *Ind. Eng. Chem.*, 28, 1429, 1936.

[15] F. W. Dittus and L. M. K. Boelter, University of California, Publ. Eng., 2, 443, 1930.

[16] J. Storer and J. H. Haynes, *The Haynes Welding Manual*, Haynes Publishing Group, California, 1994.

TECHNICAL ARTICLES

[17] ISO 4063.

[18] S. Harshad, *Gun Control: GTAW torch design innovations enhance productivity, quality*, November 15, 2001 PRACTICAL WELDING TODAY®.

[19] J. Haidar and A. J. D. Farmer, *Surface temperature measurements for tungsten-based cathodes of high-current free-burning arcs*, 9 May 1995, CSIRO Division of Applied Physics, Australia.

[20] P. J. Li and Y. M. Zhang, *Analysis of an Arc Light Mechanism and Its Application in Sensing of the GTAW Process*, September 2000, Center for Robotics and Manufacturing Systems and Electrical Engineering Department, University of Kentucky.

[21] A. Shacklock, L. Hong, H. Sheng, J. W Jie, *Intelligent Robotic GTAW System for 3D Welding*, 2001, Automated Material Processing Group, Automation Technology Division, Singapore Institute of Manufacturing Technology.

[22] M. Goodarzi, R. Choo and J. M. Toguri, *The effect of the cathode tip angle on the GTAW arc and weld pool: Mathematical model of the arc*, 26 June 1997, Department of Metallurgy and Materials Science, University of Toronto.

WEBPAGES

[23] www.thefabricator.com/ArcWelding/ArcWelding_TechCell.cfm

[24] www.arczone.com

[25] www.mece.ualberta.ca/tutorials/ansys/

[26] www.wikipedia.com

[27] www.twi.co.uk

FIGURE INDEX

PICTURE INDEX

TABLE INDEX

APPENDIX A

EXPERIMENTAL RESULTS*

1 GEOMETRY INFLUENCE

1.1 Experiment 1

1.1.1 Parameters

Table A-1.1.1 Parameters of Experiment 1.

	Model C	Material	Features
Accessories	Back cap	Steel	-
	Back cap insulator	Teflon	-
	Collet	Copper	length: long type: without BET*
	Collet body	Steel	length: long
	Coupler handle/cable	Copper	-
	Electrode	Tungsten	diameter: 2.4 mm length: 65 mm number: 1
	External block	Copper	-
	Handle	Copper	type: hollow
	Internal block	Steel	-
	Nozzle	Alumina	number: 6
	Torch body	Teflon	-
Intensity	150 A		
Gas	argon flow: 10 l/ min		laminar
Geometry	distance workpiece - electrode		5 mm
	distance electrode - nozzle		5 mm
Welding time	3’5 min	1 cycle	

* BET means “becoming element of turbulence”.

1.1.2 Results

Table A-1.1.2 Results of Experiment 1.

	T1	T2	T3	T4
Model C	(K)	(K)	(K)	(K)
measurement 1	133.3	100.6	76.88	59.71

1.1.3 Commentaries

- Collet appearance: it has a small deformation.
- Collet body appearance: it is normal, good.
- Electrode appearance: the electrode kept a good condition except at the point, there is no peak. It didn't darken so much.
- Nozzle appearance: it was melted a little at the down border, also there is some metal drops on the wall.

1.1.4 Pictures

The experiment 1 was made to check that everything was right. It didn't take pictures of electrode number 1.

1.2 Experiment 2

1.2.1 Parameters

Table A-1.2.1 Parameters of Experiment 2.

	Model C	Material	Features
Accessories	Back cap	Steel	-
	Back cap insulator	Teflon	-
	Collet	Copper	length: long type: without BET
	Collet body	Steel	length: long
	Coupler handle/cable	Copper	-
	Electrode	Tungsten	diameter: 2.4 mm length: 65 mm number: 5
	External block	Copper	-
	Handle	Copper	type: hollow
	Internal block	Steel	-
	Nozzle	Alumina	number: 6
	Torch body	Teflon	-
Intensity	150 A		
Gas	argon flow: 10 l/ min		laminar
Geometry	distance piece - electrode		5 mm
	distance electrode - nozzle		5 mm
Welding time	3’5 min	1 cycle	

1.2.2 Results

Table A-1.2.2 Results of Experiment 2.

	T1	T2	T3	T4
Model C	(K)	(K)	(K)	(K)
measurement 1	168.9	124.5	93.36	65.49
measurement 2	168.5	131.3	98.95	69.75
measurement 3	165.6	128.4	98.33	66.87

1.2.3 Commentaries

- Collet appearance: good status.
- Collet body appearance: its condition is good; there were drops in interior wall.
- Electrode appearance: it got dark and the spike was broken.
- Nozzle appearance: there were many drops on the wall.

1.2.4 Pictures

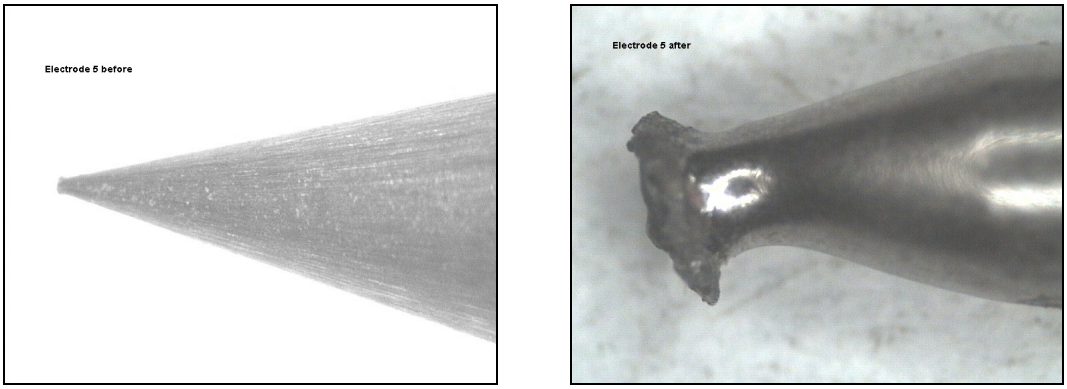

(a) (b)

Picture A-1.2.1 Electrode 5 used for experiment number 2: (a) before welding; (b) after welding.

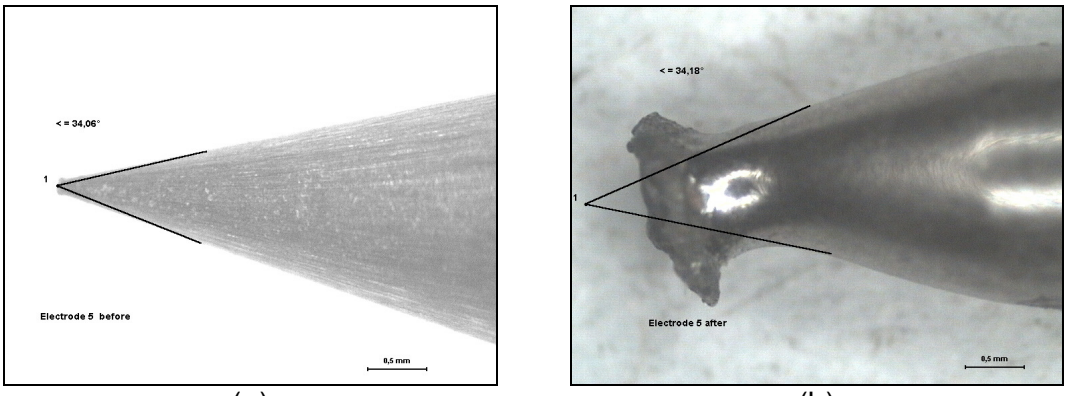

(a) (b)

Picture A-1.2.2 Angle of Electrode 5 used for experiment number 2: (a) before welding < = 34.06 º; (b) after welding >> 34 º.

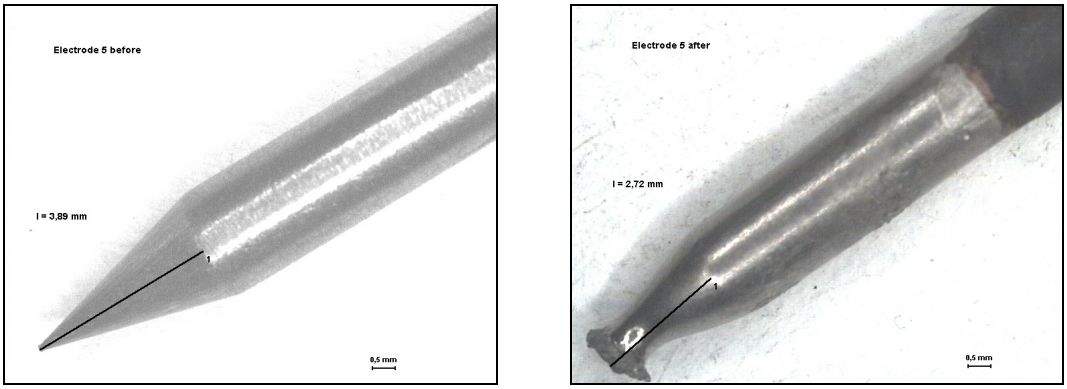

(a) (b)

Picture A-1.2.3 Cone height of Electrode 5 used for experiment number 2: (a) before welding l = 3.89 mm; (b) after welding l = 2.72 mm.

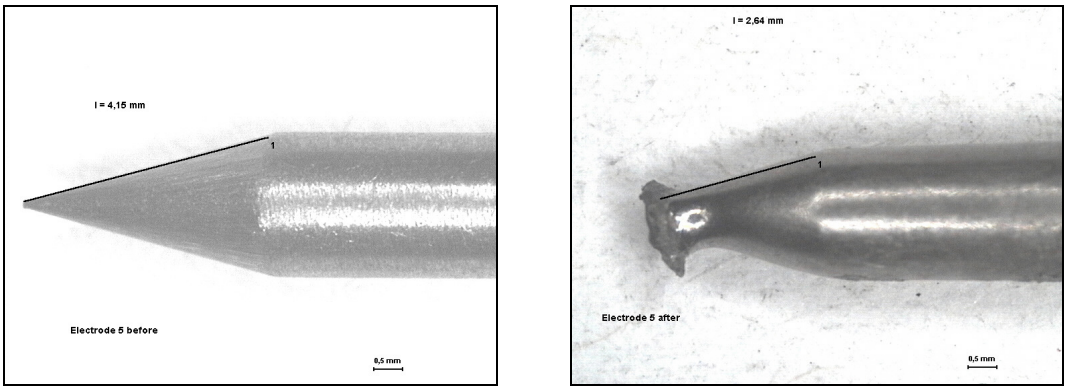

(a) (b)

Picture A-1.2.4 Cone hypotenuse of Electrode 5 used for experiment number 2: (a) before welding l = 4.15 mm; (b) after welding l = 2.64 mm.

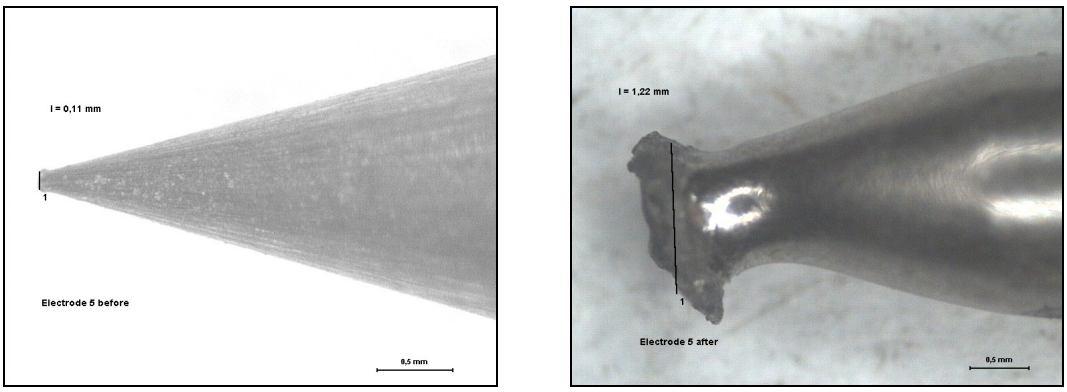

(a) (b)

Picture A-1.2.5 Spike of Electrode 5 used for experiment number 2: (a) before welding l = 0.11 mm; (b) after welding l = 1.22 mm.

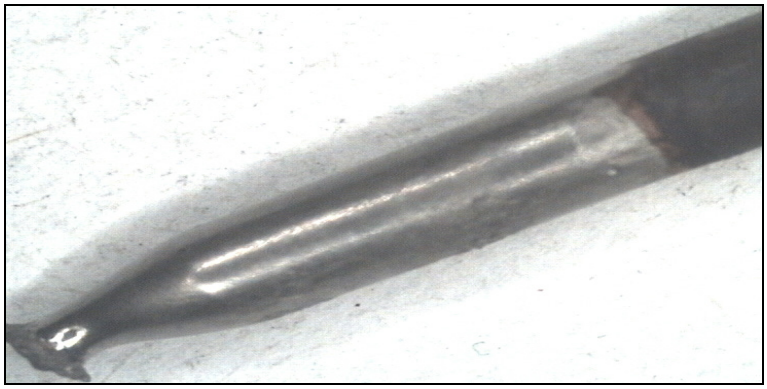

Picture A-1.2.6 Status of Electrode 5 used for experiment number 2 after welding three times during 3.5 min.

1.3 Experiment 3

1.3.1 Parameters

Table A-1.3.1 Parameters of Experiment 3.

	Model A	Material	Features
Accessories	Back cap	Steel	-
	Back cap insulator	Teflon	-
	Collet	Copper	length: long type: without BET
	Collet body	Steel	length: long
	Coupler torch/gas pipe	Brass	-
	Coupler handle/cable	Copper	-
	Electrode	Tungsten	diameter: 2.4 mm length: 64 mm number: 2
	External block	Copper	-
	Handle	Copper	type: solid
	Internal block	Steel	-
	Nozzle	Alumina	number: 6
	Torch body	Teflon	-
Intensity	150 A		
Gas	argon flow: 10 l/ min		laminar
Geometry	distance piece - electrode		5 mm
	distance electrode - nozzle		5 mm
Welding time	3’5 min	1 cycle	

1.3.2 Results

Table A-1.3.2 Results of Experiment 3.

	T1	T2	T3	T4
Model A	(K)	(K)	(K)	(K)
measurement 1	137.1	105.0	93.36	77.40
measurement 2	130.8	100.2	91.27	75.54
measurement 3	138.7	111.8	103.6	86.11

1.3.3 Commentaries

- Collet appearance: it had a big deformation.
- Collet body appearance: its condition was not good because it was melted a little.
- Electrode appearance: On wall of the spike there were many drops coming from the liquid metal.
- Nozzle appearance: many drops on interior wall.

1.3.4 Pictures

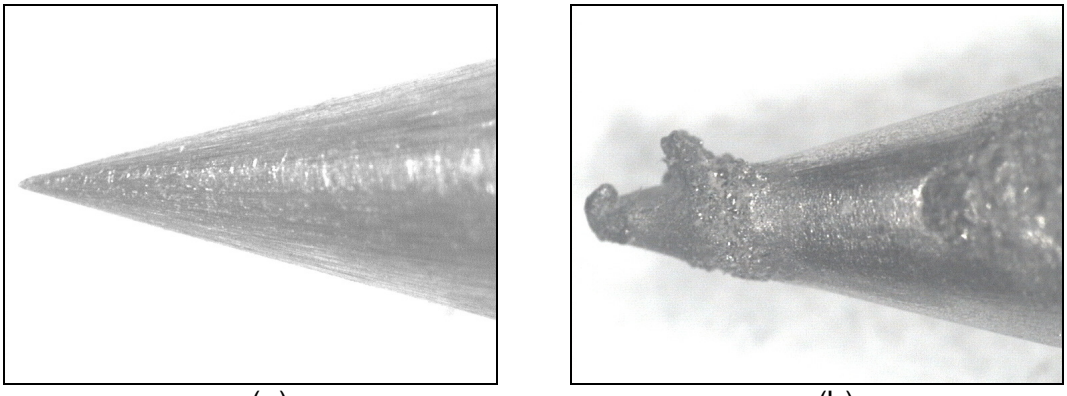

(a) (b)

Picture A-1.3.1 Electrode 2 used for experiment number 3: (a) before welding; (b) after welding.

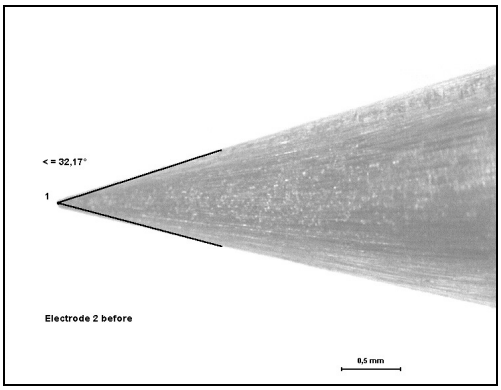

(a)

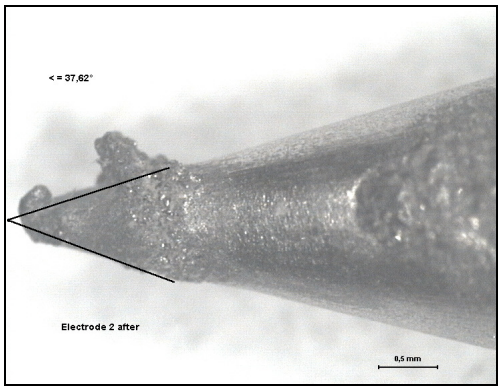

(b)

Picture A-1.3.2 Angle of Electrode 2 used for experiment number 3: (a) before welding < = 32.17 º; (b) after welding < = 37.62 º.

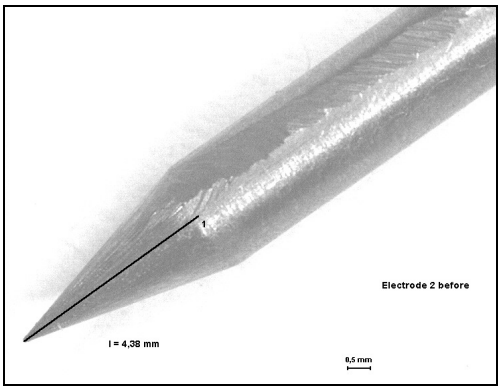

(a)

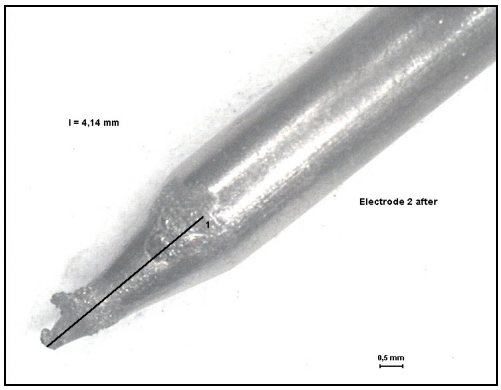

(b)

Picture A-1.3.3 Cone height of Electrode 2 used for experiment number 3: (a) before welding l = 4.38 mm; (b) after welding l = 4.14 mm.

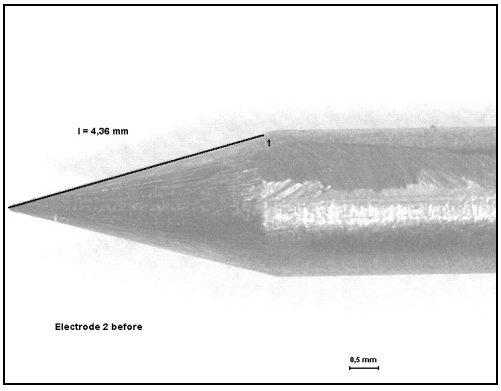

(a)

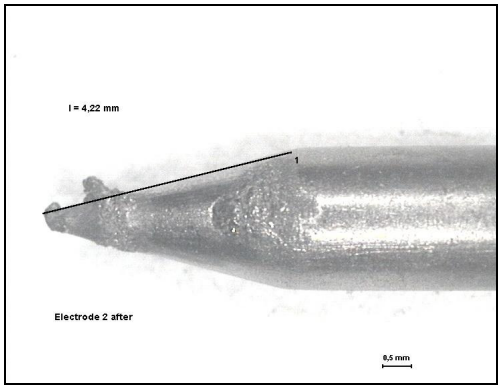

(b)

Picture A-1.3.4 Cone hypotenuse of Electrode 2 used for experiment number 3: (a) before welding l = 4.36 mm; (b) after welding l = 4.22 mm.

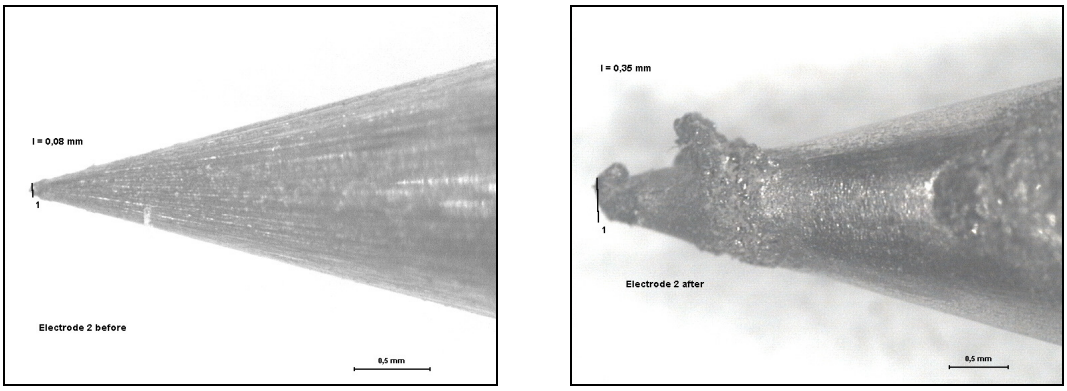

(a) (b)

Picture A-1.3.5 Spike of Electrode 2 used for experiment number 3: (a) before welding l = 0.08 mm; (b) after welding l = 0.35 mm.

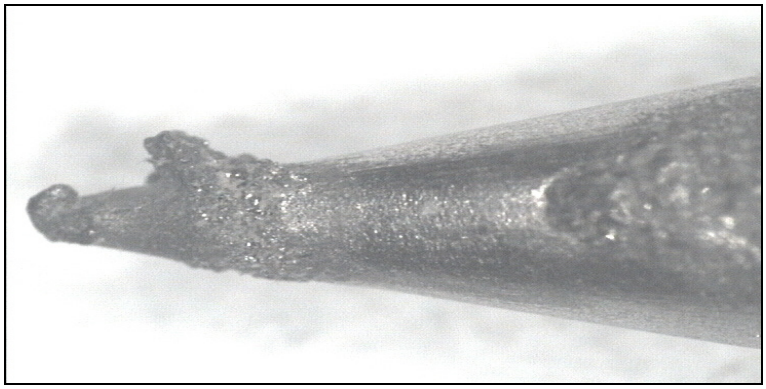

Picture A-1.3.6 Status of Electrode 2 used for experiment number 3 after welding three times during 3.5 min.

1.4 Experiment 4

1.4.1 Parameters

Table A-1.4.1 Parameters of Experiment 4.

	Model D	Material	Features
Accessories	Back cap	Steel	-
	Back cap insulator	Teflon	-
	Collet	Copper	length: short type: without BET
	Collet body	Steel	length: short
	Coupler handle/cable	Copper	-
	Electrode	Tungsten	diameter: 2.4 mm length: 65 mm number: 3
	External block	Copper	-
	Handle	Copper	type: hollow
	Internal block	Steel	-
	Nozzle	Alumina	number: 6
	Torch body	Teflon	-
Intensity	150 A		
Gas	argon flow: 10 l/ min		laminar
Geometry	distance piece - electrode		5 mm
	distance electrode - nozzle		5 mm
Welding time	3’5 min	1 cycle	

1.4.2 Results

Table A-1.4.2 Results of Experiment 4.

	T1	T2	T3	T4
Model D	(K)	(K)	(K)	(K)
measurement 1	157.4	107.4	86.13	61.78
measurement 2	162.2	114.7	90.12	64.18
measurement 3	166.2	118.0	97.05	71.72

1.4.3 Commentaries

- Collet appearance: really good condition; there is no damaged.
- Collet body appearance: its condition is good.
- Electrode appearance: the spike is so damaged, however there are no drops on its.
- Nozzle appearance: no change.

1.4.4 Pictures

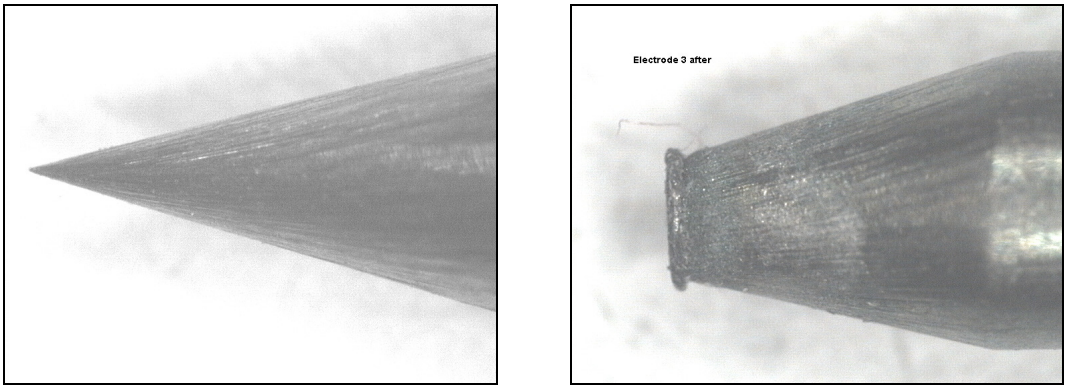

(a) (b)

Picture A-1.4.1 Electrode 3 used for experiment number 4: (a) before welding; (b) after welding.

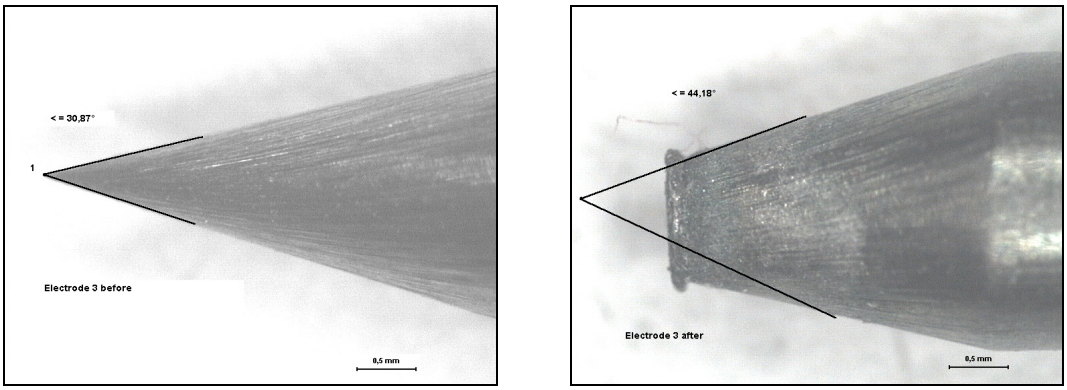

(a) (b)

Picture A-1.4.2 Angle of Electrode 3 used for experiment number 4: (a) before welding < = 30.87 º; (b) after welding < = 44.18 º.

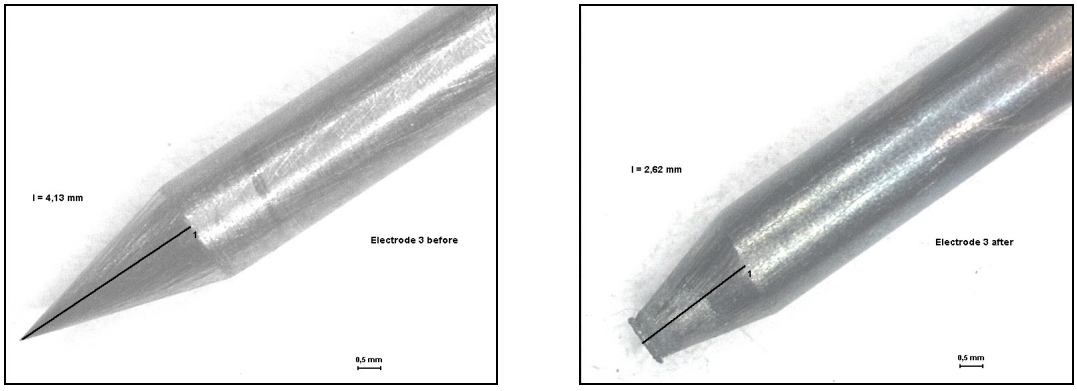

(a) (b)

Picture A-1.4.3 Cone height of Electrode 3 used for experiment number 4: (a) before welding l = 4.13 mm; (b) after welding l = 2.62 mm.

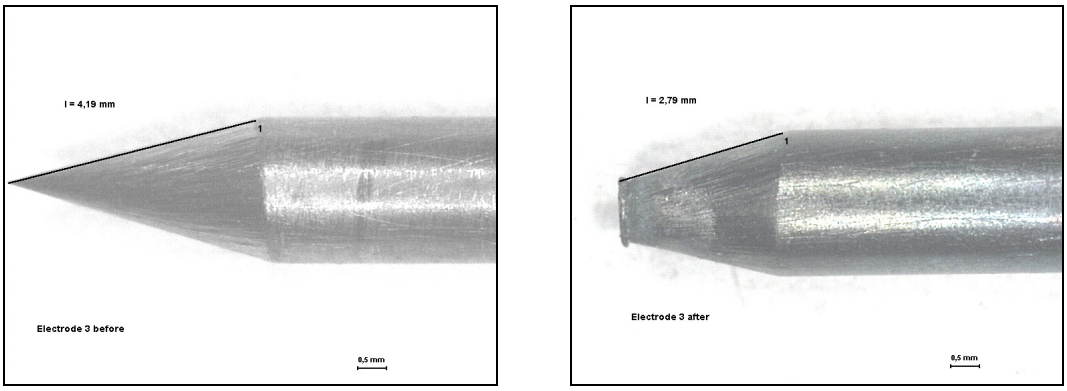

(a) (b)

Picture A-1.4.4 Cone hypotenuse of Electrode 3 used for experiment number 4: (a) before welding l = 4.19 mm; (b) after welding l = 2.79 mm.

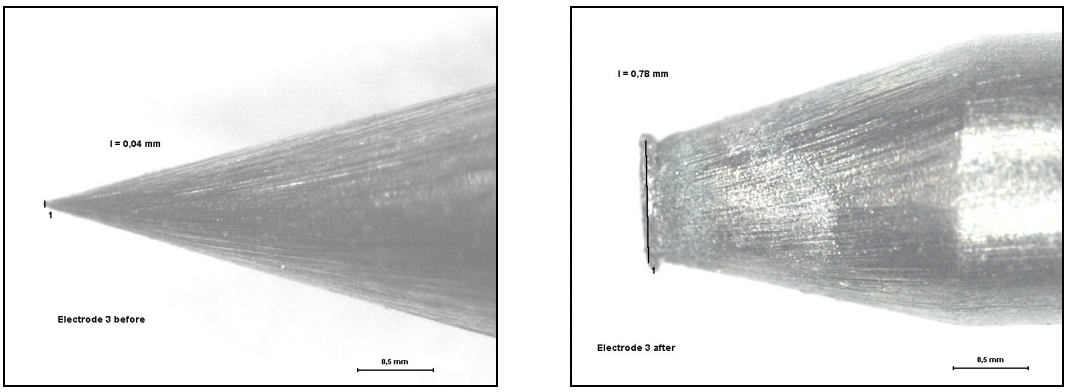

(a) (b)

Picture A-1.4.5 Spike of Electrode 3 used for experiment number 4: (a) before welding l = 0.04 mm; (b) after welding l = 0.78 mm.

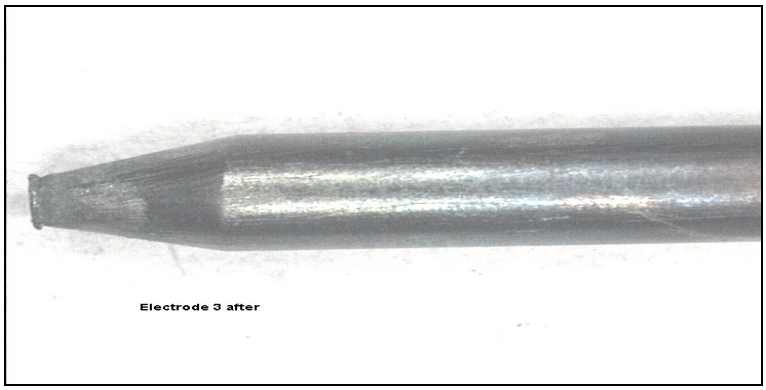

Picture A-1.4.6 Status of Electrode 3 used for experiment number 4 after welding three times during 3.5 min.

1.5 Experiment 5

1.5.1 Parameters

Table A-1.5.1 Parameters of Experiment 5.

	Model B	Material	Features
Accessories	Back cap	Steel	-
	Back cap insulator	Teflon	-
	Collet	Copper	length: short type: without BET
	Collet body	Steel	length: short
	Coupler torch/gas pipe	Brass	-
	Coupler handle/cable	Copper	-
	Electrode	Tungsten	diameter: 2.4 mm length: 65 mm number: 4
	External block	Copper	-
	Handle	Copper	type: solid
	Internal block	Steel	-
	Nozzle	Alumina	number: 6
	Torch body	Teflon	-
Intensity	150 A		
Gas	argon flow: 10 l/ min		laminar
Geometry	distance piece - electrode		5 mm
	distance electrode - nozzle		5 mm
Welding time	3’5 min	1 cycle	

1.5.2 Results

Table A-1.5.2 Results of Experiment 5.

Model B	T1 (K)	T2 (K)	T3 (K)	T4 (K)
measurement 1	145.4	93.29	87.24	73.33
measurement 2	160.8	105.6	99.96	84.23
measurement 3	176.9	113.9	102.8	86.56

1.5.3 Commentaries

- Collet appearance: there was almost no deformation; in general good condition.
- Collet body appearance: its condition was good, it didn't present any wear with respect of before experiment.
- Electrode appearance: the electrode was so blackened; there is no spike; there are no drops on interior wall.
- Nozzle appearance: no change.

1.5.4 Pictures

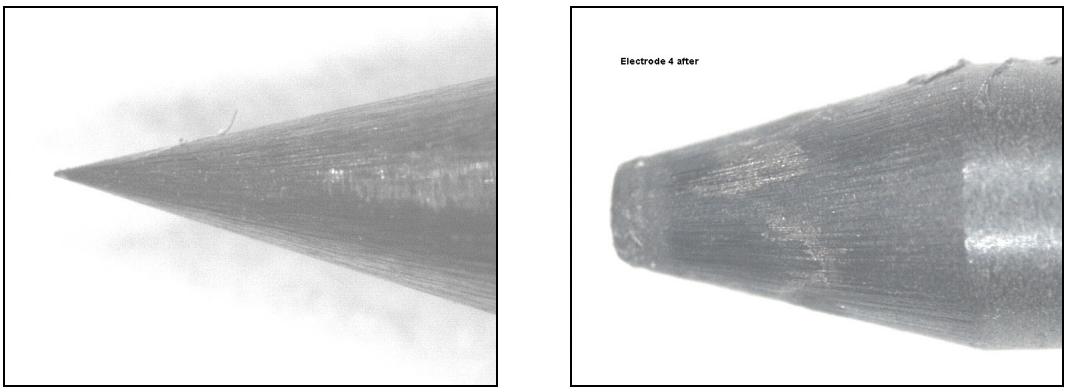

(a) (b)

Picture A-1.5.1 Electrode 4 used for experiment number 5: (a) before welding; (b) after welding.

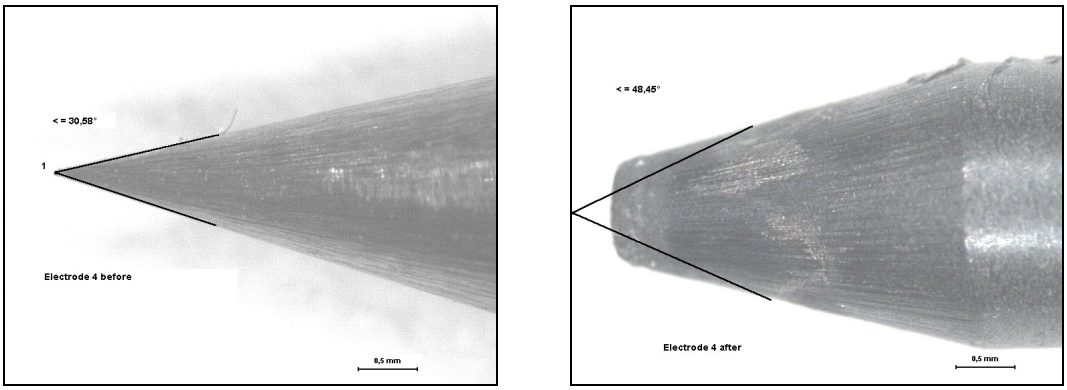

(a) (b)

Picture A-1.5.2 Angle of Electrode 4 used for experiment number 5: (a) before welding < = 30.58 º; (b) after welding < = 48.45 º.

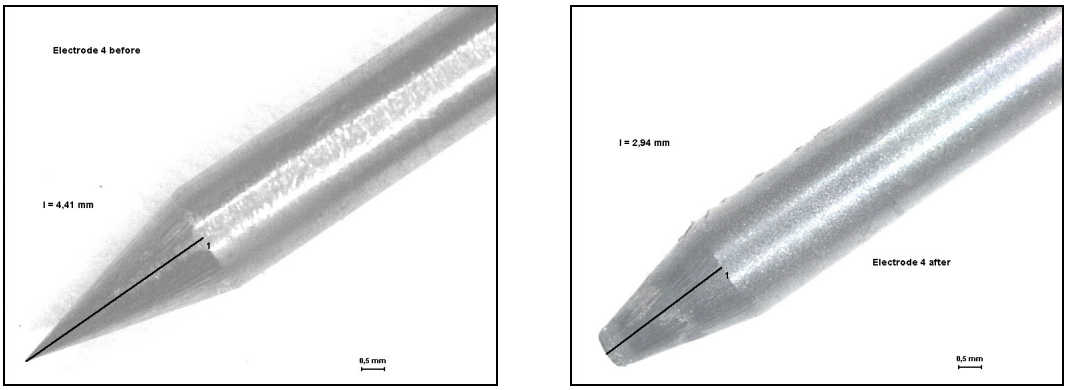

(a) (b)

Picture A-1.5.3 Cone height of Electrode 4 used for experiment number 5: (a) before welding l = 4.41 mm; (b) after welding l = 2.94 mm.

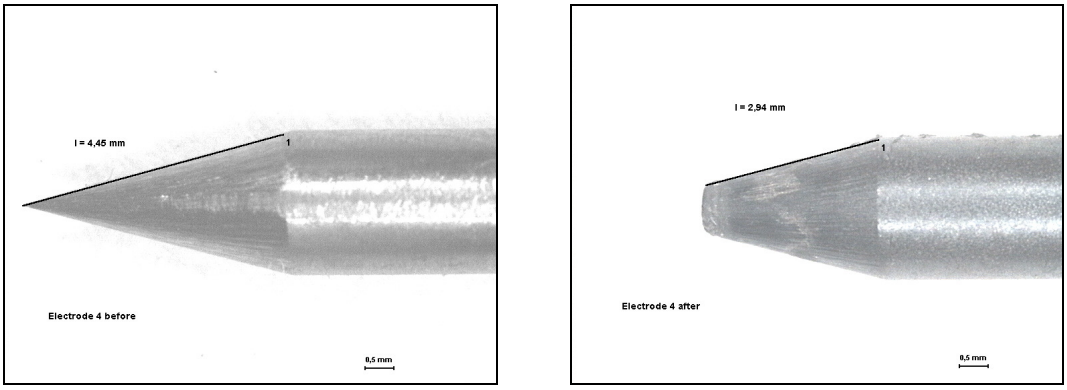

(a) (b)

Picture A-1.5.4 Cone hypotenuse of Electrode 4 used for experiment number 5: (a) before welding l = 4.45 mm; (b) after welding l = 2.94 mm.

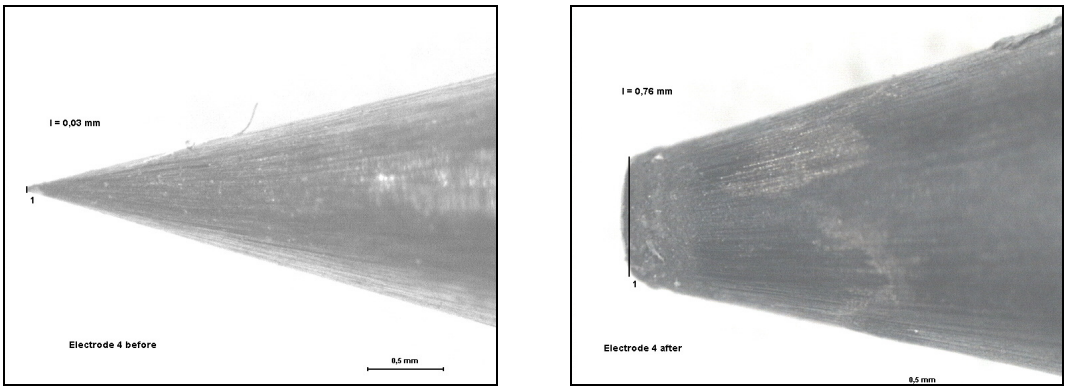

(a) (b)

Picture A-1.5.5 Spike of Electrode 4 used for experiment number 5: (a) before welding l = 0.03 mm; (b) after welding l = 0.76 mm.

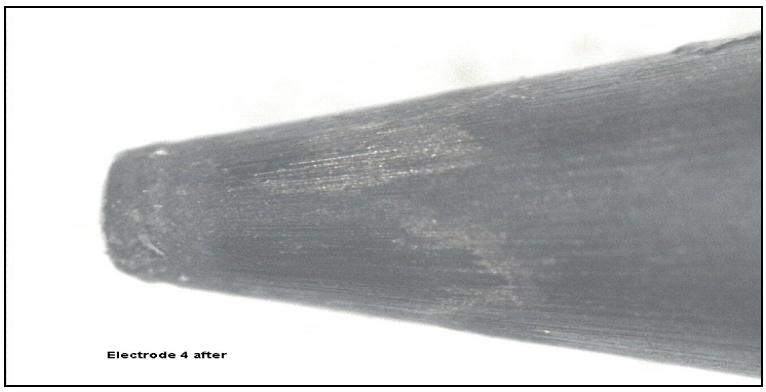

Picture A-1.5.6 Status of Electrode 4 used for experiment number 5 after welding three times during 3.5 min.

2 DIAMETER INFLUENCE

2.1 Experiment 6

2.1.1 Parameters

Table A-2.1.1 Parameters of Experiment 6.

	Model B	Material	Features
Accessories	Back cap	Steel	-
	Back cap insulator	Teflon	-
	Collet	Copper	length: short type: without BET
	Collet body	Steel	length: short
	Coupler torch/gas pipe	Brass	-
	Coupler handle/cable	Copper	-
	Electrode	Tungsten	diameter: 4 mm length: 65 mm number: 6
	External block	Copper	-
	Handle	Copper	type: solid
	Internal block	Steel	-
	Nozzle	Alumina	number: 6
	Torch body	Teflon	-
Intensity	150 A		
Gas	argon flow: 10 l/ min		laminar
Geometry	distance piece - electrode		5 mm
	distance electrode - nozzle		5 mm
Welding time	3’5 min	1 cycle	

2.1.2 Results

Table A-2.1.2 Results of Experiment 6.

	T1	T2	T3	T4
Model B	(K)	(K)	(K)	(K)
measurement 1	208.0	116.7	105.1	80.39
measurement 2	157.5	122.0	106.1	85.08
measurement 3	180.1	102.1	98.30	80.15

2.1.3 Commentaries

- Collet appearance: it hasn't suffered any deformation because of the heat, it wasn't melted.
- Collet body appearance: It got dark a little on the down part. It wasn't melted and there are no drops liquid metal on its.
- Electrode appearance: the electrode is totally blackened; there is still spike, there is some material on its.
- Nozzle appearance: good shape; there is no wear, just a little dirty.

2.1.4 Pictures

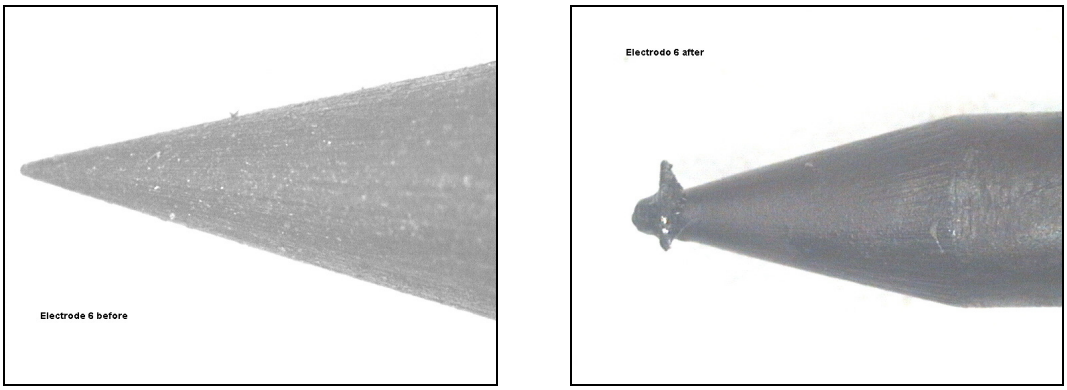

(a) (b)

Picture A-2.1.1 Electrode 6 used for experiment number 6: (a) before welding; (b) after welding.

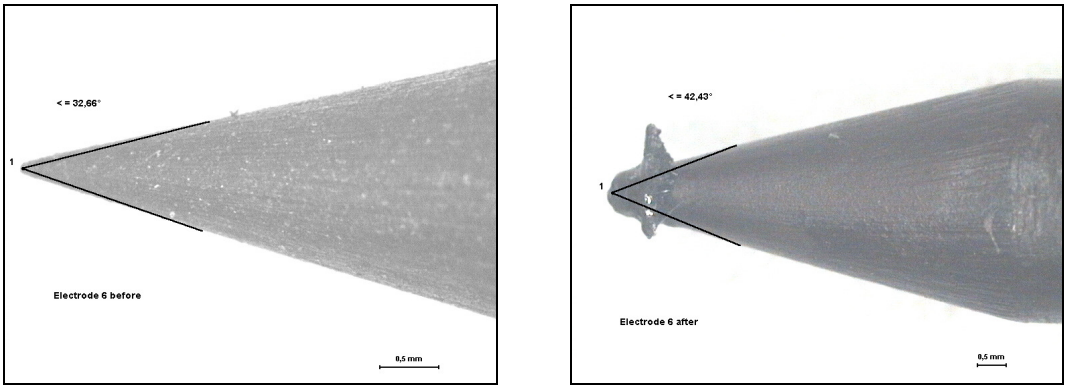

(a) (b)

Picture A-2.1.2 Angle of Electrode 6 used for experiment number 6: (a) before welding < = 32.66 º; (b) after welding < = 42.43 º.

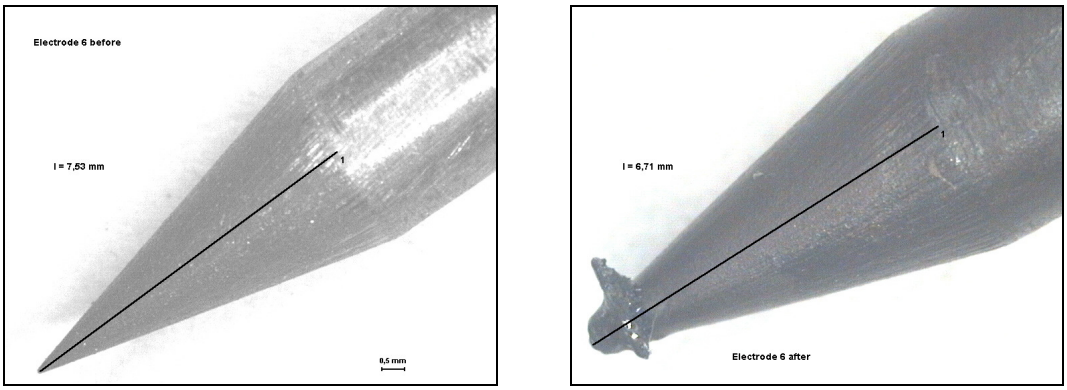

(a) (b)

Picture A-2.1.3 Cone height of Electrode 6 used for experiment number 6: (a) before welding l = 7.53 mm; (b) after welding l = 6.71 mm.

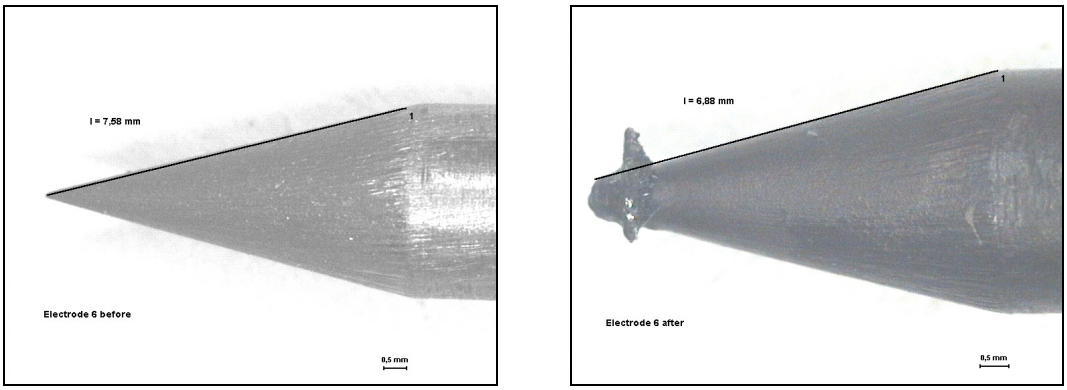

(a) (b)

Picture A-2.1.4 Cone hypotenuse of Electrode 6 used for experiment number 6: (a) before welding l = 7.58 mm; (b) after welding l = 6.88 mm.

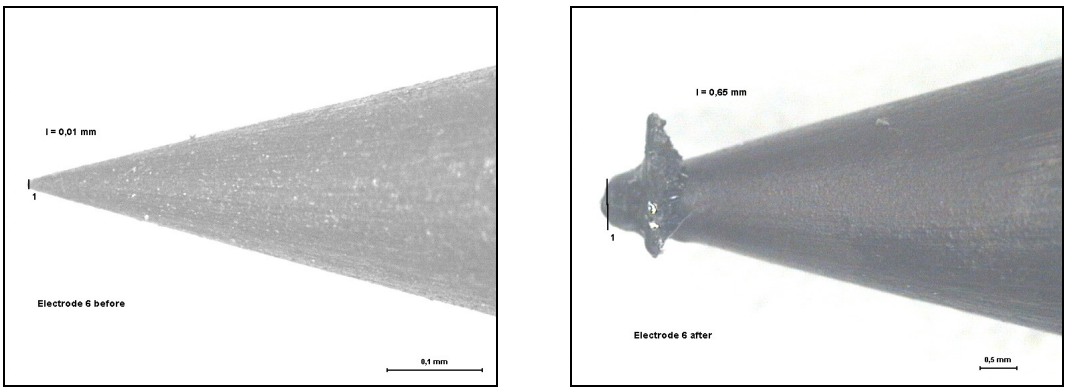

(a) (b)

Picture A-2.1.5 Spike of Electrode 6 used for experiment number 6: (a) before welding l = 0.01 mm; (b) after welding l = 0.65 mm.

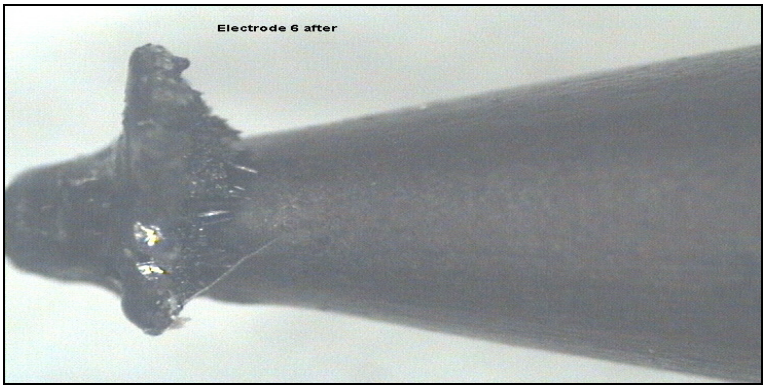

Picture A-2.1.6 Status of Electrode 6 used for experiment number 6 after welding three times during 3.5 min.

3 VOLUMETRIC FLOW RATE INFLUENCE

3.1 Experiment 7

3.1.1 Parameters

Table A-1.7.1 Parameters of Experiment 7.

	Model B	Material	Features
Accessories	Back cap	Steel	-
	Back cap insulator	Teflon	-
	Collet	Copper	length: short type: with BET
	Collet body	Steel	length: short
	Coupler torch/gas pipe	Brass	-
	Coupler handle/cable	Copper	-
	Electrode	Tungsten	diameter: 2.4 mm length: 65 mm number: 7
	External block	Copper	-
	Handle	Copper	type: solid
	Internal block	Steel	-
	Nozzle	Alumina	number: 6
	Torch body	Teflon	-
Intensity	150 A		
Gas	argon flow: 10 l/ min		laminar
Geometry	distance piece - electrode		5 mm
	distance electrode - nozzle		5 mm
Welding time	3’5 min	1 cycle	

3.1.2 Results

Table A-3.1.2 Results of Experiment 7.

Model B	T1 (K)	T2 (K)	T3 (K)	T4 (K)
measurement 1	148.8	90.44	85.55	70.90
measurement 2	161.7	102.0	94.57	78.29
measurement 3	190.3	109.2	103.1	84.55

3.1.3 Commentaries

- Collet appearance: perfect status.
- Collet body appearance: its condition is in general good; there are no drops in interior down wall, it wasn't melted. Just it has a little black coloring at the bottom part.
- Electrode appearance: the electrode shows blue coloration and the spike is completely trite.
- Nozzle appearance: no change.

3.1.4 Pictures

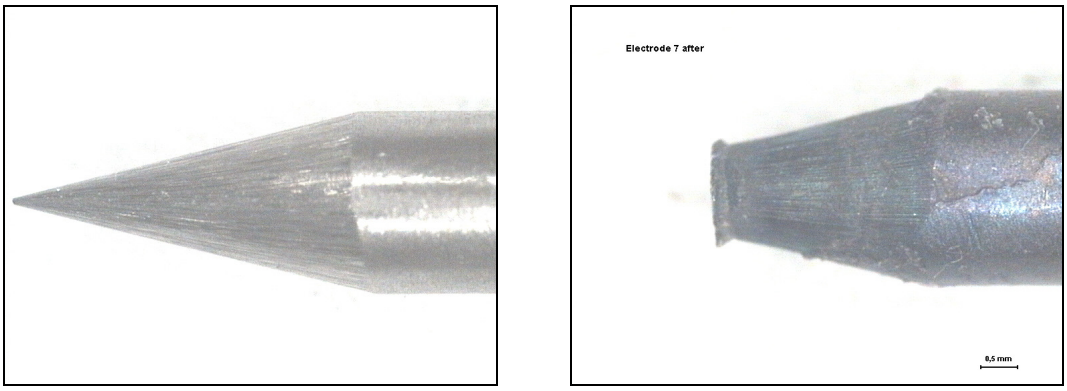

(a) (b)

Picture A-3.1.1 Electrode 7 used for experiment number 7: (a) before welding; (b) after welding.

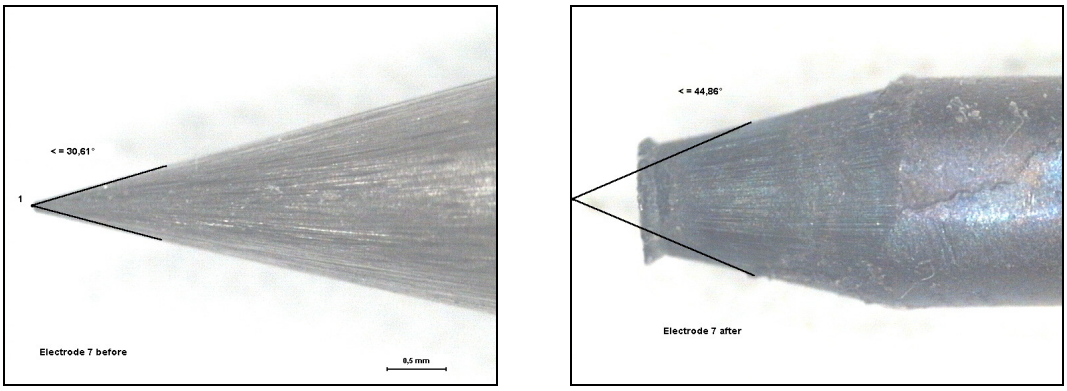

(a) (b)

Picture A-3.1.2 Angle of Electrode 7 used for experiment number 7: (a) before welding < = 30.61 º; (b) after welding < = 44.86 º.

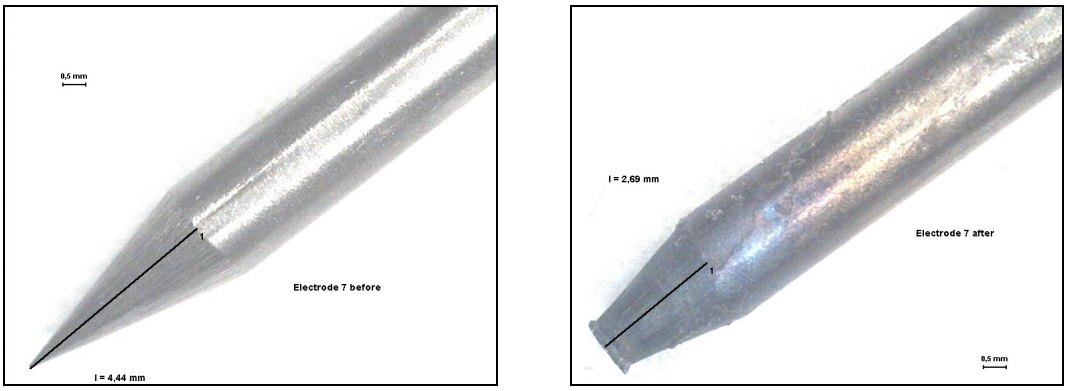

(a) (b)

Picture A-3.1.3 Cone height of Electrode 7 used for experiment number 7: (a) before welding l = 4.44 mm; (b) after welding l = 2.69 mm.

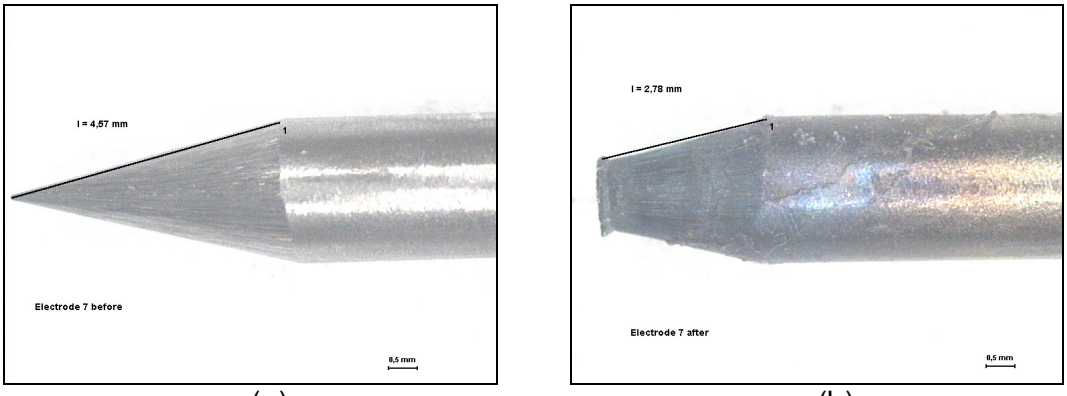

(a) (b)

Picture A-3.1.4 Cone hypotenuse of Electrode 7 used for experiment number 7: (a) before welding l = 4.57 mm; (b) after welding l = 2.78 mm.

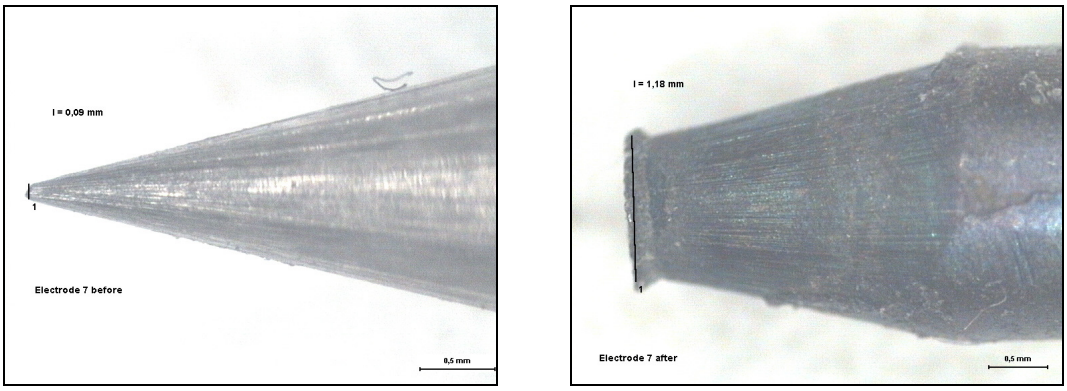

(a) (b)

Picture A-3.1.5 Spike of Electrode 7 used for experiment number 7: (a) before welding l = 0.09 mm; (b) after welding l = 1.18 mm.

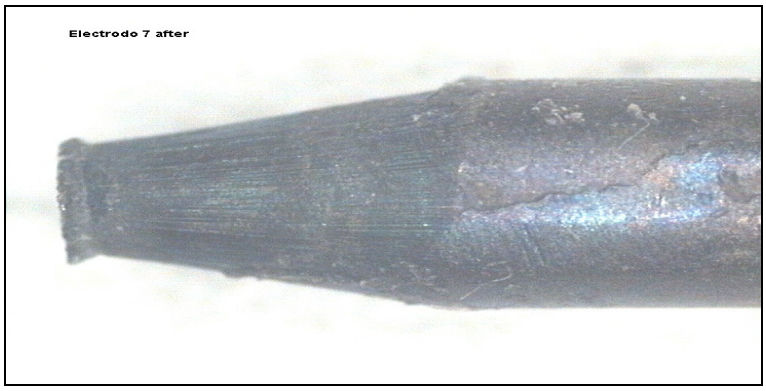

Picture A-3.1.6 Status of Electrode 7 used for experiment number 7 after welding three times during 3.5 min.

3.2 Experiment 8

3.2.1 Parameters

Table A-3.2.1 Parameters of Experiment 8.

	Model A	Material	Features
Accessories	Back cap	Steel	-
	Back cap insulator	Teflon	-
	Collet	Copper	length: long type: without BET
	Collet body	Steel	length: long
	Coupler torch/gas pipe	Brass	-
	Coupler handle/cable	Copper	-
	Electrode	Tungsten	diameter: 2.4 mm length: 65 mm number: 8
	External block	Copper	-
	Handle	Copper	type: solid
	Internal block	Steel	-
	Nozzle	Alumina	number: 6
	Torch body	Teflon	-
Intensity	150 A		
Gas	argon flow: 15 l/ min		turbulent
Geometry	distance piece - electrode		5 mm
	distance electrode - nozzle		5 mm
Welding time	3’5 min	1 cycle	

3.2.2 Results

Table A-3.2.2 Results of Experiment 8.

	T1	T2	T3	T4
Model A	(K)	(K)	(K)	(K)
measurement 1	184.8	124.0	110.1	81.93

3.2.3 Commentaries

- Collet appearance: it changed its color at its down part.
- Collet body appearance: there are some green drops on its interior wall.
- Electrode appearance: Just after welding once the electrode is totally damaged and it is impossible use it again. It shows really black color and the electrode lost its entire spike.
- Nozzle appearance: it reached so high temperatures than it was red.

3.2.4 Pictures

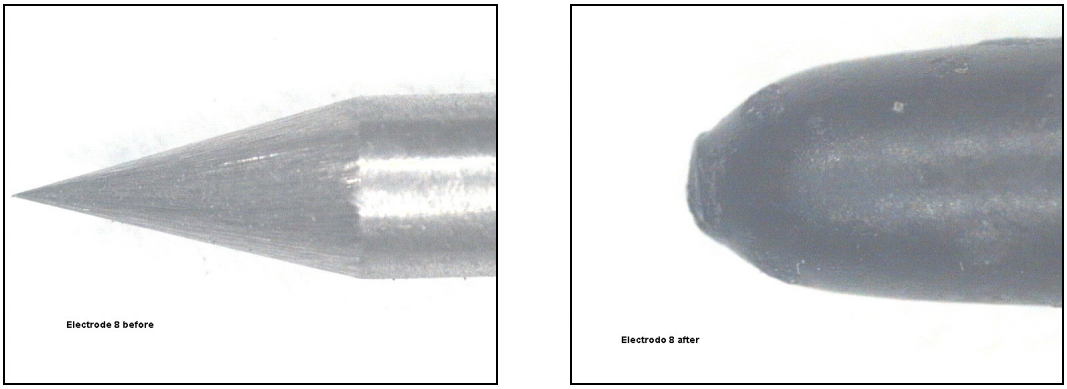

(a) (b)

Picture A-3.2.1 Electrode 8 used for experiment number 8: (a) before welding; (b) after welding.

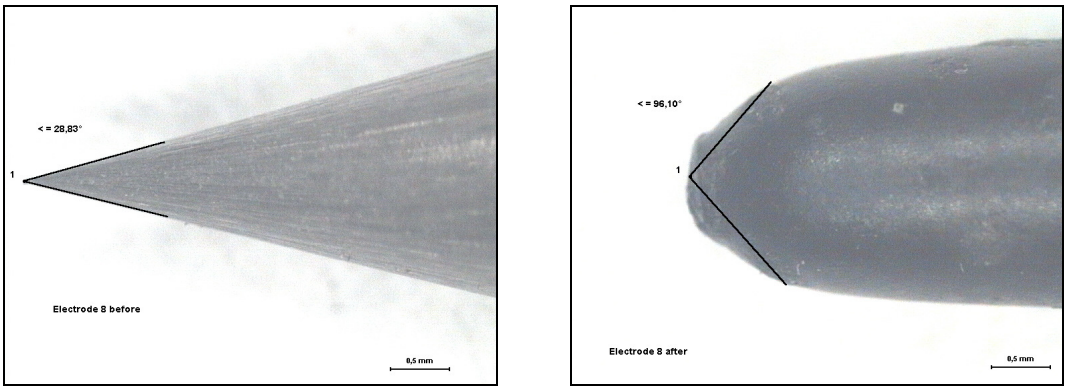

(a) (b)

Picture A-3.2.2 Angle of Electrode 8 used for experiment number 8: (a) before welding < = 28.83 º; (b) after welding < = 96.10 º.

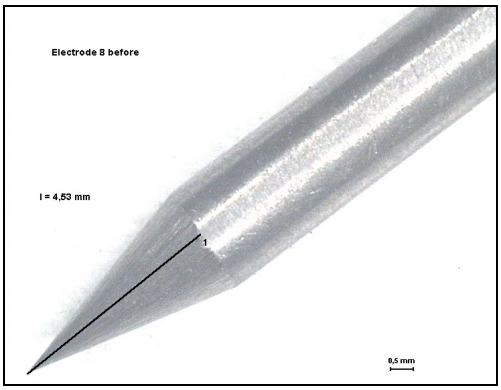

(a)

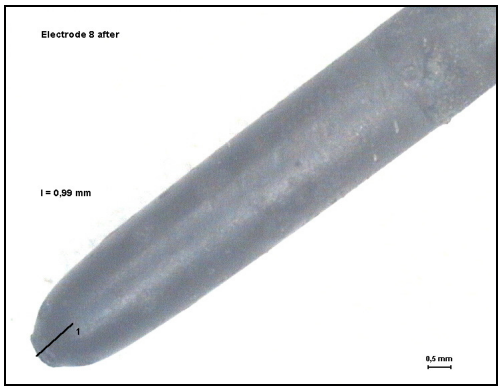

(b)

Picture A-3.2.3 Cone height of Electrode 8 used for experiment number 8: (a) before welding l = 4.53 mm; (b) after welding l = 0.99 mm.

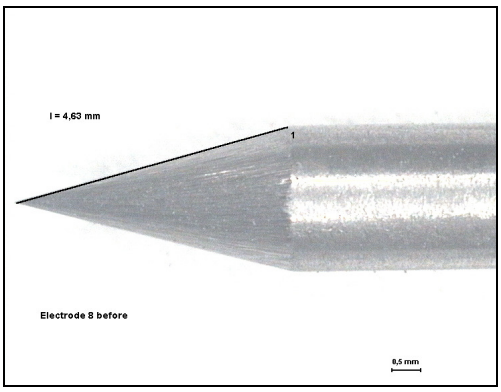

(a)

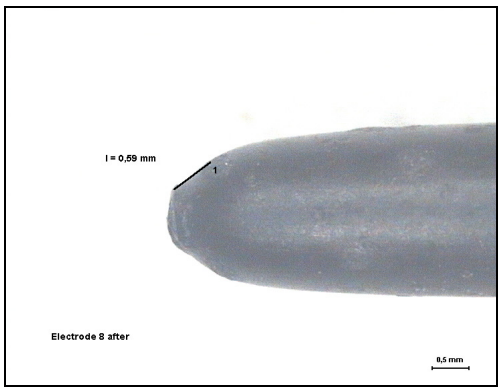

(b)

Picture A-3.2.4 Cone hypotenuse of Electrode 8 used for experiment number 8: (a) before welding l = 4.63 mm; (b) after welding l = 0.59 mm.

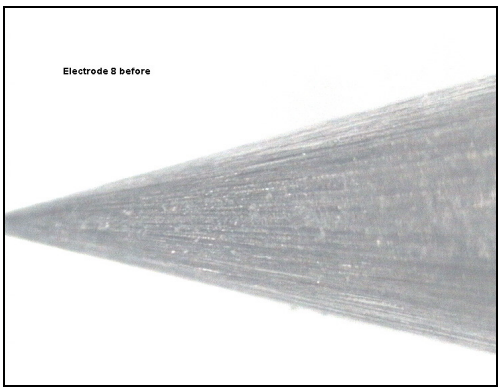

(a)

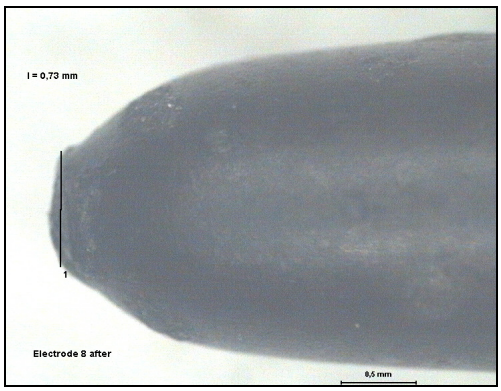

(b)

Picture A-3.2.5 Spike of Electrode 8 used for experiment number 8: (a) before welding l = 0.03 mm; (b) after welding l = 0.73 mm.

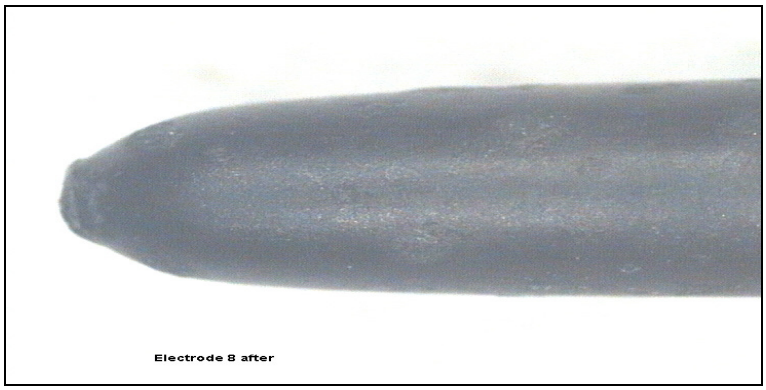

Picture A-3.2.6 Status of Electrode 8 used for experiment number 8 after welding once during 3.5 min.

3.3 Experiment 9

3.3.1 Parameters

Table A-3.3.1 Parameters of Experiment 9.

	Model A	Material	Features
Accessories	Back cap	Steel	-
	Back cap insulator	Teflon	-
	Collet	Copper	length: long type: with BET
	Collet body	Steel	length: long
	Coupler torch/gas pipe	Brass	-
	Coupler handle/cable	Copper	-
	Electrode	Tungsten	diameter: 2.4 mm length: 65 mm number: 9
	External block	Copper	-
	Handle	Copper	type: solid
	Internal block	Steel	-
	Nozzle	Alumina	number: 6
	Torch body	Teflon	-
Intensity	150 A		
Gas	argon flow: 15 l/ min		turbulent
Geometry	distance piece - electrode		5 mm
	distance electrode - nozzle		5 mm
Welding time	3’5 min	1 cycle	

3.3.2 Results

Table A-3.3.2 Results of Experiment 9.

	T1	T2	T3	T4
Model A	(K)	(K)	(K)	(K)
measurement 1	123.0	82.94	75.28	67.23

3.3.3 Commentaries

- Collet appearance: perfect condition.
- Collet body appearance: good status.
- Electrode appearance: there is deformation at the spike and the most important observation is there is much material on its. After using once the electrode was completely damaged, it was no possible to use again. The electric arc was irregular and too high.
- Nozzle appearance: no change.

3.3.4 Pictures

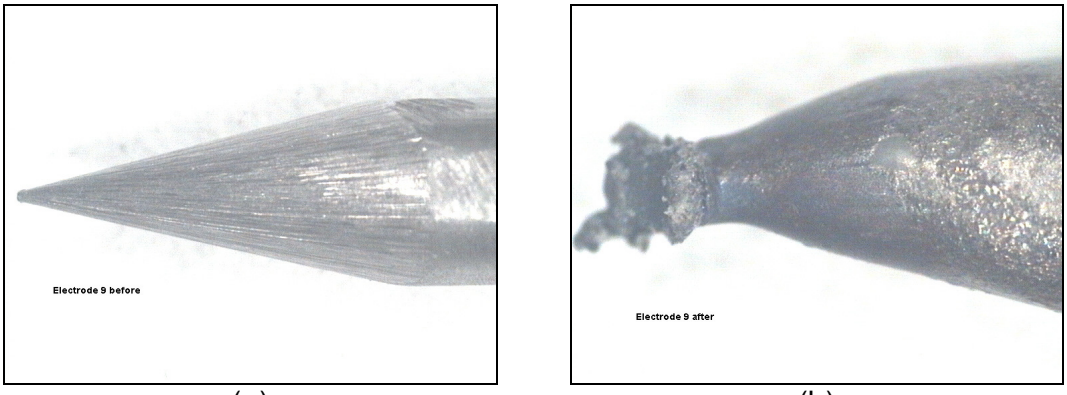

(a) (b)

Picture A-3.3.1 Electrode 9 used for experiment number 9: (a) before welding; (b) after welding.

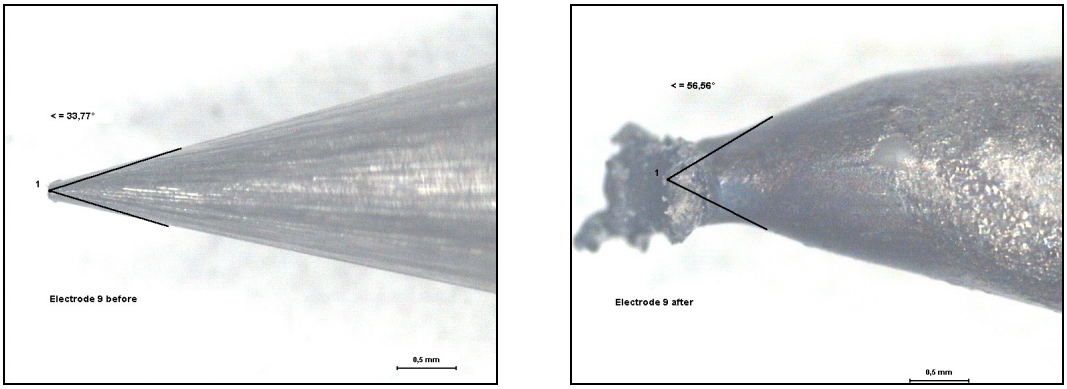

(a) (b)

Picture A-3.3.2 Angle of Electrode 9 used for experiment number 9: (a) before welding < = 33.77 º; (b) after welding < = 56.56 º.

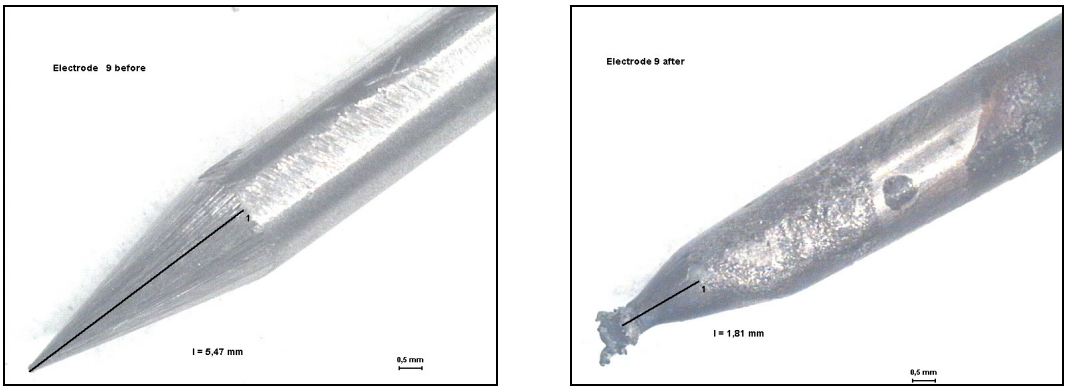

(a) (b)

Picture A-3.3.3 Cone height of Electrode 9 used for experiment number 9: (a) before welding l = 5.47 mm; (b) after welding l = 1.81 mm.

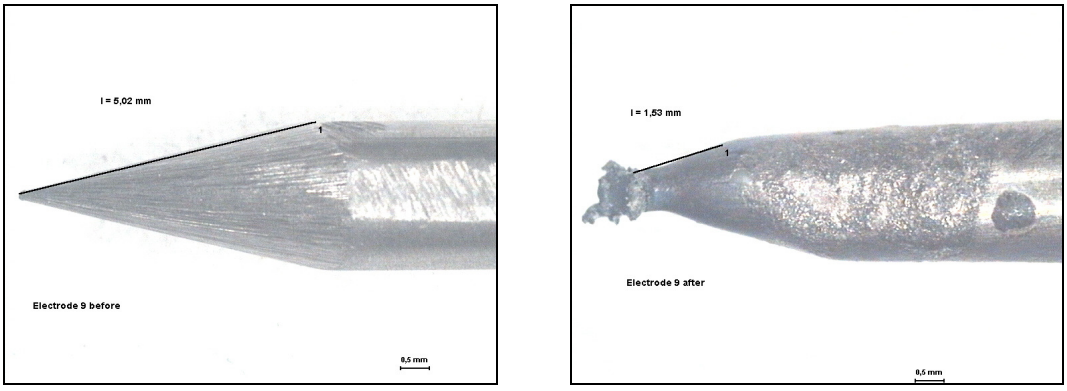

(a) (b)

Picture A-3.3.4 Cone hypotenuse of Electrode 9 used for experiment number 9: (a) before welding l = 5.02 mm; (b) after welding l = 1.53 mm.

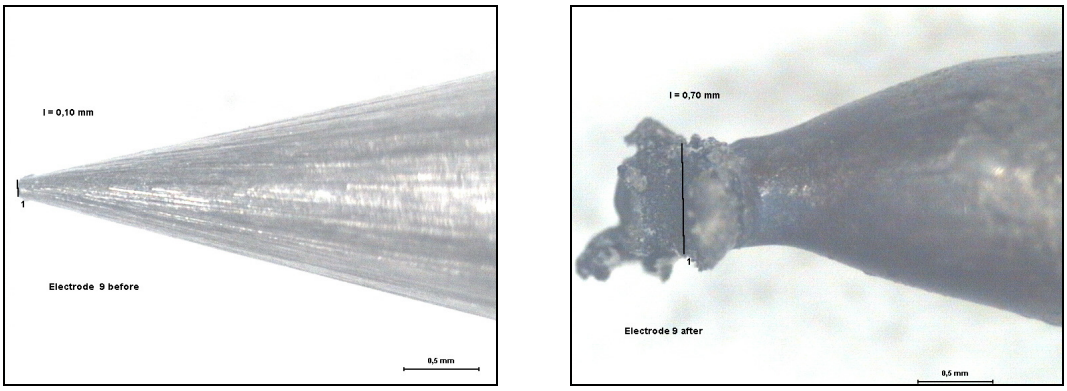

(a) (b)

Picture A-3.3.5 Spike of Electrode 9 used for experiment number 9: (a) before welding l = 0.1 mm; (b) after welding l = 0.7 mm.

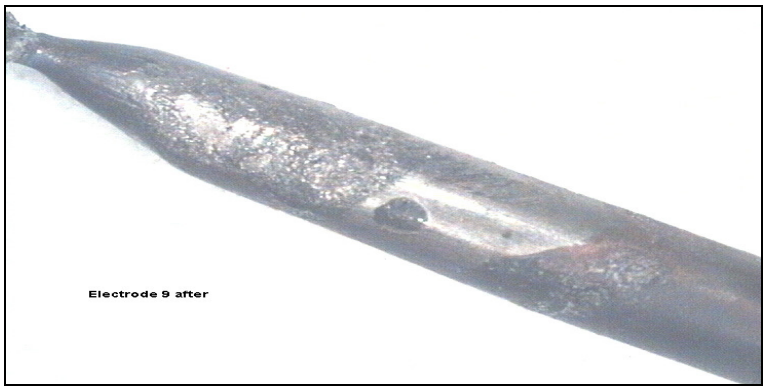

Picture A-3.3.6 Status of Electrode 9 used for experiment number 9 after welding once during 3.5 min.

3.4 Experiment 10

3.4.1 Parameters

Table A-3.4.1 Parameters of Experiment 10.

	Model A	Material	Features
Accessories	Back cap	Steel	-
	Back cap insulator	Teflon	-
	Collet	Copper	length: long type: with BET
	Collet body	Steel	length: long
	Coupler torch/gas pipe	Brass	-
	Coupler handle/cable	Copper	-
	Electrode	Tungsten	diameter: 2.4 mm length: 65 mm number: 10
	External block	Copper	-
	Handle	Copper	type: solid
	Internal block	Steel	-
	Nozzle	Alumina	number: 6
	Torch body	Teflon	-
Intensity	260 A		
Gas	argon flow: 15 l/ min		turbulent
Geometry	distance piece - electrode		5 mm
	distance electrode - nozzle		5 mm
Welding time	3’5 min	1 cycle	

3.4.2 Results

Table A-3.4.2 Results of Experiment 10.

	T1	T2	T3	T4
Model A	(K)	(K)	(K)	(K)
measurement 1	254.7	159.1	140.0	120.5

3.4.3 Commentaries

- Collet appearance: good condition.
- Collet body appearance: good status.
- Electrode appearance: temperatures are higher than before experiment because of this the electrode got a dark coloration, however its wear is much less and with less material on itself. It could be because the electric arc was wider, what means less energy density and less metal evaporated.
- Nozzle appearance: no change.

3.4.4 Pictures

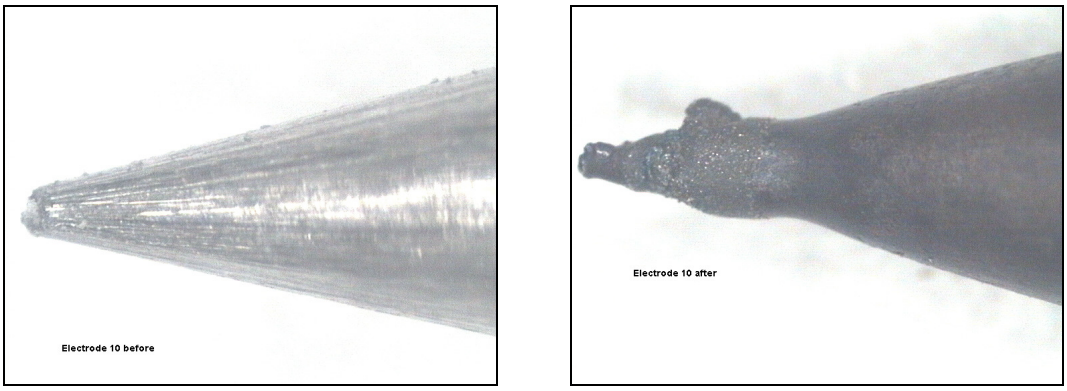

(a) (b)

Picture A-3.4.1 Electrode 10 used for experiment number 10: (a) before welding; (b) after welding.

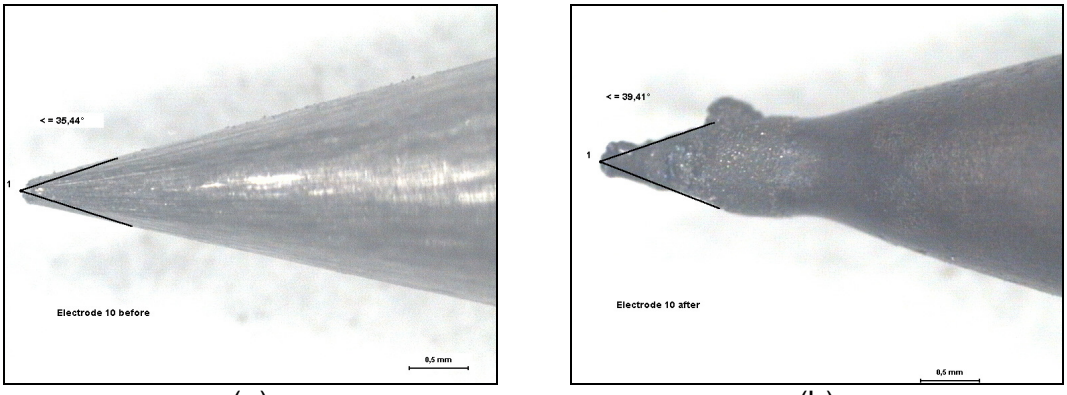

(a) (b)

Picture A-3.4.2 Angle of Electrode 10 used for experiment number 10: (a) before welding < = 35.44 º; (b) after welding < = 39.41 º.

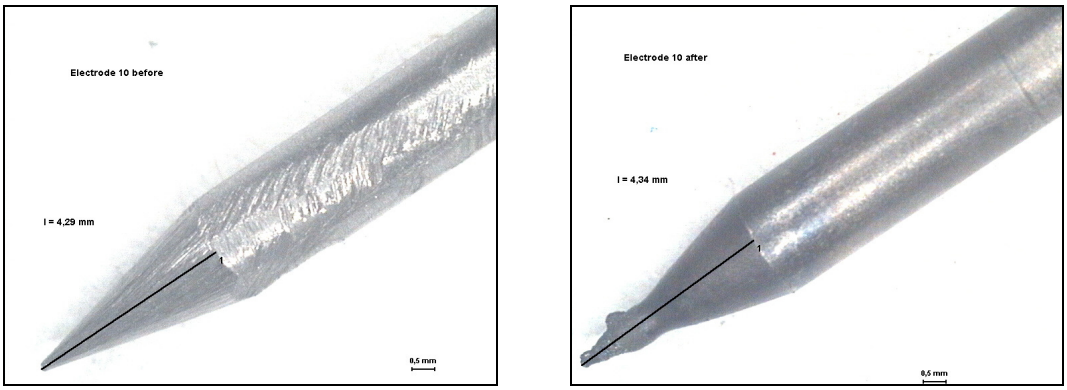

(a) (b)

Picture A-3.4.3 Cone height of Electrode 10 used for experiment number 10: (a) before welding l = 4.29 mm; (b) after welding l = 4.34 mm.

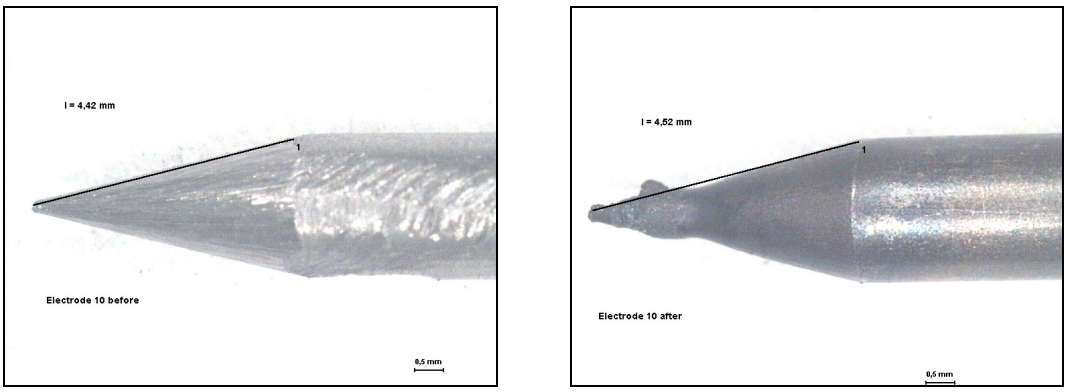

(a) (b)

Picture A-3.4.4 Cone hypotenuse of Electrode 10 used for experiment number 10: (a) before welding l = 4.42 mm; (b) after welding l = 4.52 mm.

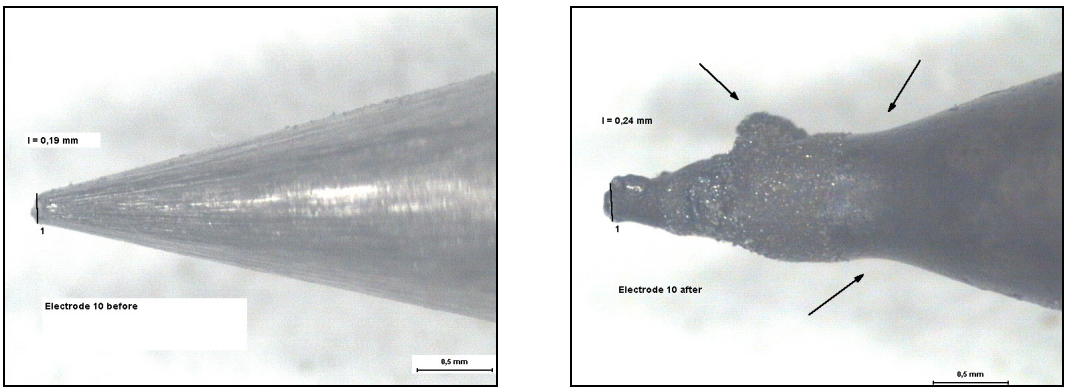

(a) (b)

Picture A-3.4.5 Spike of Electrode 10 used for experiment number 10: (a) before welding l = 0.19 mm; (b) after welding l = 0.24 mm.

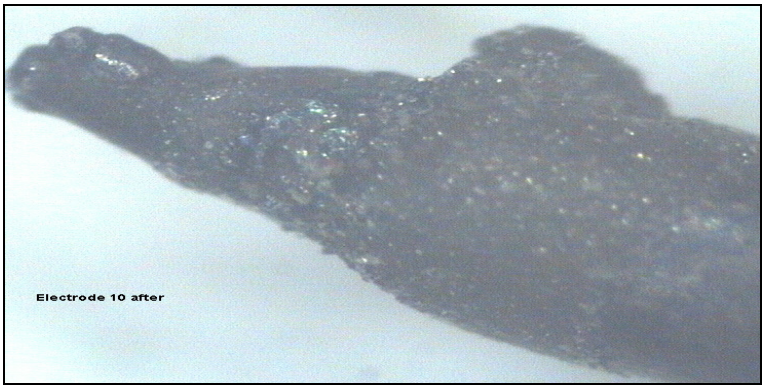

Picture A-3.4.6 Status of Electrode 10 used for experiment number 10 after welding once during 3.5 min.

3.5 Experiment 11

3.5.1 Parameters

Table A-3.5.1 Parameters of Experiment 11.

	Model A	Material	Features
Accessories	Back cap	Steel	-
	Back cap insulator	Teflon	-
	Collet	Copper	length: long type: with BET
	Collet body	Steel	length: long
	Coupler torch/gas pipe	Brass	-
	Coupler handle/cable	Copper	-
	Electrode	Tungsten	diameter: 4 mm length: 65 mm number: without
	External block	Copper	-
	Handle	Copper	type: solid
	Internal block	Steel	-
	Nozzle	Alumina	number: 10
	Torch body	Teflon	-
Intensity	260 A		
Gas	argon		
	flow: 15 l/ min		turbulent
Geometry	distance piece - electrode		5 mm
	distance electrode - nozzle		5 mm
Welding time	3’5 min	1 cycle	

3.5.2 Results

Table A-3.5.2 Results of Experiment 11.

	T1	T2	T3	T4
Model A	(K)	(K)	(K)	(K)
measurement 1	238.8	172.1	138.4	105.5

3.5.3 Commentaries

- Electrode appearance: reached temperatures are too high; the electrode was fallen down at 2 min and thirty six seconds and shows dark coloration. The spike is completely damaged because of the fall.

3.5.4 Pictures

It wasn't taken photos of the electrode.

3.6 Experiment 12

3.6.1 Parameters

Table A-3.6.1 Parameters of Experiment 12.

	Model B	Material	Features
Accessories	Back cap	Steel	-
	Back cap insulator	Teflon	-
	Collet	Copper	length: short type: with BET
	Collet body	Steel	length: short
	Coupler torch/gas pipe	Brass	-
	Coupler handle/cable	Copper	-
	Electrode	Tungsten	diameter: 2.4 mm length: 65 mm number: 11
	External block	Copper	-
	Handle	Copper	type: solid
	Internal block	Steel	-
	Nozzle	Alumina	number: 8
	Torch body	Teflon	-

Table A-3.6.1 Continued.

Intensity	260 A	
Gas	argon	
	flow: 15 l/ min	turbulent
Geometry	distance piece - electrode	5 mm
	distance electrode - nozzle	5 mm

3.6.2 Results

Table A-3.6.2 Results of Experiment 12.

	T1	T2	T3	T4
Model B	(K)	(K)	(K)	(K)
measurement 1	100.2	83.76	85.42	75.33
measurement 2	105.0	92.01	92.9	82.39
measurement 3	112.8	95.22	96.07	86.36

3.6.3 Commentaries

- Collet appearance: good condition.
- Collet body appearance: good status.
- Electrode appearance: in general electrode status is good, it still has spike, there is no so much coloration and there is no material on its.

3.6.4 Pictures

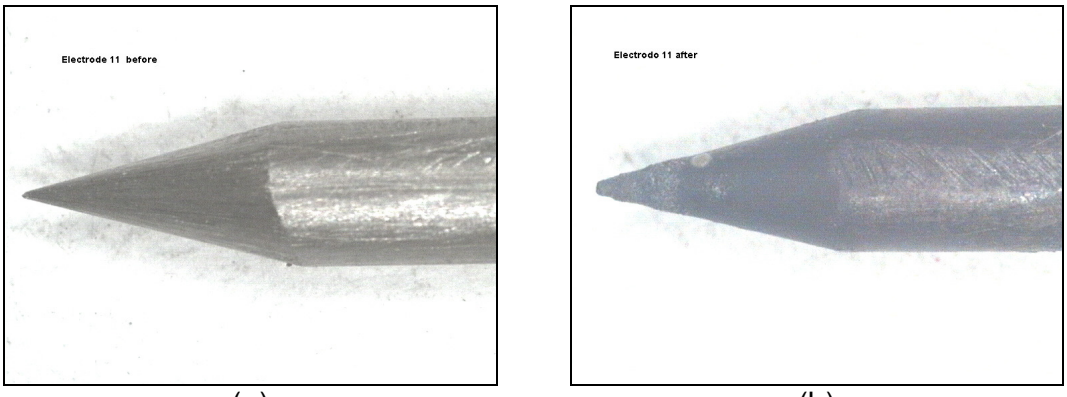

(a) (b)

Picture A-3.6.1 Electrode 11 used for experiment number 12: (a) before welding; (b) after welding.

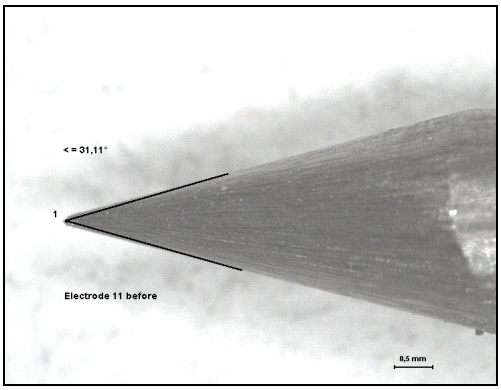

(a)

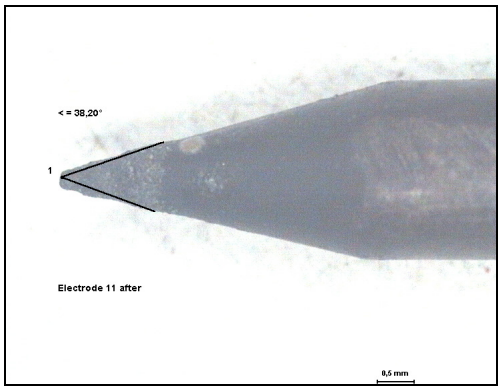

(b)

Picture A-3.6.2 Angle of Electrode 11 used for experiment number 12: (a) before welding < = 31.11 º; (b) after welding < = 38.20 º.

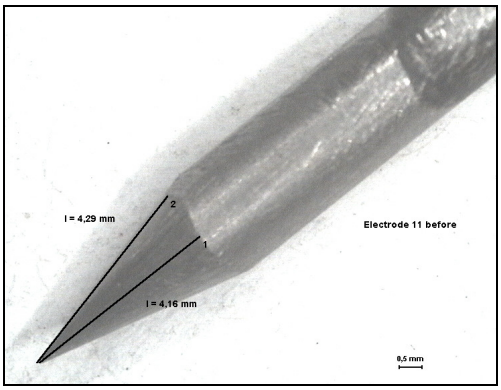

(a)

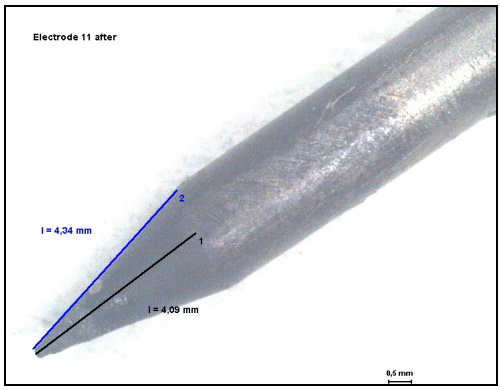

(b)

Picture A-3.6.3 Cone hypotenuse and height of Electrode 11 used for experiment number 12: (a) before welding l_1 = 4.16 mm l_2 = 4.29 mm; (b) after welding l_1 = 4.09 mm l_2 = 4.34 mm.

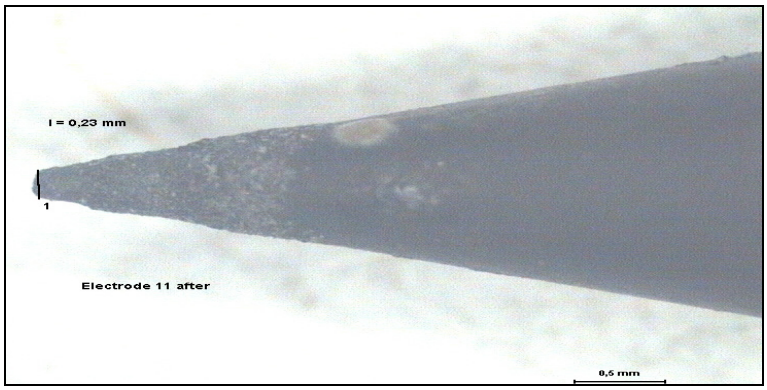

Picture A-3.6.4 Status of Electrode 11 used for experiment number 12 after welding three times during 3.5 min. Spike of Electrode 11 after welding; l = 0.23 mm.

3.7 Experiment 13

3.7.1 Parameters

Table A-3.7.1 Parameters of Experiment 13.

	Model B	Material	Features
Accessories	Back cap	Steel	-
	Back cap insulator	Teflon	-
	Collet	Copper	length: short type: with BET
	Collet body	Steel	length: short
	Coupler torch/gas pipe	Brass	-
	Coupler handle/cable	Copper	-
	Electrode	Tungsten	diameter: 3.2 mm length: 65 mm number: without
	External block	Copper	-
	Handle	Copper	type: solid
	Internal block	Steel	-
	Nozzle	Alumina	number: 8
	Torch body	Teflon	-
Intensity	150 A		
Gas	argon flow: 15 l/ min		turbulent
Geometry	distance piece - electrode		5 mm
	distance electrode - nozzle		5 mm
Welding time	3’5 min	1 cycle	

3.7.2 Results

Table A-3.7.2 Results of Experiment 13.

Model B	T1 (K)	T2 (K)	T3 (K)	T4 (K)
measurement 1	111.0	96.0	87.1	71.7
measurement 2	116.4	108.5	99.77	82.72
measurement 3	134.6	111.3	101.2	83.93

3.7.3 Commentaries

- Collet appearance: perfect condition, no damaged, no melted.
- Collet body appearance: good status.
- Electrode appearance: the electrode is very good condition, without material on its and without damage.

3.7.4 Pictures

It wasn't taken photos of the electrode.

3.8 Experiment 14

3.8.1 Parameters

Table A-3.8.1 Parameters of Experiment 14.

	Model A	Material	Features
Accessories	Back cap	Steel	-
	Back cap insulator	Teflon	-
	Collet	Copper	length: long type: with BET
	Collet body	Steel	length: long
	Coupler torch/gas pipe	Brass	-
	Coupler handle/cable	Copper	-
	Electrode	Tungsten	diameter: 3.2 mm length: 65 mm number: 14
	External block	Copper	-
	Handle	Copper	type: solid
	Internal block	Steel	-
	Nozzle	Alumina	number: 8
	Torch body	Teflon	-
Intensity	150 A		
Gas	argon flow: 15 l/ min		turbulent
Geometry	distance piece - electrode		5 mm
	distance electrode - nozzle		5 mm
Welding time	3'5 min	1 cycle	

3.8.2 Results

Table A-3.8.2 Results of Experiment 14.

Model A	T1 (K)	T2 (K)	T3 (K)	T4 (K)
measurement 1	116.2	89.56	82.02	72.61
measurement 2	142.1	101.7	93.75	81.15
measurement 3	169.5	103.2	93.49	81.83

3.8.3 Commentaries

- Collet appearance: normal.
- Collet body appearance: normal.
- Electrode appearance: there is material on its spike and there is coloration and it shows dark coloration.

3.8.4 Pictures

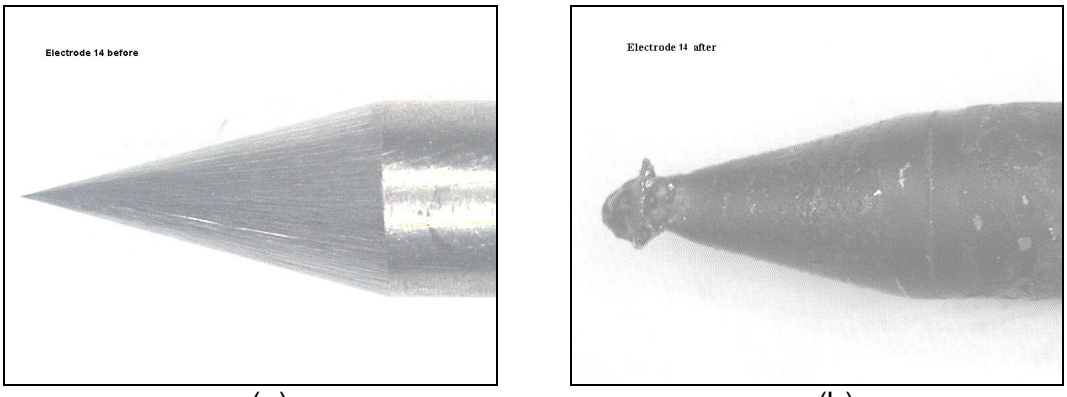

(a) (b)

Picture A-3.8.1 Electrode 14 used for experiment number 14: (a) before welding; (b) after welding.

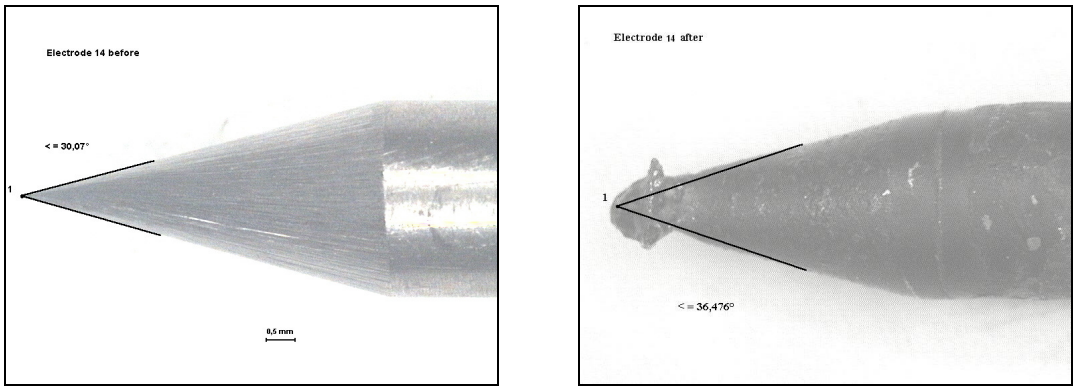

(a) (b)

Picture A-3.8.2 Angle of Electrode 14 used for experiment number 14: (a) before welding < = 30.07 º; (b) after welding < = 36.47 º.

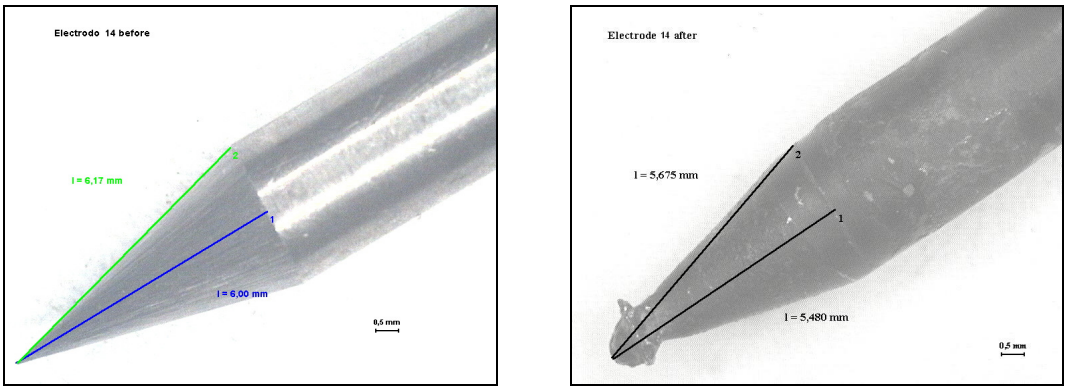

(a) (b)

Picture A-3.8.3 Cone hypotenuse and height of Electrode 14 used for experiment number 14: (a) before welding l_1 = 6 mm l_2 = 6.17 mm; (b) after welding l_1 = 5.48 mm l_2 = 5.675 mm.

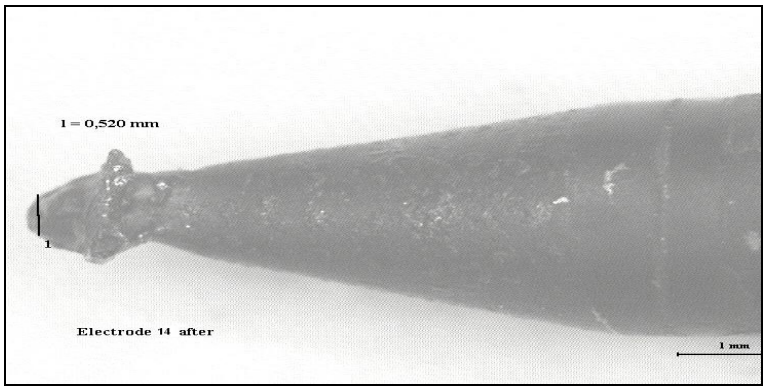

Picture A-3.8.4 Status of Electrode 14 used for experiment number 14 after welding three times during 3.5 min. Spike of Electrode 14 after welding; l = 0.52 mm.

3.9 Experiment 15

3.9.1 Parameters

Table A-3.9.1 Parameters of Experiment 15.

	Model A	Material	Features
Accessories	Back cap	Steel	-
	Back cap insulator	Teflon	-
	Collet	Copper	length: long type: with BET
	Collet body	Steel	length: long
	Coupler torch/gas pipe	Brass	-
	Coupler handle/cable	Copper	-
	Electrode	Tungsten	diameter: 3.2 mm length: 65 mm number: without
	External block	Copper	-
	Handle	Copper	type: solid
	Internal block	Steel	-
	Nozzle	Alumina	number: 8
	Torch body	Teflon	-
Intensity	300 A		
Gas	argon flow: 15 l/ min		turbulent
Geometry	distance piece - electrode		5 mm
	distance electrode - nozzle		5 mm
Welding time	3’5 min	1 cycle	

3.9.2 Results

Table A-3.9.2 Results of Experiment 15.

	T1	T2	T3	T4
Model A	(K)	(K)	(K)	(K)
measurement 1	207.9	175.7	155.1	137.4

3.9.3 Commentaries

The electrode fell down at 2 min and forty-four seconds.

3.9.4 Pictures

It wasn't taken photos of the electrode.

3.10 Experiment 16

3.10.1 Parameters

Table A-3.10.1 Parameters of Experiment 16.

	Model A	Material	Features
Accessories	Back cap	Steel	-
	Back cap insulator	Teflon	-
	Collet	Copper	length: long type: with BET
	Collet body	Steel	length: long
	Coupler torch/gas pipe	Brass	-
	Coupler handle/cable	Copper	-
	Electrode	Tungsten	diameter: 3.2 mm length: 65 mm number: without
	External block	Copper	-
	Handle	Copper	type: solid
	Internal block	Steel	-
	Nozzle	Alumina	number: 8
	Torch body	Teflon	-
Intensity	300 A		
Gas	argon flow: 15 l/ min		turbulent
Geometry	distance piece - electrode		5 mm
	distance electrode - nozzle		5 mm
Welding time	3'5 min	1 cycle	

3.10.2 Results

Table A-3.10.2 Results of Experiment 16.

	T1	T2	T3	T4
Model A	(K)	(K)	(K)	(K)
measurement 1	268.9	171.2	150.6	122.3

3.10.3 Commentaries

The electrode fell down at 2 min and forty-four seconds. The collet was melted a little at the bottom part.

3.10.4 Pictures

It wasn't taken photos of the electrode.

3.11 Experiment 17

3.11.1 Parameters

Table A-3.11.1 Parameters of Experiment 17.

	Standard model: TBISR26	Material	Features
Accessories	Collet	Copper	length: long type: without BET
	Collet body	Copper	length: long
	Coupler handle/cable	Copper	-
	Electrode	Tungsten	diameter: 3.2 mm number: without
	External block	Copper	-
	Handle	Copper	type: hollow
	Internal block	Copper	-
	Nozzle	Alumina	number: 8
	Torch body	Teflon	-

Table A-3.11.1 Continued.

Intensity	260 A		
Gas	argon		
	flow: 15 l/ min		
Geometry	distance piece - electrode		5 mm
	distance electrode - nozzle		5 mm
Welding time	3.5 min	1 cycle	

3.11.2 Results

Table A-3.11.2 Results of Experiment 17.

	T2	T3
Model TBISR26	(K)	(K)
measurement 1	181.0	151.9

3.12 Experiment 18

3.12.1 Parameters

Table A-3.12.1 Parameters of Experiment 18.

	Standard model: TBISR26	Material	Features
Accessories	Collet	Copper	length: long type: without BET
	Collet body	Copper	length: long
	Coupler handle/cable	Copper	-
	Electrode	Tungsten	diameter: 3.2 mm number: without
	External block	Copper	-
	Handle	Copper	type: hollow
	Internal block	Copper	-
	Nozzle	Alumina	number: 8
	Torch body	Teflon	-

Table A-3.12.1 Continued.

Intensity	260 A		
Gas	argon		
	flow: 15 l/ min		
Geometry	distance piece - electrode		5 mm
	distance electrode - nozzle		5 mm
Welding time	6 min	1 cycle	

3.12.2 Results

Table A-3.12.2 Results of Experiment 18.

	T2	T3
Model TBISR26	(K)	(K)
measurement 1	188.4	162.3

3.13 Experiment 19

3.13.1 Parameters

Table A-3.13.1 Parameters of Experiment 19.

	Standard model: TBISR26	Material	Features
Accessories	Collet	Copper	length: long type: without BET
	Collet body	Copper	length: long
	Coupler handle/cable	Copper	-
	Electrode	Tungsten	diameter: 3.2 mm number: without
	External block	Copper	-
	Handle	Copper	type: hollow
	Internal block	Copper	-
	Nozzle	Alumina	number: 8
	Torch body	Teflon	-

Table A-3.13.1 Continued.

Intensity	240 A		
Gas	argon		
	flow: 15 l/ min		
Geometry	distance piece - electrode		5 mm
	distance electrode - nozzle		5 mm
Welding time	6 min	1 cycle	

3.13.2 Results

Table A-3.13.2 Results of Experiment 19.

	T2	T3
Model TBISR26	(K)	(K)
measurement 1	171.0	148.0
measurement 2	187.4	166.2
measurement 3	175.4	153.6

3.14 Experiment 20

3.14.1 Parameters

Table A-3.14.1 Parameters of Experiment 20.

	Model A	Material	Features
Accessories	Back cap	Steel	-
	Back cap insulator	Teflon	-
	Collet	Copper	length: long type: with BET
	Collet body	Steel	length: long
	Coupler torch/gas pipe	Brass	-
	Coupler handle/cable	Copper	-
	Electrode	Tungsten	diameter: 3.2 mm length: 65 mm number: without
	External block	Copper	-
	Handle	Copper	type: solid
	Internal block	Steel	-
	Nozzle	Alumina	number: 8
	Torch body	Teflon	-

Table A-3.14.1 Continued.

Intensity	300 A		
Gas	argon		
	flow: 15 l/ min		
Geometry	distance piece - electrode		5 mm
	distance electrode - nozzle		5 mm
Welding time	6 min	1 cycle	

3.14.2 Results

Table A-3.14.2 Results of Experiment 20.

	T1	T2	T3	T4
Model A	(K)	(K)	(K)	(K)
measurement 1	320.6	211.0	201.9	167.9

3.14.3 Commentaries

The temperatures were so high than insulation was burnt. The electrode doesn't have spike and shows really dark coloration. The collet was melted.

3.15 Experiment 21

3.15.1 Parameters

Table A-3.15.1 Parameters of Experiment 21.

	Model A	Material	Features
Accessories	Back cap	Steel	-
	Back cap insulator	Teflon	-
	Collet	Copper	length: long type: with BET
	Collet body	Copper	length: long
	Coupler torch/gas pipe	Brass	-
	Coupler handle/cable	Copper	-
	Electrode	Tungsten	diameter: 3.2 mm length: 65 mm number: without
	External block	Copper	-
	Handle	Copper	type: solid
	Internal block	Steel	-
	Nozzle	Alumina	number: 8
	Torch body	Teflon	-
Intensity	300 A		
Gas	argon flow: 15 l/ min		turbulent
Geometry	distance piece - electrode		5 mm
	distance electrode - nozzle		5 mm
Welding time	6 min	1 cycle	

3.15.2 Results

Table A-3.15.2 Results of Experiment 21.

	T1	T2	T3	T4
Model A	(K)	(K)	(K)	(K)
measurement 1	278.9	191.8	176.8	162

4 CURRENT FLOW INFLUENCE

4.1 Experiment 22

4.1.1 Parameters

Table A-4.1.1 Parameters of Experiment 22.

	Model D	Material	Features
Accessories	Back cap	Brass	-
	Back cap insulator	Teflon	-
	Collet	Copper	length: short type: with BET
	Collet body	Copper	length: short
	Coupler handle/cable	Copper	-
	Electrode	Tungsten	diameter: 3.2 mm length: 65 mm number: without
	External block	Copper	-
	Handle	Copper	type: hollow
	Internal block	Copper	-
	Nozzle	Alumina	number: 6
	Torch body	Teflon	-
Intensity	320 A		
Gas	argon flow: 15 l/ min		turbulent
Geometry	distance piece - electrode		5 mm
	distance electrode - nozzle		5 mm
Welding time	3.5 min	1 cycle	

4.1.2 Results

Table A-4.1.2 Results of Experiment 22.

	T1	T2	T3	T4
Model D	(K)	(K)	(K)	(K)
measurement 1	225.8	205.8	131.5	90.05

4.2 Experiment 23

4.2.1 Parameters

Table A-4.2.1 Parameters of Experiment 23.

	Model D	Material	Features
Accessories	Back cap	Brass	-
	Back cap insulator	Teflon	-
	Collet	Copper	length: short type: with BET
	Collet body	Copper	length: short
	Coupler handle/cable	Copper	-
	Electrode	Tungsten	diameter: 3.2 mm length: 65 mm number: without
	External block	Copper	-
	Handle	Copper	type: hollow
	Internal block	Copper	-
	Nozzle	Alumina	number: 6
	Torch body	Teflon	-
Intensity	340 A		
Gas	argon flow: 15 l/ min		turbulent
Geometry	distance piece - electrode		5 mm
	distance electrode - nozzle		5 mm
Welding time	3.5 min	1 cycle	

4.2.2 Results

Table A-4.2.2 Results of Experiment 23.

	T1	T2	T3	T4
Model D	(K)	(K)	(K)	(K)
measurement 1	249.3	221.7	145.4	101.1

4.3 Experiment 24

4.3.1 Parameters

Table A-4.3.1 Parameters of Experiment 24.

	Model D	Material	Features
Accessories	Back cap	Brass	-
	Back cap insulator	Teflon	-
	Collet	Copper	length: short type: with BET
	Collet body	Copper	length: short
	Coupler handle/cable	Copper	-
	Electrode	Tungsten	diameter: 3.2 mm length: 65 mm number: without
	External block	Copper	-
	Handle	Copper	type: hollow
	Internal block	Copper	-
	Nozzle	Alumina	number: 6
	Torch body	Teflon	-
Intensity	300 A		
Gas	argon flow: 15 l/ min		turbulent
Geometry	distance piece - electrode		5 mm
	distance electrode - nozzle		5 mm
Welding time	3.5 min	4 cycle	
Cooling time	6.5 min		

4.3.2 Results

Table A-4.3.2 Results of Experiment 24.

Model D		T1 (K)	T2 (K)	T3 (K)	T4 (K)
cycle	1	212.0	190.0	120.7	81.2
cycle	2	235.3	224.5	150.6	11.4
cycle	3	232.4	235.4	160.6	122.8
cycle	4	238	241.3	167.3	126.7

5 MATERIAL INFLUENCE

5.1 Experiment 25

5.1.1 Parameters

Table A-5.1.1 Parameters of Experiment 25.

	Model D	Material	Features
Accessories	Back cap	Brass	-
	Back cap insulator	Teflon	-
	Collet	Copper	length: short type: with BET
	Collet body	Copper	length: short
	Coupler handle/cable	Copper	-
	Electrode	Tungsten	diameter: 3.2 mm length: 65 mm number: without
	External block	Copper	-
	Handle	Copper	type: hollow
	Internal block	Steel	-
	Nozzle	Alumina	number: 6
	Torch body	Teflon	-
Intensity	320 A		
Gas	argon flow: 15 l/ min		turbulent
Geometry	distance piece - electrode		5 mm
	distance electrode - nozzle		5 mm
Welding time	3.5 min	1 cycle	

5.1.2 Results

Table A-5.1.2 Results of Experiment 25.

	T1	T2	T3	T4
Model D	(K)	(K)	(K)	(K)
measurement 1	314.4	230.1	117.7	81.03

5.2 Experiment 26

5.2.1 Parameters

Table A-5.2.1 Parameters of Experiment 26.

	Model D	Material	Features
Accessories	Back cap	Brass	-
	Back cap insulator	Teflon	-
	Collet	Copper	length: short type: with BET
	Collet body	Steel	length: short
	Coupler handle/cable	Copper	-
	Electrode	Tungsten	diameter: 3.2 mm length: 65 mm number: without
	External block	Copper	-
	Handle	Copper	type: hollow
	Internal block	Steel	-
	Nozzle	Alumina	number: 6
	Torch body	Teflon	-
Intensity	300 A		
Gas	argon flow: 15 l/ min		turbulent
Geometry	distance piece - electrode		5 mm
	distance electrode - nozzle		5 mm
Welding time	3.5 min	3 cycle	
Cooling time	6.5 min		

5.2.2 Results

Table A-5.2.2 Results of Experiment 26.

		T1	T2	T3	T4
Model D		(K)	(K)	(K)	(K)
cycle	1	229.0	219.7	112.8	76.1
cycle	2	247.6	255.0	144.1	103.5
cycle	3	255.5	276.0	156.2	116.3

6 DUTY CYCLE INFLUENCE

6.1 Experiment 27

6.1.1 Parameters

Table A-6.1.1 Parameters of Experiment 27.

	Model D	Material	Features
Accessories	Back cap	Brass	-
	Back cap insulator	Teflon	-
	Collet	Copper	length: short type: with BET
	Collet body	Copper	length: short
	Coupler handle/cable	Copper	-
	Electrode	Tungsten	diameter: 3.2 mm length: 65 mm number: without
	External block	Copper	-
	Handle	Copper	type: hollow
	Internal block	Steel	-
	Nozzle	Alumina	number: 6
	Torch body	Teflon	-
Intensity	300 A		
Gas	argon flow: 15 l/ min		turbulent
Geometry	distance piece - electrode		5 mm
	distance electrode - nozzle		5 mm
Welding time	3.5 min	3 cycle	
Cooling time	6.5 min		

6.1.2 Results

Table A-6.1.2 Results of Experiment 27.

Model D		T1 (K)	T2 (K)	T3 (K)	T4 (K)
cycle	1	307. 8	202.8	117.7	79.2
cycle	2	330.4	250.5	157.1	114.4
cycle	3	344.7	263.9	169.8	127.3

6.2 Experiment 28

6.2.1 Parameters

Table A-6.2.1 Parameters of Experiment 28.

	Model D	Material	Features
Accessories	Back cap	Brass	-
	Back cap insulator	Teflon	-
	Collet	Copper	length: short type: with BET
	Collet body	Copper	length: short
	Coupler handle/cable	Copper	-
	Electrode	Tungsten	diameter: 3.2 mm length: 65 mm number: without
	External block	Copper	-
	Handle	Copper	type: hollow
	Internal block	Steel	-
	Nozzle	Alumina	number: 6
	Torch body	Teflon	-
Intensity	340 A		
Gas	argon flow: 15 l/ min		turbulent
Geometry	distance piece - electrode		5 mm
	distance electrode - nozzle		5 mm
Welding time	3.5 min	1 cycle	

6.2.2 Results

Table A-6.2.2 Results of Experiment 28.

	T1	T2	T3	T4
Model D	(K)	(K)	(K)	(K)
measurement 1	350.0	253.3	133.6	94.20

6.3 Experiment 29

6.3.1 Parameters

Table A-6.3.1 Parameters of Experiment 29.

	Model D	Material	Features
Accessories	Back cap	Brass	-
	Back cap insulator	Teflon	-
	Collet	Copper	length: short type: with BET
	Collet body	Copper	length: short
	Coupler handle/cable	Copper	-
	Electrode	Tungsten	diameter: 3.2 mm length: 65 mm number: without
	External block	Copper	-
	Handle	Copper	type: hollow
	Internal block	Steel	-
	Nozzle	Alumina	number: 6
	Torch body	Teflon	-
Intensity	352 A		
Gas	argon flow: 15 l/ min		turbulent
Geometry	distance piece - electrode		5 mm
	distance electrode - nozzle		5 mm
Welding time	3.5 min	1 cycle	

6.3.2 Results

Table A-6.3.2 Results of Experiment 29.

	T1	T2	T3	T4
Model D	(K)	(K)	(K)	(K)
measurement 1	372.7	277.5	147.0	102.9

6.4 Experiment 30

6.4.1 Parameters

Table A-6.4.1 Parameters of Experiment 30.

	Model D	Material	Features
Accessories	Back cap	Brass	-
	Back cap insulator	Teflon	-
	Collet	Copper	length: short type: with BET
	Collet body	Copper	length: short
	Coupler handle/cable	Copper	-
	Electrode	Tungsten	diameter: 3.2 mm length: 65 mm number: without
	External block	Copper	-
	Handle	Copper	type: hollow
	Internal block	Steel	-
	Nozzle	Alumina	number: 6
	Torch body	Teflon	-
Intensity	300 A		
Gas	argon flow: 15 l/ min		turbulent
Geometry	distance piece - electrode		5 mm
	distance electrode - nozzle		5 mm
Welding time	6 min	1 cycle	

6.4.2 Results

Table A-6.4.2 Results of Experiment 30.

	T1	T2	T3	T4
Model D	(K)	(K)	(K)	(K)
measurement 1	304.4	229.1	129.2	98.65

6.5 Experiment 31

6.5.1 Parameters

Table A-6.5.1 Parameters of Experiment 31.

	Model D	Material	Features
Accessories	Back cap	Brass	-
	Back cap insulator	Teflon	-
	Collet	Copper	length: short type: with BET
	Collet body	Copper	length: short
	Coupler handle/cable	Copper	-
	Electrode	Tungsten	diameter: 3.2 mm length: 65 mm number: without
	External block	Copper	-
	Handle	Copper	type: hollow
	Internal block	Copper	-
	Nozzle	Alumina	number: 6
	Torch body	Teflon	-
Intensity	300 A		
Gas	argon flow: 15 l/ min		turbulent
Geometry	distance piece - electrode		5 mm
	distance electrode - nozzle		5 mm
Welding time	6 min	1 cycle	

6.5.2 Results

Table A-6.5.2 Results of Experiment 31.

	T1	T2	T3	T4
Model D	(K)	(K)	(K)	(K)
measurement 1	274.0	200.1	134.0	98.22

6.6 Experiment 32

6.6.1 Parameters

Table A-6.6.1 Parameters of Experiment 32.

	Model D	Material	Features
Accessories	Back cap	Brass	-
	Back cap insulator	Teflon	-
	Collet	Copper	length: short type: with BET
	Collet body	Steel	length: short
	Coupler handle/cable	Copper	-
	Electrode	Tungsten	diameter: 3.2 mm length: 65 mm number: without
	External block	Copper	-
	Handle	Copper	type: hollow
	Internal block	Steel	-
	Nozzle	Alumina	number: 6
	Torch body	Teflon	-
Intensity	300 A		
Gas	argon flow: 15 l/ min		turbulent
Geometry	distance piece - electrode		5 mm
	distance electrode - nozzle		5 mm
Welding time	6 min	1 cycle	

6.6.2 Results

Table A-6.6.2 Results of Experiment 32.

	T1	T2	T3	T4
Model D	(K)	(K)	(K)	(K)
measurement 1	242.3	250.3	139.0	100.9

6.6.3 Commentaries

The electrode fell down at 3’ 36”.

7 VALIDATION

7.1 Validation of model A: experiment 33

7.1.1 Parameters

Table A-7.1.1 Parameters of Experiment 33.

	Model A	Material	Features
Accessories	Back cap	Steel	-
	Back cap insulator	Teflon	-
	Collet	Copper	length: long type: with BET
	Collet body	Copper	length: long
	Coupler handle/cable	Copper	-
	Electrode	Tungsten	diameter: 3.2 mm length: 65 mm number: without
	External block	Copper	-
	Handle	Copper	type: solid
	Internal block	Copper	-
	Nozzle	Alumina	number: 6
	Torch body	Teflon	-
Intensity	250 A		
Gas	argon flow: 15 l/ min		turbulent
Geometry	distance piece - electrode		5 mm
	distance electrode - nozzle		5 mm
Welding time	3.5 min	1 cycle	

7.1.2 Results

Table A-7.1.2 Results of Experiment 33.

	T1	T2	T3	T4
Model A	(K)	(K)	(K)	(K)
measurement 1	234.6	178.3	161.3	130.2

2.1.3 Commentaries

It was impossible to finish the experiment; the electric arc was so irregular, inclined and bigger and bigger. The turbulent regime caused an entrance of air, so the temperature on the electrode and the piece rose abruptly. The consequence is that the piece we used to weld has yellow oxide on its surface. The electrode is completely destroyed.

7.2 Validation of model B: experiment 34

7.2.1 Parameters

Table A-7.2.1 Parameters of Experiment 34.

	Model B	Material	Features
Accessories	Back cap	Steel	-
	Back cap insulator	Teflon	-
	Collet	Copper	length: short type: with BET
	Collet body	Copper	length: short
	Coupler handle/cable	Copper	-
	Electrode	Tungsten	diameter: 3.2 mm length: 65 mm number: without
	External block	Copper	-
	Handle	Copper	type: solid
	Internal block	Copper	-
	Nozzle	Alumina	number: 6
	Torch body	Teflon	-
Intensity	250 A		
Gas	argon flow: 15 l/ min		turbulent
Geometry	distance piece - electrode		5 mm
	distance electrode - nozzle		5 mm
Welding time	3.5 min	1 cycle	

7.2.2 Results

Table A-7.2.2 Results of Experiment 34.

Model B	T1 (K)	T2 (K)	T3 (K)	T4 (K)
measurement 1	158.3	124.7	115.5	93.51
measurement 2	163.5	128.8	121.2	100.2
measurement 3	184.5	138	130.9	117.1

7.3 Validation of model C: experiment 35

7.3.1 Parameters

Table A-7.3.1 Parameters of Experiment 35.

	Model C	Material	Features
Accessories	Back cap	Steel	-
	Back cap insulator	Teflon	-
	Collet	Copper	length: long type: with BET
	Collet body	Copper	length: long
	Coupler handle/cable	Copper	-
	Electrode	Tungsten	diameter: 3.2 mm length: 65 mm number: without
	External block	Copper	-
	Handle	Copper	type: hollow
	Internal block	Copper	-
	Nozzle	Alumina	number: 6
	Torch body	Teflon	-
Intensity	250 A		
Gas	argon flow: 15 l/ min		turbulent
Geometry	distance piece - electrode		5 mm
	distance electrode - nozzle		5 mm
Welding time	3.5 min	1 cycle	

7.3.2 Results

Table A-2.6 Results of Experiment 24

	T1	T2	T3	T4
Model C	(K)	(K)	(K)	(K)
measurement 1	196.1	186.2	118.6	78.1

7.3.3 Commentaries

The electrode is completely broken. The electric arc was irregular and some dust appeared on the workpiece surface.

7.4 Validation of model D: experiment 36

7.4.1 Parameters

Table A-7.4.1 Parameters of Experiment 36.

	Model C	Material	Features
Accessories	Back cap	Steel	-
	Back cap insulator	Teflon	-
	Collet	Copper	length: short type: with BET
	Collet body	Copper	length: short
	Coupler handle/cable	Copper	-
	Electrode	Tungsten	diameter: 3.2 mm length: 65 mm number: without
	External block	Copper	-
	Handle	Copper	type: hollow
	Internal block	Copper	-
	Nozzle	Alumina	number: 6
	Torch body	Teflon	-
Intensity	250 A		
Gas	argon flow: 15 l/ min		turbulent
Geometry	distance piece - electrode		5 mm
	distance electrode - nozzle		5 mm
Welding time	3.5 min	1 cycle	

7.4.2 Results

Table A-7.4.2 Results of Experiment 36.

Model D	T1 (K)	T2 (K)	T3 (K)	T4 (K)
measurement 1	193.3	158.6	84.47	65.87
measurement 2	194.2	162.5	84.89	66.70
measurement 3	201.0	168.2	88.8	69.3

7.4.3 Commentaries

The electrode is really perfect. The collet and collet body hasn't suffered any damage.

APPENDIX B

PHYSICAL PROPERTIES OF SOLIDS

1 DENSITY, HEAT SPECIFIC, METLTING POINT AND THERMAL CONDUCTIVITY

Table D.1 Physical properties of solids *

	ρ	c_p	k $(W/m \cdot K)$			T_{mp}
Material	(Kg/m^3) (293 K)	$(J/kg \cdot ^\circ K)$ (293 K)	(293 K)	K (373 K)	(573 K)	(ºC)
Aluminum	2701.1	938.3	229	229	230	660
Brass (70%Cu,30%Zn)	8520	381.2	107	128	148	920-980
Copper	8890	385.4	386	379	369	1083
Stainless steel	7820	460.8	16	17.3	23	1350
Teflon(PTFE)**	2200	1040	0.23			327
Tungsten	19320	134.0	160	150	130	3410

* J. R. Welty, C. E. Wicks, R. E. Wilson, and G. Rorrer, *Fundamentals of Momentum, Heat, and Mass Transfer*, Wiley Book Company, New York, 2000, Appendix H.
** A. Bejan, *Convection Heat Transfer*, Wiley Book Company, New York, 2004, Appendix B.

2 ELECTRICAL CONDUCTIVITY AND RESISTIVITY

The electrical conductivity of metals is expressed by the equation:

$$\sigma = n \cdot q \cdot \mu \tag{D1}$$

where n is the number of charge carries, q is the charge of the ion and μ is the mobility of the charged species. [5]
As the resistivity is the inverse of the electrical conductivity, is represented by the following equation:

$$\Re = \frac{1}{\sigma} \tag{D2}$$

When resistivity is dependent on temperature is often calculated by the empirical relationship:

$$\Re = \Re_0 + \alpha.T \tag{D3}$$

Table D.2 shows $\Re_0$ and α of some metals along with the calculated resistivity at 100 ºC.

More accurate equation is given by Mathesson´s rule, where is combined effect of thermal, impurity and defects on the resistivity:

$$\Re_{total} = \Re_{thermal} + \Re_{impurity} + \Re_{defect} \tag{D4}$$

For pure elements the contribution of defects is on the order of 0.1 percent of the total but for heavily cold worked metals it can be as high as 5 percent.

Table D.2 Resistivity values of common metals [6].

Material	$\Re_0$* ($\mu\Omega \cdot cm$) (293 ºK)	α ($\mu\Omega \cdot cm / {}^\circ K$) (298 ºK)	$\Re$ at 100ºC ($\mu\Omega \cdot cm$) (293 ºK)
Aluminum	2.284	0.0039	3.064
Brass	7	0.002	7.4
Copper	1.7241	0.00393	2.5101
Stainless steel	10.4	0.005	11.4
Tungsten	5.6	0.0045	6.5

* Determined at 25 ºC.

APPENDIX C

PHYSICAL PROPERTIES OF GASES*

Table E.1 Physical properties of Argon. [12]

T	ρ	μ	ע	c_P	k	Pr
$^\circ K$	$\frac{kg}{m^3}$	$\frac{kg}{m \cdot s}$	$\frac{m^2}{s}$	$\frac{J}{kg \cdot ^\circ K}$	$\frac{W}{m \cdot ^\circ K}$	dimensionless
300	1,622E+00	2,268E-05	1,398E-05	5,2032E+02	1,7703E-02	6,6666092E-01
400	1,217E+00	2,862E-05	2,352E-05	5,2032E+02	2,2338E-02	6,6664690E-01
500	9,734E-01	3,392E-05	3,485E-05	5,2032E+02	2,6477E-02	6,6666676E-01
600	8,112E-01	3,876E-05	4,778E-05	5,2032E+02	3,0253E-02	6,6666591E-01
700	6,953E-01	4,325E-05	6,220E-05	5,2032E+02	3,3753E-02	6,6665952E-01
800	6,084E-01	4,745E-05	7,800E-05	5,2032E+02	3,7036E-02	6,6666878E-01
900	5,408E-01	5,144E-05	9,511E-05	5,2032E+02	4,0146E-02	6,6667215E-01
1000	4,867E-01	5,524E-05	1,135E-04	5,2032E+02	4,3115E-02	6,6665887E-01
1100	4,425E-01	5,890E-05	1,331E-04	5,2032E+02	4,5971E-02	6,6666743E-01
1200	4,056E-01	6,243E-05	1,539E-04	5,2032E+02	4,8729E-02	6,6665967E-01

* All gas properties are for atmospheric pressure.

Table E.2 Physical properties of Air. [4]

T	ρ	μ	ע	c_P	k	Pr
$^\circ K$	$\frac{kg}{m^3}$	$\frac{kg}{m \cdot s}$	$\frac{m^2}{s}$	$\frac{J}{kg \cdot ^\circ K}$	$\frac{W}{m \cdot ^\circ K}$	dimensionless
0	1,2923E+00	1,72E-05	1,331E-05	1,0057E+03	2,41E-02	7,1836E-01
10	1,2467E+00	1,77E-05	1,419E-05	1,0058E+03	2,49E-02	7,1542E-01
20	1,2042E+00	1,82E-05	1,509E-05	1,0061E+03	2,56E-02	7,1298E-01
30	1,1644E+00	1,87E-05	1,601E-05	1,0064E+03	2,60E-02	7,2162E-01
40	1,1273E+00	1,91E-05	1,696E-05	1,0068E+03	2,71E-02	7,0996E-01
50	1,0924E+00	1,96E-05	1,792E-05	1,0074E+03	2,78E-02	7,0891E-01
60	1,0596E+00	2,00E-05	1,890E-05	1,0080E+03	2,85E-02	7,0793E-01
70	9,9960E-01	2,05E-05	1,990E-05	1,0087E+03	2,92E-02	7,0664E-01
80	9,7210E-01	2,09E-05	2,092E-05	1,0095E+03	2,99E-02	7,0608E-01
90	9,7210E-01	2,14E-05	2,196E-05	1,0130E+03	3,06E-02	7,0701E-01

* All gas properties are for atmospheric pressure.

APPENDIX D

CONVECTION COEFFIECIENTS

Table D.1 Summary of convection coefficients used for each model at T = 25ºC.

	Solid Handle						Hollow Handle			
	Model A		Model B		Model C		Model D			
	Q = 10 l/min	Q= 15 l/min	Q= 10 l/min	Q= 15 l/min	Q= 10 l/min	Q= 15 l/min	Q= 10 l/min	Q= 15 l/min		
$h_{0,A}$	-	-	$h_{0,B}$	-	-	$h_{0,C}$	5.1786e1	8.1724e1	$h_{0,D}$	5.1786e1	8.1724e1
$h_{1,A}$	8.5598e1	1.2292e2	$h_{1,B}$	8.5598e1	1.2292e2	$h_{1,C}$	4.8040e1	7.5813e1	$h_{1,D}$	4.8040e1	7.5813e1
$h_{2,A}$	4.0257e1	6.6099e1	$h_{2,B}$	4.0257e1	6.6099e1	$h_{2,C}$	1.0837e2	1.2769e2	$h_{2,D}$	1.0837e2	1.2769e2
$h_{3,A}$	6.4160e1	7.6079e1	$h_{3,B}$	6.4160e1	7.6079e1	$h_{3,C}$	6.4160e1	7.6079e1	$h_{3,D}$	6.4160e1	7.6079e1
$h_{4,A}$	7.2867e1	8.1025e1	$h_{4,B}$	7.8114e1	8.8048e1	$h_{4,C}$	7.2867e1	8.1025e1	$h_{4,D}$	7.8114e1	8.8048e1
$h_{5,A}$	1.7281e2	4.2192e2	$h_{5,B}$	1.7281e2	4.2192e2	$h_{5,C}$	1.7281e2	4.2192e2	$h_{5,D}$	1.7281e2	4.2192e2
$h_{6,A}$	9.518e1	1.0998e2	$h_{6,B}$	1.3381e2	1.5748e2	$h_{6,C}$	9.518e1	1.0998e2	$h_{6,D}$	1.3381e2	1.5748e2
$h_{7,A}$	2.2	2.2	$h_{7,B}$	2.2	2.2	$h_{7,C}$	2.2	2.2	$h_{7,D}$	2.2	2.2
h_a	9.957	9.957	h_a	9.957	9.957	h_a	9.957	9.957	h_a	9.957	9.957

Table D.2 Summary of convection coefficients used for each model at T = 40ºC.

	Solid Handle						Hollow Handle			
	Model A		Model B		Model C		Model D			
	Q = 10 l/min	Q= 15 l/min	Q= 10 l/min	Q= 15 l/min	Q= 10 l/min	Q= 15 l/min	Q= 10 l/min	Q= 15 l/min		
$h_{0,A}$	-	-	$h_{0,B}$	-	-	$h_{0,C}$	4,8130e1	7.7051e1	$h_{0,D}$	4,8130e1	7.705e1
$h_{1,A}$	8.1752e1	1.1796e2	$h_{1,B}$	8.1752e1	1.1796e2	$h_{1,C}$	4,4648e1	7.1477e1	$h_{1,D}$	4,4648e1	7.147e1
$h_{2,A}$	3.6931e1	6.1896e1	$h_{2,B}$	3.6931e1	6.1896e1	$h_{2,C}$	1,0855e2	1.2777e2	$h_{2,D}$	1,0855e2	1.277e2
$h_{3,A}$	6.4144e1	7.6038e1	$h_{3,B}$	6.4144e1	7.6038e1	$h_{3,C}$	6,4144e1	7.6038e1	$h_{3,D}$	6,4144e1	7.603e1
$h_{4,A}$	7.4097e1	8.2003e1	$h_{4,B}$	7.9173e1	8.8861e1	$h_{4,C}$	7.4097e1	8.2003e1	$h_{4,D}$	7.9173e1	8.886e1
$h_{5,A}$	1.7296e2	2.0419e2	$h_{5,B}$	1.7296e2	2.0419e2	$h_{5,C}$	1,7296e2	4.0179e2	$h_{5,D}$	1,7296e2	4.017e2
$h_{6,A}$	9.5858e1	1.1045e2	$h_{6,B}$	1,3407e2	1.5761e2	$h_{6,C}$	9,5858e1	1.1045e2	$h_{6,D}$	1,3407e2	1.576e2
$h_{7,A}$	1.80	1.80	$h_{7,B}$	1.80	1.80	$h_{7,C}$	1.80	1.80	$h_{7,D}$	1.80	1.80
h_a	8.78	8.78	h_a	8.78	8.78	h_a	8.78	8.78	h_a	8.78	8.78

Table D.3 Summary of convection coefficients used for each model at T = 5 ºC.

	Solid Handle						Hollow Handle			
	Model A		Model B		Model C		Model D			
	Q = 10 l/min	Q= 15 l/min	Q= 10 l/min	Q= 15 l/min	Q= 10 l/min	Q= 15 l/min	Q= 10 l/min	Q= 15 l/min		
$h_{0,A}$	-	-	$h_{0,B}$	-	-	$h_{0,C}$	5.7550e1	8.9185e1	$h_{0,D}$	5.7550e1	8.9185e1
$h_{1,A}$	9.1789e1	1.3099e2	$h_{1,B}$	9.1789e1	1.3099e2	$h_{1,C}$	5.3387e1	8.2734e1	$h_{1,D}$	5.3387e1	8.2734e1
$h_{2,A}$	4.5457e1	7.2764e1	$h_{2,B}$	4.5457e1	7.2764e1	$h_{2,C}$	1.0855e2	1.2807e2	$h_{2,D}$	1.0855e2	1.2807e2
$h_{3,A}$	6.4425e1	7.6421e1	$h_{3,B}$	6.4425e1	7.6421e1	$h_{3,C}$	6.4425e1	7.6421e1	$h_{3,D}$	6.4425e1	7.6421e1
$h_{4,A}$	7.1472e1	8.0017e1	$h_{4,B}$	7.6981e1	8.0017e1	$h_{4,C}$	7.1472e1	8.0017e1	$h_{4,D}$	7.6981e1	8.7299e1
$h_{5,A}$	3.0741e2	4.5447e2	$h_{5,B}$	3.0741e2	4.5447e2	$h_{5,C}$	3.0741e2	4.5447e2	$h_{5,D}$	3.0741e2	4.5447e2
$h_{6,A}$	9.4642e1	1.0977e2	$h_{6,B}$	1.3398e2	1.5791e2	$h_{6,C}$	9.4642e1	1.0977e2	$h_{6,D}$	1.3398e2	1.5791e2
$h_{7,A}$	2.51	2.51	$h_{7,B}$	2.51	2.51	$h_{7,C}$	2.51	2.51	$h_{7,D}$	2.51	2.51
h_a	10.61	10.61	h_a	10.61	10.61	h_a	10.61	10.61	h_a	10.61	10.61

APPENDIX E

GRAPHS OF EXPERIMENTAL RESULTS

1 GEOMETRY

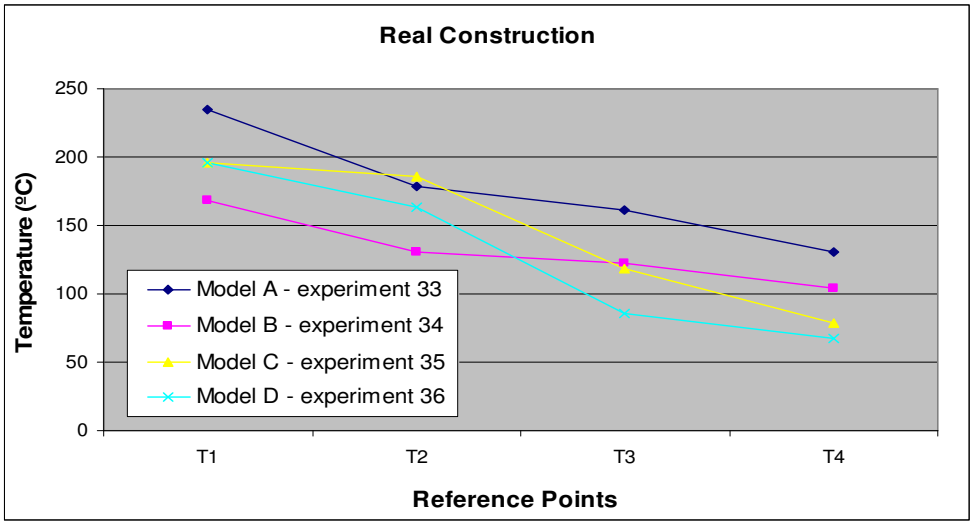

Figure E-1 Experimental temperatures at main reference points used for the Ansys model validation. Experimental conditions; welding time 3.5 min, 3.2 mm electrode diameter, z_{ne} 5 mm , z_{ew} 5 mm, turbulent regime with "becoming element of turbulence", 250 A, 25 º C. Model A: long collet body with heavy handle; Model B: short collet body with heavy handle; Model C: long collet body with hollow handle; Model D: short collet body with hollow handle.

It is observed that temperature profiles for the configuration with long collet body (model A and model C) are higher than for the configuration with short collet body (model B and D)*. Also, the configuration with solid handle (model A and model B) shows greater temperatures at handle zone (at reference points T3 and T4) than the configuration with hollow handle (model C and model D) **. The model with less temperature at handle zone is the model D.

* Compare model A with model B and model C with model D.
** Compare model A with model C and model B with model D.

2 MATERIALS

Table E-1 Material combinations used to make the experiments: material for each element of the real construction.

	Combination 1	Combination 2	Combination 3
Back Cap	Brass	Brass	Brass
Back Cap Insulator	Teflon	Teflon	Teflon
Collet	Copper	Copper	Copper
Collet Body	Copper	Copper	Steel
Coupler handle/cable	Copper	Copper	Copper
Coupler torch/gas pipe	Brass	Brass	Brass
Electrode	Tungsten	Tungsten	Tungsten
External Block	Copper	Copper	Copper
Handle	Copper	Copper	Copper
Internal Block	Steel	Copper	Steel
Torch Body	Teflon	Teflon	Teflon

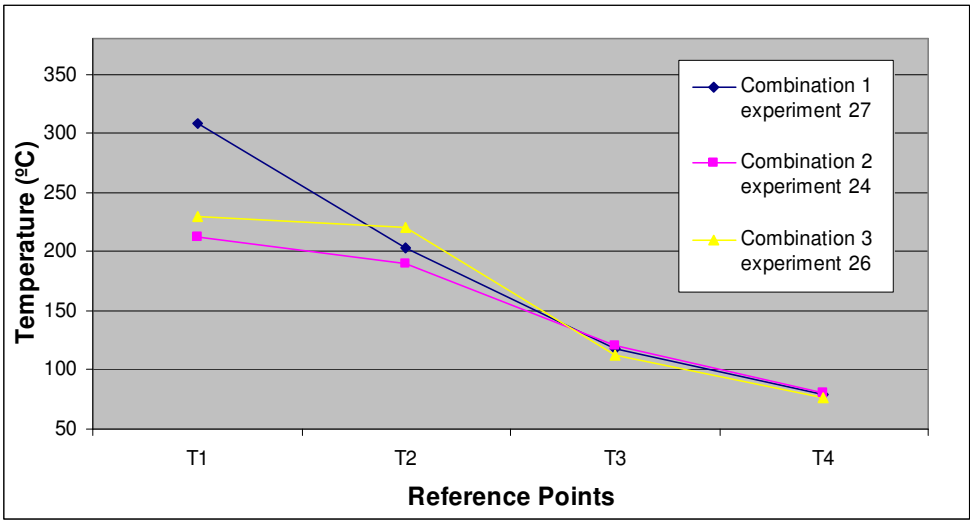

Figure E-2 Diagram of temperature at reference points dependent on material combination. Parameters: welding time 3.5 min, 3.2 mm electrode diameter, z_{ew} 5 mm, z_{ne} 5 mm, 300 A, 25 º C, turbulent regime with “becoming element of turbulence. Model D: short collet body with hollow handle.

The following observations are obtained by looking Figure E-2:
(1) The use of copper collet body make conduction heat to up welding torch be faster than conduction with steel collet body. This slower heat transfer causes that temperatures at the handle and at T1 with steel collet body are a little lower than with copper collet body.
(2) The use of steel internal block gets temperatures higher than with copper block.
(3) The use of steel collet body and steel internal block at the same combination gives singular results at T2; this temperature has a value higher as it was expected.

3 CURRENT FLOW

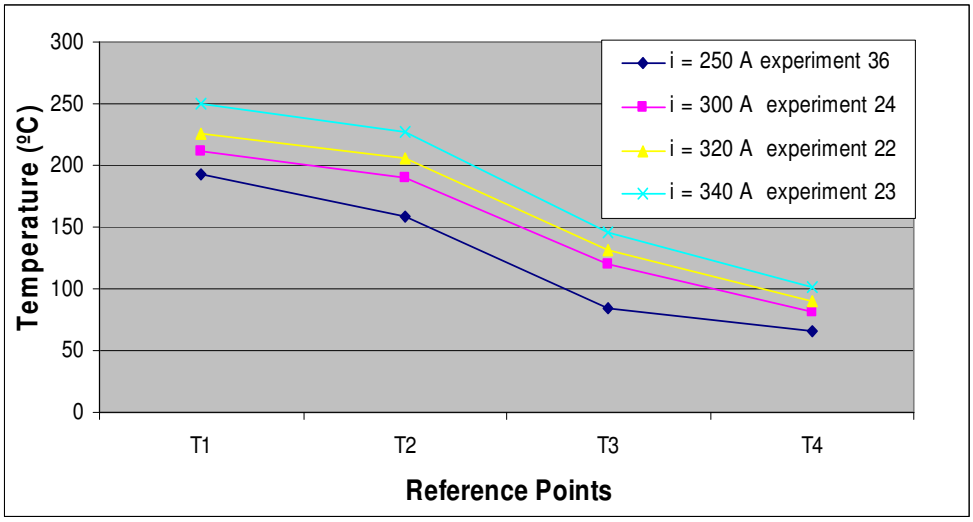

Figure E-3 Temperature profiles of experimental results at reference points for different current values. Parameters: welding time 3.5 min, 25 º C, 3.2 mm electrode diameter, z_{ne} = 5 mm, z_{ew} 5 mm, turbulent regime with “becoming element of turbulence”. Model D: short collet body with hollow handle.

As Figure 6.2.5 illustrates, temperatures rise as current flow increases. The temperature increased between a curve and the next up one at T1 and T2 is bigger than at T4 and T3, that is, the increase of current has more effect at these points than at T4 and T3.

One of possible explanations might be the resistance of the welding elements to electrical current running through them, what generates joule heat. This resistance depends on material and geometry. As the material for collet body, external block and handle is the same. This means that the geometry in the handle is less favourable for current running through.

4 ELECTRODE DIAMETER

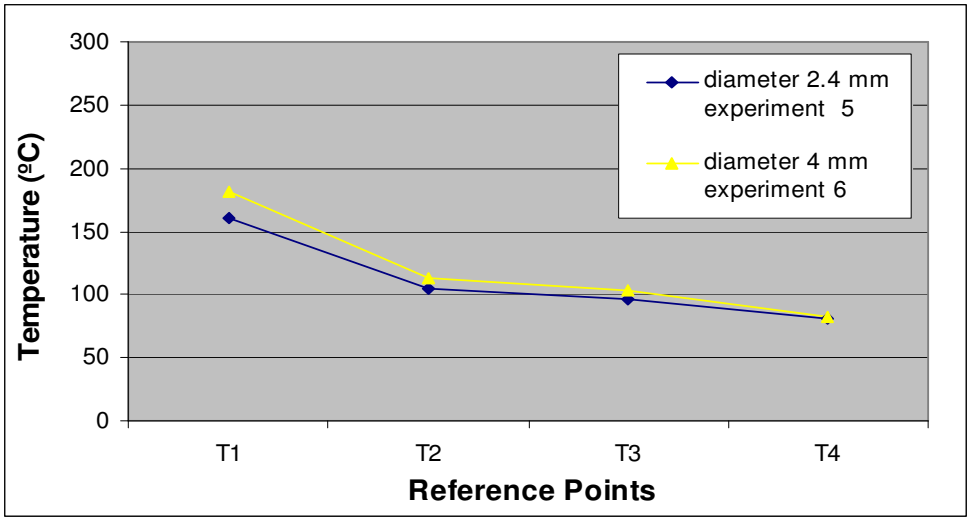

Figure E-4 Temperature profiles of experimental results at reference points for different electrode diameter. Parameters: welding time 3.5 min, 25 º C, z_{ew} 5 mm, z_{ne} = 5 mm, 150 A, laminar flow without "becoming element of turbulence". Model B: short collet body with solid handle.

5 VOLUMETRIC FLOW RATE

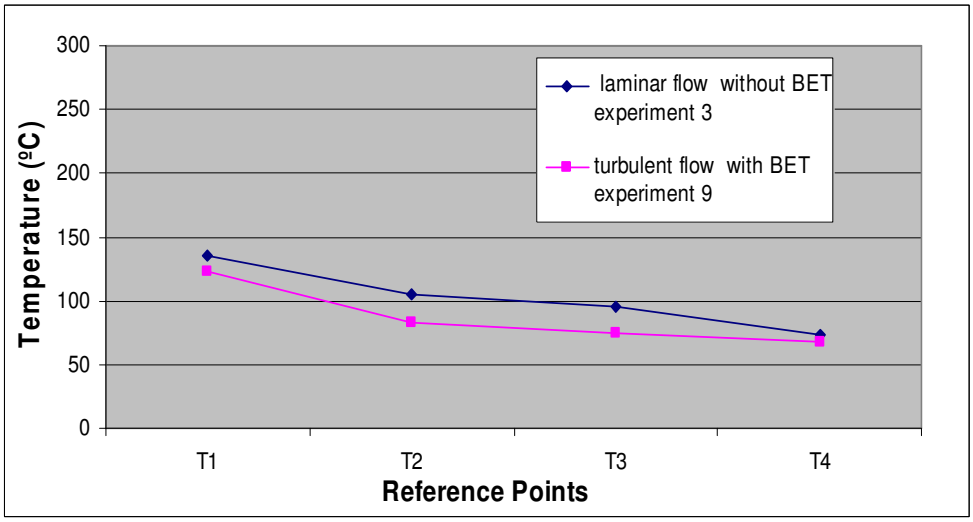

Figure E-5 Temperature profiles of experimental results at reference points for different flow regimen. Parameters: welding time 3.5 min, 25 º C, z_{ew} 5 mm, z_{ne} = 5 mm, 150 A. Model A: long collet body with solid handle.

BET means "becoming element of turbulence".

6 DUTY CYCLE

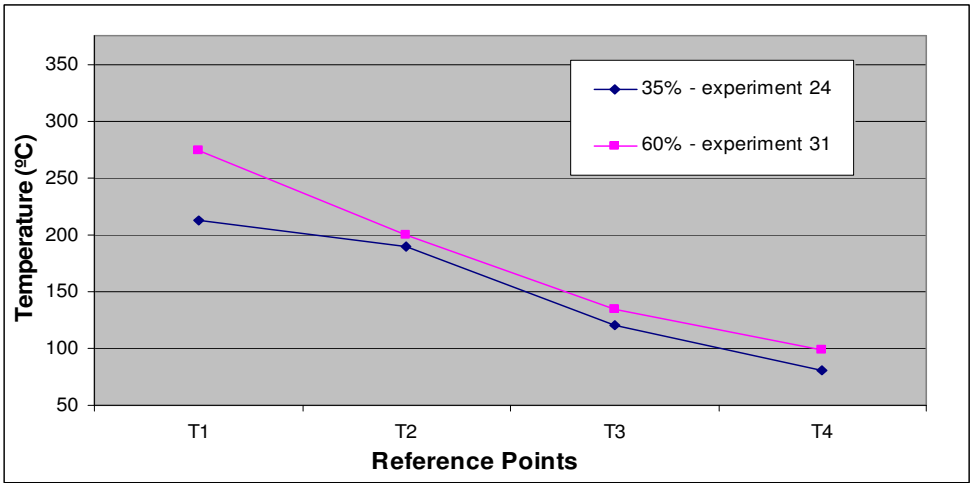

Figure E-6 Temperature profile at reference points for different duty cycle: 35% and 60%. Parameters: 25 º C, z_{ew} = 5 mm, z_{ne} = 5 mm, 300 A, diameter electrode 3.2 mm, turbulent regime, collet with "becoming element of turbulence". Model D: short collet body with hollow handle.

Figure E-7 shows that temperature profiles go up for each next cycle.

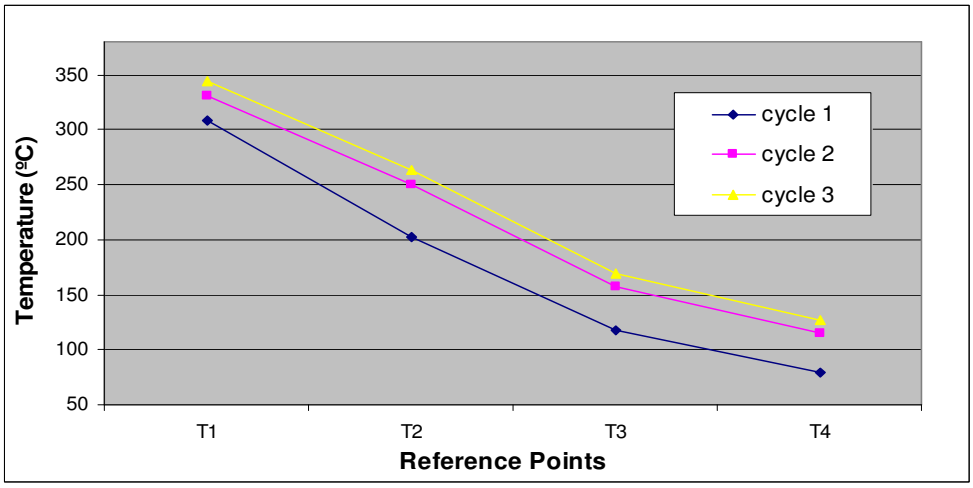

Figure E-7 Temperature profile of experiment 26 at reference points after each cycle. Parameters: 25 º C, z_{ew} = 5 mm, z_{ne} = 5 mm, 300 A, diameter electrode 3.2 mm, turbulent regime, collet with "becoming element of turbulence" and welding time 3.5 min, cooling time is 6.5 min per cycle. Model D: short collet body with hollow handle.

APPENDIX F

ANSYS PLOTS

1 GEOMETRY PLOTS

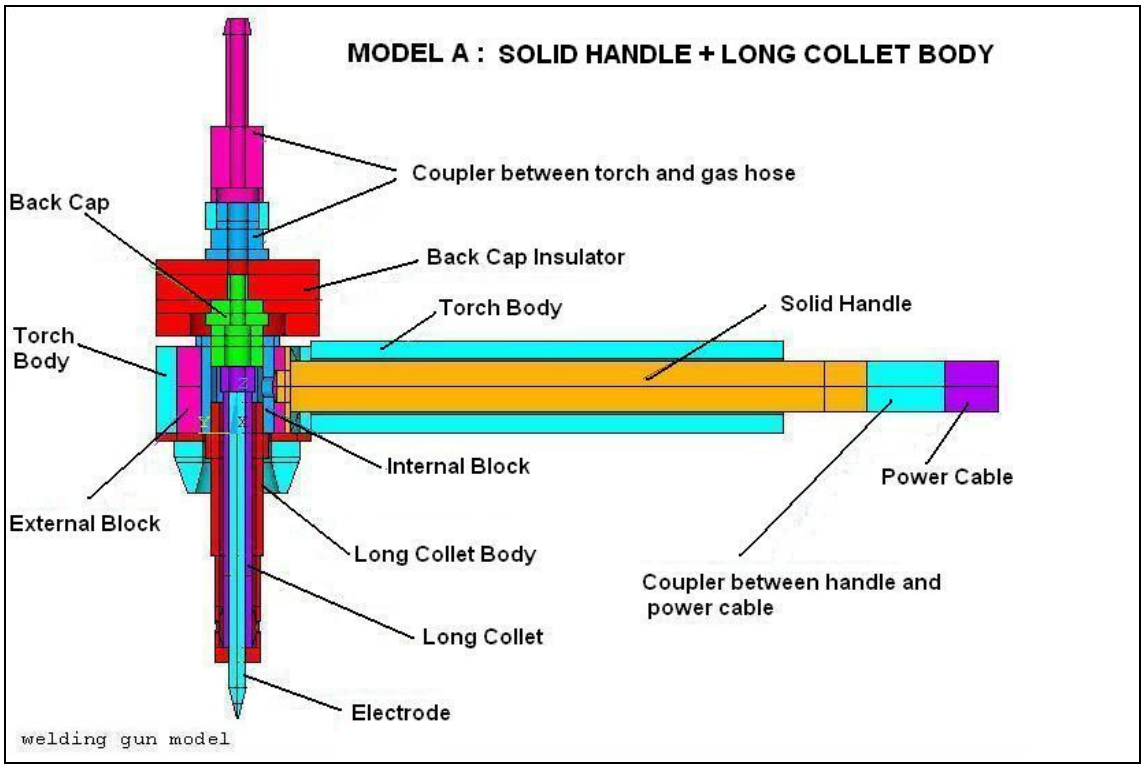

Figure F-1.1 Cross-sectional view of welding torch model A.

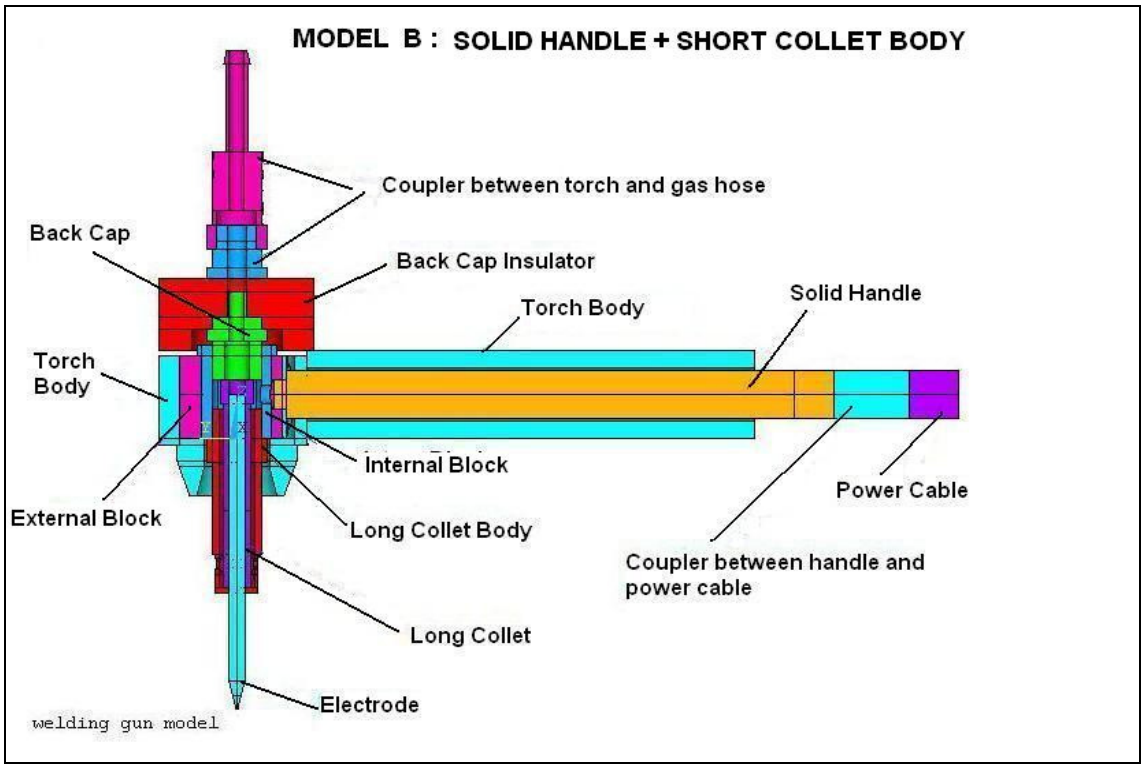

Figure F-1.2 Cross-sectional view of welding torch model B.

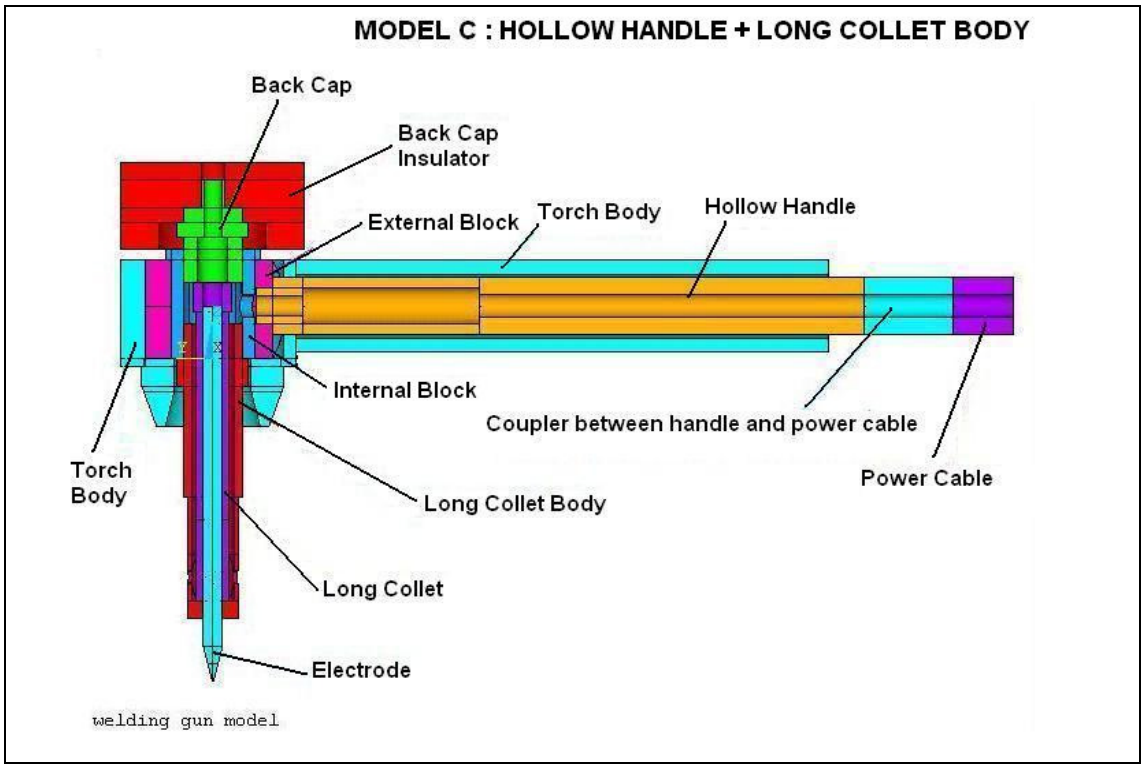

Figure F-1.3 Cross-sectional view of welding torch model C.

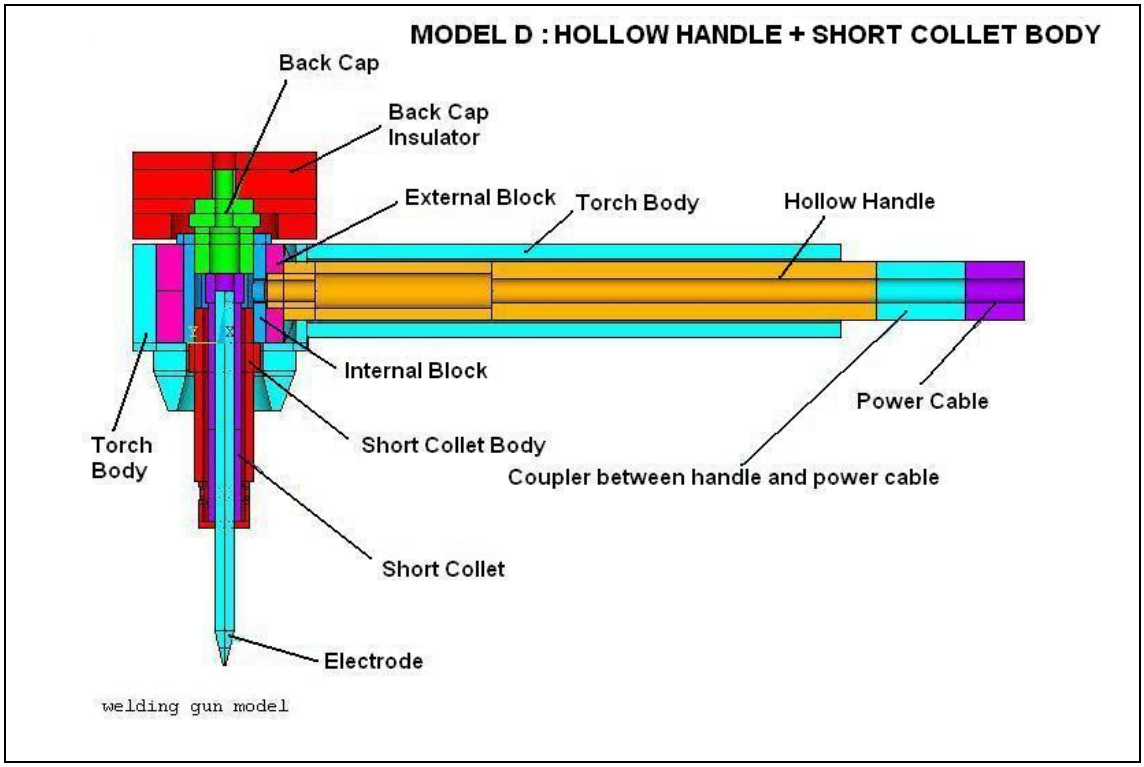

Figure F-1.4 Cross-sectional view of welding torch model D.

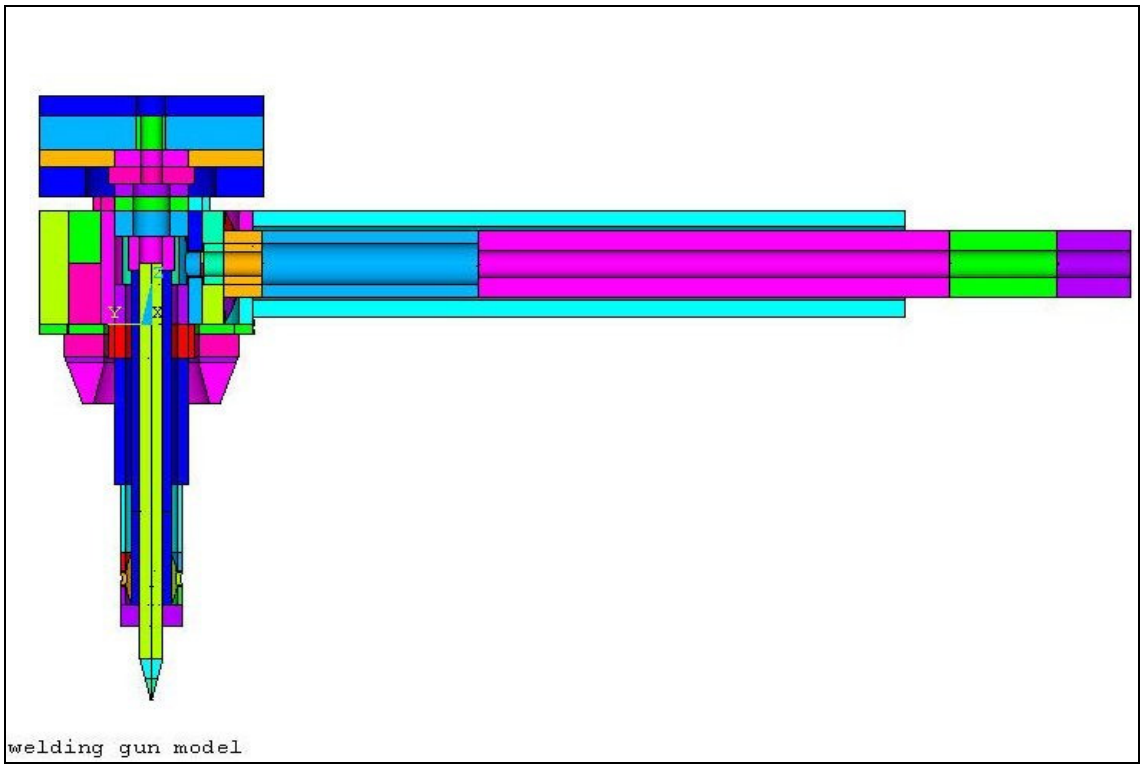

Figure F-1.5 Schematic diagram of model C divided in small volumes for being meshed.

2 MESH

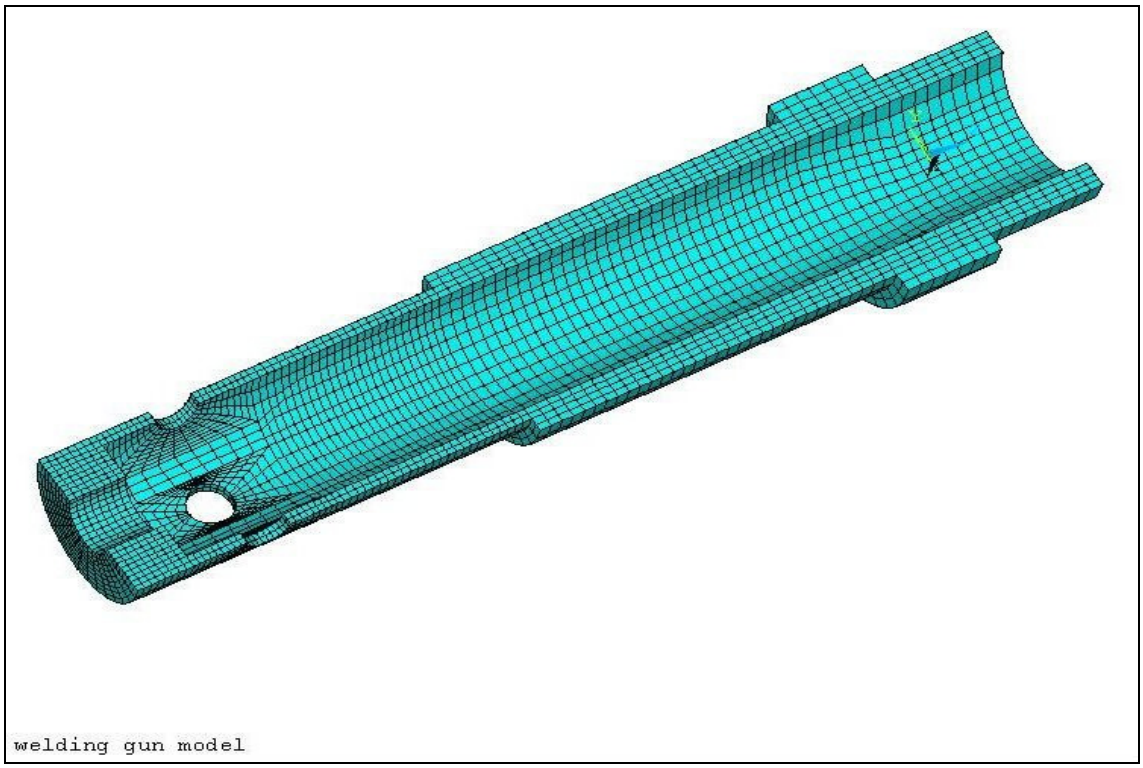

Figure F-2.1 Meshing long collet body of the welding torch model in Ansys.

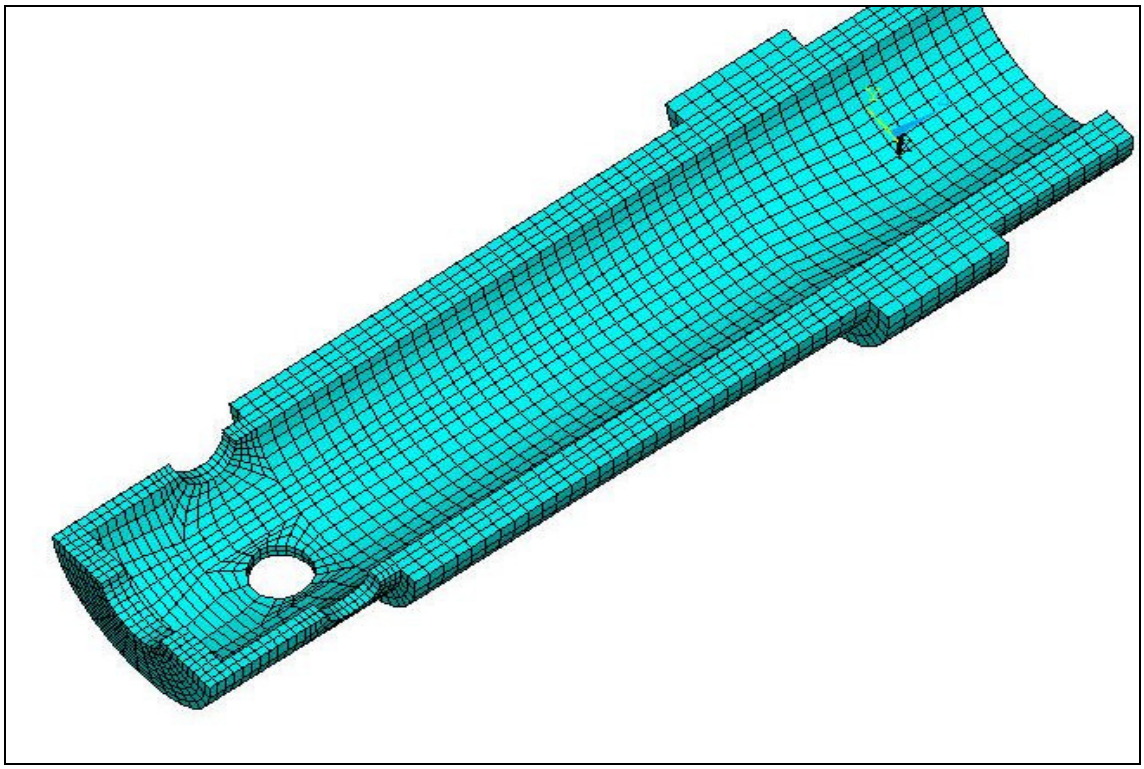

Figure F-2.2 Meshing short collet body of the welding torch model in Ansys.

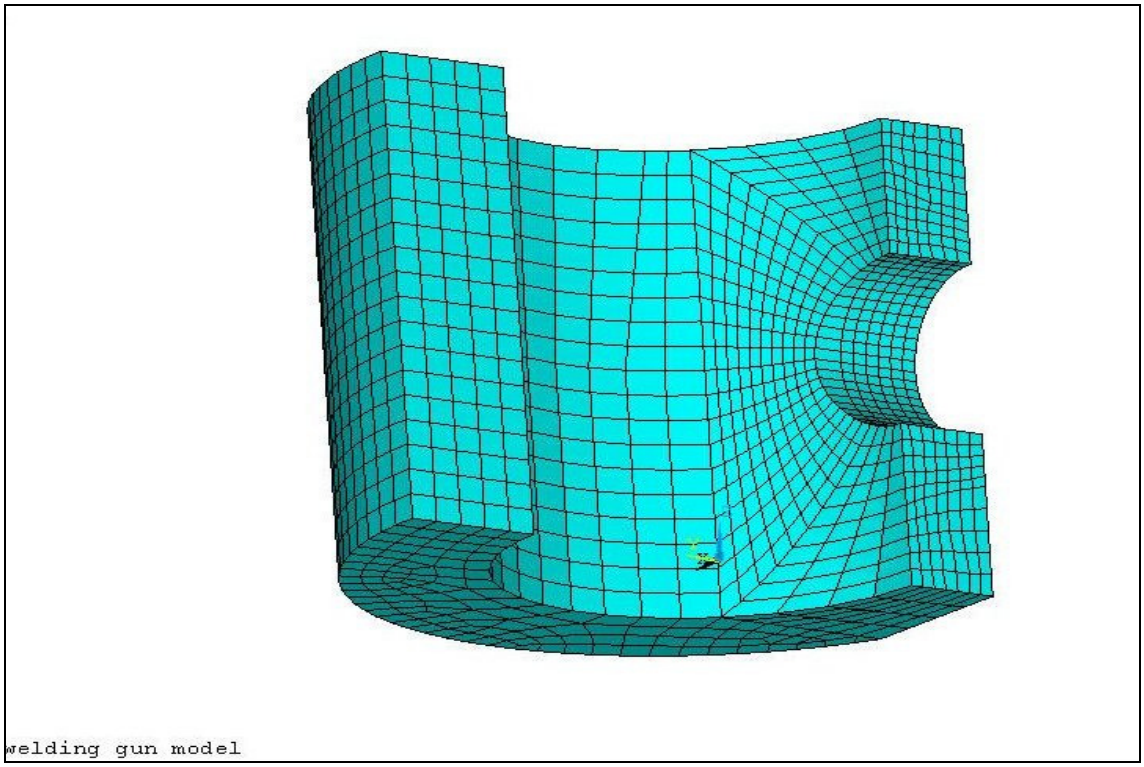

Figure F-2.3 Meshing external block of the welding torch model in Ansys.

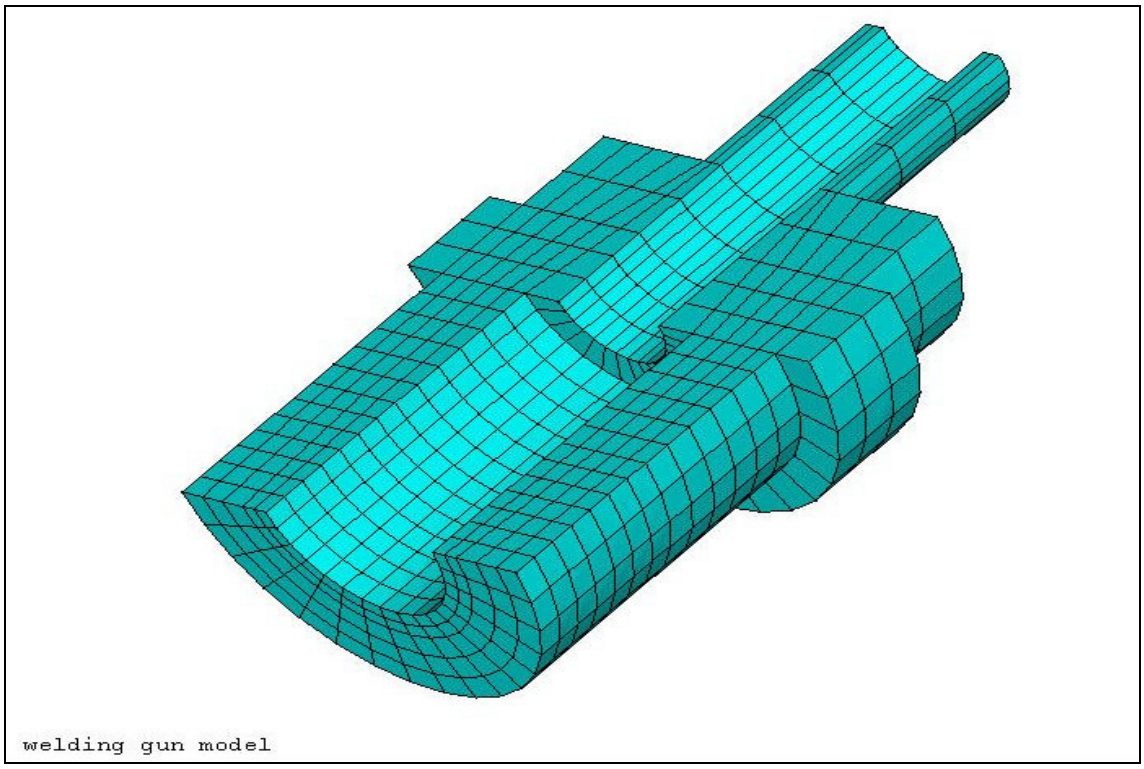

Figure F-2.4 Meshing back cap of the welding torch model in Ansys.

3 BOUNDARY CONDITIONS AND LOADS

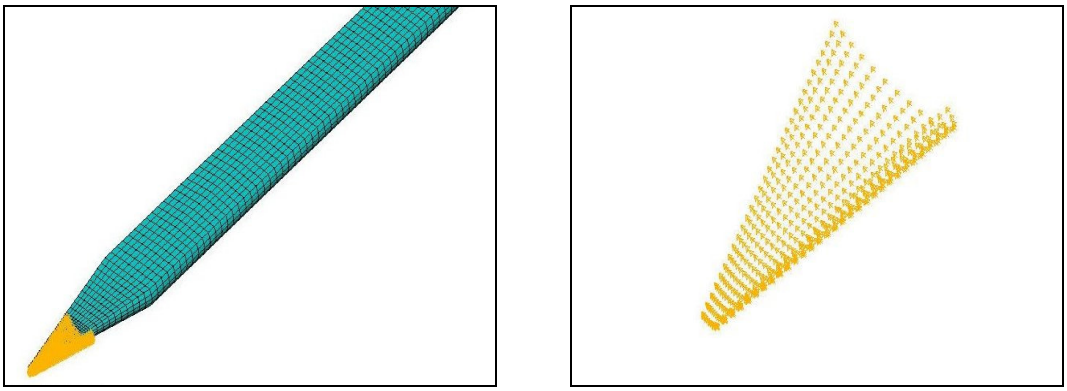

(a) (b)

Figure F-3.1 (a) Temperature boundary condition on nodes at surface of the tip of electrode along 3 mm. (b) Detail of temperature boundary on nodes.

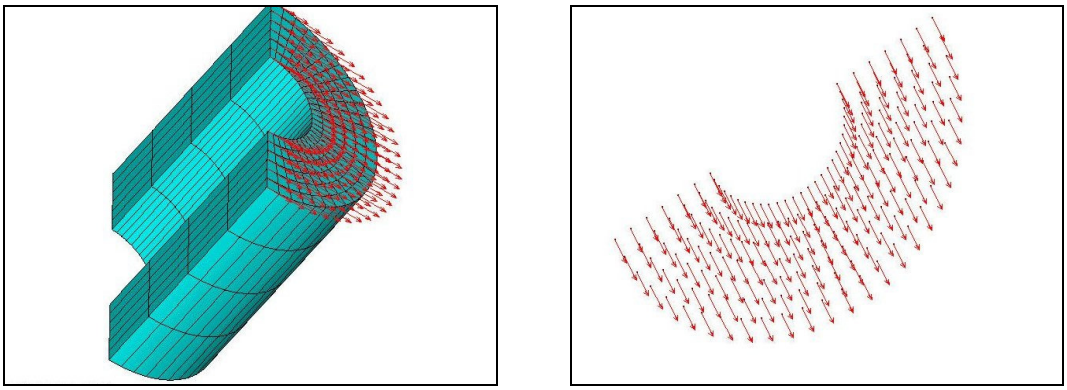

(a) (b)

Figure F-3.2 (a) Temperature boundary condition on nodes at surface of the tip of electrode along 3 mm. (b) Detail of temperature boundary on nodes.

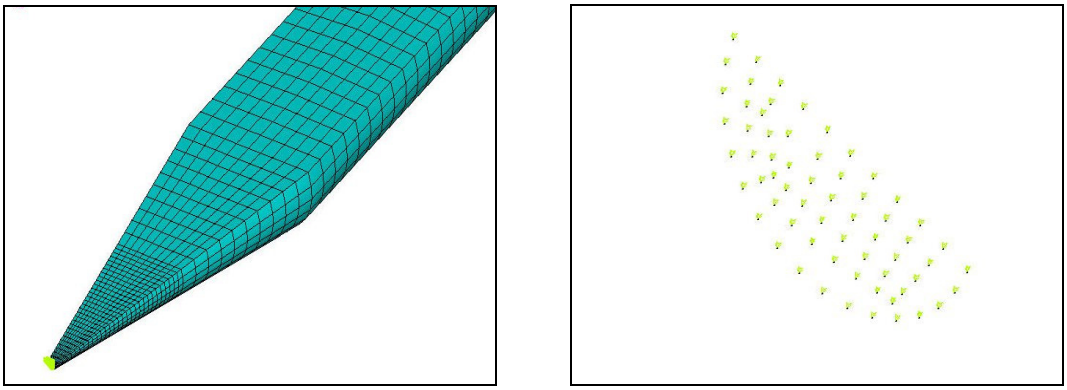

(a) (b)

Figure F-3.3 (a) Temperature boundary condition on nodes at surface of the tip of electrode along 3 mm. (b) Detail of temperature boundary on nodes.

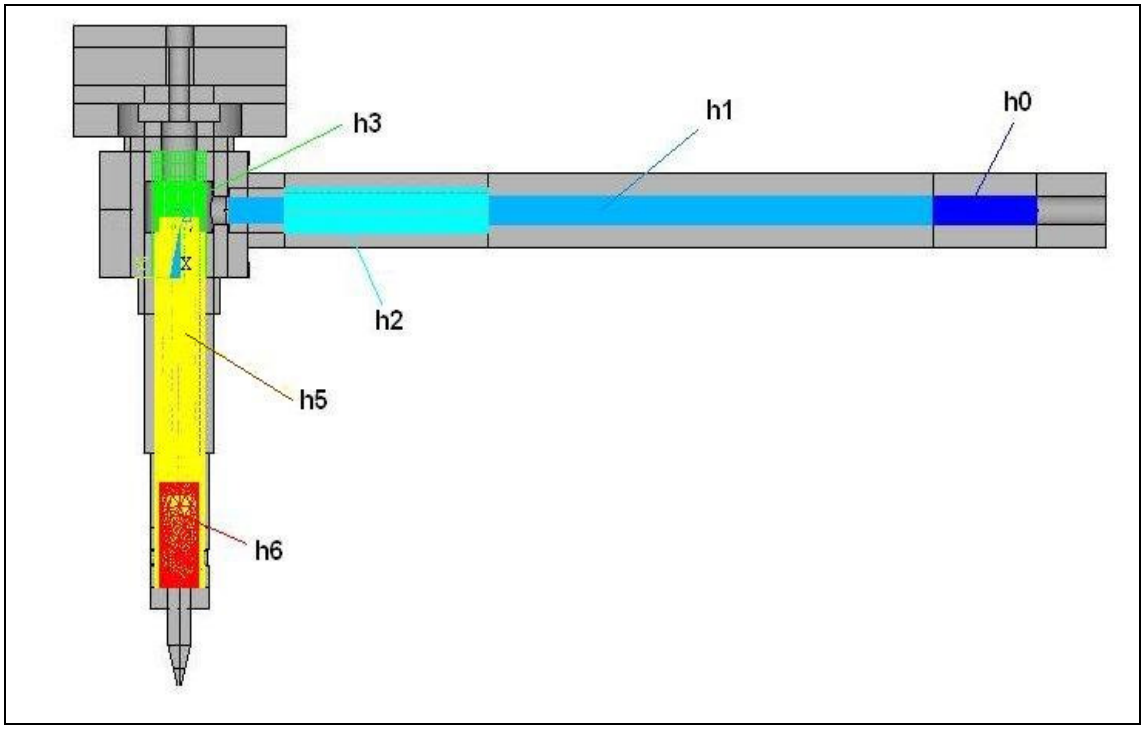

Figure F-3.4 Convective coefficients for different regions in welding torch due to forced convection. Geometry: model C.

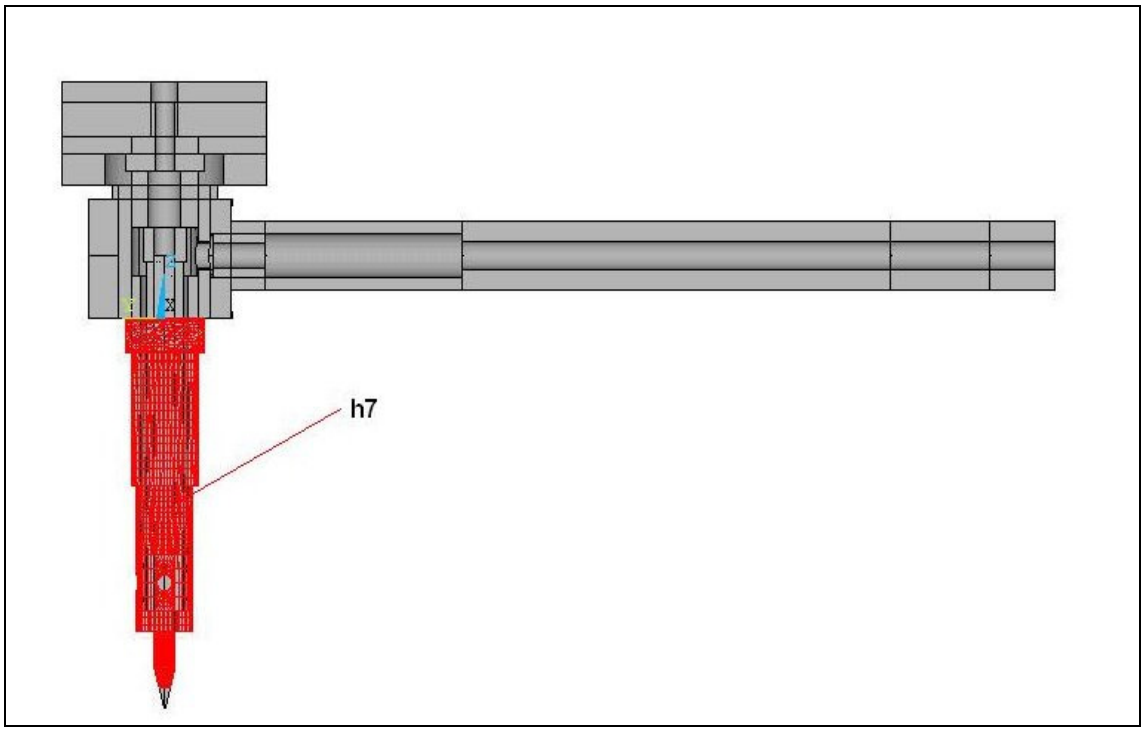

Figure F-3.5 Convective coefficient (h_7) in welding torch due to free convection between the nozzle and the external surface of collet body and the electrode. Geometry: model C.

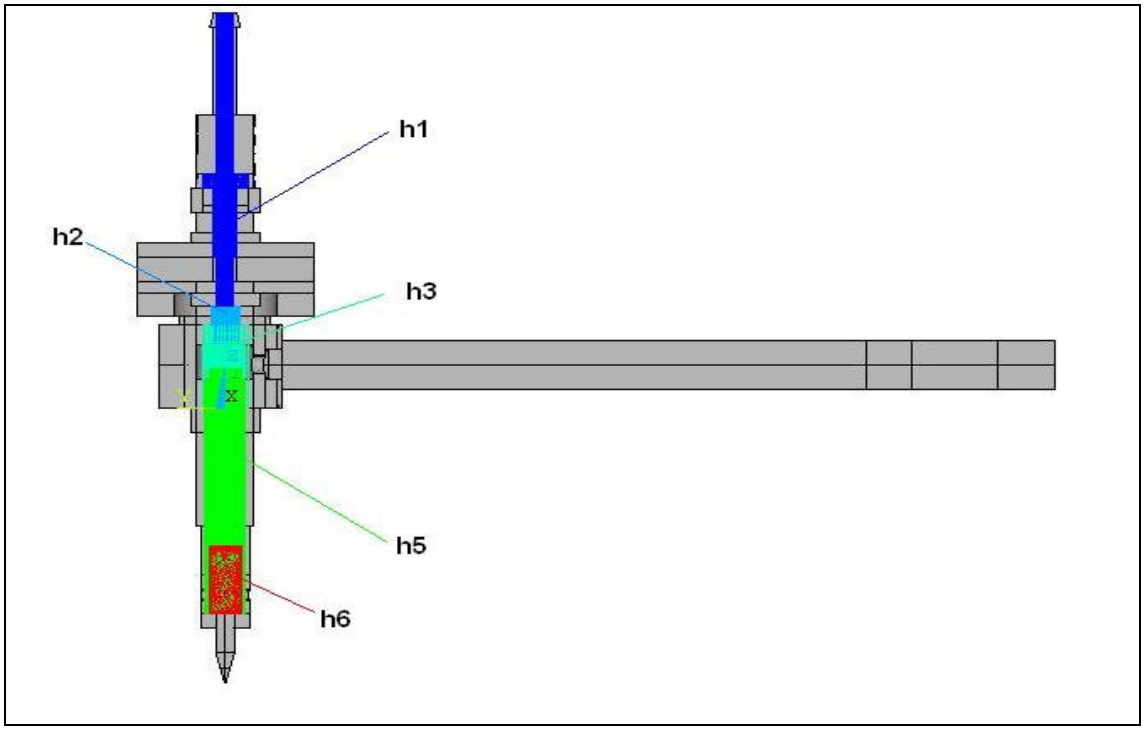

Figure F-3.6 Convective coefficients for different regions in welding torch due to forced convection. Geometry: model A.

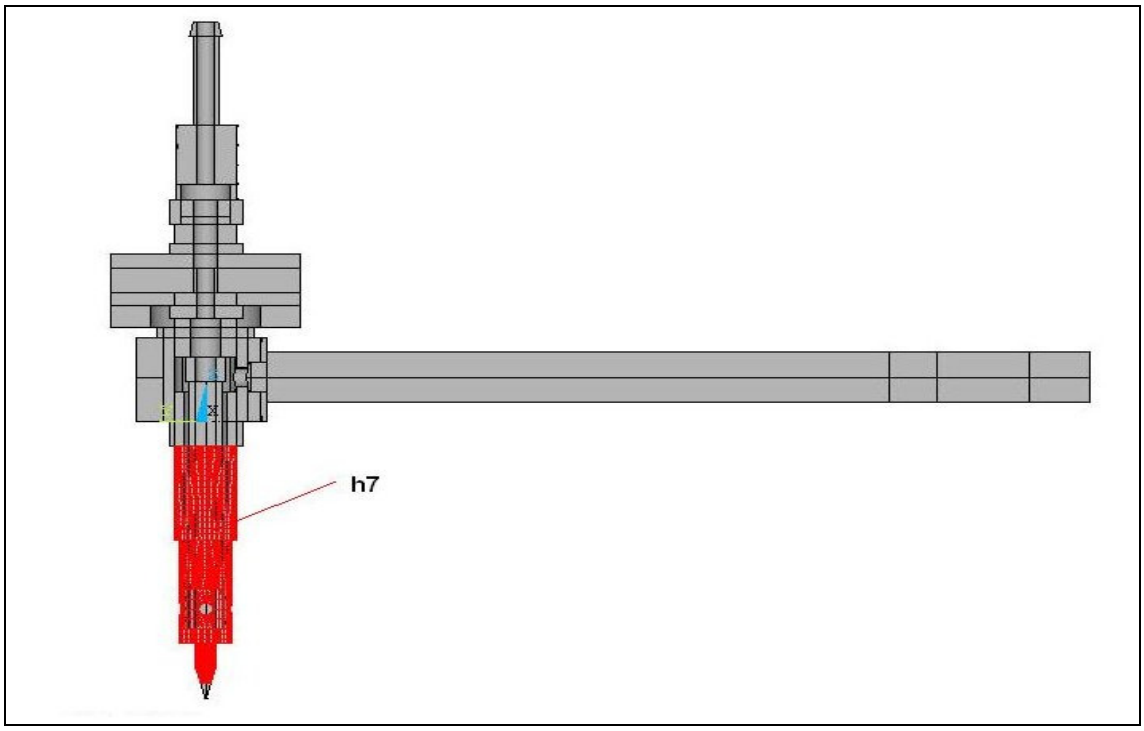

Figure F-3.7 Convective coefficient (h_7) in welding torch due to free convection between the nozzle and the external surface of collet body and the electrode. Geometry: model C.

4 SIMULATION PLOT

4.1 Simulation of geometry

4.1.1 Model A: solid handle + long collet body

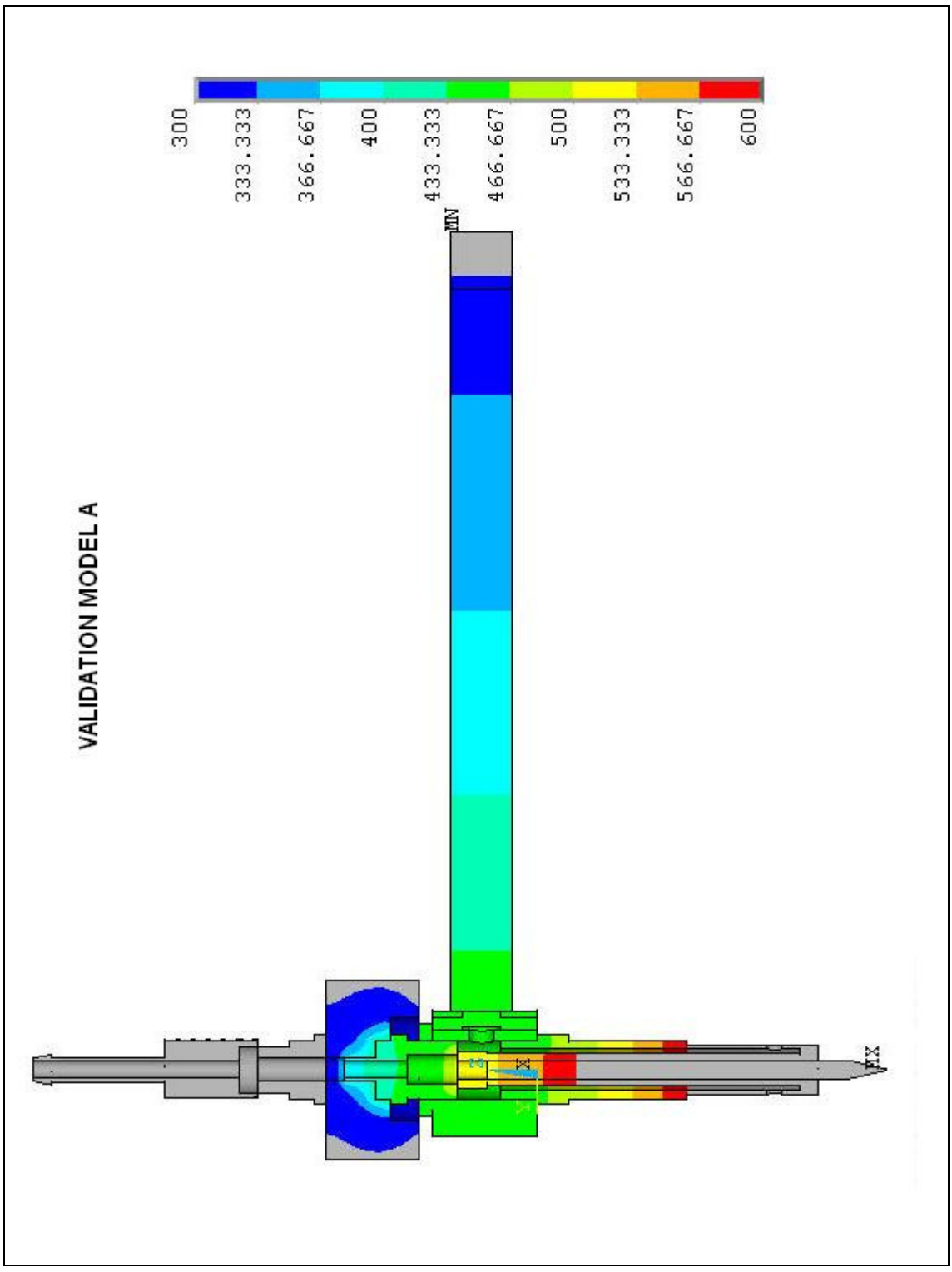

Figure F-4.1.1 Temperature plot in welding torch for model A. Scale from 300 to 600 K. Simulation conditions; 250 A, material combination number 0, diameter 3.2 mm, turbulent regime, collet with “becoming element of turbulence” and simulating time 3’ 30”.

4.1.2 Model B: solid handle + short collet body

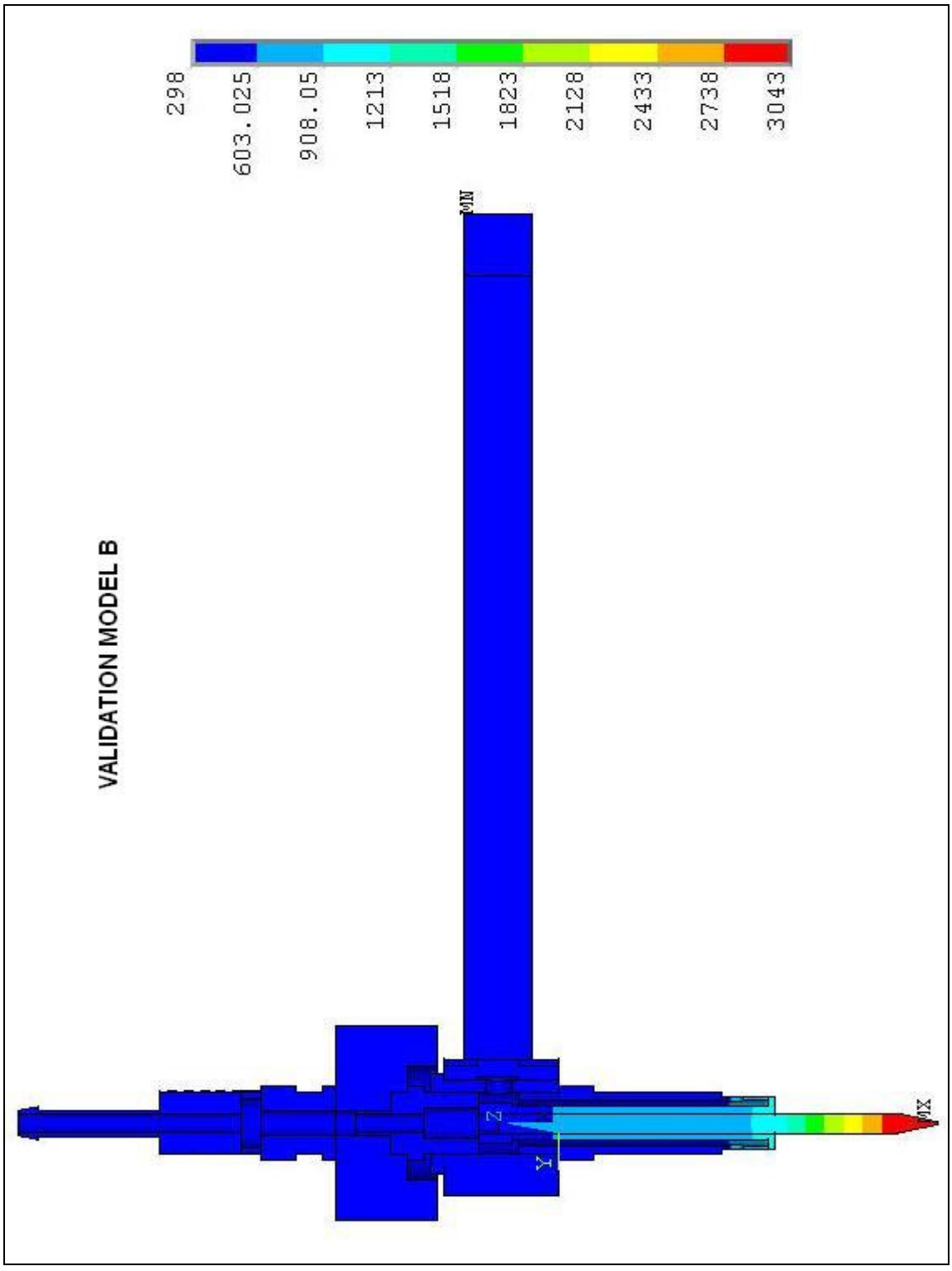

Figure F-4.1.2 Temperature plot in welding torch for model B. Scale from 298 to 3043 K. Simulation conditions; 250 A, material combination number 0, diameter 3.2 mm, turbulent regime, collet with “becoming element of turbulence” and simulating time 3’ 30”.

4.1.3 Model C: Hollow handle + long collet body

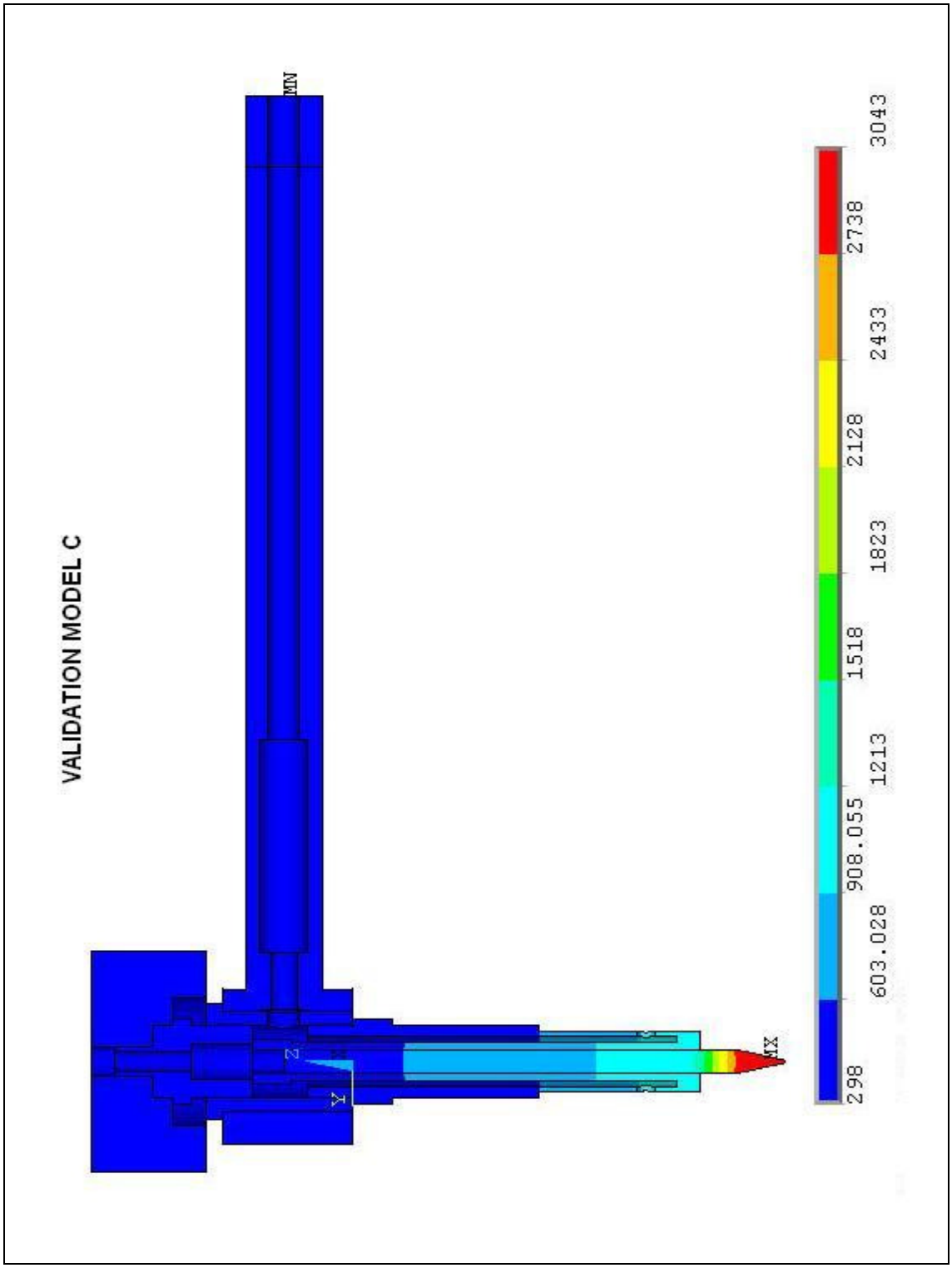

Figure F-4.1.3 Temperature plot in welding torch for model C. Scale from 298 to 3043 K. Simulation conditions; 250 A, material combination number 0, diameter 3.2 mm, turbulent regime, collet with “becoming element of turbulence” and simulating time 3’ 30”.

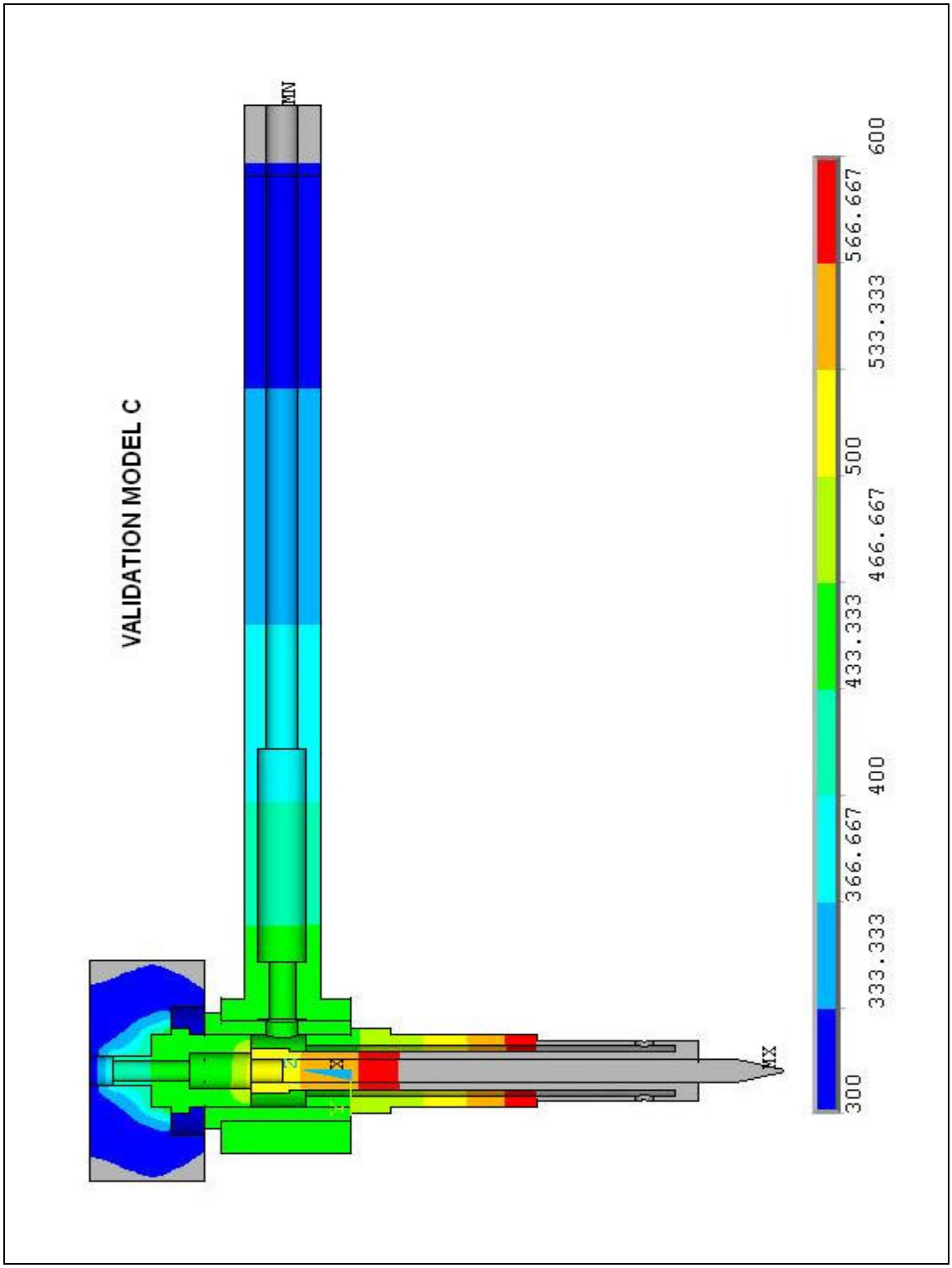

Figure F-4.1.4 Temperature plot in welding torch for model C. Scale from 300 to 600 K. Simulation conditions; 250 A, material combination number 0, diameter 3.2 mm, turbulent regime, collet with “becoming element of turbulence” and simulating time 3’ 30”.

4.1.4 Model D: hollow handle + short collet body

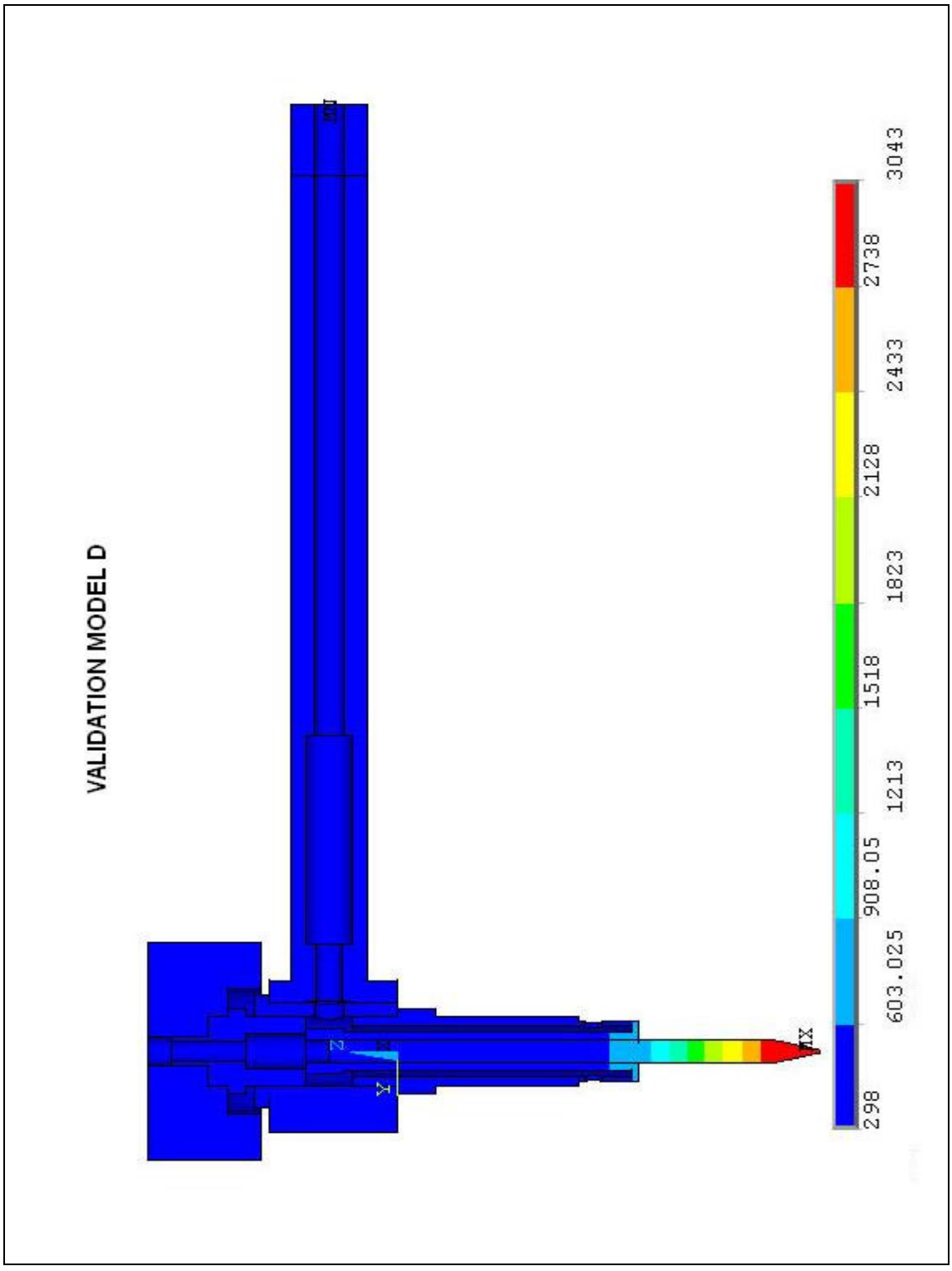

Figure F-4.1.5 Temperature plot in welding torch for model D. Scale from 298 to 3043 K. Simulation conditions; 250 A, material combination number 0, diameter 3.2 mm, turbulent regime, collet with “becoming element of turbulence” and simulating time 3’ 30”.

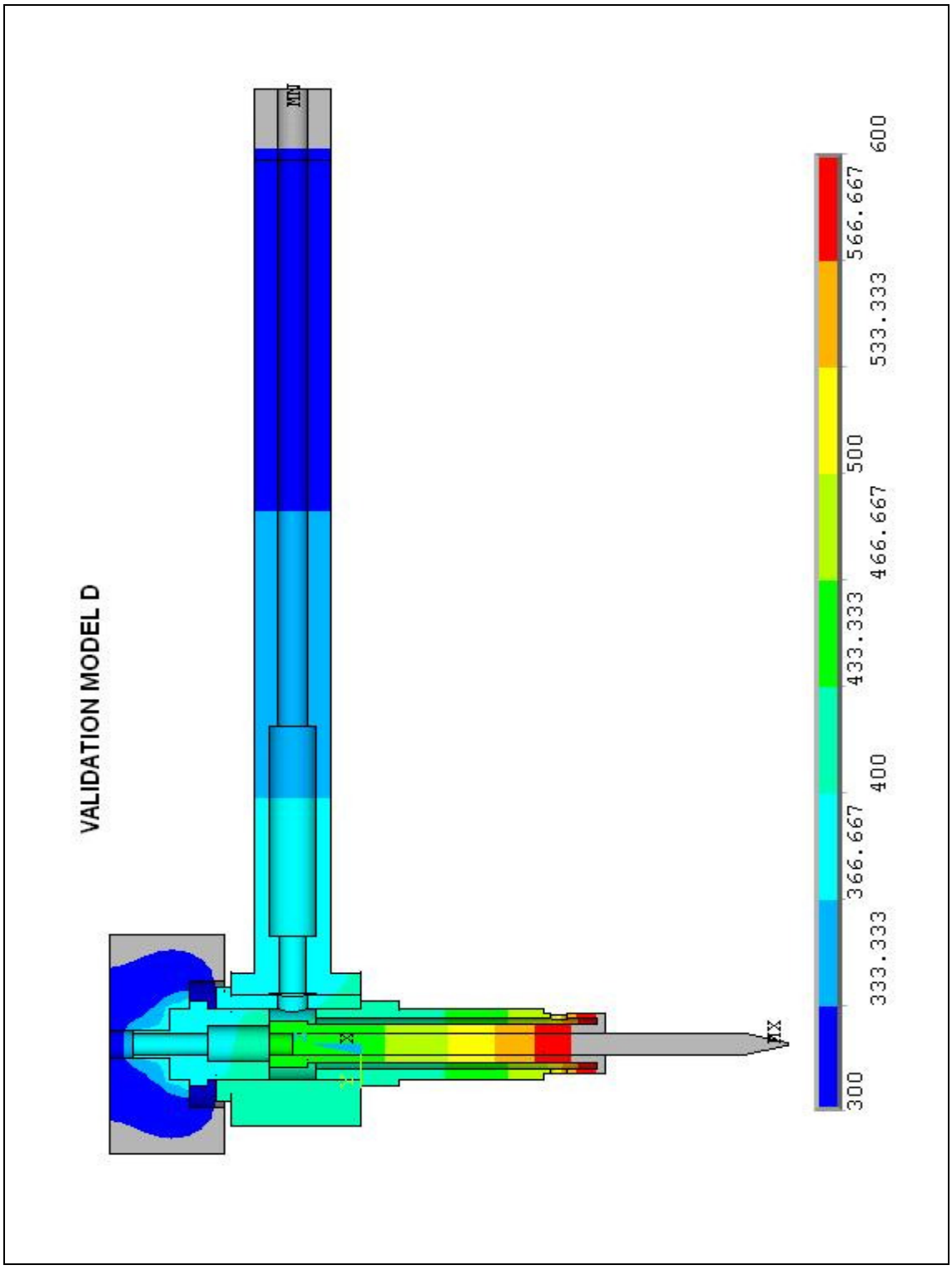

Figure F-4.1.6 Temperature plot in welding torch for model D. Scale from 300 to 600 K. Simulation conditions; 250 A, material combination number 0, diameter 3.2 mm, turbulent regime, collet with "becoming element of turbulence" and simulating time 3' 30".

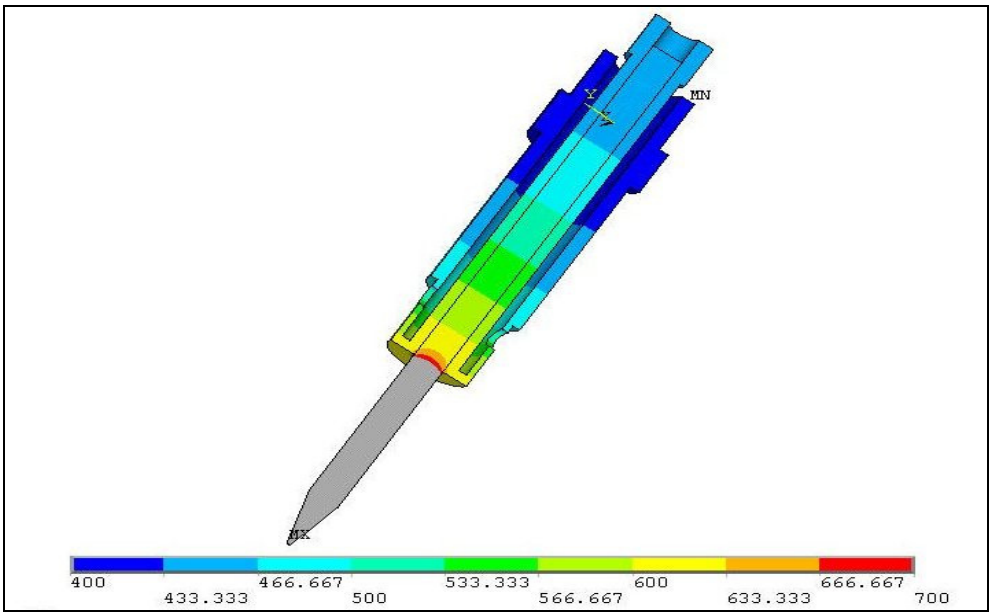

Figure F-4.1.7 Temperature plot in welding torch for model D. Detail of the collet, collet body and electrode. Scale from 400 to 700 K. Simulation conditions; 250 A, material combination number 0, diameter 3.2 mm, turbulent regime, collet with "becoming element of turbulence" and simulating time 3' 30".

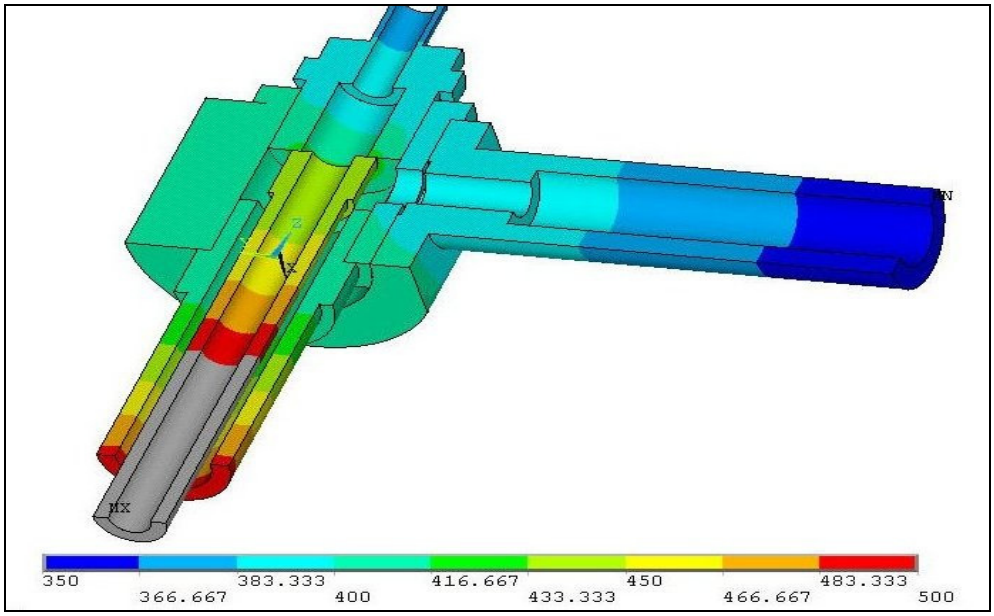

Figure F-4.1.8 Temperature plot in welding torch for model D. Detail of elements close to block internal and block external. Scale from 350 to 500 K. Simulation conditions; 250 A, material combination number 0, diameter 3.2 mm, turbulent regime, collet with "becoming element of turbulence" and simulating time 3' 30".

4.2 Simulation of Material Combinations

4.2.0 Combination 0

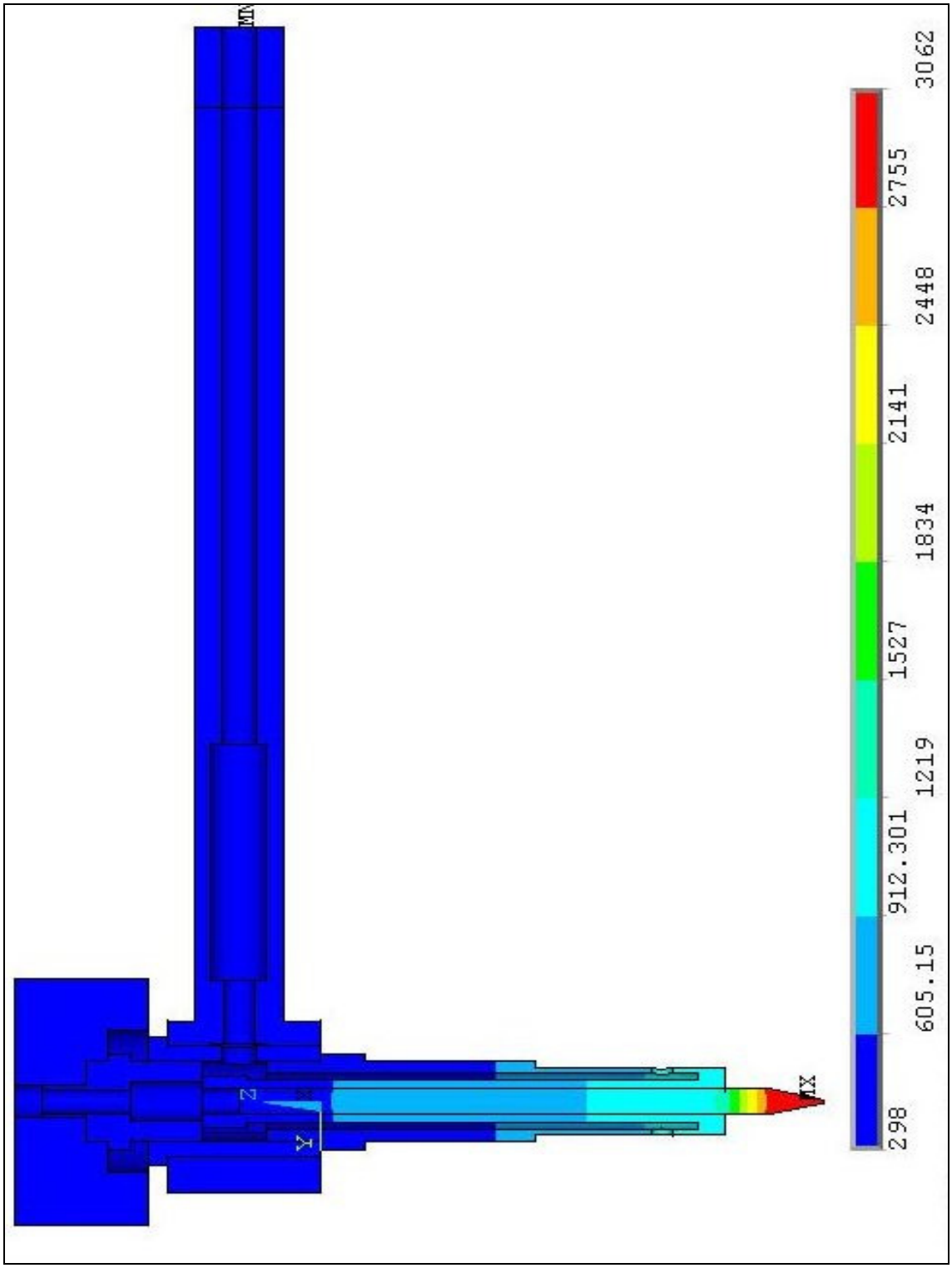

Figure F-4.2.1 Temperature plot in welding torch for the material combination number 0. Scale from 298 to 3062 K. Simulation conditions; 300 A, model C, uniform temperature 298 K, diameter 3.2 mm, turbulent regime, collet with “becoming element of turbulence” and simulating time 3’ 30”.

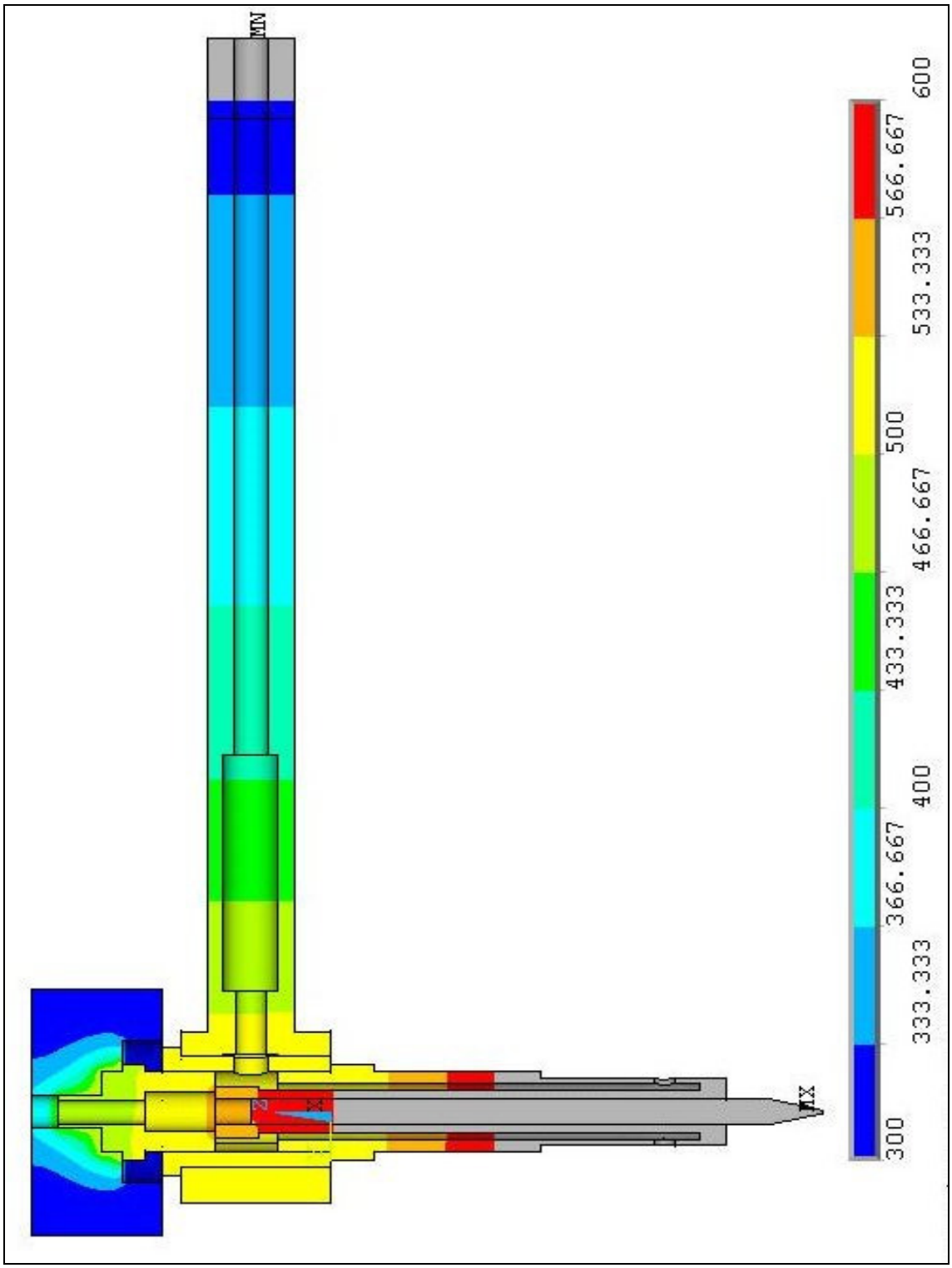

Figure F-4.2.2 Temperature plot in welding torch for material combination number 0. Scale from 300 to 600 K. Simulation conditions; 300 A, model C, uniform temperature 298 K, diameter 3.2 mm, turbulent regime, collet with “becoming element of turbulence” and simulating time 3’ 30”.

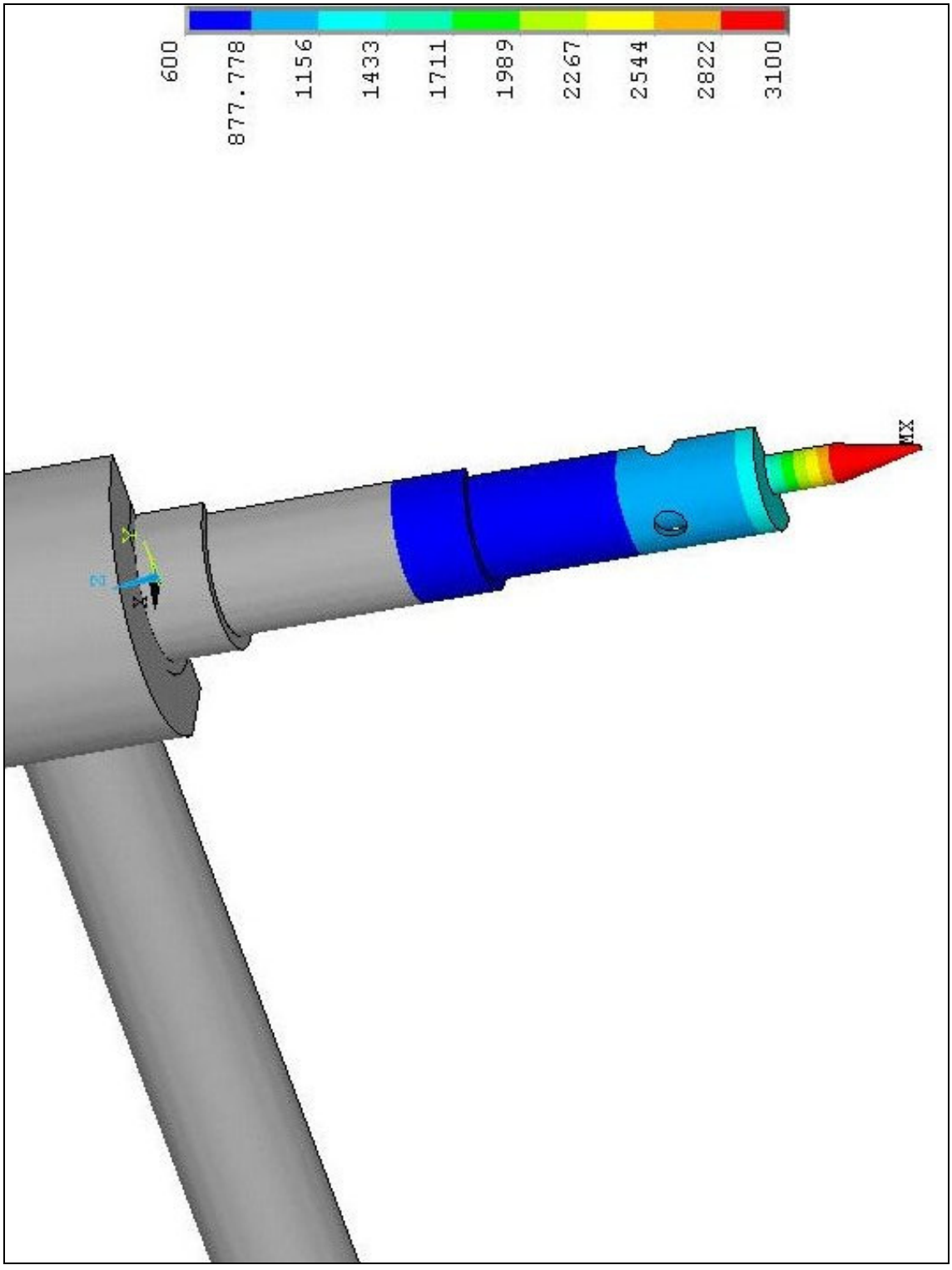

Figure F-4.2.3 Temperature plot of collet body for material combination number 0. Scale from 600 to 3100 K. Simulation conditions; 300 A, model C, uniform temperature 298 K, diameter 3.2 mm, turbulent regime, collet with “becoming element of turbulence” and simulating time 3’ 30”.

4.2.1 Combination 1

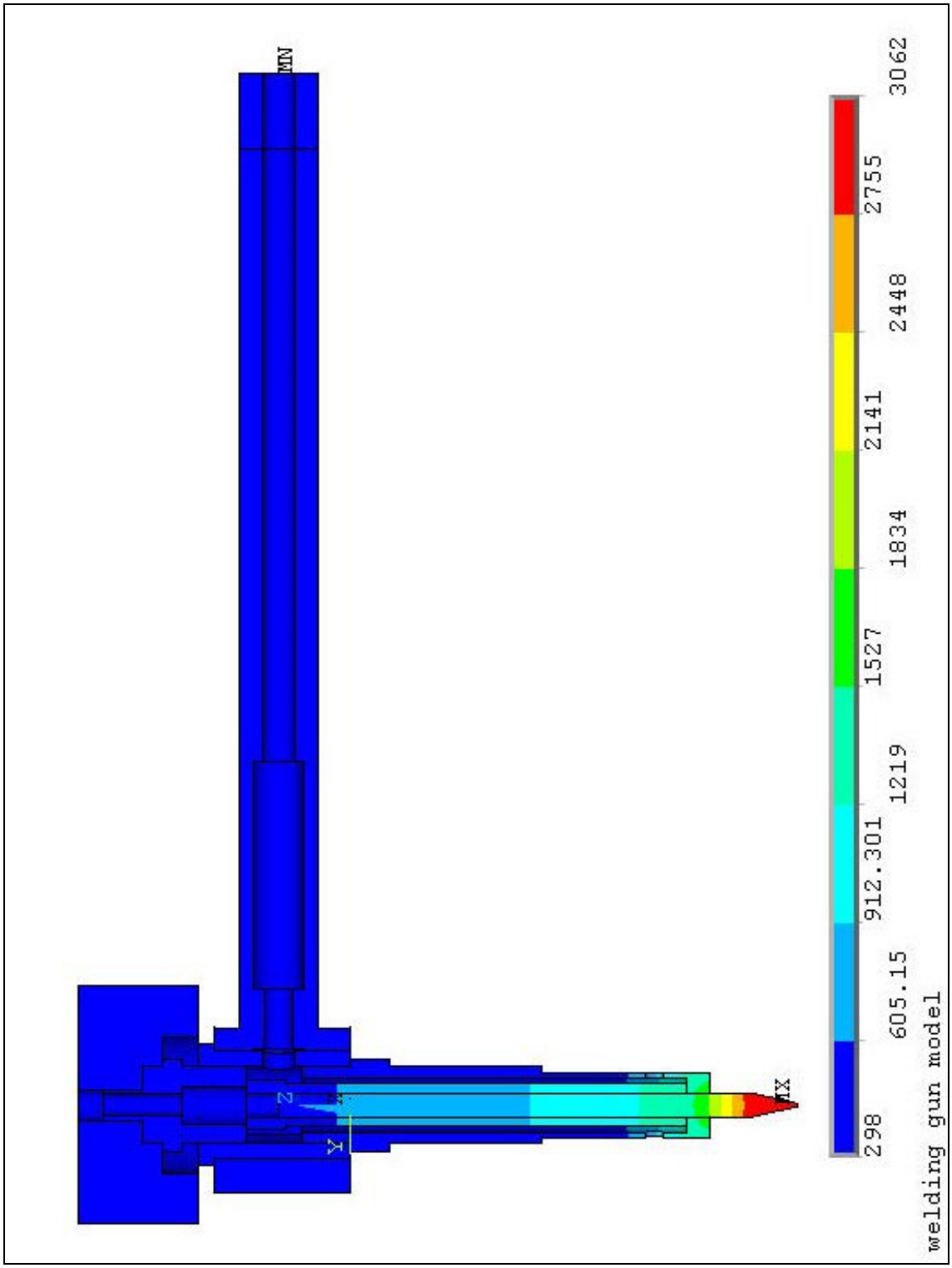

Figure F-4.2.4 Temperature plot in welding torch for the material combination number 1. Scale from 298 to 3062 K. Simulation conditions; 300 A, model C, uniform temperature 298 K, diameter 3.2 mm, turbulent regime, collet with “becoming element of turbulence” and simulating time 3’ 30”.

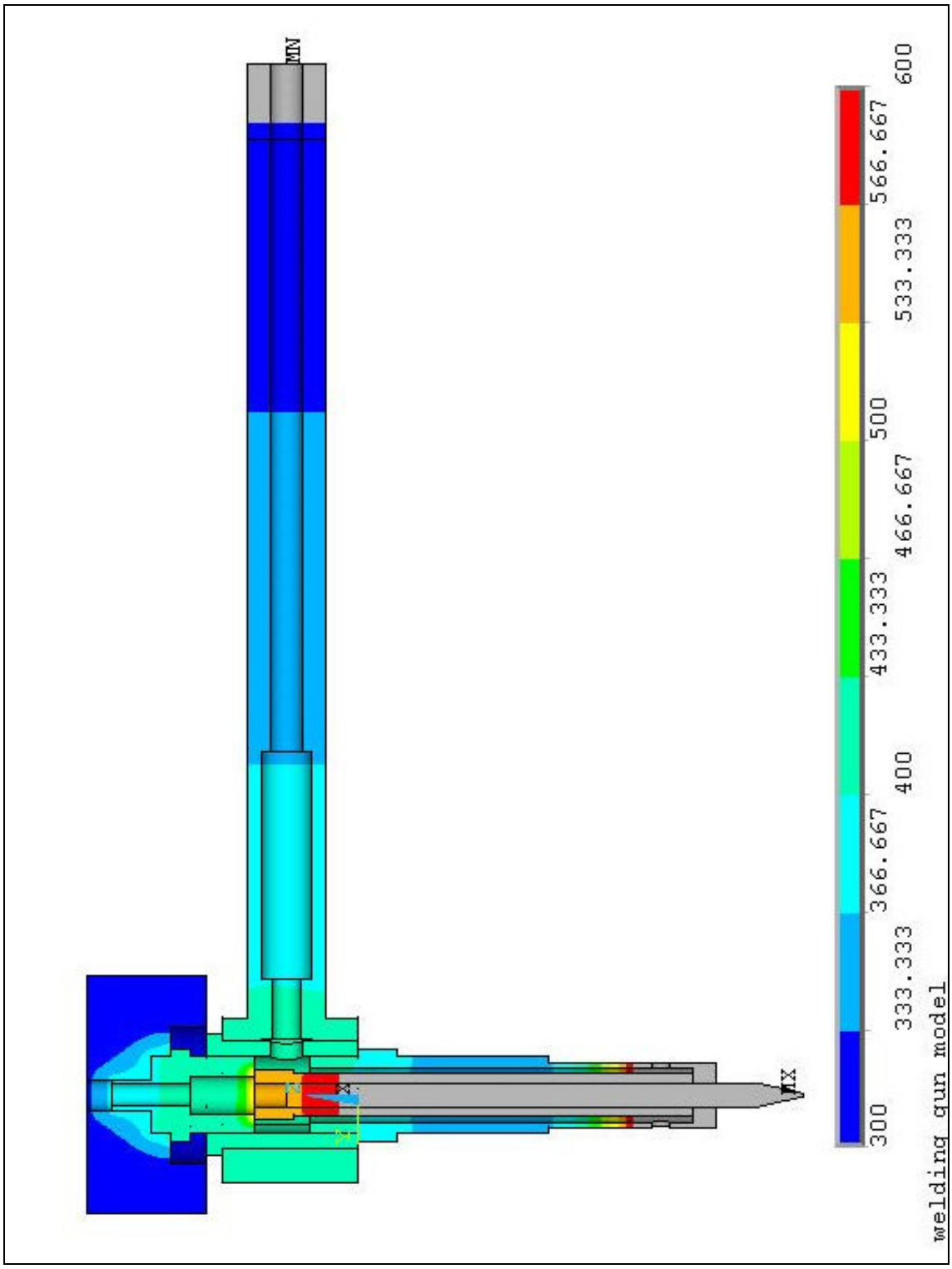

Figure F-4.2.5 Temperature plot in welding torch for material combination number 1. Scale from 300 to 600 K. Simulation conditions; 300 A, model C, uniform temperature 298 K, diameter 3.2 mm, turbulent regime, collet with “becoming element of turbulence” and simulating time 3’ 30”.

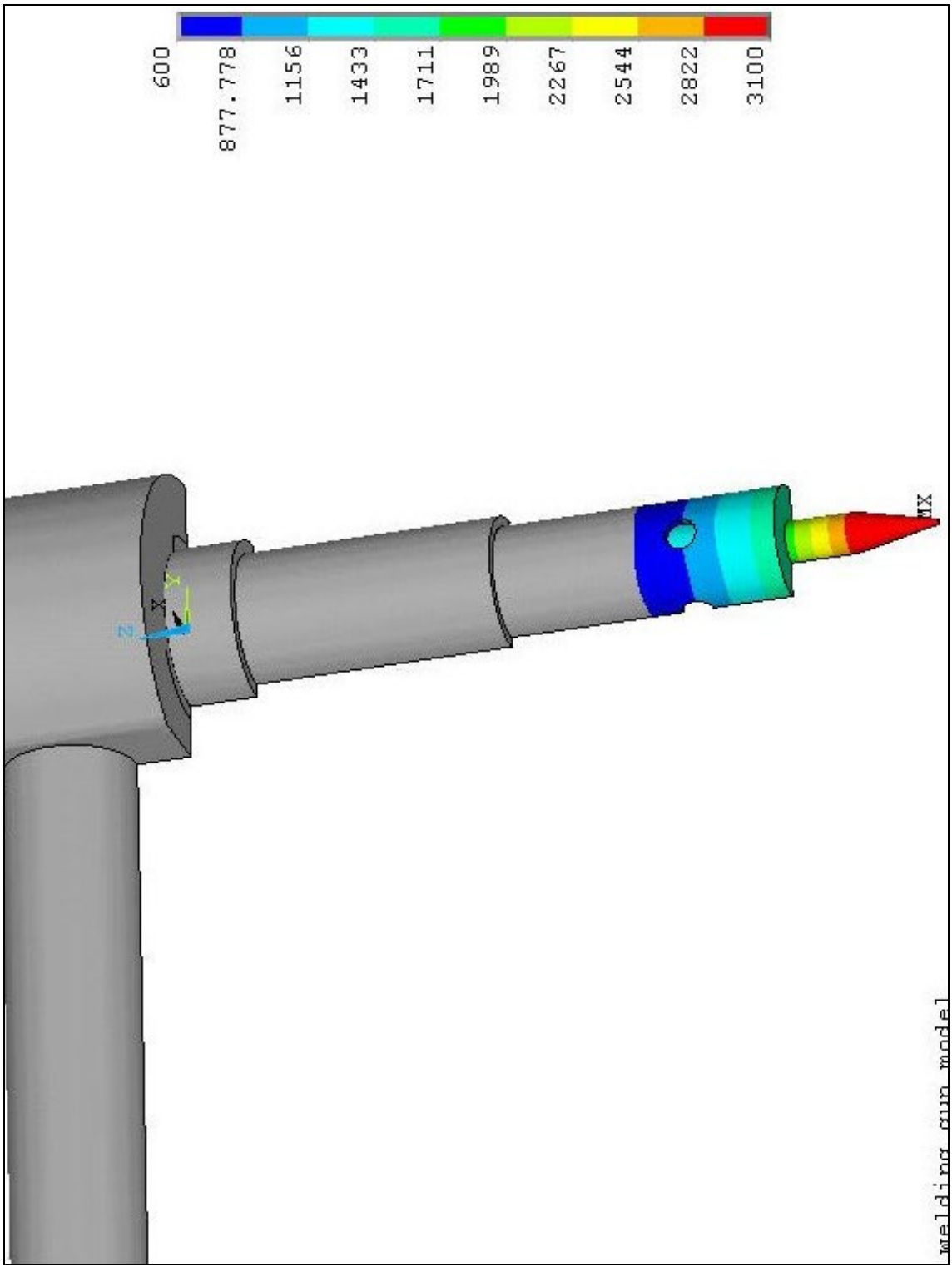

Figure F-4.2.6 Temperature plot of collet body for material combination number 1. Scale from 600 to 3100 K. Simulation conditions; 300 A, model C, uniform temperature 298 K, diameter 3.2 mm, turbulent regime, collet with “becoming element of turbulence” and simulating time 3’ 30”.

4.2.2 Combination 4

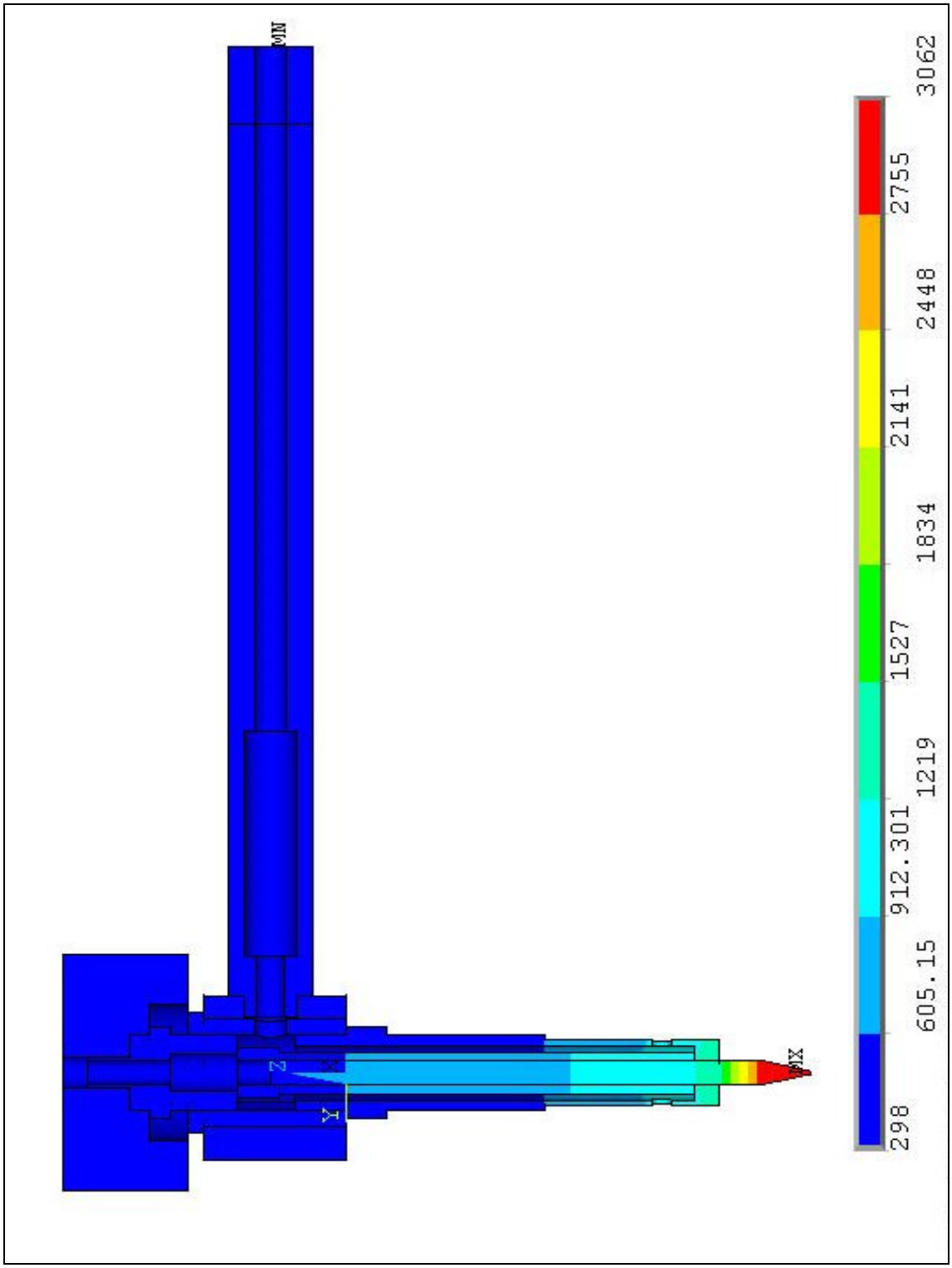

Figure F-4.2.7 Temperature plot in welding torch for the material combination number 4. Scale from 298 to 3062 K. Simulation conditions; 300 A, model C, uniform temperature 298 K, diameter 3.2 mm, turbulent regime, collet with “becoming element of turbulence” and simulating time 3’ 30”.

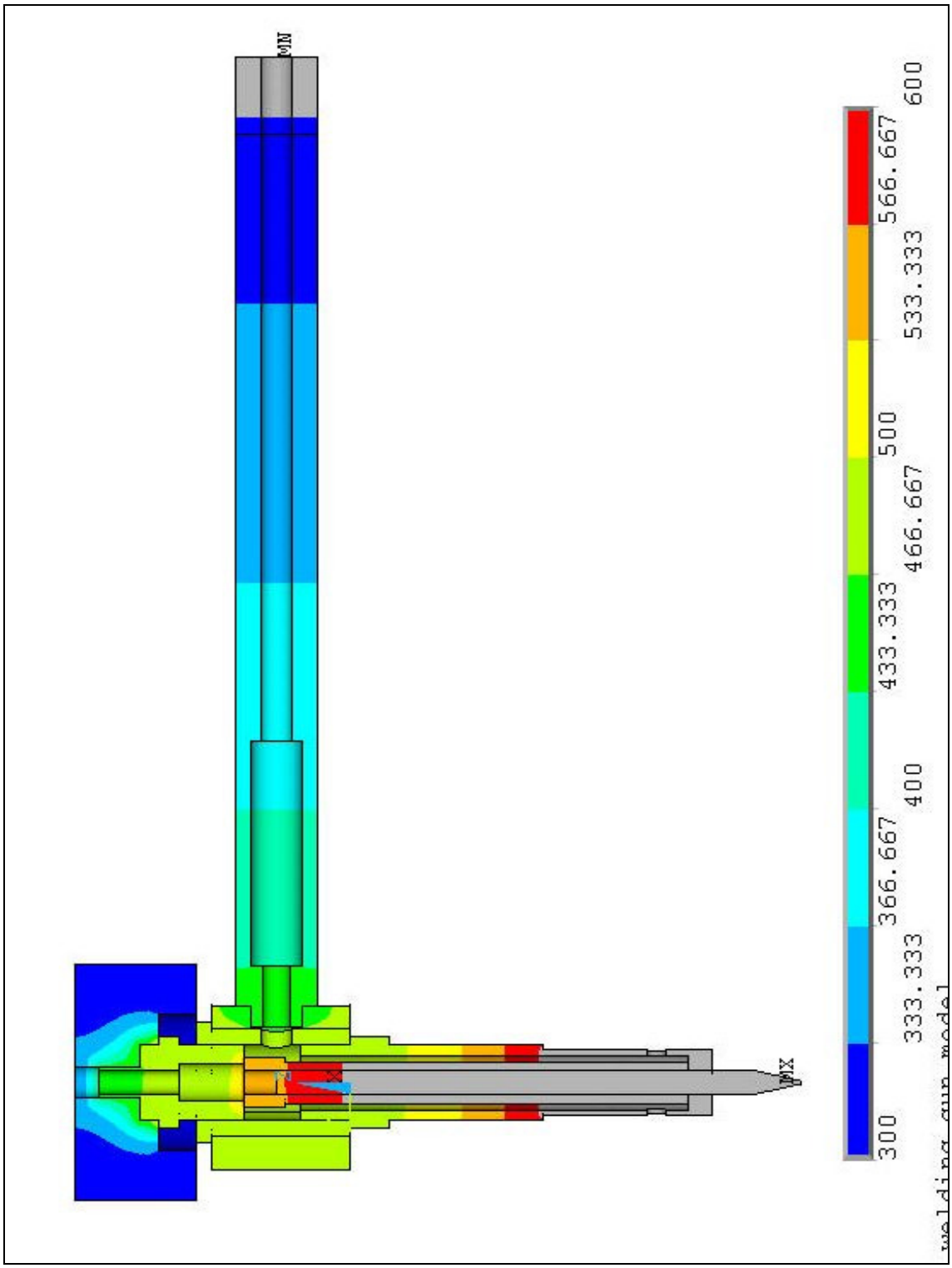

Figure F-4.2.8 Temperature plot in welding torch for material combination number 4. Scale from 300 to 600 K. Simulation conditions; 300 A, model C, uniform temperature 298 K, diameter 3.2 mm, turbulent regime, collet with “becoming element of turbulence” and simulating time 3’ 30”.

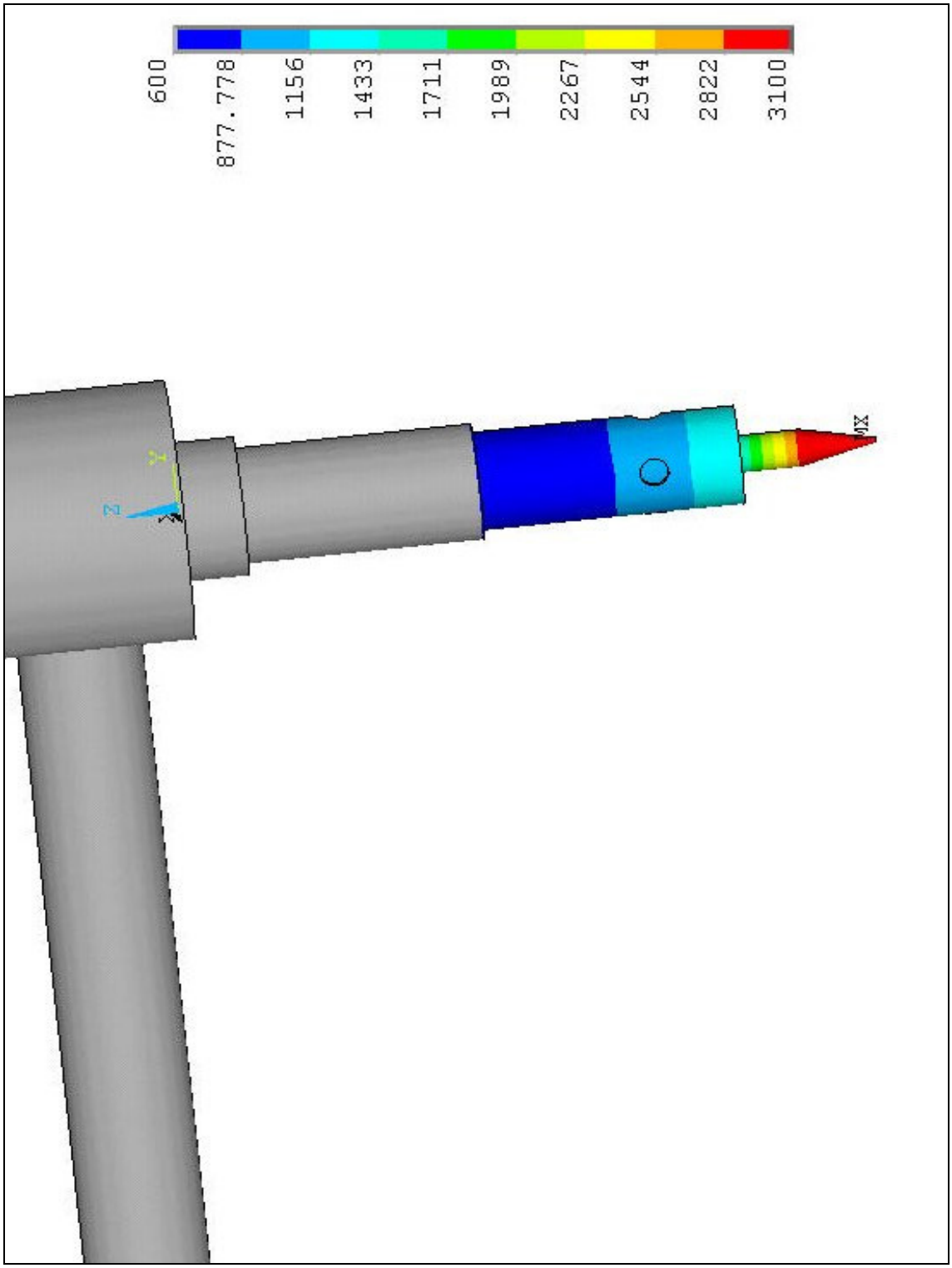

Figure F-4.2.9 Temperature plot of collet body for material combination number 4. Scale from 600 to 3100 K. Simulation conditions; 300 A, model C, uniform temperature 298 K, diameter 3.2 mm, turbulent regime, collet with “becoming element of turbulence” and simulating time 3’ 30”.

4.2.3 Combination 7

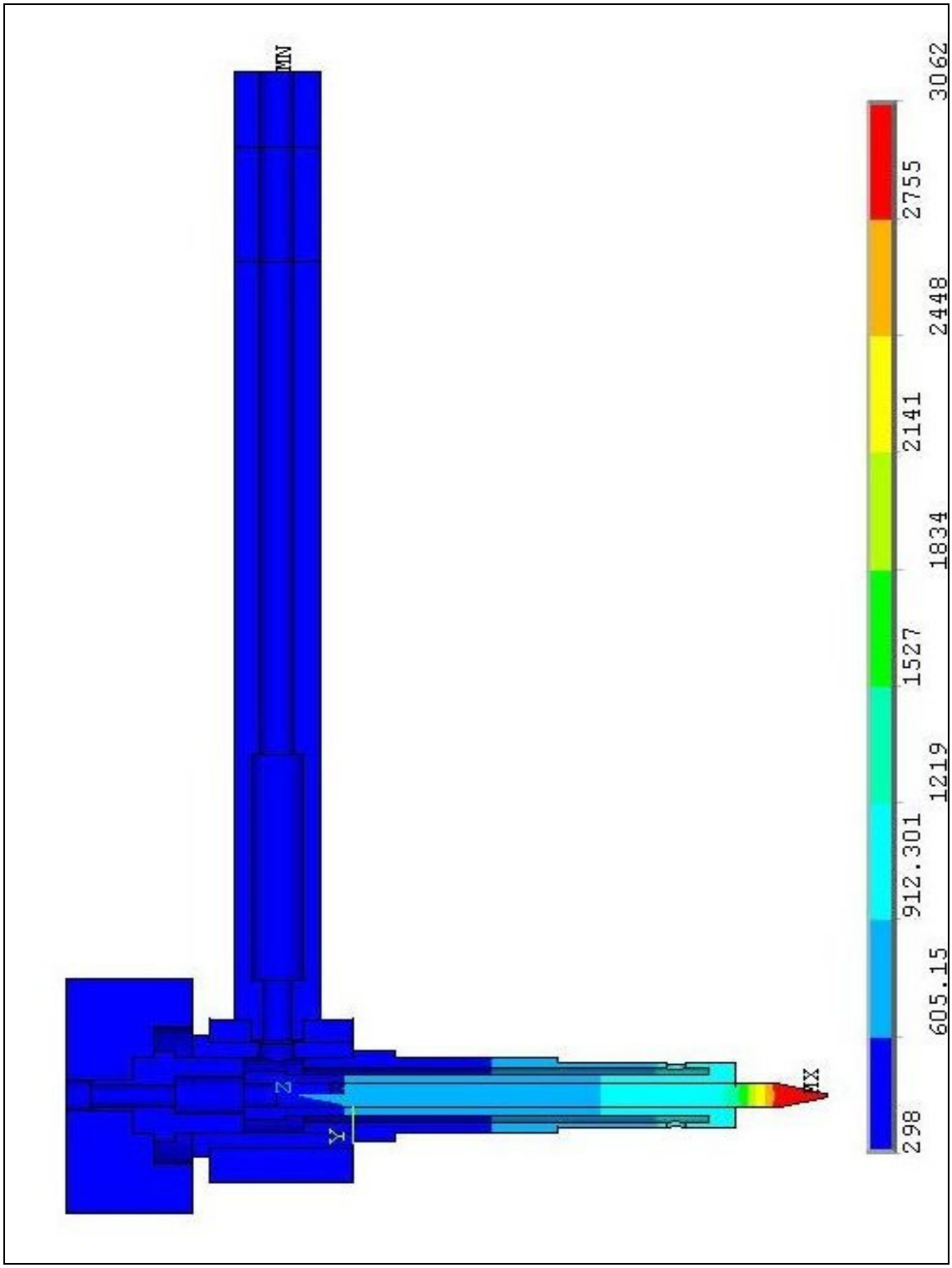

Figure F-4.2.10 Temperature plot in welding torch for the material combination number 7. Scale from 298 to 3062 K. Simulation conditions; 300 A, model C, uniform temperature 298 K, diameter 3.2 mm, turbulent regime, collet with “becoming element of turbulence” and simulating time 3’ 30”.

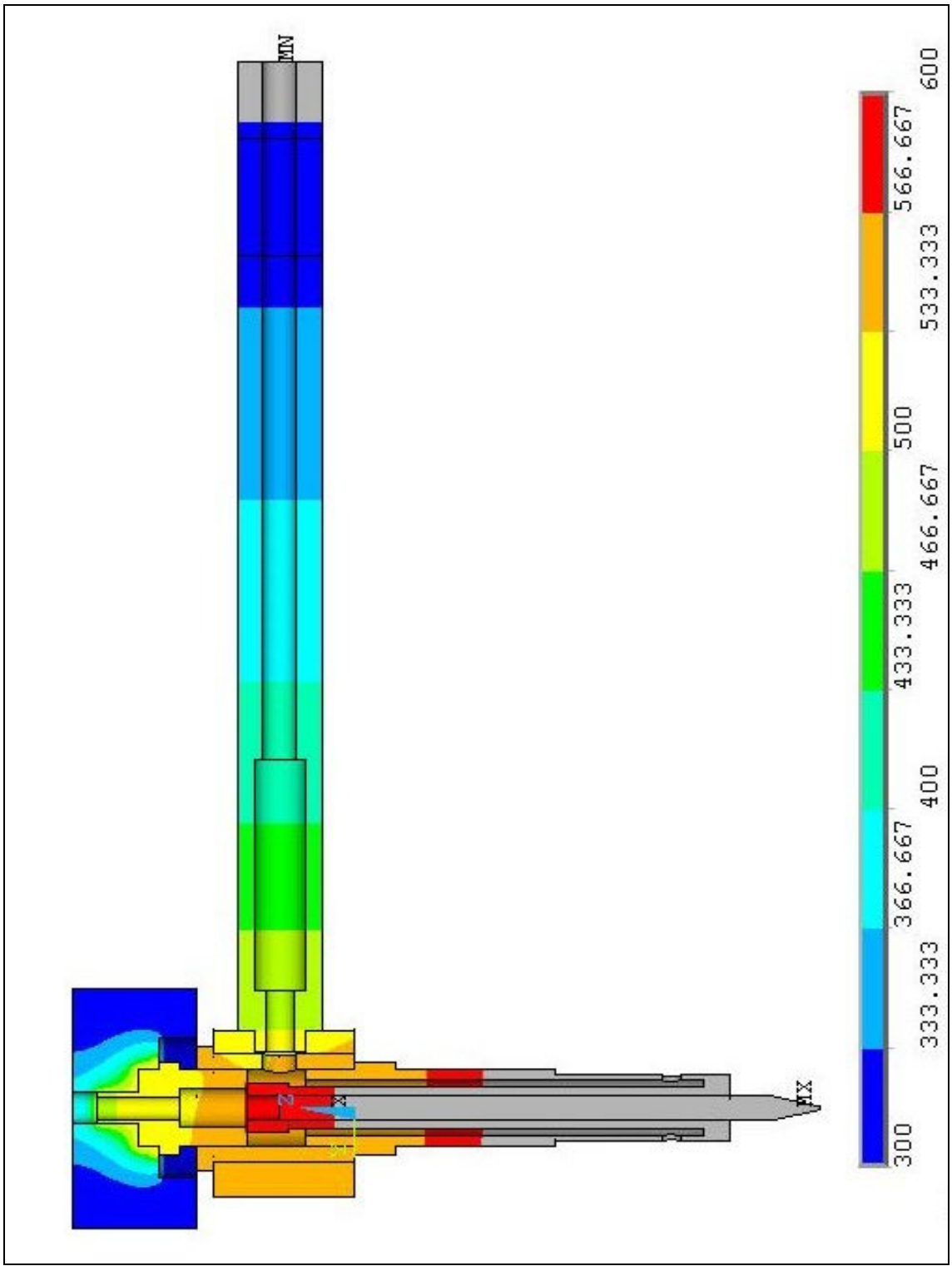

Figure F-4.2.11 Temperature plot in welding torch for material combination number 7. Scale from 300 to 600 K. Simulation conditions; 300 A, model C, uniform temperature 298 K, diameter 3.2 mm, turbulent regime, collet with “becoming element of turbulence” and simulating time 3’ 30”.

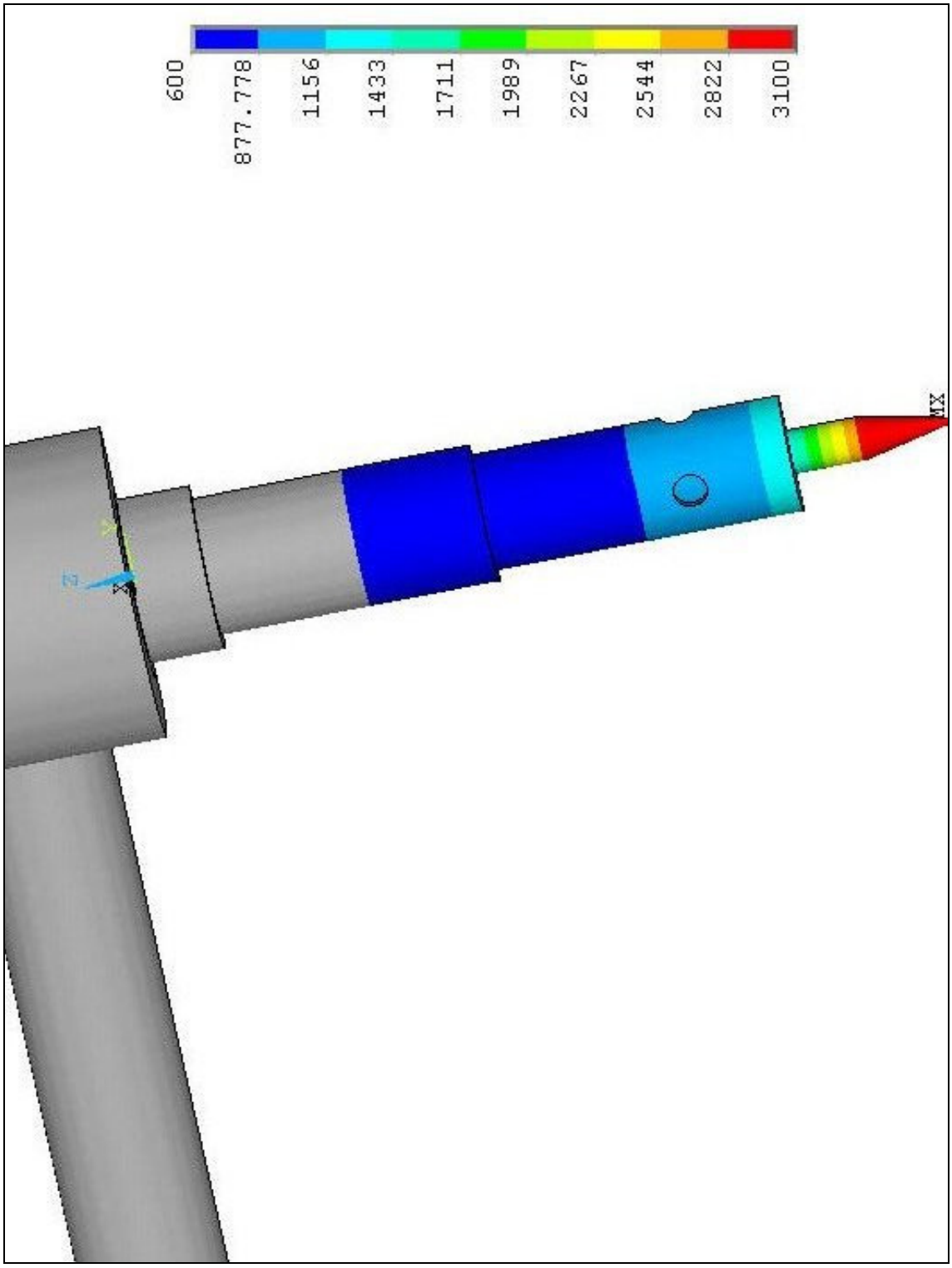

Figure F-4.2.12 Temperature plot of collet body for material combination number 7. Scale from 600 to 3100 K. Simulation conditions; 300 A, model C, uniform temperature 298 K, diameter 3.2 mm, turbulent regime, collet with “becoming element of turbulence” and simulating time 3’ 30”.

4.3 Simulation of Electrode Diameter

4.3.1 Diameter 2.4 mm

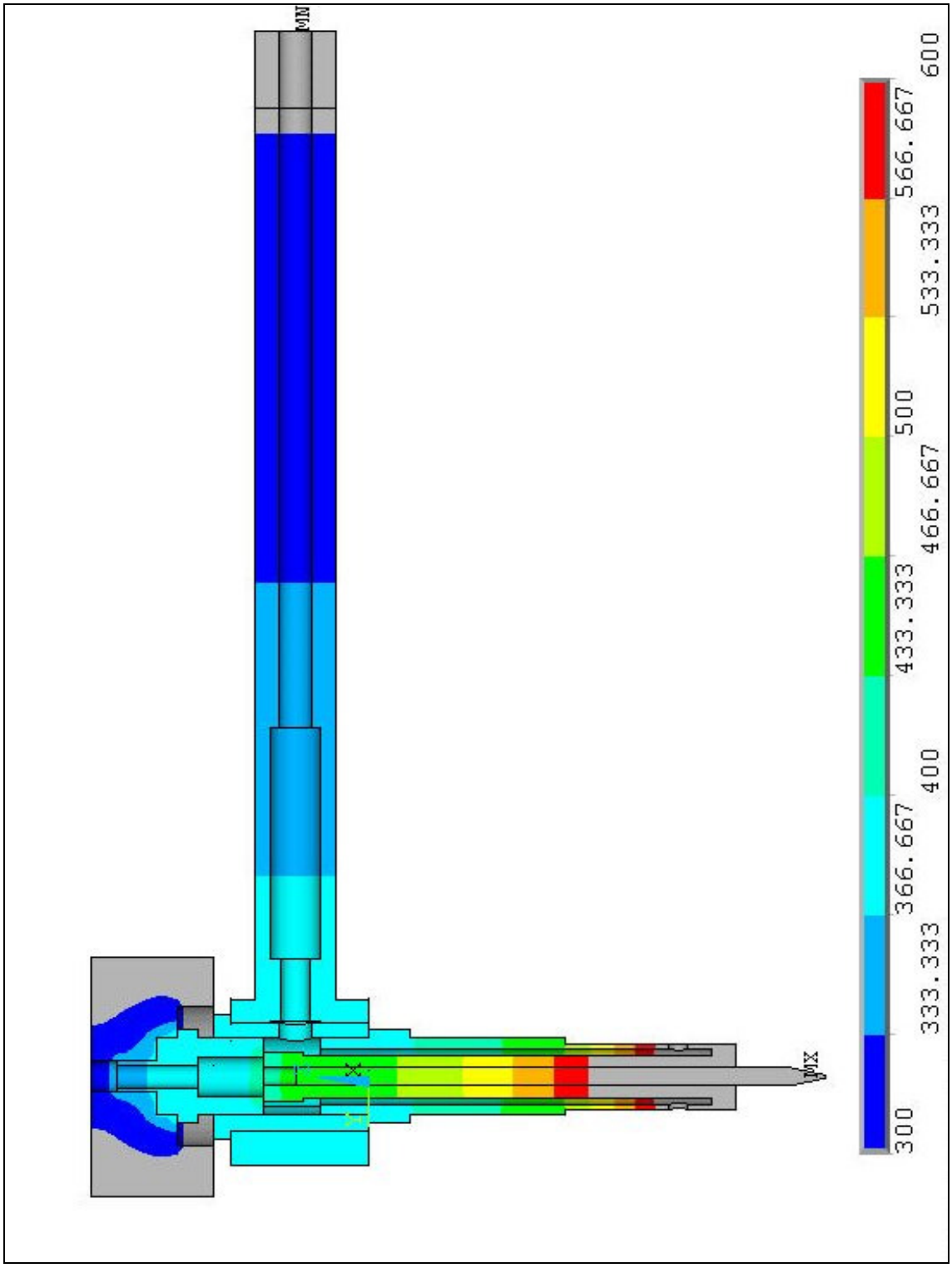

Figure F-4.3.1 Temperature plot in welding torch for diameter 2.4 mm. Scale from 300 to 600 K. Simulation conditions; 250 A, material combination number 0, model C, uniform temperature 298 K, turbulent regime, collet with “becoming element of turbulence” and simulating time 3’ 30”.

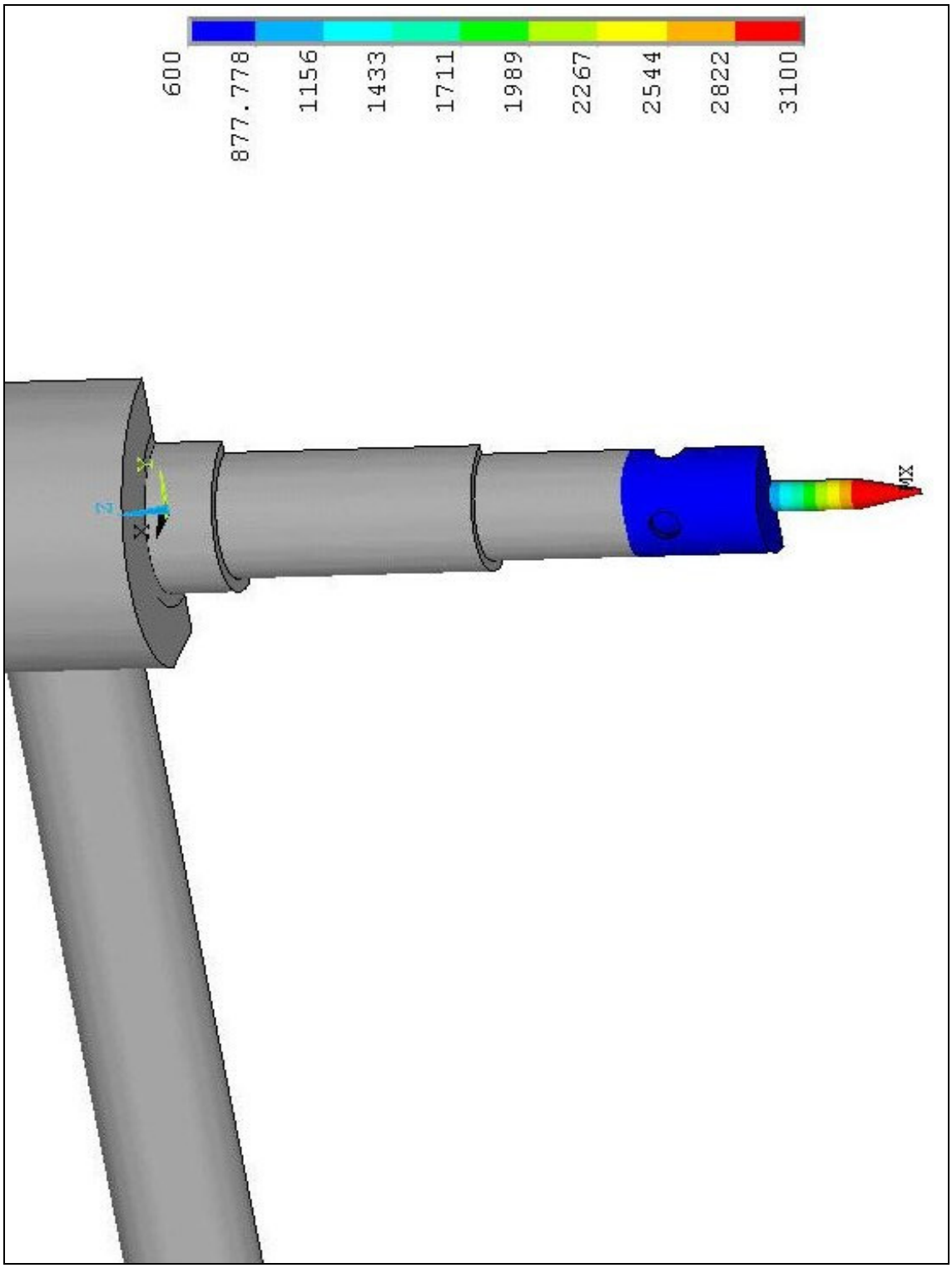

Figure F-4.3.2 Temperature plot of the collet body for diameter 2.4 mm. Scale from 600 to 3100 K. Simulation conditions; 250 A, material combination number 0, model C, uniform temperature 298 K, turbulent regime, collet with “becoming element of turbulence” and simulating time 3’ 30”.

4.4.3 Diameter 4 mm

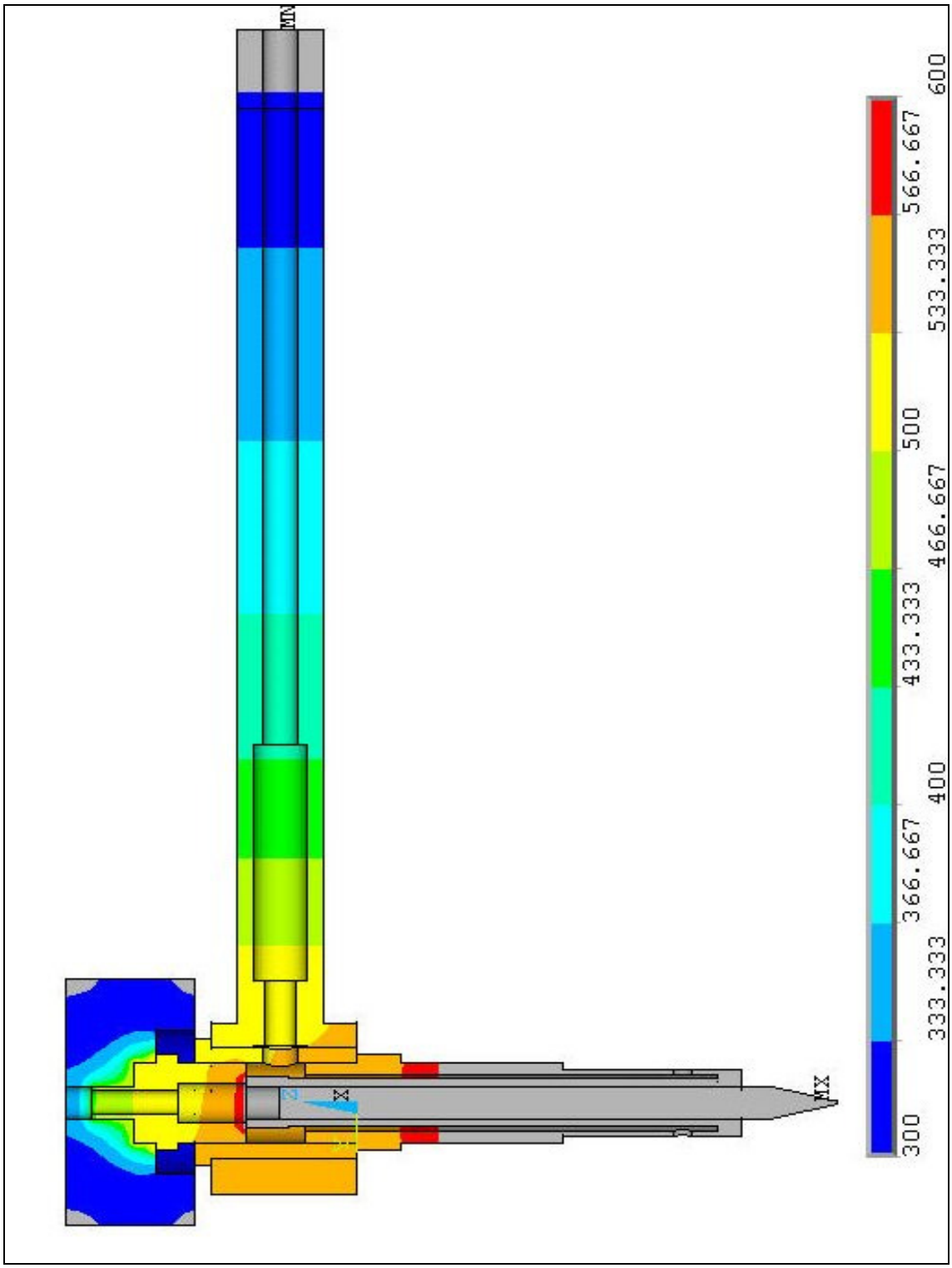

Figure F-4.3.3 Temperature plot in welding torch for 4 mm. Scale from 300 to 600 K. Simulation conditions; 250 A, material combination number 0, model C, uniform temperature 298 K, turbulent regime, collet with “becoming element of turbulence” and simulating time 3’ 30”

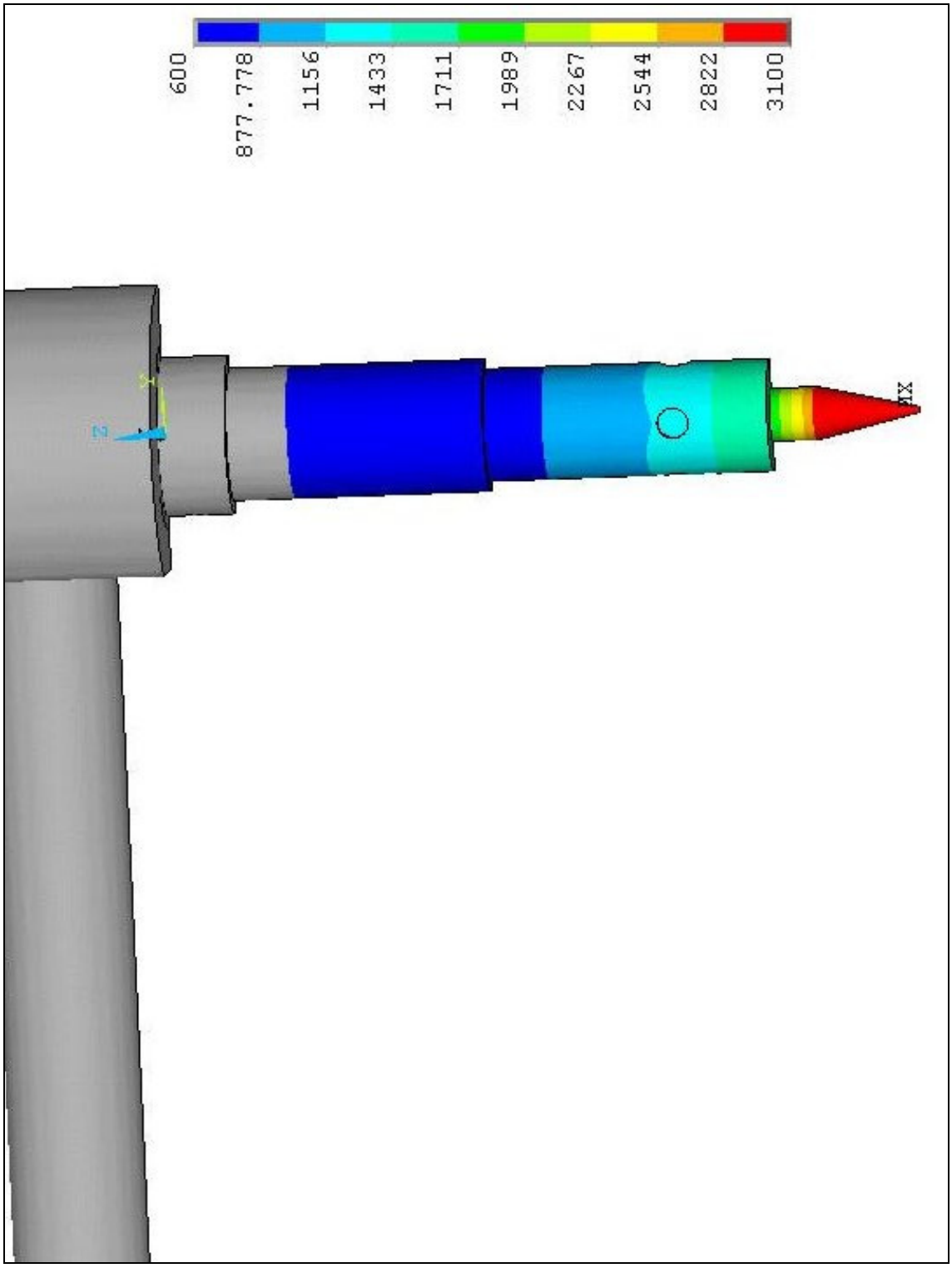

Figure F-4.3.4 Temperature plot in welding torch for diameter 4 mm. Scale from 600 to 3100 K. Simulation conditions; 250 A, material combination number 0, model C, uniform temperature 298 K, turbulent regime, collet with “becoming element of turbulence” and simulating time 3’ 30”.

4.4 Simulation of Volumetric Flow Rate

4.4.1 Laminar Flow and collet without “becoming element of turbulence”

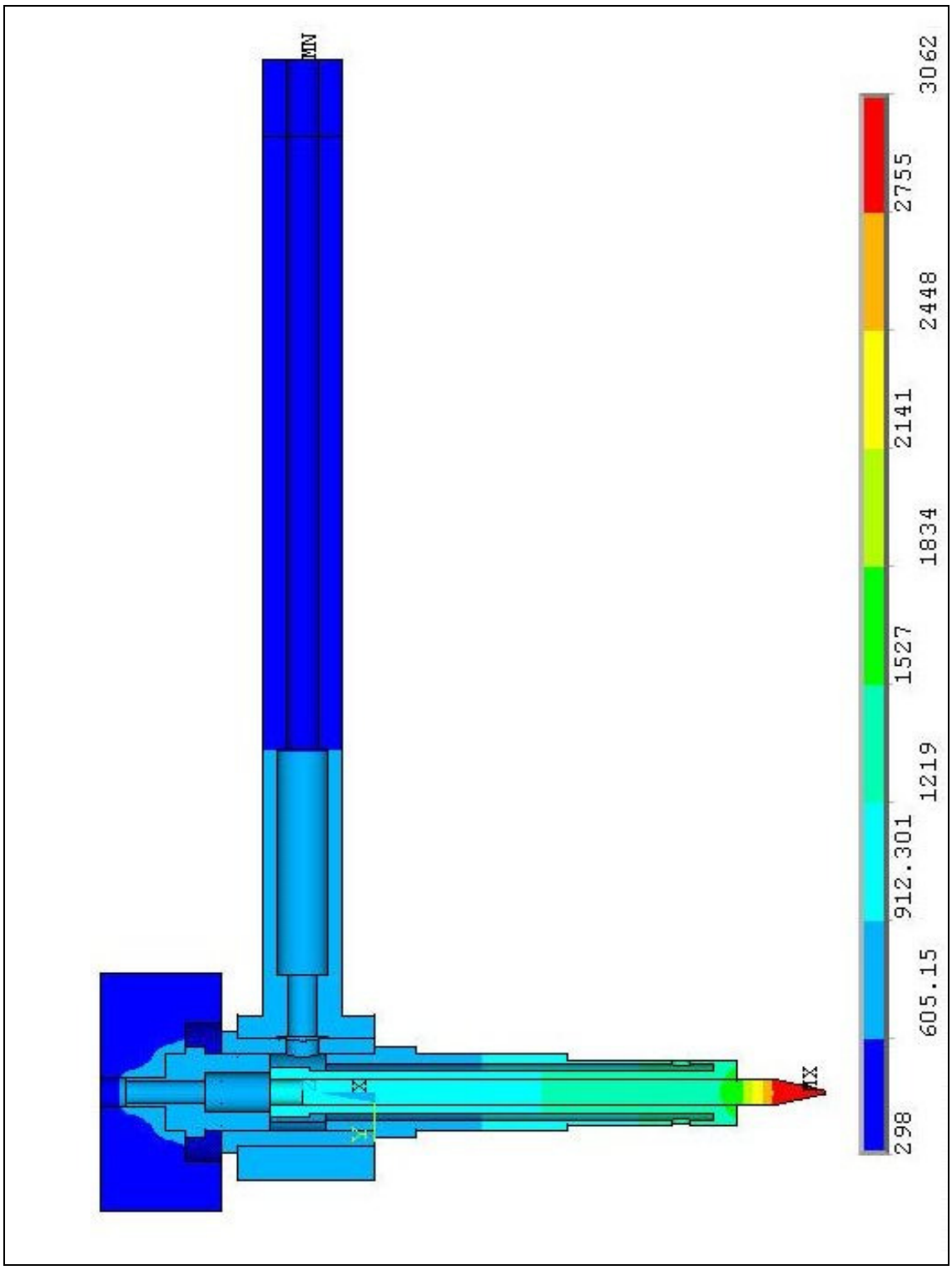

Figure F-4.4.1 Temperature plot in welding torch for laminar flow and collet without “becoming element of turbulence”. Scale from 298 to 3062 K. Simulation conditions; electrode diameter 3.2 mm, uniform temperature 298 K, material combination number 0, model C, 300 A, laminar flow, collet without “becoming element of turbulence” and simulating time 3’ 30”.

4.4.2 Turbulent regime and collet with “becoming element of turbulence”

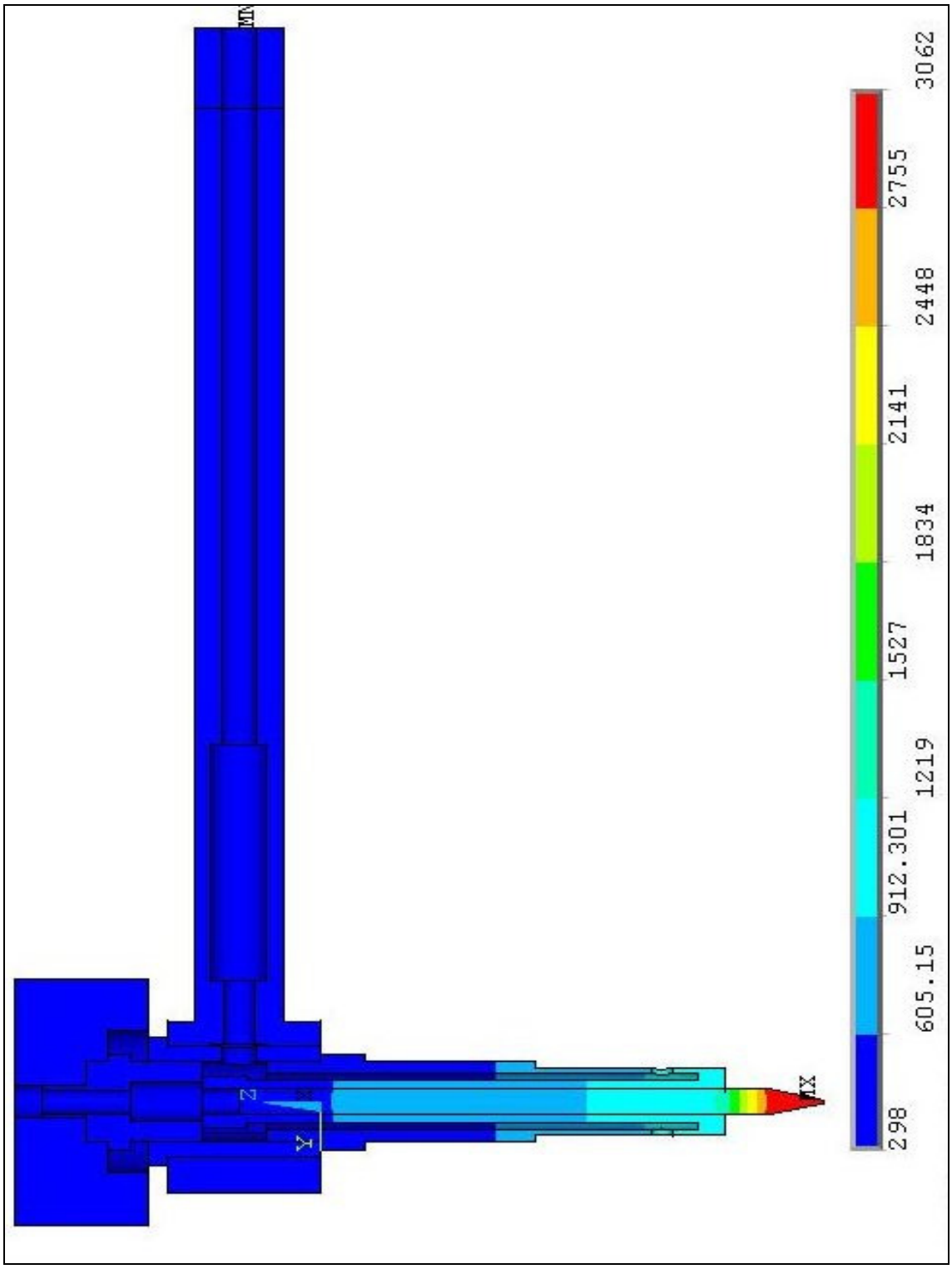

Figure F-4.4.2 Temperature plot in welding torch for turbulent regime and collet with “becoming element of turbulence”. Scale from 298 to 3062 K. Simulation conditions; electrode diameter 3.2 mm, uniform temperature 298 K, material combination number 0, model C, 300 A, turbulent regime, collet with “becoming element of turbulence” and simulating time 3’ 30”.